

Studies of Drug-drug and Drug-metal Interactions of Some Selected Antidiabetic, Antihypertensive and Lipid Lowering Drugs

The dissertation submitted to the Department of Pharmaceutical Chemistry, Faculty of Pharmacy, University of Dhaka, Bangladesh in partial fulfillment of the requirements for the degree of Doctor of Philosophy (PhD).



SUBMITTED BY

Reg. No.: 75/2015-2016 and 107/2019-2020 (Re-Reg.)

Department of Pharmaceutical Chemistry
Faculty of Pharmacy
University of Dhaka, Bangladesh

October 2021

DECLARATION

I, hereby, declare that the dissertation entitled “**Studies of Drug-drug and Drug-metal Interactions of Some Selected Antidiabetic, Antihypertensive and Lipid Lowering Drugs**” is my original research work carried out in the Department of Pharmaceutical Chemistry, Faculty of Pharmacy, University of Dhaka, Dhaka-1000, Bangladesh. I also declare that I have not submitted this dissertation either in part or full or in any other form to any other University or Institution for any Degree or any other purpose.



(Fahima Aktar)

PhD Student

Department of Pharmaceutical Chemistry

Faculty of Pharmacy

University of Dhaka

Dhaka-1000

Bangladesh

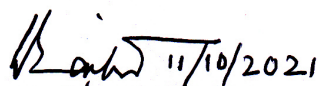
Date and Place

October 11, 2021

Dhaka University

SUPERVISORS' CERTIFICATE

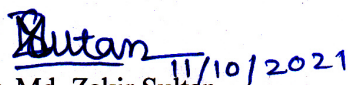
This is to certify that the research work in this Thesis entitled “**Studies of Drug-drug and Drug-metal Interactions of Some Selected Antidiabetic, Antihypertensive and Lipid Lowering Drugs**” described by Fahima Aktar, is an original work and has been carried out under our supervision in the Department of Pharmaceutical Chemistry, Faculty of Pharmacy, University of Dhaka, Dhaka-1000, Bangladesh, for the degree of Doctor of Philosophy (PhD). No part of this thesis has previously been submitted to any University/Institute for any Degree.

 11/10/2021

Dr. Mohammad A. Rashid

Professor

Department of Pharmaceutical Chemistry
Faculty of Pharmacy, University of Dhaka
Dhaka-1000, Bangladesh.

 11/10/2021

Dr. Md. Zakir Sultan

Principal Scientist

Centre for Advanced Research in Sciences (CARS)
University of Dhaka
Dhaka-1000, Bangladesh.

Dedicated to

My Father

MD. FAZLUR RAHMAN PRODHAN

&

My Mother

MRS. JOSNA RAHMAN

ACKNOWLEDGEMENTS

First and foremost I am grateful to the Almighty **Allah** for giving me the patience, dedications and ability to complete my PhD works.

I would like to express my heartfelt gratitude and profound thanks to my supervisor **Dr. Mohammad A. Rashid**, Professor, Department of Pharmaceutical Chemistry, University of Dhaka, Bangladesh for his valuable support, guidance and considerations during my entire research work. Despite extremely busy schedule, he took his time out to help me whenever necessary.

I am also indebted and grateful to **Dr. Md. Zakir Sultan**, Principal Scientist, Centre for Advanced Research in Sciences (CARS), University of Dhaka, co-supervisor of my PhD project for his co-operation and support throughout the research work.

I would also express my heartfelt gratitude and profound thanks to **Professor Dr. S. M. Abdur Rahman**, Dean, Faculty of Pharmacy, University of Dhaka for his valuable support and guidance.

Very sincerely, I acknowledge my special gratitude to **Dr. Md. Shah Amran**, Professor and Chairman, Department of Pharmaceutical Chemistry, University of Dhaka for his sincere suggestions and co-operation.

I am grateful to my colleagues, officers and staff of the Department of Pharmaceutical Chemistry as well as Faculty of Pharmacy for their sincere cooperation. I want to thank the authority, scientists, officers and staff of the Centre for Advanced Research in Sciences (CARS), University of Dhaka for their support to conduct my research.

I am indebted to my parents for their endless encouragement, love and advice. I would like to express my gratitude to my husband Nahid-Uz-Zaman Khan for his belief in me and his continuous support in taking decisions both now and in the past. I would like to acknowledge my children: Nabha and Naham, my parents in law, my sisters and relatives for their continuous support, cooperation and patience throughout my research period.

CONTENTS

	Page
CONTENTS	I-VI
LIST OF TABLES	VII-IX
LIST OF FIGURES	X-XV
ABSTRACT	XVI-XX
CHAPTER ONE: INTRODUCTION	1-25
1.1. COMPLEXATION LEADS TO DRUG DISCOVERY	2
1.1.1. Drug-drug interaction	3
1.1.2. Drug-metal interaction	3
1.2. SELECTION OF DRUGS AND METALS	4
1.3. DIABETES AND ANTIDIABETIC DRUGS	4
1.3.1. Metformin	5
1.3.2. Vildagliptin	6
1.3.3. Glimepiride	7
1.3.4. Dapagliflozin	8
1.4. HYPERTENSION AND ANTIHYPERTENSIVE DRUGS	9
1.4.1. Olmesartan medoxomil	10
1.4.2. Perindopril erbumine	11
1.5. HYPERLIPIDEMIA AND LIPID LOWERING DRUGS	12
1.5.1. Rosuvastatin	12
1.5.2. Atorvastatin calcium	13
1.6. METALS AND DRUG-METAL COMBINATION	14
1.6.1. Chromium(III)	14
1.6.1.1. Necessity of chromium	16
1.6.1.2. Chromium requirement in people with diabetes and glucose intolerance	16
1.6.1.3. Chromium level connectivity with fats and lipids	16
1.6.1.4. Chromium and diabetes	17
1.6.1.5. Chromium: mechanism of activity	17
1.6.1.6. Safety of supplemental chromium	18

1.6.2.	Lead(II)	18
1.6.2.1.	Mechanism of lead to induce diabetes	20
1.6.2.2.	Risk of lead in provoking diabetes	20
1.6.3.	Iron(II)	21
1.6.4.	Copper(II)	21
1.6.5.	Zinc(II)	21
1.7.	INTERACTION OF PROTEIN WITH THE DRUGS FOR SYNTHESIS OF NEW COMPLEXES	22
1.8.	OBJECTIVES OF THE PRESENT WORK	23
1.9.	SOCIO-ECONOMIC IMPORTANCE	24
CHAPTER TWO: MATERIALS AND METHODS		26-49
2.1.	MATERIALS	27
2.1.1.	Drugs and chemicals	27
2.1.1.1.	Preparation of pH 7.4 buffer solutions	28
2.1.2.	Instruments	28
2.1.3.	Animals	30
2.2.	METHODS	31
2.2.1.	Formation of drug-drug complexes by co-evaporated dispersion method	31
2.2.2.	Characterization of synthesized complexes	33
2.2.3.	Induction of diabetes in mice	35
2.2.4.	Serum creatinine study	36
2.2.5.	Uric acid determination	37
2.2.6.	Determination of SGPT and SGOT	37
2.2.7.	Histopathological studies of liver and kidney tissues of experimental mice	38
2.2.8.	Lipid lowering activity of rosuvastatin and its complexes in rabbits	38
2.2.8.1.	Experimental design	38
2.2.8.2.	Chemical analysis of biological sample	39
2.2.8.3.	Total cholesterol measurement procedure in serum	39
2.2.8.4.	Serum triglycerides measurement procedure	40
2.2.8.5.	LDL Cholesterol determination	40

2.2.8.6.	HDL Cholesterol determination	41
2.2.9.	Thrombolytic activity of rosuvastatin and its complexes	42
2.2.9.1.	Method of working sample preparation	42
2.2.9.2.	Measurement of thrombolytic activity	43
2.2.10.	Membrane stabilizing property of rosuvastatin and its complexes	43
2.2.10.1.	Preparation of the samples	43
2.2.10.2.	Erythrocytes (RBC) collection	43
2.2.10.3.	Preparation of phosphate buffer solution	44
2.2.10.4.	Preparation of isotonic solution	44
2.2.10.5.	Preparation of hypotonic solution	44
2.2.10.6.	Preparation of erythrocyte suspension	44
2.2.10.7.	Hypotonic solution-induced hemolysis	45
2.2.11.	<i>In vitro</i> antioxidant study of rosuvastatin and its complexes	45
2.2.11.1.	DPPH free radical scavenging property	45
2.2.11.2.	Preparation of standard for antioxidant activity determination	46
2.2.11.3.	Preparation of test sample	46
2.2.11.4.	Preparation of DPPH solution	46
2.2.11.5.	Evaluation of antioxidant property	46
2.2.12.	Fluorescence quenching characteristics of drugs and drug-drug complexes	47
2.2.12.1.	Quenching analysis by fluorescence spectrophotometer	47
2.2.12.2.	Evaluation of the binding constant and binding sites	48
2.2.12.3.	Thermodynamic parameters and binding forces	48

CHAPTER THREE: RESULTS AND DISCUSSION 50-187

3.1.	OLMESARTAN MEDOXOMIL AND THREE ANTIDIABETIC DRUGS COMPLEXATION: SYNTHESIS, CHARACTERIZATION AND BIOLOGICAL ACTIVITY EVALUATION	51
3.1.1.	TLC characterization of the drug complexes	51
3.1.2.	Analysis of parent drugs and drug complexes by HPLC	52
3.1.3.	Analysis of parent drugs and drug complexes by DSC	55
3.1.4.	Determination of melting point	60

3.1.5.	Analysis of parent drugs and drug complexes by TGA	61
3.1.6.	Analysis of drugs and drug complexes by FT-IR	69
3.1.7.	¹ H NMR spectra of parent drug and drug complexes	74
3.1.8.	Postulation of the complex formation	89
3.1.9.	Fluorescence quenching studies	90
3.1.9.1.	Analysis of thermodynamic parameters and the binding forces	96
3.1.9.2.	Analysis of binding constants (n) and no of binding points (K _b)	97
3.1.10.	Analysis of blood glucose level in mice	100
3.1.11.	Histopathological study results of drugs and drug complexes	103
3.1.12.	Serum creatinine analysis of drugs and complexes treated mice	104
3.1.13.	Analysis of serum uric acid in mice treated with drugs and drug complexes	106
3.1.14.	Serum SGPT and SGOT analysis in different mice groups	107
3.2.	ROSUVASTATIN, PERINDOPRIL ERBUMINE AND VILDAGLIPTIN COMPLEXATION: SYNTHESIS, CHARACTERIZATION AND ASSESSMENT OF BIOLOGICAL ACTIVITY	109
3.2.1.	TLC characterization of drugs and drug complexes	109
3.2.2.	Analysis of melting points of drugs and drug complexes	110
3.2.3.	TGA thermogram analysis of parent drugs and drug complexes	110
3.2.4.	FT-IR spectra analysis of drugs and drugs complexes	116
3.2.5.	<i>In vivo</i> study: Assessment of hypolipidemic activity of rosuvastatin and its complexes	122
3.2.6.	<i>In vitro</i> study: Determination of thrombolytic activity of drugs and drugs complexes	124
3.2.7.	<i>In vitro</i> study: Membrane stabilizing activity assay	126
3.2.8.	<i>In vitro</i> study of antioxidant activity	126
3.2.9.	Analyses of fluorescence quenching by perindopril, rosuvastatin, vildagliptin, and three drug complexes PR, PV	130

and RV	
3.2.9.1. Analysis of thermodynamic parameters and the binding forces	134
3.2.9.2. Analysis of binding constants (n) and no of binding points (K _b)	135
3.3. COMPLEXATION OF CHROMIUM(III) WITH FOUR ANTIDIABETIC DRUGS: SYNTHESIS, CHARACTERIZATION AND ASSESSMENT OF BIOLOGICAL ACTIVITY	138
3.3.1. TLC analysis of drugs and chromium complexes	138
3.3.2. Analysis of drugs and drug chromium complexes by DSC	139
3.3.3. TGA Analysis of drugs and drug chromium complexes	141
3.3.4. FT-IR spectra analysis of drugs and chromium drug complexes	148
3.3.5. ¹ H NMR spectra analysis for drugs and chromium drug complexes	151
3.3.6. Antidiabetic property of drugs and their Cr-complexes in mice	159
3.3.7. Histopathological studies of mice treated with chromium(III) drug complexes	160
3.4. COMPLEXATION OF HEAVY METAL LEAD WITH FOUR ANTIDIABETIC DRUGS: SYNTHESIS, CHARACTERIZATION AND ASSESSMENT OF BIOLOGICAL ACTIVITY AND TOXICITY	163
3.4.1. TLC characterization of drugs and lead drug complexes	163
3.4.2. Analysis of drugs and lead drug complexes by DSC	163
3.4.3. Analysis of drugs and lead drug complexes by TGA	166
3.4.4. Analysis of drugs and lead drug complexes by FT-IR	168
3.4.5. Evaluation of antidiabetic activity of drugs and lead drug complexes	170
3.4.6. Evaluation of toxicity in terms of serum creatinine and uric acid level determinations in mice	172
3.4.7. Histopathological studies of mice treated with drugs and lead	174

3.5. LIPID LOWERING DRUG ATORVASTATIN CALCIUM TRIHYDRATE COMPLEXATION WITH COPPER(II), IRON(II) AND ZINC(II): SYNTHESIS AND CHARACTERIZATION	177
3.5.1. Physical, analytical and thermal characteristics of drug and metal drug complexes	177
3.5.2. TLC characteristics of the drug and metal drug complexes	178
3.5.3. Analysis of drug and metal drug complexes by UV Spectroscopy	178
3.5.4. Analysis of drug and metal drug complexes by FT-IR	179
3.5.5. Analysis of atorvastatin and its metal complexes by ¹ H NMR spectroscopy	182
CHAPTER FOUR: CONCLUSION	188-193
CHAPTER FIVE: REFERENCES	194-215
LIST OF PAPERS PUBLISHED FROM THE THESIS	216

LIST OF TABLES

Table 3.1.	R _f values of precursor drugs and their complexes	51
Table 3.2.	Melting points from DSC thermograms	55
Table 3.3.	Melting points of olmesartan and three antidiabetic drugs and their complexes, OD, OV and OM	60
Table 3.4.	Percent (%) degradation of drugs and drug complexes from TGA thermograms	68
Table 3.5.	Stern-Volmer quenching rate constant K _{sv} and K _q of the olmesartan-BSA, dapagliflozin-BSA, vildagliptin-BSA, metformin-BSA, OD-BSA, OV-BSA and OM-BSA system at different temperatures	96
Table 3.6.	Thermodynamic parameters of drugs and newly synthesized drug complexes mediated quenching of BSA at 298 K, 308 K and 318 K	97
Table 3.7.	Binding constant (K _b) and number of binding sites(n) of the pure drugs and drug complexes at three different temperatures like 298 K 308 K and 318 K	99
Table 3.8.	Fasting blood glucose level (mmol/L) of different group of mice at different days	100-102
Table 3.9.	Anti-diabetic activity of the pure drugs and drug complexes	103
Table 3.10.	Serum creatinine level in different drugs and drug complexes treated mice group	105
Table 3.11.	Serum Uric acid level after treatment with the drugs and drug complexes in different mice groups	106
Table 3.12.	Serum SGPT and SGOT level in mice after treatment with drug and drug-complexes	107
Table 3.13.	R _f values of rosuvastatin, perindopril, vildagliptin and their complexes	109
Table 3.14.	Different melting points of the drugs rosuvastatin, perindopril, vildagliptin and the newly formed complexes PR, RV and PV	110
Table 3.15.	Percent (%) degradation of pure drugs and drug complexes with increasing temperature from TGA thermograms	116
Table 3.16.	Level of HDL, cholesterol, triglycerides, LDL cholesterol,	123

	VLDL cholesterol and non HDL cholesterol of different groups of drugs treated rabbits	
Table 3.17.	Thrombolytic activity of newly formed drug complexes PR, PV and RV	125
Table 3.18.	Membrane stabilizing activity of the drug rosuvastatin, drug complex PR, PV and RV in terms of % of inhibition of hemolysis of RBC in hypotonic solution	126
Table 3.19.	Antioxidant activity of rosuvastatin and the complexes PR, PV and RV	127
Table 3.20.	IC ₅₀ value of <i>tert</i> -butyl-1-hydroxytoluene (BHT)	127
Table 3.21.	IC ₅₀ value of the standard drug rosuvastatin	128
Table 3.22.	IC ₅₀ value of the new drug complex PR	128
Table 3.23.	IC ₅₀ value of the new drug complex PV	129
Table 3.24.	IC ₅₀ value of the new drug complex RV	129
Table 3.25.	Stern-Volmer quenching constant K _{sv} and K _q of the perindopril-BSA, rosuvastatin-BSA, vildagliptin-BSA, PR-BSA, PV-BSA and RV-BSA system at different temperatures	134
Table 3.26.	Thermodynamic parameters of drugs and newly synthesized drug complexes mediated quenching of BSA at 298 K and 308 K	135
Table 3.27.	Binding constant (K _b) and number of binding sites (n) of the pure drugs and drug complexes at two different temperatures at 298 K and 308 K	137
Table 3.28.	R _f values of drugs and the metal-drug complexes on F ₂₅₄ TLC plate	138
Table 3.29.	Percent (%) degradation of pure drugs and metal drug complexes with increasing temperature from TGA thermograms	148
Table 3.30.	<i>In vivo</i> antidiabetic property of antidiabetic drugs and their Cr-complexes in mice	159
Table 3.31.	R _f values of reference drugs and their respective lead complexes on silica gel F ₂₅₄ TLC plate	163
Table 3.32.	<i>In vivo</i> antidiabetic property of pure drugs (metformin, glimepiride, vildagliptin and dapagliflozin) and their Pb-	171

	complexes (Pb-met, Pb-glim, Pb-vilda and Pb-dapa) in mice model	
Table 3.33.	Serum creatinine levels after treatment with pure drugs (metformin, glimepiride, vildagliptin and dapagliflozin) and their Pb-complexes (Pb-met, Pb-glim, Pb-vilda and Pb-dapa) in mice model	172
Table 3.34.	Serum uric acid levels after treatment with pure drugs (metformin, glimepiride, vildagliptin and dapagliflozin) and their Pb-complexes (Pb-met, Pb-glim, Pb-vilda and Pb-dapa) in mice model	173
Table. 3.35.	Physical, analytical and thermal characteristics of atorvastatin and its three complexes	178

LIST OF FIGURES

Figure 1.1.	Structures of metformin (1), vildagliptin (2), glimepiride (3) and dapagliflozin (4)	5
Figure 1.2.	Mechanism of action of metformin	6
Figure 1.3.	Mechanism of action of vildagliptin	7
Figure 1.4.	Mechanism of action of glimepiride	8
Figure 1.5.	Mechanism of action of dapagliflozin	9
Figure 1.6.	Structures of two antihypertensive drugs: olmesartan medoxomil (1) perindopril erbumine (2)	10
Figure 1.7.	Mechanism of action of olmesartan medoxomil	10
Figure 1.8.	Investigation of perindopril on morbidity and/or mortality	11
Figure 1.9.	Structures of: rosuvastatin (1) atorvastatin calcium (2)	12
Figure 1.10.	Mechanism of actions of statins	13
Figure 2.1.	Some instruments used in the experiment: (1) Reaction bath, (2) Digital melting point measuring instrument, (3) DSC, (4) Fluorescence spectrophotometer, (5) ELISA reader, (6) HPLC	28-30
Figure 2.2.	Experimental rodents: (1) mice and (2) rabbits.	31
Figure 2.3.	TLC determination	33
Figure 2.4.	RBC collection	44
Figure 2.5.	Antioxidant activity by DPPH assay	47
Figure 3.1.	HPLC chromatograms of O, D and OD	53
Figure 3.2.	HPLC chromatograms of O, V and OV	54
Figure 3.3.	HPLC chromatograms of O, M and OM	55
Figure 3.4.	DSC thermograms of drugs: (1) olmesartan medoxomil, (2) dapagliflozin, (3) vildagliptin, (4) metformin, (5) OD, (6) OV and (7) OM	57-59
Figure 3.5.	Overlaid DSC thermograms of olmesartan medoxomil, dapagliflozin, vildagliptin, metformin HCl and the newly formed complexes viz. OD, OV and OM	60
Figure 3.6.	TGA thermograms of pure drugs, drug complexes: (1) olmesartan medoxomil, (2) metformin HCl, (3) dapagliflozin, (4) vildagliptin, (5) OD, (6) OV, (7) OM, (8) Overlaid thermograms of dapagliflozin, olmesartan and the complex OD, (9) Overlaid	61-65

	thermograms of vildagliptin, olmesartan and the complex OV,	
	(10) Overlaid thermograms of metformin, olmesartan and the complex OM	
Figure 3.7.	Overlaid TGA thermograms of precursor drugs and their complexes	66
Figure 3.8.	Degradation pattern of olmesartan medoxomil	66
Figure 3.9.	Degradation pattern of dapagliflozine	67
Figure 3.10.	Degradation pattern of vildagliptin	67
Figure 3.11.	Decomposition pattern of metformin HCl	67
Figure 3.12.	FT-IR spectra of pure drugs and complexes: (1) olmesartan medoxomil, (2) dapagliflozin, (3) vildagliptin, (4) metformin HCl, (5) OD, (6) OV and (7) OM	69-72
Figure 3.13.	Overlaid FT-IR spectra of olmesartan medoxomil and its complexes: (1) olmesartan medoxomil, dapagliflozin and complex OD, (2) olmesartan medoxomil, vildagliptin and complex OV, (3) olmesartan medoxomil, metformin and complex OM	73-74
Figure 3.14.	¹ H NMR spectra of olmesartan medoxomil (1-3), dapagliflozin (4-6), reacted complex OD (7-9) and unreacted solid mixture of olmesartan medoxomil and dapagliflozin (10-11)	75-80
Figure 3.15.	¹ H NMR spectra of olmesartan medoxomil (12), vildagliptin (13), reacted complex OV (14-16) and unreacted solid mixture of olmesartan medoxomil, vildagliptin (17-19)	81-84
Figure 3.16.	¹ H NMR spectra of olmesartan medoxomil (20), metformin HCl (21), complex OM (22-24) and unreacted solid mixture of olmesartan medoxomil and metformin HCl (25-27)	85-88
Figure 3.17.	Emission spectra of BSA in presence of different concentrations of olmesartan medoxomil, dapagliflozin, vildagliptin, metformin, complex OD, complex OV, complex OM	91-93
Figure 3.18.	BSA quenching Stern-Volmer plots with increased concentrations of olmesartan, dapagliflozin, vildagliptin, metformin, complex OD, complex OV and complex OM at 298 K, 308 K and 318 K	94
Figure 3.19.	Arrhenius plot (1) and Van't Hoff plot (2), for the interaction of BSA with olmesartan, dapagliflozin, vildagliptin, metformin, OD	95

- complex, OV complex and OM complex to determine the energy of activation of the quenching process at pH 7.4
- Figure 3.20.** Log plot for determination of binding constant (K_b) and no of binding point (n) for different systems like (1) Olmesartan-BSA, (2) dapagliflozin-BSA, (3) Vildagliptin-BSA, (4) metformin-BSA, (5) OD-BSA, (6) OV-BSA and (7) OM-BSA at 298 K, 308 K and 318 K **98-99**
- Figure 3.21.** Antidiabetic activity of drug complexes OD, OV and OM in comparison to metformin, dapagliflozin and vildagliptin **103**
- Figure 3.22.** Histopathology of kidney and liver tissues of the experimental mice treated with dapagliflozin, vildagliptin, glimepiride, OD, OV and OM **104**
- Figure 3.23.** Serum creatinine level of mice groups treated with drugs and drug complexes **105**
- Figure 3.24.** Serum uric acid levels in different mice treated with drug and drug complexes **106**
- Figure 3.25.** Serum SGPT and SGOT levels of mice after treatment with drugs and drug complexes **108**
- Figure 3.26.** TGA thermograms of the drugs and newly formed drug complexes: (1) perindopril, (2) Rosuvastatin, (3) Vildagliptin, (4) Drug complex PR, (5) Drug complex PV, (6) Drug complex RV **110-113**
- Figure 3.27.** The three overlaid TGA thermograms of the drugs and newly formed drug complexes: (1) Overlaid TGA thermograms of perindopril, vildagliptin and the complex PV, (2) Overlaid TGA thermograms of perindopril, rosuvastatin and the complex PR and (3) Overlaid TGA thermograms of vildagliptin, rosuvastatin and the complex RV **114-115**
- Figure 3.28.** FT-IR spectra of the drugs and drugs complexes: (1) perindopril erbumine, (2) rosuvastatin, (3) vildagliptin, (4) drug complex PR, (5) drug complex PV and (6) drug complex RV **117-119**
- Figure 3.29.** Overlaid FT-IR spectra of: (1) perindopril, rosuvastatin the drug complex PR; (2) perindopril, vildagliptin and their complex PV; (3) rosuvastatin, vildagliptin and their complex RV; (4) perindopril, rosuvastatin, vildagliptin, PR, PV and RV **120-121**

Figure 3.30.	Comparison of levels of HDL, cholesterol, triglycerides, LDL cholesterol, VLDL cholesterol and non HDL cholesterol of different groups of drugs treated rabbits	124
Figure 3.31.	Thrombolytic activity exhibited by rosuvastatin, PR, PV and RV in a way of % of clot lysis	125
Figure 3.32.	Membrane stabilizing activity of the drug rosuvastatin, drug complex PR, PV and RV in terms of % of inhibition of hemolysis of RBC in hypotonic solution	126
Figure 3.33.	IC ₅₀ values of BHT, rosuvastatin and three drug complexes	127
Figure 3.34.	IC ₅₀ value of <i>tert</i> -butyl-1-hydroxytoluene (BHT)	127
Figure 3.35.	IC ₅₀ value of the standard drug rosuvastatin	128
Figure 3.36.	IC ₅₀ value of the new drug complex PR	128
Figure 3.37.	IC ₅₀ value of the new drug complex PV	129
Figure 3.38.	IC ₅₀ value of the new drug complex RV	129
Figure 3.39.	Emission spectra of BSA in presence of different concentrations of perindopril, rosuvastatin, vildagliptin, complex PR, complex PV, complex RV	130-131
Figure 3.40.	BSA quenching Stern-Volmer plots with increased concentration of (1) perindopril, (2) rosuvastatin, (3) vildagliptin, (4) complex PR, (5) complex PV and (6) complex RV at 298 K and 308 K	132
Figure 3.41.	Arrhenius plot (1) and Van't Hoff plot (2) for the interaction of BSA with perindopril, rosuvastatin, vildagliptin, PR complex, PV complex and RV complex to determine the activation energy of the quenching process at pH 7.4	133
Figure 3.42.	Graphical log plot for determination of binding constant (K _b) and number of binding points (n) for (1) perindopril-BSA, (2) rosuvastatin-BSA, (3) vildagliptin-BSA, (4) PR-BSA, (5) PV-BSA and (6) RV-BSA at 298 K and 308 K	136
Figure 3.43.	Overlaid DSC thermograms for (1) metformin and Cr-metformin complex, (2) dapagliflozin and Cr-dapagliflozin complex, (3) vildagliptin and Cr-vildagliptin complex and (4) glimepiride and Cr-glimepiride complex	139-141
Figure 3.44.	TGA thermograms: (1) metformin, (2) Cr-metformin complex, (3) glimepiride, (4) Cr-glimepiride complex, (5) vildagliptin, (6)	142-145

- Cr-vildagliptin complex, (7) dapagliflozin and (8) Cr-dapagliflozin complex
- Figure 3.45.** Overlaid TGA thermograms: (1) metformin and Cr-metformin complex, (2) glimepiride and Cr-glimepiride complex, (3) vildagliptin and Cr-vildagliptin complex and (4) dapagliflozin and Cr-dapagliflozin complex **146-147**
- Figure 3.46.** Overlaid IR spectra: (1) metformin and Cr-metformin complex, (2) glimepiride and Cr-glimepiride complex, (3) vildagliptin and Cr-vildagliptin complex and (4) dapagliflozin and Cr-dapagliflozin complex **149-150**
- Figure 3.47.** ¹H NMR spectra of: (1) metformin, (2) Cr-metformin, (3) Glimepiride, (4) Cr-glimepiride, (5) vildagliptin, (6) Cr-vildagliptin, (7) dapagliflozin and (8) Cr-dapagliflozin **151-158**
- Figure 3.48.** Graphical presentation of antidiabetic property of reference drugs and their Cr-complexes in mice model **159**
- Figure 3.49.** Histopathological reports of metformin, Cr-metformin, glimepiride, Cr-glimepiride, vildagliptin, Cr-vildagliptin, dapagliflozin and Cr-dapagliflozin treated mice liver and kidney tissues **160-162**
- Figure 3.50.** Overlaid DSC thermograms of: (1) metformin and Pb-metformin, (2) dapagliflozin and Pb-dapagliflozin, (3) glimepiride and Pb-glimepiride and (4) vildagliptin and Pb-vildagliptin complex **164-165**
- Figure 3.51.** Overlaid TGA thermograms: (1) metformin and Pb-metformin complex, (2) glimepiride and Pb-glimepiride complex, (3) vildagliptin and Pb-vildagliptin complex and (4) dapagliflozin and Pb-dapagliflozin complex **166-167**
- Figure 3.52.** Overlaid IR spectra of: (1) metformin and Pb-met complex, (2) glimepiride and Pb-glim complex, (3) vildagliptin and Pb-vilda complex and (4) dapagliflozin and Pb-dapa complex **168-170**
- Figure 3.53.** *In vivo* antidiabetic property of pure drugs (metformin, glimepiride, vildagliptin and dapagliflozin) and their Pb-complexes (Pb-met, Pb-glim, Pb-vilda and Pb-dapa) in mice model **171**
- Figure 3.54.** Serum creatinine levels after treatment with pure drugs **173**

(metformin, glimepiride, vildagliptin and dapagliflozin) and their Pb-complexes (Pb-met, Pb-glim, Pb-vilda and Pb-dapa) in mice model

- Figure 3.55.** Serum uric acid levels after treatment with pure drugs (metformin, glimepiride, vildagliptin and dapagliflozin) and their Pb-complexes (Pb-met, Pb-glim, Pb-vilda and Pb-dapa) in mice model **174**
- Figure 3.56.** Histopathological reports of metformin, Pb-metformin, glimepiride, Pb-glimepiride, vildagliptin, Pb-vildagliptin, dapagliflozin and Pb-dapagliflozin treated mice liver and kidney tissues **174-176**
- Figure 3.57.** Crystals of Fe-atorvastatin, Cu-atorvastatin and Zn-atorvastatin **177**
- Figure 3.58.** Overlaid UV spectra of atorvastatin calcium and three new complexes Fe-atorvastatin, Cu-atorvastatin and Zn-atorvastatin. **179**
- Figure 3.59.** FT-IR spectra of: (1) atorvastatin calcium, (2) Fe-atorvastatin, (3) Cu-atorvastatin and (4) Zn-atorvastatin **180-181**
- Figure 3.60.** ^1H NMR spectra: (1-3) atorvastatin calcium, (4-6) Fe-atorvastatin, (7-9) Cu-atorvastatin and (10-12) Zn-atorvastatin **182-187**

ABSTRACT

Drug-drug and drug-metal interactions are important area of research in drug discovery as well as pharmacodynamic actions of the drugs. Drug-drug and drug-metal complexation may introduce new molecules having new and/or better therapeutic activities in the body.

In this research work, various types of complexes from antidiabetic, antihypertensive and lipid lowering drugs were investigated while interacting with each other and with the metal ions like chromium(III), lead(II), zinc(II), iron(II) and copper(II). Different types of physicochemical properties and *in vivo* as well as *in vitro* pharmacological effects of the complexes were also studied.

Drug-drug interactions of three antidiabetic agents (metformin, dapagliflozin and vildagliptin) with an antihypertensive drug (olmesartan medoxomil) were performed by co-evaporated dispersion method and three complexes were synthesized as olmesartan-metformin (OM), olmesartan-dapagliflozin (OD) and olmesartan-vildagliptin (OV).

Three complexes of a lipid lowering drug (rosuvastatin) with an antidiabetic drug (vildagliptin), as well as an antihypertensive drug (perindopril) were synthesized viz. perindopril-vildagliptin (PV), perindopril-rosuvastatin (PR) and rosuvastatin-vildagliptin (RV).

Eleven drug metal complexes were also synthesized viz. Cr-metformin, Cr-glimepiride, Cr-vildagliptin, Cr-dapagliflozin, Pb-metformin, Pb-glimepiride, Pb-vildagliptin, Pb-dapagliflozin, Zn-atorvastatin, Cu-atorvastatin and Fe-atorvastatin.

The co-evaporated dispersion method was used for the synthesis of both drug-drug and drug-metal complexes. TLC, HPLC, FT-IR, UV, DSC and NMR studies confirmed the synthesis of the complexes. The melting points, DSC and TGA analyses demonstrated the thermal stability as well as thermochemical properties of the synthesized complexes. The thermodynamic parameters of the interactions of BSA (bovine serum albumin) with these pure drugs and synthesized complexes were observed using fluorescence quenching method.

For TLC studies of the precursor drugs and complexes, the R_f values were found to be different from each other. Although, the NMR spectra of the pure drugs (metformin,

dapagliflozin, vildagliptin, glimepiride, olmesartan medoxomil, perindopril, rosuvastatin, atorvastatin) and synthesized complexes (OM, OD, OV, Cr-metformin, Cr-glimepiride, Cr-vildagliptin, Cr-dapagliflozin, Zn-atorvastatin, Cu-atorvastatin and Fe-atorvastatin) were recorded. No attempt was taken for in-depth analysis of the NMR spectral data. The main objective of acquiring the ^1H NMR spectra of the above mentioned drugs and complexes was to see the differences in the spectral patterns between the parent drug(s) and the corresponding synthesized complex(es). Careful analysis of the ^1H NMR spectra demonstrated that differences could be seen between the spectra of the parent drug and synthesized complex. This was only to show that complexes were formed which was further supported by TLC, TGA, DSC and FTIR analyses. Melting points were found to be 221-225 °C, 80-85 °C, 150-154 °C, 175-180 °C, 126-130 °C, 156-160 °C and 163-167 °C for metformin, dapagliflozin, vildagliptin, olmesartan medoxomil, perindopril, rosuvastatin and atorvastatin, respectively. The synthesized complexes exhibited melting points at 68-72 °C, 80-85 °C, 100-105 °C, 55-60 °C, 110-115 °C, 115-118 °C, 102-107.6 °C, 106.5-111 °C and 105.6-110 °C for OM, OD, OV, PR, RV, PV, Zn-atorvastatin, Cu-atorvastatin and Fe-atorvastatin, respectively which were also different from the precursor drugs and the complexes. The DSC thermograms of metformin, dapagliflozin, vildagliptin, olmesartan medoxomil, OD, OV, OM, Cr-metformin, Cr-glimepiride, Cr-vildagliptin, Cr-dapagliflozin, Pb-metformin, Pb-glimepiride, Pb-vildagliptin and Pb-dapagliflozin revealed the melting endotherms which were found to be different from each other. The R_t of HPLC chromatograms were found to not be identical of some parent drugs and drug complexes in the same analytical conditions.

The mechanism of interactions of olmesartan, dapagliflozin, vildagliptin, metformin, and OD, OV and OM complexes with BSA were studied and found as dynamic quenches because the values of K_{sv} were increased with increasing temperature. The thermodynamic factors were determined from the linear plot of Van't Hoff which indicated the spontaneous (negative value of ΔG) interaction where hydrophobic interaction was the major contributing force (positive values of ΔH and ΔS) except for olmesartan. For olmesartan-BSA, it was found that $\Delta H < 0 < \Delta S$ which indicated that the interaction was electrostatic force driven. The binding constants and number of binding sites were also calculated and found that one mole of the reactant (drug) and/or complex interacted with one mole of BSA.

On the other hand, the interaction mechanisms of rosuvastatin, perindopril, vildagliptin, RV, PV and PR with BSA were also studied and found that perindopril, vildagliptin, PV and PR showed dynamic quenches as the values of K_{sv} increased along with increasing temperature. But the rosuvastatin-BSA and RV-BSA systems were developed by static quenching where, K_{sv} values decreased with increasing temperature. The interactions of perindopril, vildagliptin, PR, PV with BSA were mediated by enthalpy driven hydrophobic bonding (negative value of ΔG). But the rosuvastatin-BSA and RV-BSA systems were driven by the Vander Waal's forces and H-bonds (negative value of ΔH along with $\Delta S < 0$). The binding constants and number of binding sites were also analyzed and found that one mole of the reactant (drug) and/or complex interacted with one mole of BSA.

In vivo exploration of anti-diabetic activity was done on alloxan induced mice. The study revealed that after 14 days of treatment the antidiabetic drugs e.g. metformin, dapagliflozin and vildagliptin reduced the blood sugar by 39.70%, 56.73% and 51.22%, respectively while the newly synthesized complexes e.g. OM, OD and OV reduced the blood sugar by 42.95%, 50.50% and 48.66%, respectively. Hence only OM demonstrated synergistic effect as it reduced the blood sugar level more than that exhibited by metformin. Other complexes OD and OV did not show better effect than the parent drugs dapagliflozin and vildagliptin, respectively. The OM can be demonstrated as safe because the complex revealed no damage to hepatic and nephrotic tissues. But the other complexes OD and OV produced moderate to severe dysplasia in kidney and liver tissues after 14 days of treatment. All the three complexes elevated levels of serum creatinine and uric acid than that for metformin, dapagliflozin and vildagliptin itself. The levels of serum creatinine for control, metformin, dapagliflozin, vildagliptin were found as 3.8 mg/dL, 3.38 mg/dL, 3.42 mg/dL and 3.60 mg/dL, respectively but for OM, OD and OV the concentrations were found as 4.09 mg/dL, 4.56 mg/dL and 5.95 mg/dL, respectively. Uric acid levels for control, metformin, dapagliflozin, vildagliptin, OM, OD and OV were found as 17.59 mg/dL, 10.06 mg/dL, 11.37mg/dL, 16.84 mg/dL, 12.75 mg/dL, 15.64 mg/dL and 17.81 mg/dL, respectively. The serum SGPT level for control, metformin, dapagliflozin, vildagliptin, complex OM, OD and OV treated mice were calculated as 23.85 U/L, 20.28 U/L, 21.02 U/L, 21.17 U/L, 17.35 U/L, 20.15 U/L and 27.78 U/L, respectively. Serum SGOT level in mice after treatment with drugs and drug complexes were found 21.23 U/L, 18.42 U/L, 17.24 U/L, 17.70 U/L, 15.54 U/L, 18.91 U/L and 25.67 U/L, respectively for control,

metformin, dapagliflozin, vildagliptin, OM, OD and OV. Serum SGPT and SGOT levels were elevated by the treatment with OV. But OM treatment revealed reduced serum SGPT and SGOT levels than by only metformin treatment (20.28 U/L to 17.35 U/L and 18.42 U/L to 15.54 U/L, respectively). Considering all the issues the complex OM can be demonstrated as safe and promising ligand and can be suggested for further extensive studies to evaluate as therapeutic agent.

In case of antidiabetic activity of four Cr-complexes viz. Cr-metformin, Cr-glimepiride, Cr-vildagliptin and Cr-dapagliflozin, they improved glucose metabolism in alloxan induced hyperglycemic mice. The treatment with the Cr-complexes significantly reduced the blood glucose level than that of the positive control group mice. Among the four Cr-drug complexes, Cr-dapagliflozin complex reduced blood glucose level significantly and it was found to be 64.20% more effective than the standard dapagliflozin. The result was followed by Cr-glimepiride by 26.72% blood glucose reduction, Cr-metformin by 23.35% reduction and Cr-vildagliptin by 7.61% reduction than the standard glimepiride, metformin and vildagliptin, respectively. But Cr-vildagliptin and Cr-dapagliflozin showed moderate dysplasia in hepatic tissues after 14 days of treatment. So, whether Cr-complexes can offer long-term health benefits or not is still unknown as extensive toxicological data could not be established yet.

In case of Pb-antidiabetic drug complexes, they did not show significant positive effect to reduce the blood glucose level. After 14 days of treatment with metformin, glimepiride, vildagliptin, dapagliflozin, it was found that the average glucose levels of mice decreased from 31.54, 30.24, 31.50 and 30.37 to 19.02, 17.20, 19.70 and 17.60 mmol/L, respectively in mice whereas the complexes Pb-metformin, Pb-glimepiride, Pb-vildagliptin and Pb-dapagliflozin did not reduce blood glucose level considerably and blood sugar levels were found as 25.82, 29.23, 25.32 and 29.32 mmol/L, respectively. Moreover, the Pb-complexes increased serum creatinine and serum uric acid levels of mice as well as produced necrosis of the hepatic and nephrotic tissues which suggested cellular damage in liver and kidney of mice. After treatment with metformin, glimepiride, vildagliptin, dapagliflozin, the serum creatinine levels of mice were found to be 3.38, 3.96, 3.60 and 3.42 mg/dL, respectively whereas for Pb-metformin, Pb-glimepiride, Pb-vildagliptin and Pb-dapagliflozin the creatinine levels were increased to 4.57, 5.36, 5.21 and 5.24 mg/dL, respectively. The levels of uric acid of the experimental mice were elevated into 53.13 from 42.91, 57.40 from 44.83, 49.36 from 40.21 and 53.32 from 41.49 mg/dL for Pb-metformin, Pb-glimepiride, Pb-

vildagliptin and Pb-dapagliflozin, respectively than that of metformin, glimepiride, vildagliptin and dapagliflozin.

In vivo evaluation of lipid lowering activity was done on high fat diet fed rabbits and from the experiment, it was found that all the synthesized complexes viz. complex PR, PV and RV reduced cholesterol, triglycerides, low density lipoprotein (LDL) cholesterol, very low density lipoprotein (VLDL) cholesterol, non high density lipoprotein (HDL) cholesterol levels but enhanced the high density lipoprotein (HDL) cholesterol level. The complex PR decreased the levels of serum cholesterol, triglycerides, low density lipoprotein (LDL) cholesterol, very low density lipoprotein (VLDL) cholesterol to 139.92 ± 8.23 mg/dL, 210.1 ± 38.34 mg/dL, 81.0 ± 10.12 mg/dL, 30.0 ± 2.12 mg/dL and 112.0 ± 8.79 mg/dL, respectively while the reference drug rosuvastatin lowered the levels at 144.8 ± 9.12 mg/dL, 280.13 ± 40.25 mg/dL, 87.0 ± 12.10 mg/dL, 37.0 ± 3.23 mg/dL and 114.0 ± 9.23 mg/dL, respectively. The complex RV also decreased cholesterol, triglycerides, low density lipoprotein (LDL) cholesterol, very low density lipoprotein (VLDL) cholesterol 172.35 ± 10.12 mg/dL, 152.01 ± 41.45 mg/dL, 111.0 ± 10.11 mg/dL, 27.0 ± 3.32 mg/dL and 137 ± 8.32 mg/dL, respectively than the reference drug rosuvastatin did. The promising complex PV reduced the LDL and VLDL to 69.0 ± 10.65 mg/dL and 26.0 ± 4.13 mg/dL, respectively. But rosuvastatin as well as the three newly formed complexes PR, RV, PV increased HDL cholesterol levels to 30.34 ± 2.01 mg/dL, 28.33 ± 2.5 mg/dL, 34.9 ± 2.7 mg/dL and 49.44 ± 2.3 mg/dL, respectively than that of the control group of rabbits (12.48 ± 2.3 mg/dL).

In support of lipid lowering activity the antioxidant, thrombolytic and membrane stabilizing activities of the complexes PR, PV and RV were also evaluated *in vitro*. Three complexes showed better thrombolytic activity than rosuvastatin. Among the complexes, the RV demonstrated the highest thrombolytic activity ($29.52 \pm 0.09\%$) whereas PR, PV and rosuvastatin showed $26.39 \pm 0.06\%$, 20.97% and $20.96 \pm 0.09\%$ activities, respectively. The synthesized complexes PR, PV and RV displayed better antioxidant activity than the lipid lowering drug rosuvastatin. For free radical scavenging activity, the highest IC_{50} was produced by PV (67.71 μ g/mL) among all the samples followed by RV (56.83 μ g/mL), PR (54.79 μ g/mL) and rosuvastatin (131.6 μ g/mL). Three new complexes also were investigated for membrane stabilizing activity and showed significant effect. The rosuvastatin inhibited 39.92% hemolysis of RBCs followed by RV (35.18%), PR (26.55%) and PV (19.43%) in the condition of induced by hypotonic solution.

CHAPTER ONE

INTRODUCTION

CHAPTER ONE

INTRODUCTION

Drug discovery is a procedure that encourages to the commencement of a new drug into clinical therapy. Isolation from plants, synthesis, drug-drug and drug-metal complexations, structure-activity relationship analysis, combinatorial chemistry and computer aided drug design etc. help to find out new molecule as therapeutic candidate.

1.1. COMPLEXATION LEADS TO DRUG DISCOVERY

Complexation is the alliance between two or more molecules to form a nonbonded structure with a well-defined stoichiometry. It is the covalent or noncovalent interlinkage between two or more compounds that are competent of free existence. The ligand i.e. drug molecule is a particle that interacts with another fragment, the substrate, to form a complex. It also occurs between a metal ion and a molecular or ionic entity that carries at least one atom with an unshared pair of electrons. The complexation influences the structure activity relationship (SAR) which is the association between the chemical structure of a molecule and its biological activity. This allows moderations of the action or the power of a bioactive compound (typically a drug) by modifying its chemical structure. Complexation may change the action or the potency (i.e. activity) of drug.

This technique is applied in the chemical synthesis to place new molecules into the biomedical compounds and trail the alterations to mimic their efficacy or for different biological effects. Complexation of one drug with another drug or metal ion is a very prospective field of research in the agriculture, industrial chemistry, medicinal chemistry and pharmacology. The therapeutic applications of metal complexes with traditional drugs in the treatment of different diseases has been comprehensively studied (Borhade *et al.*, 2011; Habib *et al.*, 2011; Munde *et al.*, 2012; Sabastiyan *et al.*, 2012; Sheikshoaie *et al.*, 2012). Metal complex of respective drug may possess different modes of activities, allowing the evolution of metal complexes to offer a different route of novel drug delivery system (Kostova *et al.*, 2006). Recent researches with metal drug complexes have shown that joining a drug with metalloelement increases its therapeutic activity and in many areas the complex may have new activity that the respective parent drug does not possesses (Adekunle *et al.*, 2010). Thus, we motivated to study some drug-drug and drug-metal complexes and evaluated their biological properties.

1.1.1. Drug-drug interaction

Drug-drug interaction occurs while two or more drugs react with each other. When the effects of first drug (target drug) are changed by the co-administration of second drug (precipitant drug), food, drink, herbal medicine or other environmental chemical agents the interaction is claimed to happen. Two drugs are given together in the following cases (Brody, 2018):

- a) In a fixed drug combination (FDC) formulation in single dosage form two different drugs are physically complexed.
- b) Where package label requires the dispensed dosage form administration along with another new therapeutic agent, then the required drug is dispensed as a separate pill or capsule.
- c) Physicians prescribe method named off label uses, where the physician wants better control over the disease and agree in recommending two different therapeutic agents in case of same illness, thus the patient has to grab two drugs.

Drug interactions can have minimal undesired effects. The possibility of interactions rises with the number of drugs administered. Due to poly-therapy drug-drug interaction (DDI) is the most frequent reason for drug error especially for geriatric patients in developed countries with a prevalence of 20-40% (Caterina *et al.*, 2013). DDIs are classified under two major groups called pharmacokinetic drug-drug interaction and pharmacodynamic drug-drug interaction. Pharmacokinetic DDI implies absorption, distribution, metabolism and excretion behavior with drugs which may result in treatment failure and/or toxicity of the respective agent. Pharmacodynamic DDIs are classified under following further subgroups: (1) direct effect at receptor function, (2) involvement of a biological or physiological control process and (3) synergistic or antagonistic behaviors.

1.1.2. Drug-metal interaction

The therapeutic application and requisition of metals with chelate compounds is the emerging field both commercially and clinically. This growing economic and therapeutic discipline has been found in monographs, major reviews and dedicated volumes (Berthon, 1995; Clarke, 1989; Clarke, 1999; Farrell, 1989; Farrell, 1999; Fricker, 1994; Guo, 1999; Keppler, 1993; Orvig, 1999; Roat, 2002; Sadler, 1999). A

rational estimate for the whole field is approaching US\$5 billion yearly and made the field commercially important. A good example of the use of chelating agents is in the treatment of Wilson's disease which revealed how medical problems due to excess free metal ion [Cu(II)] may be improved (Sarkar, 1999).

1.2. SELECTION OF DRUGS AND METALS

In medical research different drugs are subjected to react with each other for the search of new therapeutic agent with better or different therapeutic potential. In this thesis three classes of drugs were selected namely antidiabetic drugs, antihypertensive drugs and lipid lowering drugs and made to interact with each other in search of new therapeutics. Chromium, lead, iron, copper and zinc were also selected as metals to do some interactions with some selected drugs.

1.3. DIABETES AND ANTIDIABETIC DRUGS

Hyperglycemia is the frequently occurring long-term illness as well as a major reason of fatality in developed and developing countries. According to a recent report it is evaluated that 382 million of people are suffering from diabetes mellitus (DM) and the number of diabetic patients will reach to 592 million by the year of 2035. Diabetes means combination of metabolic disorders about chronic hyperglycemia as a result of defective action of hormone insulin as well as improper secretion of the hormone, or either any one (Guariguata *et al.*, 2014). This results in metabolic disorders of macromolecules like carbohydrates, fat and protein, which leads to other fundamental problems as well as treatment resistant conditions like heart and kidney collapse. DM can be principally divided into two categories insulin dependent and insulin independent. First one progresses by the pathogenic action of T-lymphocytes on insulin-producing β -cells and a chronic autoimmune disease (Mandrup *et al.*, 2010). Insulin independent DM or Type 2 DM is of result from insulin opposing in combination with inappropriate secretion of the hormone and characterized by hyperglycemia (Guariguata *et al.*, 2014). Pathogenesis of Type 2 DM may be triggered by new lifestyle of modern societies, pathogenic elements, genetic factors etc. (McCarthy, 2010). To control hyperglycemia most of the Type 2 DM patients require complicated treatment procedures. Firstly, it requires the food intake alteration with physical exercise then leading to single agent treatment, double agent treatment, or multi-agent treatment which at the end may need hormone therapy in combination with or without oral

antidiabetic agents (Colberg *et al.*, 2010). Therefore, the stipulation for oral antihyperglycemic agents is elevated day by day and new products are regularly introduced.

In this thesis most commonly prescribed four antidiabetic agents were selected e.g. metformin, vildagliptin, glimepiride and dapagliflozin for the study of complexation. The structures of these antidiabetic drugs are given in Figure 1.1.

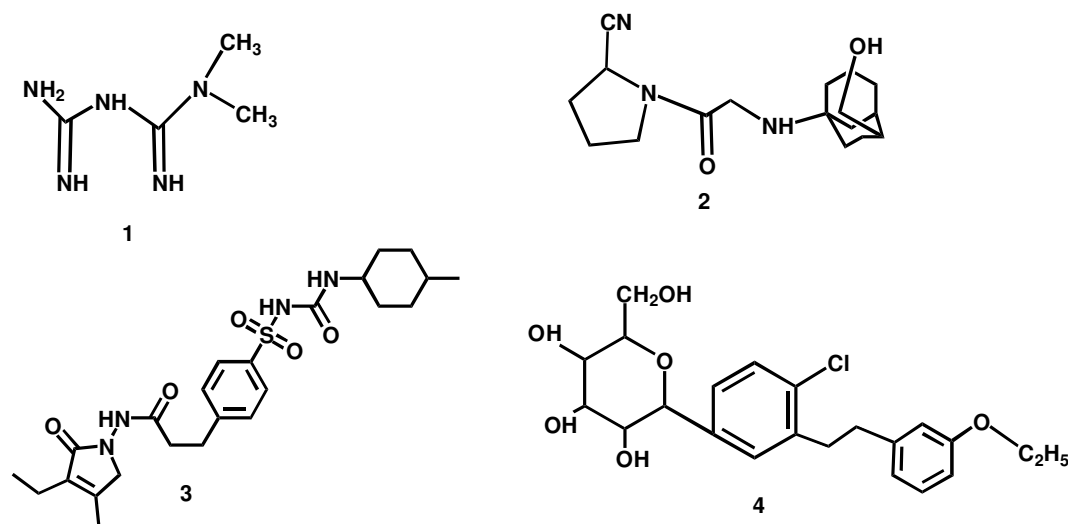


Figure 1.1. Structures of metformin (1), vildagliptin (2), glimepiride (3) and dapagliflozin (4).

1.3.1. Metformin

It is a drug of biguanide class used worldwide (Bailey, 1992; Williams and Palmer, 1975). For more than 50 years metformin is being employed to treat Type 2 DM. Along with diet and exercise it is considered as the major choice of treatment (Stumvoll *et al.*, 1995). It is an insulin secretagogue agent that work by reducing the amount of sugar from liver (i.e., reduced gluconeogenesis) (Alves *et al.*, 2014) by regulating flux of gluconeogenic, rather than straight stoppage of gene expression (Viollet and Foretz, 2013). As insulin sensitizer the drug reduces insulin resistance hence cells become able to use and absorb sugar more effectively. It also decreases the absorption of glucose in the intestinal mucosa as well as increases the utilization of glucose by skeletal muscle reuptake (Musi *et al.*, 2002) as shown in Figure 1.2. The exact mechanisms of action of metformin yet remain unknown though the research was done over 60 years (Ikeda *et al.*, 2000). The main priority of metformin over other biguanides is its very low accountability in producing lactic acid, however, its major disadvantage is adverse

gastrointestinal effects (Inzucchi *et al.*, 2012). Though it is considered as the primary choice for Type 2 DM patients, the drug is insufficient to reach glycemic control in many individuals and a second drug is needed for glycemic control (Ahren, 2008; Rendell, 2004).

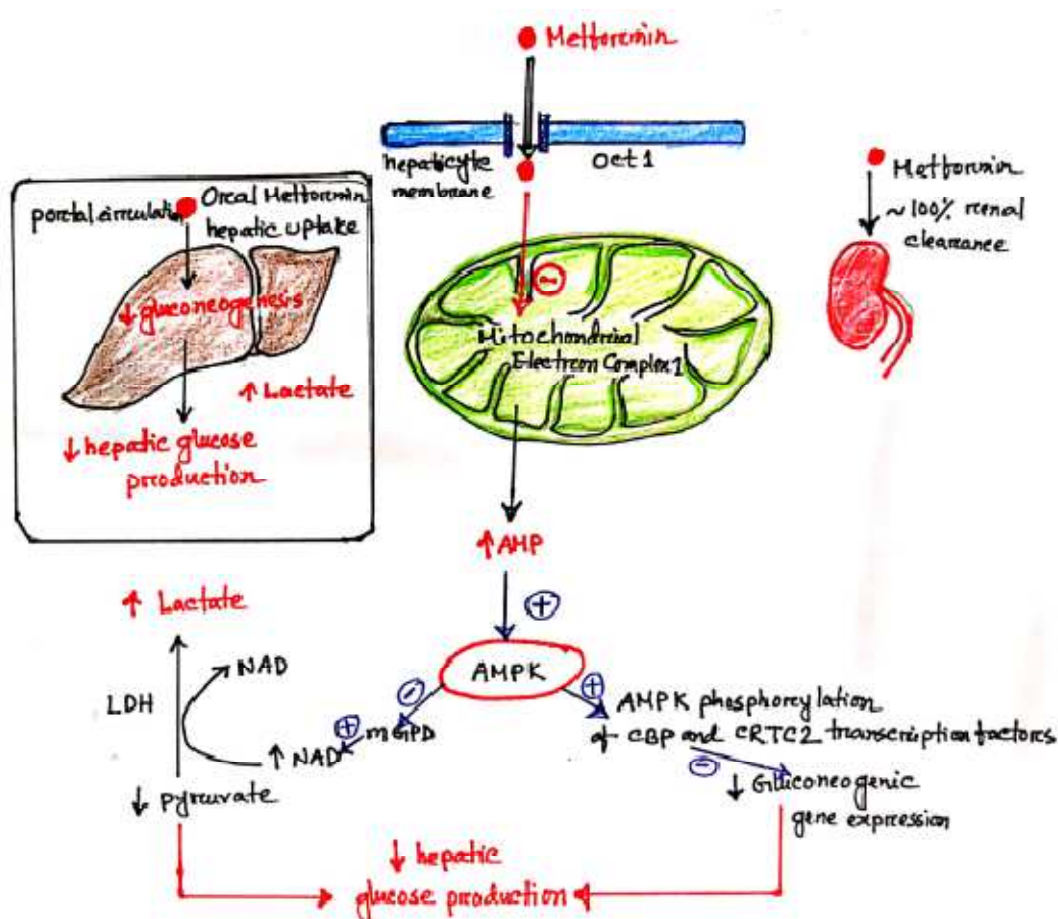


Figure 1.2. Mechanism of action of metformin (Pernicova and Korbonits, 2014).

1.3.2. Vildagliptin

Oral antidiabetic drug vildagliptin is incretin (an enzyme) enhancer and work by enhancing blood levels of the hormone glucagon-like peptide (GLP)-1 by suppressing the dipeptidyl peptidase Type 4 enzyme which deactivates GLP-1 (Drucker, 2007), as depicted by Makrilakis (2019) in Figure 1.3. Treatment with vildagliptin enhances β -cell sensitivity to glucose, by increasing insulin secretion irrespective to both postprandial and fasting glucose states. It also shows better α -cell function (rebuilding of appropriate glucose-related suppression of glucagon) resulting in decreased production of endogenous glucose in both postprandial and fasting periods. Prolonged

therapy with vildagliptin sometimes decreases fundamental degradation of β -cell activity in diabetic patients. Vildagliptin and metformin combination therapy may produce potential synergistic effect by enhancing active GLP-1 levels and can produce long-term advancements in pancreatic cell function in DM2 patients. Vildagliptin therapy also gives extra helpful pancreatic activity, such as increased peripheral insulin sensitivity and enhanced postprandial lipoprotein metabolism (Bellary, 2011). Improved β - and α -cell activity via incretin level improvement by vildagliptin gives better meal-related and fasting functional glycemic index (Mathieu, 2009).

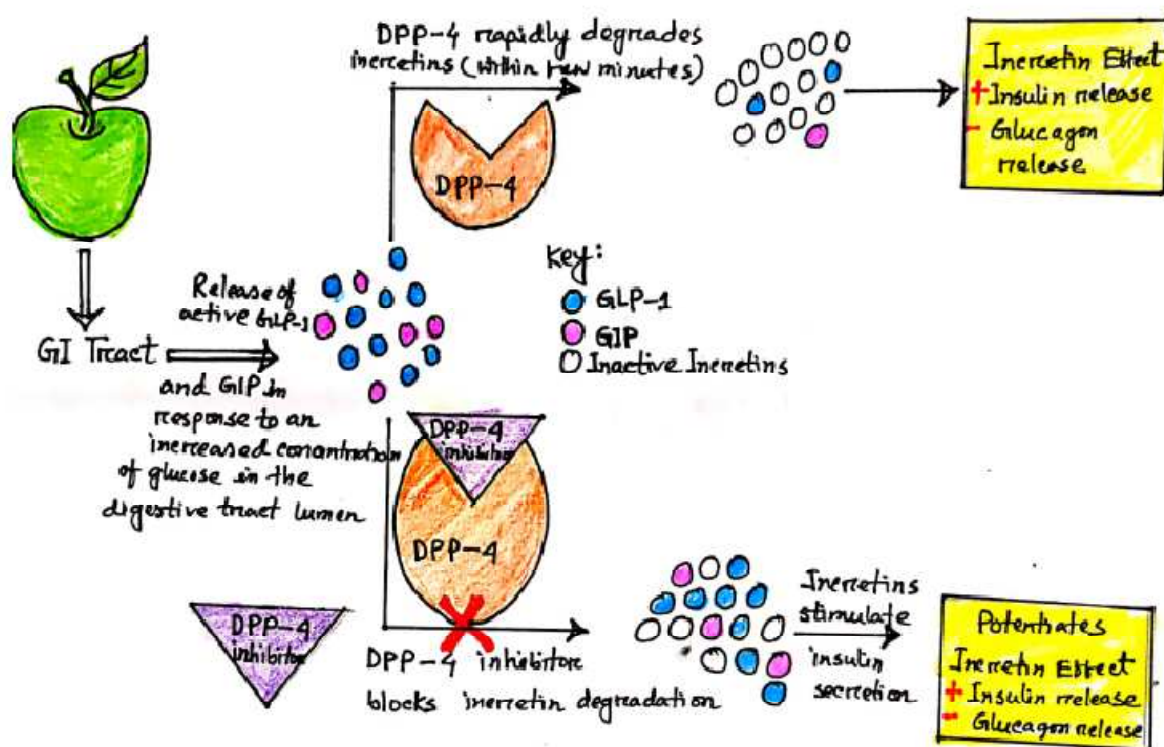


Figure 1.3. Mechanism of action of vildagliptin (Makrilakis, 2019).

1.3.3. Glimepiride

Some researchers consider glimepiride as a second generation (DeFronzo, 1999), and others as third generation of sulfonylureas (Tsunekawa *et al.* 2003). It performs secretagogue activity by triggering β -cell sulfonylurea receptor 1 (SUR 1), resulting shutdown of ATP-dependent potassium channels (Stumvoll *et al.*, 2005; Sturgess *et al.*, 1985). Stoppage of potassium movement produces depolarizations which unlock voltage gated calcium channels. Then entrance of extracellular calcium causes translocation of secretory granules to the cell surface and expulsion of insulin through exocytosis

(Ahren, 2011; Rorsman, 1997). Exocytosis causes merging of the secretory granule with the plasma membrane, resulting in the secretion of insulin into the extracellular space to enter the capillary blood flow (Lang, 1999; MacDonald *et al.*, 2005). Sulfonylureas have adverse effect of hypoglycemia, weight gain and hyperinsulinemia (Domecq *et al.*, 2015). The mechanism of action of glimepiride is shown in Figure 1.4.

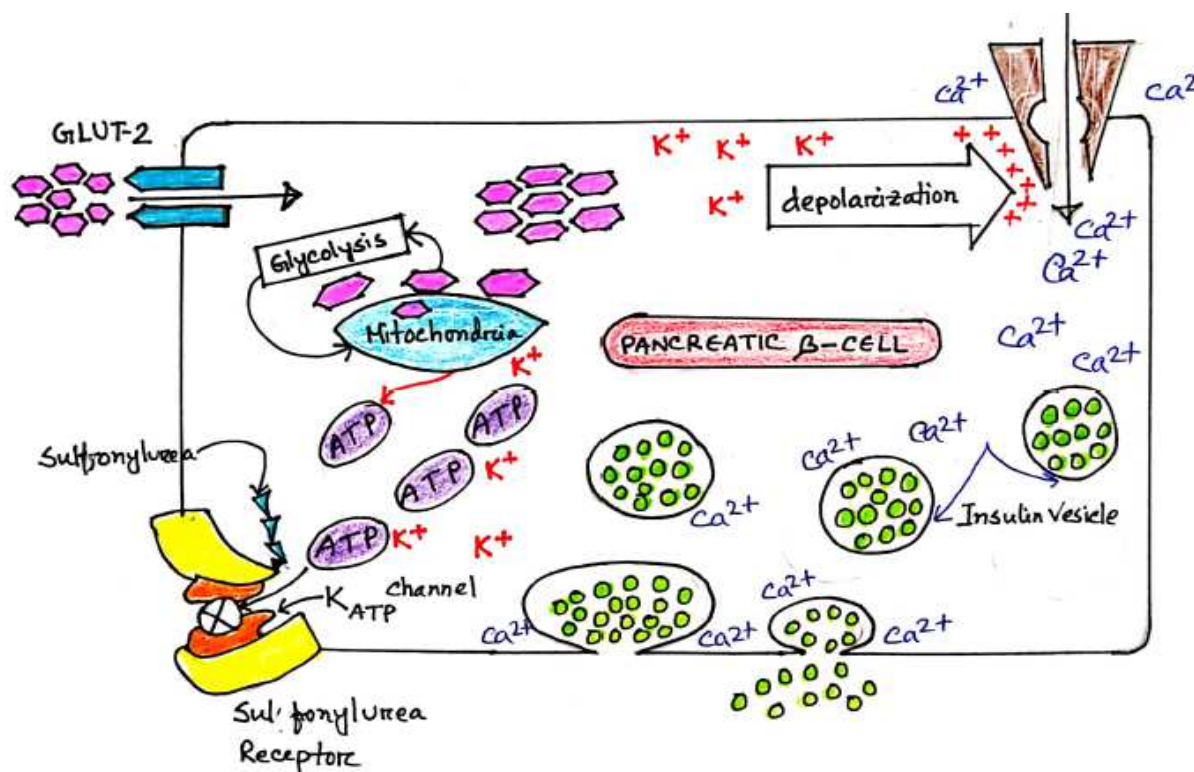


Figure 1.4. Mechanism of action of glimepiride (Al-Saleh *et al.*, 2021).

1.3.4. Dapagliflozin

Dapagliflozin is the Sodium-Dependent-Glucose-Co-Transporter 2 (SGLT2) inhibitor and was approved as therapeutics in adults with T2DM firstly by European Medicine Agency and secondly by the US Food and Drug Administration. It is resistant to β -glucosidase in the gut area justifying its oral dosage form. Dapagliflozin assists with urinary glucose excretion by decreasing tubular glucose reabsorption (Mather and Pollock, 2011). In a dose of 10 mg/day it will enhance glucose excretion in the urine of a T2DM patient by 50 -80 g/day (Plosker, 2012). The drug may be employed all alone to control hyperglycemia, or in combination with other antidiabetic drugs, like metformin (Schumm *et al.*, 2015). Mechanism of action of dapagliflozin is shown in Figure 1.5.

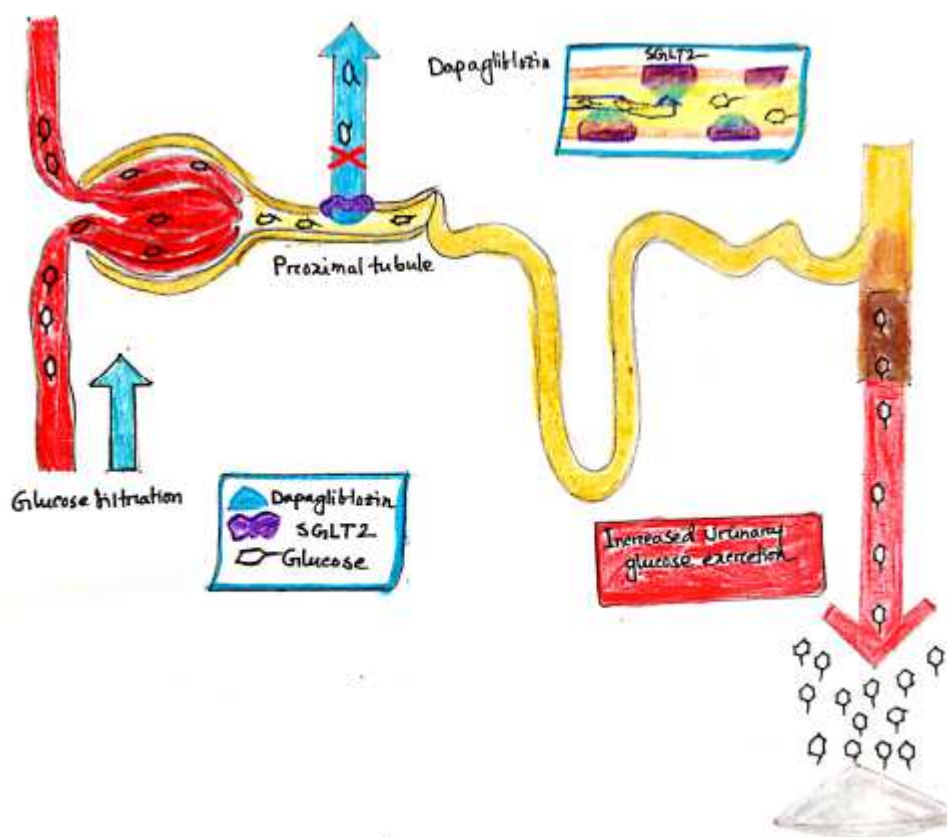


Figure 1.5. Mechanism of action of dapagliflozin (Van Bommel *et al.*, 2017).

1.4. HYPERTENSION AND ANTIHYPERTENSIVE DRUGS

Worldwide hypertension is the disease affecting an estimated one billion people (Ferro *et al.*, 2006). Hypertension is one of the major causes of stroke, congestive heart failure and coronary artery disease. Though different therapeutic tools and techniques are available, a large number of people do not get their required goal of treatment. Possible cause of this inadequate treatment may be the abnormality in keeping the target blood pressure goal. Recent advancement in knowledge related to hypertension and comorbidity resulted in reaching the blood pressure goals stricter (Krum and Gilbert, 2007). Structure of two antihypertensive drugs studied in the research is shown in Figure 1.6.

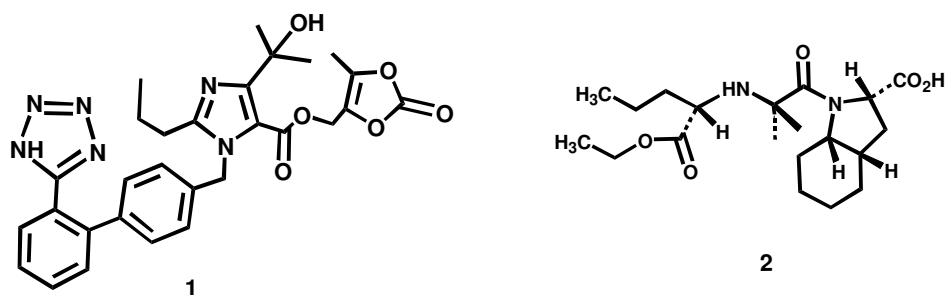


Figure 1.6. Structures of two antihypertensive drugs Olmesartan medoxomil (1), perindopril erbumine (2).

1.4.1. Olmesartan medoxomil

The ester prodrug olmesartan medoxomil is readily hydrolyzed by an enzyme, aryl esterase *in vivo* (Mire *et al.*, 2005). The prodrug has 100,000 times higher specificity for the AT1 (Type 1 angiotensin II) receptor than it has for the AT2 (Type 2 angiotensin II) receptor and inhibit the vasoconstricting as well as aldosterone releasing capacity of angiotensin (II) but without affecting the vasodilatation activity occurring by AT2-type receptor activation. This receptor selectivity in combination with binding affinity makes olmesartan unbeatable among commercially available angiotensin II Type 1 receptor blockers, (ARBs) (Mire *et al.*, 2005). Mechanism of action of olmesartan medoxomil is shown in Figure 1.7.

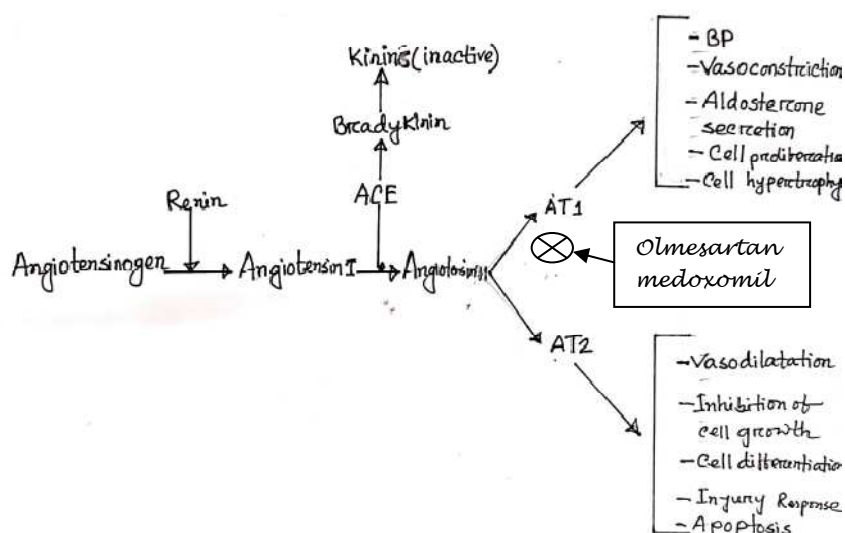


Figure 1.7. Mechanism of action of olmesartan medoxomil (Bevilacqua *et al.*, 2019).

1.4.2. Perindopril erbumine

Early 1980s discovered perindopril is a major Angiotensin Converting Enzyme (ACE) inhibitor. After extensive research it is now finalized for use as therapeutic agent for a range of patients suffering from hypertension to complex cardiovascular complications. The drug is among the latest generation of ACE inhibitors and can give day long activity by single dose administration. The drug can exhibit both blood pressure lowering activity as well as cardiovascular protecting activities and the morbidity and/or mortality of the drug is shown in Figure 1.8. The drug also exhibits better tolerability like reduced occurrence of cough and truanting of first-dose hypotension (Ferrari *et al.*, 2005).

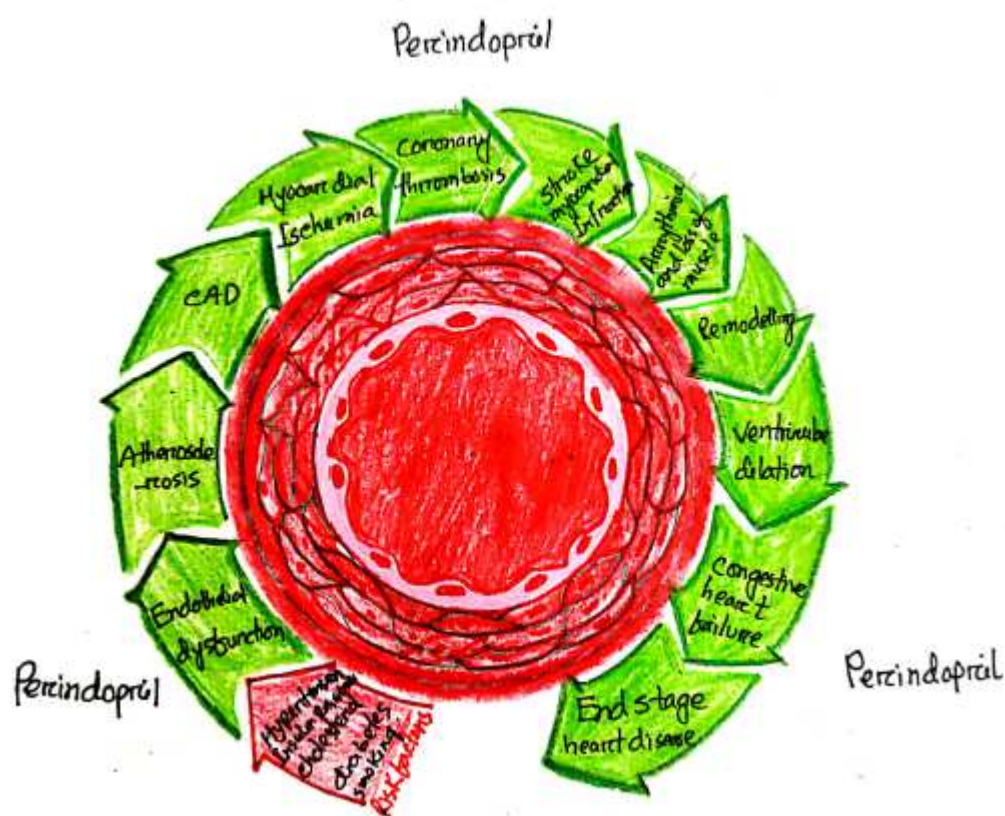


Figure 1.8. Investigation of perindopril on morbidity and/or mortality, modified from Dzauet *al.*, 2006.

1.5. HYPERLIPIDEMIA AND LIPID LOWERING DRUGS

Abnormal elevation of serum lipid levels in the blood, i.e., hyperlipidemia results in the development of atherosclerosis (Grundy, 1984). Atherosclerosis is the disease of hardening of arterial wall and may be resulted into myocardial infarction, ischemic stroke and peripheral vascular disease (Herrington *et al.*, 2016). Globally, due to high cholesterol level one-third of ischemic heart disease is resulted, which cause approximately 2.6 million death and 29.7 million disabilities (World Health Organization, WHO, 2017). Statin drugs [3-hydroxy-3-methylglutaryl-coenzyme A (HMG-CoA) reductase inhibitor] are very efficient in handling dyslipidemia. Therefore, these drugs are widely applied as prophylactic as well as therapeutic agents in cardiovascular complications (Sugiyama *et al.*, 2005). They reduce the synthesis of mevalonate, a product of HMG-CoA mediated reaction, and thus statins inhibit the synthesis of cholesterol (Rikitake and Liao, 2005).

In our research work, we used two lipid lowering drugs, rosuvastatin and atorvastatin calcium for the study. The structures of the drugs are given in figure 1.9 and mode of action is depicted in Figure 1.10.

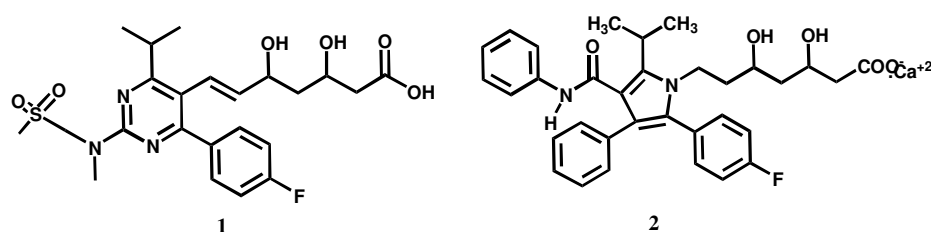


Figure 1.9. Structures of rosuvastatin (1) and atorvastatin calcium (2).

1.5.1. Rosuvastatin

Rosuvastatin [Figure 1.9(1)], the HMG-CoA reductase inhibitor is fully synthetic drug. The inherent statin moiety as well as a unique polar group, methane-sulphonamide present in rosuvastatin gives high hydrophilicity as well as increased electrovalent bonding to HMG-CoA reductase enzyme resulting in improved drug-enzyme interactions [AstraZeneca Pharmaceuticals Ltd., 2003; McTaggart, 2003; White, 2002]. The drug binds with the enzyme HMG-CoA reductase selectively and reversibly and

diminishes of the activity of enzyme in competitive way. The enzyme converts HMG-CoA to mevalonic acid, an important and major reaction in cholesterol biosynthesis. Therefore, this statin drug lowers biosynthesis of cholesterol leading to a decreased accumulation of hepatocellular sterol which is shown in Figure 1.10. In response to diminished intracellular sterol, hepatocytes increase LDL entrapment receptors for removal of LDL from hepatic circulation by LDL reuptake mechanism. Consequently, higher fractional catabolism of LDL decreases blood LDL-C availability and total sterol concentration (Buckett *et al.*, 2000; Istvan and Deisenhofer, 2011). The drug also lowers the production of ApoB (Apolipoprotein B) resulting in decreased hepatic production of very low-density lipoprotein cholesterol (VLDL-C) as well as triglycerides (Arad *et al.*, 1992).

1.5.2. Atorvastatin calcium

Atorvastatin belongs to statins group. It ambitiously depresses HMG-CoA reductase. By inhibiting the enzyme, the drug decreases the cholesterol production in liver (Figure 1.10). The drug slows down the synthesis of cholesterol to decrease the development of cholesterol on the walls of the arteries. When a patient has high blood cholesterol (Robert *et. al.*, 2003) the drug is prescribed. As a prophylactic the drug is also recommended in heart attacks and strokes.

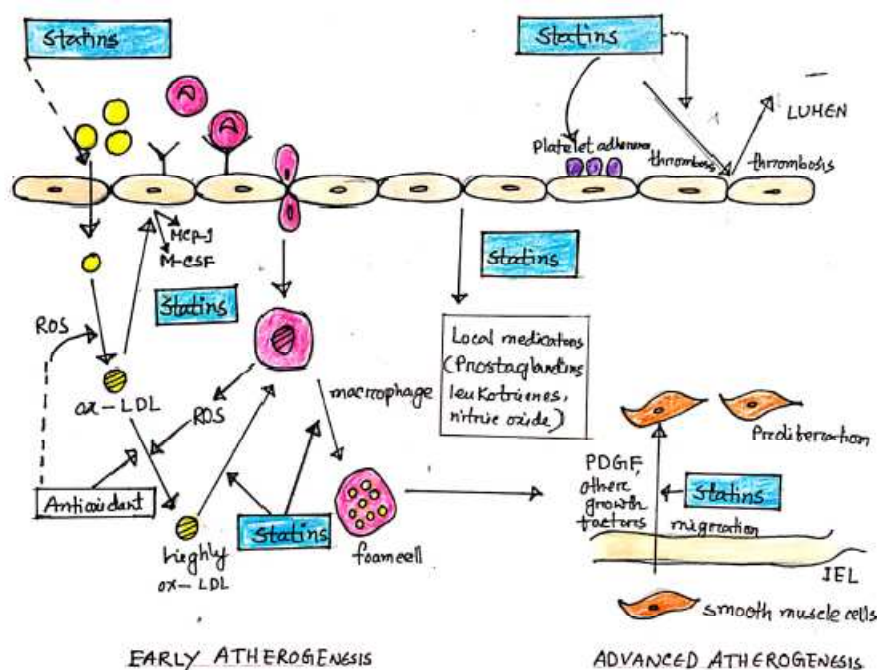


Figure 1.10. Mechanism of action of statins (Stancu and Sima, 2001).

1.6. METALS AND DRUG METAL COMBINATION

Metal-ligand interactions is a major field of medicinal chemistry especially in drug design and this is evident by two major groups of drugs, which are metallodrugs and metalloenzyme inhibitors (Mjos and Orvig, 2014; Meggers, 2007). After the recognition of antineoplastic properties of the cisplatin (cis- diamminedichloroplatinum) in 1965 (Rosenberg *et al.*, 1965), many others platinum- containing drugs have been synthesized, originated and applied for the treatment of cancer (Johnstone *et al.*, 2016; Kelland, 2007). Ruthenium-based complexes serve as prominent inhibitors of protein (Dorr and Meggers, 2014; Dyson and Sava, 2006; Hambley, 2007). Metallodrugs give enzymatic, oxidation-reduction and photosensitive characteristics *in vivo* in tagging as well as degrading proteins (Barry and Sadler, 2013; Haas and Franz, 2009; Sasmal *et al.*, 2013; Soldevila and Sadler, 2015). Therefore, the metal-drug combination and the mode of activity of this class of drug are at the heart of the inorganic chemistry research.

1.6.1. Chromium (III)

Chromium (Cr) having atomic number and relative atomic mass 24 and 52.996 g/mol respectively, is a transition metal of silvery white color (Zohdi *et al.*, 2012). The metal is brittle inherently which confirms its range limit (lower than 30-40% by weight) of content in market alloy preparations. It makes an unreactive oxide shield on the surfaces of the alloy elements to protect from oxidizing agent. A major amount of chromium is used in different alloy industries releasing harmful pollutants to contaminant breathing air and water sources (Bielicka *et al.*, 2005). For human beings, trace elements are essential and display a variety of functions e.g regulatory, catalytic, immune etc. as reported by Stoecker (1996). Chromium (Cr) was first identified to be essential for animals by Schwart and Mertz (1959). Total body stores of Cr vary between 0.4 mg and 6.0 mg according to literature. Relative to body size chromium stores may be different in neonates than in adults (Dubois and Belleville, 1991). The physiological level of Cr in human is 0.2-0.5 µg/L (Schermaier *et al.*, 1985). Transition element chromium can exhibit different valence's, among them Cr(III) is more stable and essential form but Cr (VI) performs as oxidant and is a potent carcinogen. Organic Cr is a part of a complex called "glucose tolerance factor" (GTF-Cr-nicotinic acid complex) and is better than inorganic Cr for digestive absorption. In the body, Cr (III) is better absorbed than Cr (VI) and Cr(VI) is readily converted to Cr(III) by a number of metabolic pathways

(Dubois and Belleville, 1991). Intestinal absorption of Cr(III) is low, approximately 0.5-3%, and amino acids, nicotinic acid and oxalate may accelerate its absorption. Chromium is mainly bound to transferrin in blood, but albumin and apo transferrin are also responsible for normal Cr transport. Chromium is accumulated in liver, spleen, soft tissues and bone in human. Most absorbed Cr [about sixty percent Cr(VI) and ten percent of Cr(III)] is eliminated from body by two kidneys (Under, 1991). Furthermore, little amount is excreted by other organs like hair follicles, nail extensions, milk glands, and skin. Chromium forms protein complex after binding with proteins inside the body. Other than chromium-protein complex the metal is also found in hepatic tissues, nephrotic tissues, lungs, spleen, lymph nodes and bone marrow but majority of concentration remains in the lung cells (ATSDR, 2012). Chromium (III) is found to form strong complex with nucleic acids which is thought to immune RNA from denaturation induced by heat (Pechova and Pavlata, 2007). The recommended and safe level of Cr dietary allowance remains at 50-200 µg/day but actual needs are still unknown. The adequate dietary Cr intake is normally below this lower range in many people. Some abundant sources of Cr are brewer's yeast, nuts, whole-grain cereals, corn oil, raisins, honey, grapes and refined cereal foods (Dunne and Kirschmann, 1990; Harrison *et al.*, 1994). Typically, about 100 µg of dietary chromium come from food sources like egg yolk, mushrooms, sea foods, potatoes, vegetables and fruits and grains (Bielicka *et al.*, 2005; Stoecker, 1996). Moreover, moderate to small amount of chromium also may come out from different vitamin supplements as well as oral anti-diabetic medicines (Bielicka *et al.*, 2005; Anderson, 1981).

Chromium is a necessary transition metal essential for metabolism of polysaccharides as well as fats (Anderson, 1993; Anderson, 1995; Mertz, 1993). Documented cases of Cr insufficiency have been found in a number of situations, where patients consuming usual normal diets were diagnosed with increased blood glucose, cholesterol, triglycerides as well as lower level of high density lipoproteins (HDL). Much prominent Cr deficiency symptoms have been reported for patients on total parenteral nutrition (TPN) having nerve and brain disorders (Jeejeebhoy *et al.*, 1977; Freund *et al.*, 1979; Brown *et al.*, 1986). The situation for TNP patients can be recovered by providing Cr supplement. Now, a days Cr is intentionally adjusted to TPN solutions (Anderson, 1995).

1.6.1.1. Necessity of chromium

The nutritional importance of chromium was recorded in 1977 (Jeejeebhoy *et al.*, 1977) when a woman receiving TPN was diagnosed with prominent hypoglycemic symptoms. The female patient was also observed for weight loss along with glucose intolerance and neuropathy though she was treated with 50 units/day of exogenous insulin, before Cr supplementation. The patient's side effects were diminished when 200 mg of chromium chloride was added to her TPN solutions as chromium supplement for 3 weeks and exogenous insulin treatment was no longer needed. The case was established and recorded many times in the research journals and articles on several issues (Freund *et al.*, 1979; Brown *et al.*, 1986). Necessary uses of chromium are not confined to patients receiving TPN. Moreover, aged people, children, patients with Type 1 and 2 diabetes mellitus (DM) as well as peoples with low blood sugar all categories showed beneficial effects after getting Cr supplement. Besides human, chromium treatment has shown beneficial results in horses, cattle, pigs, fish, rabbits, guinea pigs, squirrel, monkeys, mice and rats (Anderson, 1993; Anderson, 1995; Mertz, 1993).

1.6.1.2. Chromium requirement in peoples with diabetes and glucose intolerance

Chromium supplements prove to effectively regularize the function of insulin in patients having hypoglycemia as well as enhance the efficiency of the hormone insulin. Supplemental Cr also exerts benefit towards regularization of the glucose concentrations more promptly in patient with glucose intolerance in comparison to non-supplemented patients (Anderson *et al.*, 1987). The amount of Cr requirement is connected with the degree of glucose intolerance which was described by Anderson *et al.* (1991) from an experimental study where subjects were given low Cr diets. The experiment in subjects with good glucose tolerance showed that consumption of less than 20 mg of Cr daily by normal food diets showed insignificant alterations in the glucose and insulin variables, but consumption of the same diets by diabetic subjects (90-minute glucose values greater than 5.56 mmol/L) showed enhanced blood glucose level. The experiment also revealed that insulin levels can be reversed by giving the diabetic subjects a chromium supplement of 200 µg/day as Cr chloride.

1.6.1.3. Chromium level connectivity with fats and lipids

Besides improving the blood glucose tolerance and insulin efficacy chromium supplementation also showed positive results in minimizing blood lipids in experimental

non-diabetic subjects. To give a positive result in maintaining low lipid profile it may take several months (Anderson, 1995). The rate of improvement of chromium supplement in lowering lipid profile is higher in peoples with enhanced blood lipids.

1.6.1.4. Chromium and diabetes

It is evident that chromium picolinate as Cr supplement in people with Type 2 diabetes mellitus improve glucose tolerance and lower lipid levels at a dose of 200 µg/daily (Evans 1989; Ravina *et al.*, 1995). Moreover, at a supplement dose of 1000 µg/day better effect was observed (Anderson 2000; Anderson *et al.*, 1997). Same was observed in case of gestational diabetes in women where better result was found at a dose of 8 mg/kg body weight than 4 mg/kg as Cr picolinate (Jovanovic *et al.*, 1995).

1.6.1.5. Chromium: mechanism of activity

In response to enhanced number of insulin receptors chromium increases insulin binding to cells (Anderson *et al.*, 1987; Anderson, 1998). The number of insulin receptors varies from cell to cell like as more than 200,000 receptors are found in adipocytes-hepatocytes but only 40 receptors are found in erythrocyte cells (Saad, 1994). Structurally insulin receptors have two extracellular subunits called alpha subunits with a molecular weight of 135,000 D as well as two trans-membrane subunits called beta sub-units with a molecular weight of 95,000 D (Kahn, 1985). An antifungal agent Wortmanin work to suppress the enzyme phosphatidylinositol 39-kinases; by doing this the agent ultimately depress the activity of insulin-dependent cells as insulin stimulation activity is inhibited (Okaka *et al.*, 1994; Kanai *et al.*, 1930). When the hormone insulin binds with the alpha subunit of the insulin receptor phosphorylation of the beta subunit is done through a cascade of intermolecular phosphorylation reactions (Saad, 1994; Kahn, 1985; Roth *et al.*, 1994). The enzyme tyrosine kinase (which is partly responsible for the phosphorylation in insulin receptor) is stimulated through Cr bindings, leading to enhanced insulin sensitivity (Davis and Vincent, 1997). The evidence revealed that as like the hormone insulin chromium also have some activity in phosphorylation-dephosphorylation reactions of proteins.

In the absence of insulin Cr binding does not affect the protein kinase activity of rat adipocytes but in the presence of insulin Cr binding stimulates kinase activity 8-fold. A loss of kinase potentiating activity resulted when from bonded Cr is removed from low molecular weight Cr binding compound (Davis and Vincent, 1997). Therefore, Cr exerts

its effect by triggering the kinase enzyme present in insulin receptor as well as by suppressing the tyrosine phosphatase present in insulin receptor, through mediating higher phosphorylation of insulin receptor resulting more insulin hormone activity (Saad, 1994; Kahn, 1985; Roth *et al.*, 1994).

1.6.1.6. Safety of supplemental chromium

Cr (III) commonly present in different food stuffs as well as mineral supplements and is rendered as last toxic mineral. This conventional amount of nontoxic daily intake contains a relatively higher safety margin for Cr(III) in comparison to other minerals and nutrients. The ratio of the reference dose to the RDA is found 350 for chromium, in comparison to zinc which is < 2 and for manganese it is roughly 2 whereas for selenium it is found 5 to 7 (Mertz *et al.*, 1994). There was no evidence of toxicity and no reported dangerous side effect is found in any of the human studies relating Cr as supplement.

1.6.2. Lead(II)

An issue of consideration is the dramatic increase in Type 2 diabetes in developed countries due to exposure of the population from industrial chemicals, wastages and contaminants. With the increase in exposure levels of many industrial contaminants and toxicants different fatal incidence of diseases have also been elevated. Few of the metalpollutants have been found to interfere with different biological reactions *in vivo* to create damaging metabolic and/or endocrine effects. These notorious chemicals are called endocrine disrupting chemicals (EDCs). Investigations regarding these EDCs and risk of diabetes have given positive correlation (Song *et al.*, 2016). The metals with unknown role in human physiology are considered as xenobiotic which are important class of environmental chemicals. Some of these xenobiotics (e.g lead, mercury, cadmium and the metalloid arsenic) are known to cause human health hazards. Few of these xenobiotics exert detrimental effects on patophysiology leading to incidence of diabetes and other related metabolic disorders (Afridi *et al.*, 2008; Bener *et al.*, 2001; Cave *et al.*, 2010; Chen *et al.*, 2009; Chen *et al.*, 2007; Kolachi *et al.*, 2011; Moon 2013; Padilla *et al.*, 2010; Zhai *et al.*, 2017). In this regard, lead is of a particular issue. Though overall limits of lead exposure have decreased in current decennary, in certain sectors of the population there is a persistent but under-recognized incidents of exposure of this metal. By accidental ingestion of lead-based paint in childhood then in adults by sporadic exposure of lead from contaminated drinking water and others accounts for a

vast number of the peoples for exposure of lead at low concentration. The accumulation of lead in brain induce injurious pathologies and it is well documented (Ris *et al.*, 2008; Searle *et al.*, 2014; Surkan *et al.*, 2007), but little data are available for the correlation of lead exposure and chronic metabolic disorder, diabetes. The correlation of incidence of diabetes in exposure to lead should be reviewed by considering some other underlying diabetes causing factors like other metabolic, food habit, lifestyle and environmental stress factors (Joshu *et al.*, 2008). The detrimental effects of lead may be found in more cases in the underprivileged commercial city peoples than observed elsewhere. There are very little data specifically designed for examination of the effect of low level of lead on prognosis of diabetes are available, though there are considerable epidemiological results exist for the presence of low levels of various influencer xenobiotics for evolution of chronic metabolic disorder like diabetes (Jones *et al.*, 2008). Kolachi *et al.* (2011) reported that the concentration of lead is higher in blood, hair and urine sample of diabetic female patients in comparison to non-diabetic subjects. Similarly, cadmium and arsenic were also found at elevated concentration in the diabetes group and make a difficulty in assigning particular role of lead xenobiotics in diabetes evolution (Kolachi *et al.*, 2011). From an earlier study with factory workers in the United Arab Emirates remarkable pragmatic association was noticed between blood lead levels and fasting blood glucose. The study resulted that there is a possible link between low level of lead and diabetes. The experiment also established a correlation between presence of lead and blood pressure (Bener *et al.*, 2001). Numerous experiments have found the consequences of higher values of metal concentration in biological samples to disrupt the function of endocrine gland pancreas (Chen *et al.*, 2009). Although lead was not separately analyzed in these studies, together they suggested adulterous effect of metal on the function of endocrine pancreas. The form of fatty liver without association of excessive alcohol consumption is known as NAFLD (non-alcoholic fatty liver disease) and is coexisted with Type 2 diabetes. Existence of NAFLD is a reasonable predictor of Type 2 diabetes as about 70% of diabetic patient also have NAFLD (Targher *et al.*, 2007; Williamson *et al.*, 2011). Studies with lead industry workers revealed that there is a gentle connection with high blood lead levels with blood pressure (Weaver *et al.*, 2008) and kidney function (Weaver *et al.*, 2003; Weaver *et al.*, 2005; Weaver *et al.*, 2009).

1.6.2.1. Mechanism of lead to induce diabetes

One possible mechanism of lead induced diabetes is by increasing oxidative stress in biological systems (Matovic *et al.*, 2015). Reactive oxygen species (ROS) inhibit the insulin signaling pathway thus promote the genesis of diabetes and insulin resistance (Fridlyand and Philipson, 2006). Oxidative stress should be considered in the progress of lead-attributed disorders, even with populations having comparatively lower environmental exposure to lead (i.e., <10 $\mu\text{g/dL}$). Firstly, lead alters the fat compositions of membrane, developing a minimization of phosphatidyl choline and a maximization in arachidonic acid resulting in enhanced susceptibility to lipid peroxidation (Knowles and Donaldson, 1990; Lawton and Donaldson, 1991). Secondly, Pb^{++} by binding to oxyhemoglobin stimulates superoxide formation (Ribarov and Benov, 1981; Ribarov *et al.*, 1981; Ribarov and Bochev, 1982). Third, the enzyme involved in the biosynthesis of heme is porphobilinogen synthase which has prominent responsiveness to Pb^{++} ion concentration. Finally, binding with sulfhydryl groups or selenocysteine, lead ion lowers the concentration of two enzymes super oxide dismutase (SOD) and glutathione peroxidase (GPx) and thus lower the antioxidant activities of cells (Ercal *et al.*, 2011; Howard, 1974; Othman and El Missiry, 1998). Pb^{++} ion and Ca^{++} ion have similar types of electronic configuration. Major cases of lead ion mediated toxicity are evolved from interference of this toxic metal ion with variety of calcium ion mediated intracellular processes. Pb^{++} hampers with calcium mediated homeostasis and cellular reuptake by competitively binding at the same binding sites where Ca^{++} binds at pM concentrations, thus Pb^{++} enhances the level of resting intracellular Ca^{++} ions from approximately 100 nM to 200 nM (Schanne *et al.*, 1989).

1.6.2.2. Risk of lead in provoking diabetes

Studies were performed using subjects with high blood lead values (14-74 $\mu\text{g/dL}$) (Mostafalou *et al.*, 2015; Whittle *et al.*, 1983) and compared with human alarm level of 5 $\mu\text{g/dL}$ supported the hypothesis that from high to low level of lead presence in blood, probably in association with other metabolic stress conditions, lead stimulates the evolution of diabetes. Early life lead exposure might have physiological effects later in life and the statement was documented by the experiments in humans and mice. The possibility of Pb^{++} exposure resulted in particular epigenetic marks in the genome may continue throughout life and even over generations. This can give a clear mechanistic

pathway for how a limited exposure to lead might have a life-long health consequence.

1.6.3. Iron(II)

Cellular iron retention has been resulted in systemic oxidative stress, vascular inflammation and atherogenesis. Statins decrease levels of ferritin in patients with advanced CVD (DePalma *et al.*, 2003; DePalma *et al.*, 2006; DePalma *et al.*, 2010), renal disease (Sirken *et al.*, 2003) and diabetes (Ukinc *et al.*, 2009). Data from a randomized trial of iron (ferritin) reduction in participants with advanced peripheral arterial disease showed significant improvement (Zacharski *et al.*, 2011). Iron reduction may provide an alternative to statins for reducing inflammation associated with atherosclerosis is evident.

1.6.4. Copper(II)

Copper plays significant biochemical role in two ways: firstly as a crucial trace metal and as secondly as a constituent of different exogenously delivered complexes in human. As a trace metal it binds to ceruloplasmin, albumin and other proteins, while as exogenous compound it binds to different varieties of ligand compounds to react with large macromolecules, like proteins and nucleic acids. The significant role of copper in human diseases has been documented in medicinal-chemical (Brewer, 2009) and a biochemical view (Daniel *et al.*, 2004) considering the molecular physiology of Cu transport (Puig and Thiele, 2002). Major of which related to copper homeostasis (Balamurugan and Schaffner, 2006) and its collaboration to iron metabolism (Arredondo and Unez, 2005). The role of copper in major biological processes is resulted in different types of change in human physiology and pathology (Crisponi *et al.*, 2010; Uriu-Adams and Keen, 2005). A very few review studies have been found to emphasize on the various biochemical events which could be straightly affected from the use of copper complexes as medicine.

1.6.5. Zinc(II)

Zinc is one of the transition metals of the first and second series of periodic table such as Na, K, Mg and Ca, and is essential for human physiology. After iron, zinc is the second mostly available trace element in the human body. About 3 g of zinc is found in

an average adult through daily intake of 8-11 mg and mostly are localized in testicles, muscles, liver and brain (<https://ods.od.nih.gov/factsheets/Zinc-HealthProfessional>). Zinc is essential for improving the life span of cell as well as protecting tissues from necrosis. Through a specific homeostasis mechanism, a concentration of 0.6 mM of Zn is maintained in the body, a deficiency of zinc or excess amount of zinc can result in toxicity in organisms (Crichton, 2019; Finney and O'Halloran, 2003; Turel and Kljun, 2011). Deficiency of zinc may be resulted from insufficient availability of zinc in the body due to total nutritional or absorption problems, ageing, excessive losses of Zn from the body or problems in zinc homeostasis. Deficiency of zinc may compromise immunity functionality in the body because zinc exerts a vital role through functioning in cellular proliferation, RNA and DNA synthesis as well as T-lymphocyte evolution. Deficiency can further show some other problems like retardation of growth, impotence and hypogonadism. However, excess zinc, is less frequent and frequently happens via excess-supplementation. A persistent excess Zn supplement (e.g., myeloneuropathy) results in toxicity through the suppression of copper absorption and leads to a zinc-mediated copper insufficiency (Tatineni *et al.*, 2020).

1.7. INTERACTION OF PROTEIN WITH DRUGS FOR SYNTHESIS NEW COMPLEXES

In proteins, not all but only three aromatic amino acids namely phenylalanine, tyrosine and tryptophan are fluorescent. A prominent intrinsic fluorophore is tryptophan which is present at a concentration of 1 mole-percentage in proteins. When foreign compound like drug molecule or other complexes bind with natural protein, the fluorescence property of protein usually alters in association with the concentration of foreign compounds (Suryawanshi *et al.*, 2016). The change in fluorescence properties is called fluorescence quenching or fluorescence dequenching and measurement of this quenching or dequenching is the major tool in quantification of binding affinity of foreign body (i.e ligands) towards proteins. Fluorescence quenching is the decrease in measurement of fluorescence of uninterrupted natural protein in presence of external fluorophore by a series of molecular interactions. Fluorescence quenching may be dynamic or static depending on how the quencher molecules interacted with the protein (Amin *et al.*, 2016). When fluorophore is quenched in ground state by quencher then it is called static quenching but when the quencher react with fluorophore in excited state the quenching is called dynamic (Fraiji *et al.*, 1992).

1.8. OBJECTIVES OF THE PRESENT WORK

Since drug-drug and drug-metal interactions are important topics of research in drug discovery as well as pharmacodynamic actions of the drugs, and drug-drug and drug-metal complexation may introduce new molecules having new and/or more therapeutic properties in our body. Therefore, it was our main objective to synthesize new molecule possessing more potent therapeutic values by drug-drug and drug-metal interactions. In quest of new therapeutic possibilities, many biological parameters were also investigated by *in vitro* and *in vivo* analyses.

So, chemical investigations were done for five groups of newly synthesized complexes like, (i) to synthesize new complexes from antihypertensive drug olmesartan medoxomil with three antidiabetic drugs viz. dapagliflozin, vildagliptin and metformin hydrochloride (olmesartan-dapagliflozin complex, OD; olmesartan-vildagliptin complex, OV and olmesartan-metformin complex, OM), (ii) to synthesize complexes from antihypertensive drug perindopril erbumine with antidiabetic drug vildagliptin (perindopril-vildagliptin complex, PV), with lipid lowering drug rosuvastatin (perindopril-rosuvastatin complex, PR) and rosuvastatin-vildagliptin complex RV, (iii) to synthesize four chromium(III) metal complexes with four antidiabetic drugs, viz, complexes with metformin hydrochloride (Cr-met), dapagliflozin (Cr-dapa), vildagliptin (Cr-vilda), glimepiride (Cr-glim), (iv) to synthesize four lead(II) metal complexes with four antidiabetic drugs namely complexes with metformin hydrochloride (Pb-met), dapagliflozin (Pb-dapa), vildagliptin (Pb-vilda), glimepiride (Pb-glim), (v) to synthesize three metal (Fe, Cu, Zn) complexes with lipid lowering drug atorvastatin calcium trihydrate viz. Fe-atorvastatin, Cu-atorvastatin and Zn-atorvastatin. After synthesis the new drug-drug and drug-metals complexes were characterized by some analytical methods like TLC, DSC, TGA, FT-IR, HPLC and ¹H NMR.

Biological investigation is an inherent portion of research. It has been conducted to discover biological activity of pure drug or drug-drug or drug-metal complexes. Although the therapeutic activities of the standard drug are known, the research was devoted to find any unknown biological activity of the formed complexes. To evaluate the biological activities of synthesized drug complexes the following assay techniques were performed:

- ✓ Evaluation of anti-diabetic activity in swiss albino mice model (*in vivo* analysis).

- ✓ Evaluation of biochemical parameters like serum creatinine and uric acid level and SGPT-SGOT level determination by ELISA technique.
- ✓ Histopathological studies of drug complex treated liver and kidney tissue of mice.
- ✓ Evaluation of lipid lowering activity of rosuvastatin and drugs complexes in New Zealand white rabbit model (*in vivo* analysis).
- ✓ Evaluation of antioxidant activity using DPPH scavenging activity.
- ✓ Assay for thrombolytic activity using streptokinase as standard.
- ✓ Determination of membrane stabilizing activity in terms of capacity of the drug complexes to suppress the hypotonic saline mediated hemolysis of RBC.

1.9. SOCIO-ECONOMIC IMPORTANCE

For the treatment of multimorbidity in elderly patient polypharmacy is observed which enhance the possibility of drug interactions significantly (Rodrigues and Oliveira, 2016). Drug-drug interactions (DDIs) are a very ordinary reasons of untoward drug reactions (such as dysrhythmia, acute kidney injury and increased risk of falls) among geriatrics (Hines and Murphy, 2011; Lucas *et al.*, 2016; Roblek *et al.*, 2016). The prospect of untoward drug action is an obvious consequence of the direct relation between the quantity of drugs and their physio-chemical interactions. In this 21st century, hyperglycemia is doubtlessly one of the great stimulating health issues (Shrestha and Ghimire, 2012). Hypertension in hyperglycemic peoples is commonly found which is often tough to take care and ended with remarkable morbidity and mortality. The occurrence of hypertension in diabetic patient is probably 1.5-2.0 times higher than from non-diabetic people (Mitra *et al.*, 1999). The combination of hypertension and hyperglycemia in individual patients may injure similar vital organs and may result in cerebral diseases, the development of diabetic retinopathy, decrease in renal function and left ventricular hypertrophy and coronary artery disease (Grossman and Messerli, 2008). Similarly, patients with high lipid profile may have hypertension.

In this study considering the pharmaco-epidemiology, pharmacology and public health some commonly prescribed drugs (antidiabetics, antihypertensives and lipid lowering drugs) have been chosen to do some interactions among them. Cr(III) plays important roles in carbohydrate and lipid metabolism.

Therefore, to synthesize some new chromium complexes with different classes of oral antidiabetic drugs was a try and their antidiabetic potentials in mice also studied. Pb^{+2} increases oxidative pressure in living organisms (Bokara *et al.*, 2009; Coban *et al.*, 2007; Hunaiti and Soud, 2000) and oxidative stress may develop hyperglycemia by directly affecting cell signaling pathway by influencing insulin secretion. The concentration of lead in bone was connected with gradual increase in serum creatinine among diabetic patients and this was concluded from a 6-year study (Tsaih *et al.*, 2004). Four antidiabetic drugs were made to complex with lead which were metformin, glimepiride, vildagliptin and dapagliflozin, and their antidiabetic property was evaluated on mice model. Furthermore, the toxicological studies were performed by measuring serum creatinine level and uric acid level. In search of new metal combination atorvastatin calcium was reacted with iron, copper and zinc.

CHAPTER TWO

**MATERIALS AND
METHODS**

CHAPTER TWO

MATERIALS AND METHODS

2.1. MATERIALS

2.1.1. Drugs and chemicals

Olmesartan medoxomil (potency 99.98%), perindopril erbumine (potency 98.99%), dapagliflozin (purity 99.98%), vildagliptin (purity 99.99%), metformin HCl (purity 99.97%), glimepiride (purity 99%), rosuvastatin (potency 99.89%) and atorvastatin calcium trihydrate (purity 99.98%) were kind gifts from Incepta Pharmaceuticals Ltd., Dhaka, Bangladesh; ACI Pharmaceuticals Ltd., Dhaka, Bangladesh and Drug International Pharmaceuticals Ltd., Dhaka, Bangladesh.

Analytical grade chemicals like $\text{FeSO}_4 \cdot 7\text{H}_2\text{O}$, $\text{CuSO}_4 \cdot 5\text{H}_2\text{O}$ and ZnCl_2 were used for all experimental procedures. As a source of chromium(III), $\text{CrCl}_3 \cdot 6\text{H}_2\text{O}$ was used. Analytical grade lead nitrate was used as a source of lead(II). Precoated thin layer chromatography plate (Precoated TLC plate, F_{254}) was purchased from locally from Merck, Germany.

Chloroform, acetonitrile and methanol were used in the experiments and the solvents were of HPLC grade and procured locally from Sigma Aldrich, Germany. Nano pure water was used and collected from own source. Analytic grade monobasic potassium phosphate (KH_2PO_4), dipotassium hydrogen phosphate (K_2HPO_4), some other chemicals were collected from Centre for Advanced Research in Sciences (CARS), University of Dhaka. BSA solution of pH 7.4 was prepared using phosphate buffer. For determinations of triglycerides, total cholesterol, HDL cholesterol, LDL cholesterol, serum creatinine and uric acid levels colorimetric kits were purchased from Linear Chemicals, Barcelona, Spain. For studying thrombolytic property as well as membrane stabilizing property pure acetyl salicylic acid (ASA) was employed as reference standard to compare with drug complexes. To study antioxidant potential, the scavenging activity of the free radical DPPH (1,1-diphenyl-2-picrylhydrazyl) was measured and here BHT (tert-butyl-1-hydroxytoluene) was employed as reference standard. Alloxan monohydrate (98%) was purchased from Loba Chemie Pvt. Ltd., India.

2.1.1.1. Preparation of pH 7.4 buffer solution

Phosphate buffer was made ready by dissolving 235.0 mL of 0.01M K_2HPO_4 along with 65.0 mL of 0.01M KH_2PO_4 and then the mixture was raised to a volume of 1000 mL with demineralized water (Saha *et al.*, 2012).

2.1.2. Instruments

Thermostatic water bath (Unitronic Orbital, P Spectra, Spain), digital melting point instrument (model WRS-1B, Taiwan) and analytical balance (Model AS 220, Radwag, Poland) were used in the experiment. For proper mixing and preparing solution sonicator (UltrasonsMedili, J.P. Selecta, Spain) was used. In purpose of acquiring IR spectra a FT-IR instrument (model 8400S, Shimadzu, Japan) was utilized. For thermogravimetric analysis TGA 50H from Shimadzu, Japan was used. Fluorescence spectrophotometer (F-7000, Hitachi, Japan), UV-visible spectrophotometer (UV 1800, Shimadzu, Japan), DSC-60 (Shimadzu, Japan), ELISA reader (LisaScan EM, Erba, Germany), Centrifuge Instrument (Z36 HK, HermleLabortechnik GmbH, Germany) and NMR spectrometer (Bruker, 400 MHz) were in use for analysis of samples (Figure 2.1.).



(1) Reaction bath



(2) Digital melting point measuring instrument



(3) DSC (DSC-60, Shimadzu, Japan)



(4) Fluorescence spectrophotometer (F-7000)



(5) LisaScan EM ELISA reader



(6) HPLC

Figure 2.1. Some instruments used in the experiment: (1) Reaction bath, (2) Digital melting point measuring instrument, (3) DSC, (4) Fluorescence spectrophotometer, (5) ELISA reader, (6) HPLC.

2.1.3. Animals

For the experiment with animal model an ethical clearance certificate was obtained from the Faculty of Biological Sciences, University of Dhaka, Dhaka, Bangladesh (Ref.No.128/Bio.Sc.).

One hundred Albino mice [Figure 2.2 (1)] of both sexes with average weight of 50.0 g were purchased from the Animal House, Department of Pharmacy, Jahangirnagar University, Savar, Bangladesh. The mice were then maintained on a normal diet and filtered water *ad libitum*.

Twenty male and female both sex New Zealand white rabbits [Figure 2.2 (2)] were purchased having their weight in range of 1.5 ± 0.3 kg initially for measurement of the lipid lowering activity of new drug complexes. The rodents were kept in proper temperature of 21-25 °C, humid condition of 50-60% humidity and 12 h dark-light cycle. The rodents were adapted for a period of 5 days before starting the experiment.

After the experimental periods the rodents were properly disposed according to ethical guidelines.



(1) Mice



(2) Rabbits

Figure 2.2. Experimental rodents: (1) mice and (2) rabbits.

2.2. METHODS

2.2.1. Formation of drug-drug complexes by co-evaporated dispersion method

The complexes of antihypertensive drug olmesartan medoxomil with three antidiabetic drugs (dapagliflozin, vildagliptin and metformin HCl) were formed on the basis of 1:1 ratio in molarity. Twenty mL of methanolic solution of each drug was prepared by taking 0.5 mM weight of drug (0.279 g of olmesartan, 0.204 g of dapagliflozine, 0.152 g of vildagliptin and 0.082 g of metformin HCl). In the next step the drug solutions were added with each other by stirring and changing pH. Then the solutions were kept in constant heat reaction bath at 60 °C for 24 h period. Some mixtures were dried and crystallized while others were filtered and left for drying and crystallization (Aktar *et al.*, 2019; Kundu *et al.*, 2012).

Another three drug complexes such as perindopril, vildagliptin and rosuvastatin were synthesized following the previous method. 0.5 mM of each drug was accurately weighed (0.221 g of perindopril erbumine, 0.152 g of pure vildagliptin and 0.241 g of rosuvastatin) and was made a solution of volume of 20 mL using distilled water. Later on, individual drug solution was mixed with each other by stirring and changing pH. Then the solutions were kept at constant heat reaction bath for 24 h at 60°C for allowing complexation. After 24 h reaction period the mixtures were withdrawn from the reactor bath and then filtered and left for drying and crystallization at room temperature.

The Cr(III)-metformin, Cr(III)-glimepiride, Cr(III)-dapagliflozin and Cr(III)-vildagliptin complexes were synthesized by dissolving each drug i.e metformin hydrochloride (2 mmol, 0.388 g), glimepiride (0.5 mmol, 0.245 g), dapagliflozin (0.5 mmol, 0.2051 g) and vildagliptin (0.5 mmol, 0.1517 g) in methanol to form a volume of 25.0 mL. Then 25.0 mL methanol solution of 1 mmol $\text{CrCl}_3 \cdot 6\text{H}_2\text{O}$ (0.202 g) was mixed with 25 mL methanol solution of each drug. The mixtures were then heated at 70 °C in water bath with continuous stirring for 3.30 h. Finally the mixtures were left overnight for precipitation and drying.

The Pb-met, Pb-glim, Pb-vilda and Pb-dapa complexes were prepared by dissolving each drug e.g. metformin hydrochloride (2 mmol), glimepiride (0.5 mmol), vildagliptin (0.5 mmol), dapagliflozin (0.5 mmol) in 25 mL of methanol. Then 25 mL methanol solution of 1 mmol $\text{Pb}(\text{NO}_3)_2$ was poured into 25 mL of the respective drug solution. The mixtures were then heated at 70-75 °C in a water bath with occasional stirring for 4.30 h. Then the mixtures were left overnight for drying and crystallization.

The Fe(II)-atorvastatin, Cu(II)-atorvastatin and Zn(II)-atorvastatin complexes were formed by dissolving the drug e.g atorvastatin calcium (0.01 mmol) in 25.0 mL of distilled water. Then 25.0 mL aqueous solution of 0.01 mmol $\text{FeSO}_4 \cdot 7\text{H}_2\text{O}$, 0.01 mmol $\text{CuSO}_4 \cdot 5\text{H}_2\text{O}$ and 0.01 mmol ZnCl_2 were made by blending with 25.0 mL of aqueous solution of atorvastatin calcium. The mixtures then were heated at 70-75 °C in a water bath with occasional stirring for 6.30 h. Then the mixtures were kept in oven for overnight for drying and crystallization.

2.2.2. Characterization of synthesized complexes

The synthesized complexes were characterized using several analytical protocols as follows:

Thin Layer Chromatography (TLC)

TLC is a separation technique requiring very little sample and solvent. It is primarily used to determine the purity of a compound. A pure compound will show only one spot on a developed TLC plate. Possible identification of the unknown compound can be done through TLC analysis. By trial-and-error method suitable solvent system was determined to run the TLC system (Figure 2.3.).

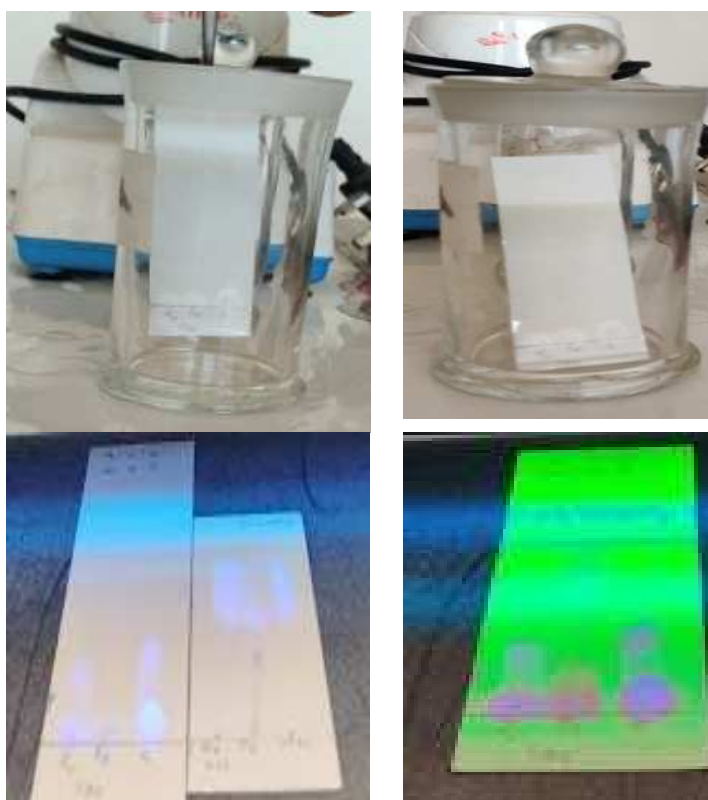


Figure 2.3. TLC determination.

High Performance Liquid Chromatography (HPLC)

For justification of the formation of complexation, reversed phase HPLC (RP-HPLC) was carried out using a C_{18} analytical column (particle size 5 μm , 25 mm \times 46 mm i.d.). The analyses were conducted using the mobile phase of a mixture of 60:40 v/v acetonitrile and 15.0 mM phosphate buffer. The flow rate of mobile phase was 1.0

mL/min and the mode was isocratic. The eluate was then monitored with a UV detector at 254 nm.

Differential Scanning Calorimetry (DSC)

DSC thermograms were recorded to study the endothermic melting point using the DSC instrument at Drug Analysis and Research Laboratory in CARS, University of Dhaka. Aluminum seal pan was used to analyze the samples and temperature range was set at 30-300 °C to record the thermograms of the samples. Temperature rising rate was maintained at 10 °C/min and inert nitrogen gas flow rate was 20 mL/min. The newly synthesized compounds as well as reference standard drugs were analyzed for phase transition determination.

Melting Points Determinations

As melting point is a determinant of the purity of the drug, a digital melting point instrument was used to determine the melting points of the newly synthesized complexes and precursor drugs. Powder form of the drugs and complexes in glass capillary were used for the experiment.

Thermo Gravimetric Analysis (TGA)

The TGA recordings were performed for confirmation of formation of complexes from the drugs. TGA were recorded in TGA 50H and degradation pattern of drug molecules as well as new complexes were compared for characterization. The sample drugs were measured in aluminum pan and temperature was set at a range usually from 25 °C to 600 °C and the temperature hold time was 5 min. Inert nitrogen gas was circulated at 10 mL/min flow rate and the temperature was raised by 10 °C/min.

Fourier Transform Infrared Spectrophotometry (FT-IR)

Fourier transform Infrared Spectroscopy (FT-IR) records an infrared absorption spectrum which reveals the types of chemical bonding among the molecular atoms. The recorded IR spectra display unique identification of individual molecule by specific stretching and bending of chemical bonds. It is an efficient tool for identification of responsible moiety and their molecular bond analysis. The FTIR analyses of drugs and complexes were carried out at the wavelength from 400 cm⁻¹ to 4000 cm⁻¹. About 100 mg of pure and moisture free potassium bromide (KBr) was added to 1.0 mg of each non-wet drug sample and then uniformly mixed in a mortar-pestle (usually in the ratio of 100:0.1). The mixture was made pellets by pressing through machinery which gave a

pressure of 8-10 tons. Then the hand made discs were examined through IR beam path for recording of the spectra. At a resolution of 4 cm^{-1} and radiation range $4000\text{-}400\text{ cm}^{-1}$ the discs were scanned for 30 times.

^1H NMR (Nuclear Magnetic Resonance) Spectroscopy

NMR spectra recording and interpretation of data reveal important information for structure elucidation of molecules. By elucidating different parameters from NMR spectrum like chemical shifts, coupling constants and integrations the structure of known and unknown compounds can be revealed. ^1H NMR spectra of the synthesized metal-drug complexes as well as the pure drugs were recorded on a Bruker 400 MHz instrument in Jahangirnagar University, Bangladesh where CDCl_3 and CD_3OD solvents were used and TMS was employed as reference standard.

UV Visible Spectrophotometry

In this procedure, absorption spectra of atorvastatin and its three complexes Fe-atorvastatin, Cu-atorvastatin and Zn-atorvastatin were compared. The stock solution of the sample was diluted to appropriate levels using buffer, then the UV spectra were measured at a radiation range of 200-800 nm.

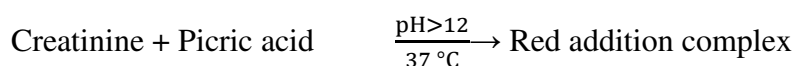
2.2.3. Induction of diabetes in mice

The mice were maintained and handled according to the guidelines of Helsinki declaration. Experiment in animal model was carried out after obtaining the ethical clearance from the Faculty of Biological Sciences, University of Dhaka, Dhaka, Bangladesh (Approval Ref.No.128/Bio.Sc.). The mice were anonymously (both male and female) divided into 16 groups and numbered as Group-I to Group-XVI containing 5 rats in each group. Group-I was referred as control group and the mice were fed normal diet only. Neither alloxan nor drug was given to the Group-I mice. Diabetes was induced in the rest of the fifteen groups from Group-II to Group-XVI by intraperitoneal injection of alloxan (Merk, India) after an overnight fasting giving a dose of 150 mg/kg body weight. Before induction of diabetes and after a period of three days of alloxan treatment, blood was drawn from tail of the all groups of fasting mice to measure the serum glucose level. Blood glucose level was measured immediately by the help of a glucometer (GlucLeader-yasee, GLM-76, Yasee Co. Ltd., Taiwan) where disposable strips were in use. The alloxan-treated mice were determined to be diabetic as they had a high serum glucose level ($>20\text{ mmol/L}$).

Group II and Group III were given a dose of 150 mg/kg metformin hydrochloride and Cr-metformin complex, respectively for 14 days as oral solution. Similarly, group IV and group V were given 150 mg/kg dapagliflozin and Cr-dapagliflozin complex, respectively. Group VI and Group VII were allowed 150 mg/kg vildagliptin and Cr-vildagliptin complex, respectively, and Group VIII and Group IX were given glimepiride and Cr-glimepiride, respectively as oral solution for 14 days. Group-X, Group-XI, Group-XII, Group-XIII, Group-XIV, Group-XV and Group-XVI were given 1.50 mg/kg body weight (b.w) of Pb-met, Pb-glim, Pb-vilda, Pb-dapa, OD, OV and OM complexes, respectively as solution for 14 days. After treatment, blood was drawn by cutting the tail of the all groups of fasting mice and blood glucose levels were measured using disposable strips. After the evaluation period all survived mice were sacrificed to collect serum for biochemical studies as well as kidney and liver were separated for histopathological studies.

2.2.4. Serum creatinine study

The procedure of serum creatinine measurement was based on modified early picrate reaction. At high pH creatinine interacts with picrate ion and forms a red complex. The rate of formation of red complex is proportional to the sample creatinine concentration and the concentration is measured at fixed interval of time in terms of increase in absorbance of radiation (Heinegaard and Tindstrom, 1973; Larsen, 1972).

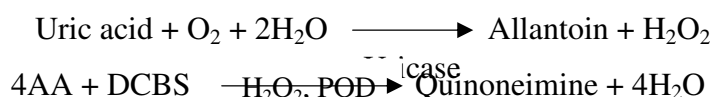


Standard, samples and reagents for the experiments were pre-incubated to reaction temperature (37 °C). The UV spectrophotometer was adjusted to level 0 using distilled water as blank. 100 µL of standard or sample and 1.0 mL of working reagent were pipetted into a cuvette and vortexed for mixing. Then the cuvettes were entered into the temperature-controlled instrument for vortexing and then stopwatch was started. Then the absorbance was measured at radiation of 510 nm after 30 seconds (A_1) and 90 seconds (A_2) of the standard or sample addition.

$$\frac{(A_2 - A_1)_{\text{Sample}}}{(A_2 - A_1)_{\text{Standard}}} \times C_{\text{standard}} = \text{mg/dL creatinine} = \text{mg/dL} \times 88.4 = \mu\text{mol/L}$$

2.2.5. Uric acid determination

By the enzyme uricase, uric acid is oxidized and produces allantoin and hydrogen peroxide. The enzyme peroxidase along with H_2O_2 oxidizes the mixture of dichlorophenol sulphonate (DCBS) and 4-aminoantipyrene (4-AA) into a dye quinoneimine. The concentration of the produced dye is proportional to the concentration of uric acid present in the serum (Barham and Trinder, 1972; Fossati *et al.*, 1980).

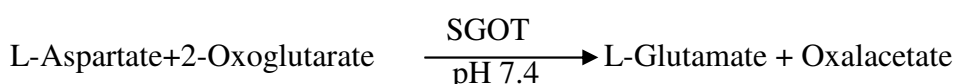


Samples and reagents were kept in room temperature and reagents were poured into three different set of tubes labelled as blank, standard and sample where these were mixed by vortexing and allowed undisturbed for 10 minutes. The absorbance (A) of the standard and samples were recorded at 520 nm using only reagent as blank.

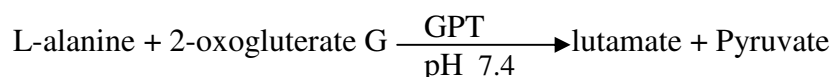
$$\frac{A_{\text{sample}}}{A_{\text{standard}}} \times C_{\text{standard}} = \text{mg/dL uric acid} = \text{mg/dL} \times 59.5 = \mu\text{mol/L}$$

2.2.6. Determination of SGPT and SGOT

The transfer of amino acid group from L-aspartate to 2-oxoglutarate is assisted by the enzyme aspartate aminotransferase (SGOT).



The movement of amino group from L-alanine to 2-oxoglutarate is assisted by the help of the enzyme Alanine aminotransferase (GPT) and from the rearrangement glutamate and pyruvate are formed.



The amino transferase activity of the enzymes is proportional to the amount of formation of oxalate or pyruvate after a certain time interval. The enzyme activity is measured by the quantifying the reaction between 2,4-dinitrophenylhydrazine (DNPH) and oxalate or pyruvate (Reitman and Frankel, 1957).

2.2.7. Histopathological studies of liver and kidney tissues of experimental mice

After the 14 days of experimental period the mice were sacrificed, and the hepatic and nephrotic tissues were collected for histopathological studies. The experiment was conducted in pathological lab of Bangabandhu Sheikh Mujib Medical University (BSMMU), Dhaka, Bangladesh.

2.2.8. Lipid lowering activity of rosuvastatin and its complexes in rabbits

2.2.8.1. Experimental design (Movahedian *et al.*, 2006)

Laboratory animals are essential for the study of human diseases and drug activities *in vivo*. Selection of proper animal model is very important for both fundamental research and evolution of therapeutic activities and diagnostic tools. Like human but unlike rodents, rabbits inherent a special resemblance of lipoproteins content and metabolism. Rabbits are sensitive to cholesterol diet and serve as delicate model to study the formation and pathogenesis of atherosclerosis. Rabbit models have served many insights into the pathogenesis and development of atherosclerosis and had been used more than a century ago as laboratory animal.

Eighteen healthy New Zealand white rabbits weighing average 1.5 ± 0.3 kg were purchased locally for the experiment. Experiment in animal model was carried out after approval of the ethical clearance from Faculty of Biological Sciences, University of Dhaka, Dhaka, Bangladesh (Approval Ref. No. 128/Bio.Sc.). The rabbits were observed with normal food and water for 5 days as adaptation period before starting the study. The rabbits were kept in suitable temperature, at 21-25 °C, 50-60% humidity and 12 hours of dark-light cycle. They were given a standard feeding of green leafy vegetables, water *ad libitum*. The experimental drug doses were given orally via gavage feeding tube. Coconut oil was used as high fat diet to make the rabbits hyperlipidemic. The rabbits were distributed into six groups where every group contained three rabbits. Group I was considered as negative control group which received only normal diet. Except group I rest of rabbits of the five groups were made hyperlipidemic by oral gavage feeding of 500 mL coconut oil/kg body weight of rabbit per day. Group II was referred as positive control which were fed only 500 mL coconut oil/kg b.w./day for 10 days. Rabbits of Group III were oil fed for 5 days then treated with reference drug rosuvastatin at a dose of 1.0 mg/day for next 5 days. Rabbits of group IV were oil fed for 5 days then treated with drug complex RP at a dose of 1.0 mg/day for next 5 days. Rabbits of group V were also oil fed for 5 days then treated with drug complex RV at a dose of 1.0 mg/day for next 5 days. The rabbits of group VI were also oil fed for 5 days then treated with drug complex PV at a dose of 1.0 mg/day for next 5 days. On the 5th,

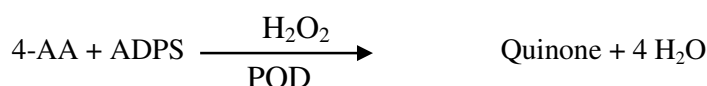
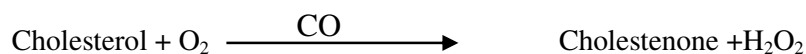
10th and 15th day of the experiment blood was withdrawn from ear veins of the rabbits. Then the blood was centrifuged and after 30 minutes serum was collected and preserved at -20 °C for biochemical study.

2.2.8.2. Chemical analysis of biological samples

By the use of special reagent kits from Linear Chemicals Pvt. Ltd., Spain, total cholesterol level, triglycerides level, high density lipoprotein level (HDL) and low-density lipoprotein level (LDL) were determined. Very low-density lipoprotein was determined by the aid of LDL calculator.

2.2.8.3. Total cholesterol measurement procedure in serum

The method (Allain *et al.*, 1974; Amundson and Zhou, 1999) used in determination of total cholesterol level in the sample requires three enzymes, cholesterol esterase (CE), cholesteroloxidase (CO) and peroxidase (PO). These three enzymes and mixture of N-ethyl-N-propyl-m-aniside (ADPS) and 4-aminoantipyrine (4-AA) produce quinone dye which is proportional of cholesterol concentration present in the sample.



First of all, reagents and samples both were set at room temperature. Three test tubes were labelled as monoreagent, sample and standard. Monoreagent containing 1.0 mL reagent was considered as blank. Standard contained 1.0 mL monoreagent and 10 µL standard cholesterol. The sample contained 1.0mL monoreagent and 10 µL sample. The test tubes were then vortexed for mixing then incubated for at least 10 mins at normal temperature and absorbance of samples and standard (A) were recorded at 550nm against the reagent as blank.

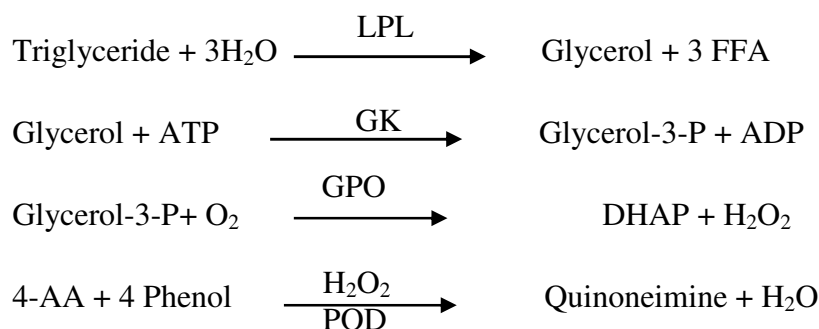
$$(A_{\text{sample}} / A_{\text{standard}}) \times C_{\text{standard}} = \text{mg/dL Cholesterol}$$

To express the results in SI units, $\text{mg/dL} \times 0.0259 = \text{mmol/L}$

2.2.8.4. Serum triglycerides measurement procedure

The method (Bucolo and David, 1973; Fossati and Prencipe, 1982) was developed on the basis of enzyme (lipoprotein lipase, LPL) catalyzed hydrolysis of triglycerides to glycerol and free fatty acids. The glycerol is phosphorylated by glycerolkinase (GK) in presence of adenosine triphosphate (ATP) into glycerol-3-phosphate (G-3-P) and adenosine diphosphate (ADP). G-3-P is then oxidized in presence of glycerolphosphate oxidase (GPO) into dihydroxy acetone phosphate (DHAP) and hydrogen peroxide (H₂O₂).

The condensation of 4-aminoantipyrine (4-AA) and phenol was assisted in presence of hydrogen peroxide and catalyst peroxidase (POD) and then a red chromogen quinoneimine is produced and the amount of which is proportional to the concentration of triglycerides present in the blood sample.



Reagents and samples were kept at room temperature. Three test tubes were labelled as monoreagent, sample and standard. Monoreagent containing 1.0 mL reagent was considered as blank. Standard contained 1.0 mL monoreagent and 10 μ L standard triglycerides. The sample contained 1.0 mL monoreagent and 10 μ L sample. The test tubes were then vortexed for proper mixing and rested in incubation for a period of 15 mins at laboratory temperature and then the absorbance of sample and standard were recorded at 500 nm against the blank (only reagent).

$$(A_{\text{sample}}/A_{\text{standard}}) \times C_{\text{standard}} = \text{mg/dL triglycerides}$$

To express the results in SI units, $\text{mg/dL} \times 0.0113 = \text{mmol/L}$

2.2.8.5. LDL cholesterol determination

LDL cholesterol determination (Arsman *et al.*, 1984) employed the technique of a unique precipitation method of LDL cholesterol by polyvinyl sulphate and then sedimentation of the precipitant. Then by determination of the concentration of rest of

lipoproteins (VLDL and HDL) present in clear upper supernatant and LDL cholesterol is calculated after subtracting the value from the total cholesterol of the sample.

For the precipitation step, reagents and samples were kept at normal temperature. Then 0.1 mL of precipitating reagent was mixed with 0.2 mL of standard/sample centrifuge tubes and the mixture was vortexed for proper mixing and kept for 10 mins for resting at room temperature. The respective tubes were then left for centrifugation for 10 mins at 6000 r.p.m. Then the supernatant part was brought for colorimetric measurement of combined VLDL and HDL. Here two series of test tubes were prepared in parallel to measure total cholesterol of the sample and HDL and VLDL in the supernatant. Three test tubes were labelled as monoreagent, supernate and standard. Monoreagent containing 1.0 mL reagent was considered as blank. Standard contained 1.0 mL monoreagent and 50 μ L standard supernate. The supernatant contained 1.0 mL monoreagent and 50 μ L sample supernate. The test tubes were vortexed for proper mixing and left for 10 mins in laboratory temperature. Then absorbance (A) of supernatant and standard was measured at 500 nm in comparison to blank (only reagent).

$$(A_{\text{supernatant}}/A_{\text{standard}}) \times C_{\text{standard}} = \text{mg/dL cholesterol}_{\text{supernatant}}$$

$$\text{LDL cholesterol} = \text{mg/dL cholesterol}_{\text{total}} - \text{mg/dL cholesterol}_{\text{supernatant}}$$

To express the results in SI units, the multiplication was used, $\text{mg/dL} \times 0.02559 = \text{mmol/L}$

2.2.8.6. HDL Cholesterol determination

This technique (Burstein *et al.*, 1980) employed a separation process after specific precipitation process (by phosphotungstic acid/ MgCl_2) of apolipoprotein B containing VLDL, LDL and apolipoprotein A, and then sedimentation of the formed precipitation by centrifugation. Then the clear supernatant part of the sample is enzymatically treated to determine the high density lipoproteins (HDL).

For the precipitation step, first of all reagents and samples were kept at laboratory temperature. Then 0.4 mL of precipitating reagent was poured into 0.2 mL standard or sample in the centrifugation tube. The mixture was then vortexed for proper mixing and kept at rest for 10 mins. The respective tubes were then placed in centrifuge machine for 10 mins for centrifugation at a speed of 4000 rpm. Then the supernatant portion was

separated for colorimetric determination of HDL. Three test tubes were labelled as monoreagent, supernatant and standard. Monoreagent containing 1.0 mL reagent was considered as blank. Standard contained 1.0 mL monoreagent and 50 μ L standard supernate. The supernate contained 1.0 mL monoreagent and 50 μ L sample supernate. The test tubes were vortexed for proper mixing and left for 10 minutes at laboratory temperature. Then the absorbance (A) of the supernatant and the reference standard was measured at 500 nm using only reagent as blank.

$$(A_{\text{supernatant}} / A_{\text{reference standard}}) \times C_{\text{reference standard}} = \text{mg/dL HDL-Cholesterol}$$

To express the results in SI units, the multiplication was used, mg/dL x 0.0259 = mmol/L

2.2.9. Thrombolytic activity of rosuvastatin and its complexes

Cerebral venous sinus thrombosis (CVT) accounts for 0.5-1% of strokes that has a dominance to occur in women (Bousser and Ferro, 2007; Star and Flaster, 2013). Anticoagulant therapy is given in CVT patients in order to promote clot resolution and prevent clot expansion. To evade the limitations of traditional anticoagulants such as heparin and warfarin novel anti-thrombotic agents are come to light (Franvis, 2005). So, the experiment was performed to determine the thrombolytic property of rosuvastatin and three drug complexes.

2.2.9.1. Method of working sample preparation

Streptokinase was employed as working standard for inhibition of formation of thrombus. For preparation of samples, accurately weighted 100.00 mg of each sample was kept in previously marked vials where 10.0 mL of distilled water poured for making solution. Ready to use lyophilized Alteplase (Streptokinase) Eppendorf tube (Becon Pharmaceuticals Ltd.) of 15,00,000 I.U., was purchased and 5 mL disinfected mineral water was poured into and assorted appropriately. The mixture was utilized as stock from which 100 μ L (30,000 I.U.) was employed for *in vitro* analysis of thrombosis. Whole blood (n=2) was collected from healthy human volunteer with no history of anticoagulant or oral contraceptives. Then 1.0 mL of blood was added to previously weighed disinfected eppendorf tube and left for formation of clot.

2.2.9.2. Measurement of Thrombolytic activity

The thrombolytic scheme was determined using the process by Prasad *et al.* (Prasad *et al.*, 2007) where streptokinase (SK) was utilized as positive control. Following the method, all samples (100 mg) were dissolved in 10 mL of distilled water and rested for overnight. After that, the soluble clear part of the sample was filtered and separated from each test tube. Then, a stock-of standard streptokinase of 100 μ L (30,000 I.U.) was measured for *in vitro* thrombolysis activity studies. Venous blood was drawn by using disinfected syringe from healthy volunteer. After this 1.0 mL of blood was added into weighed sterile Eppendorf tubes and were kept for incubation at 37 °C for 45 mins for development of thrombus. Then, the clear serum was totally decanted from all tubes without interrupting clots and clot containing tubes were then again weighed to measure the weight of individual clot weight (clot weight = weight of clot containing tube – weight of only tubes). At every pre-weighed Eppendorf tube with clot 100 μ L of streptokinase, 100 μ L of distilled water and 100 μ L aqueous solutions of our samples were added separately. Then all the tubes were left for incubation at 37 °C for 90 mins for the purpose of dissolution of clot. After the incubation period, the liberated fluids from all tubes were decanted carefully and weighed accurately to get the difference in weight of tubes after clot lysis. The differences in weight of tubes obtained before and after the clot disruption were expressed as percentage of clot lysis by following equation:

$$\% \text{ of clot lysis} = (\text{wt}_{\text{disrupted clot}} / \text{wt}_{\text{formed clot}}) \times 100\%$$

2.2.10. Membrane stabilizing property of rosuvastatin and its complexes

The membrane stabilizing property of the drugs and drug complexes were evaluated by the method used by Kawsar *et al.* (2011) by measuring their capability to inhibit hypotonic solution induced hemolysis of human erythrocyte.

2.2.10.1. Preparation of the samples

Analytical grade methanol was used to prepare the samples. Pure acetyl salicylic acid (ASA) was employed as reference standard.

2.2.10.2. Erythrocytes (RBC) collection

For the experiment human RBC was required. RBC was withdrawn from the male human free from chronic diseases with 72 kg weight (Figure 2.4.). Required RBC was

preserved in a test tube having in built anticoagulant EDTA, at 23 ± 2 °C temperature and 55 ± 2 °C humidity.

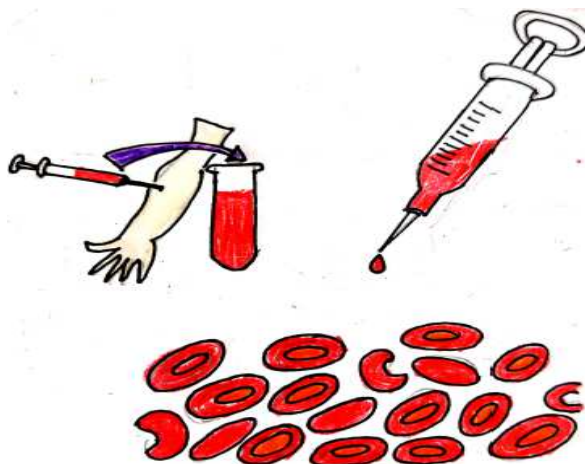


Figure 2.4. RBC collection.

2.2.10.3. Preparation of phosphate buffer solution

A buffer is a solution with stable pH. Buffer with pH 7.4 and strength of 10 mM was prepared with 0.0352% monosodium phosphate (0.352 g) dehydrate and 0.1099% disodium phosphate (1.099 g) anhydrate in a volume of 1000 mL water.

2.2.10.4. Preparation of isotonic solution

Either 0.16 M (approximately 0.95% salt in water) sodium chloride (NaCl) solution or 0.3 M nonelectrolyte solution is approximately osmolar with human red blood cells. For the making of 500 mL isotonic solution of 154 mM strength, 4.5045 g NaCl was weighed and mixed with distilled water.

2.2.10.5. Preparation of hypotonic solution

A solution of less osmotic pressure than that of an isotonic solution is termed as hypotonic solution. In preparation of 500 mL hypotonic solution of 50 mM accurately weighed 1.4625 g of NaCl was measured and mixed with distilled water

2.2.10.6. Preparation of erythrocyte suspension

The venous blood was withdrawn and preserved, and washed three times with isotonic solution in 10 mM pH 7.4 sodium phosphate buffer. The mixture was then centrifuged for 10 min at 3000 rpm. The final suspension was referred as stock erythrocyte suspension.

2.2.10.7. Hypotonic solution induced hemolysis

4.5 mL hypotonic solution in 10 mM buffer (pH 7.4) was added into each 0.5 mL of drugs and complexes (1.0 mg/mL of methanol) and to 0.5 mL of the standard acetyl salicylic acid (0.1 mg/mL of methanol). As control separately 4.5 mL of the hypotonic solution was also taken. Stock erythrocyte suspension (0.5 mL) was added to the drugs, drug complexes, standard and control. After that, the mixtures were kept at rest for 10 mins at laboratory temperature and centrifuged at 3000 rpm for 10 mins. Then the absorbances of the clear supernatant were determined at 540 nm. Membrane stabilization in terms of the percentage of inhibition of hemolysis was calculated by the help of the following equation:

$$\% \text{ inhibition of hemolysis} = 100 \times (\text{OD}_1 - \text{OD}_2 / \text{OD}_1)\%$$

Where, OD_1 = optical density of hypotonic buffered saline solution alone (control) and OD_2 = optical density or absorbance of test sample in hypotonic solution.

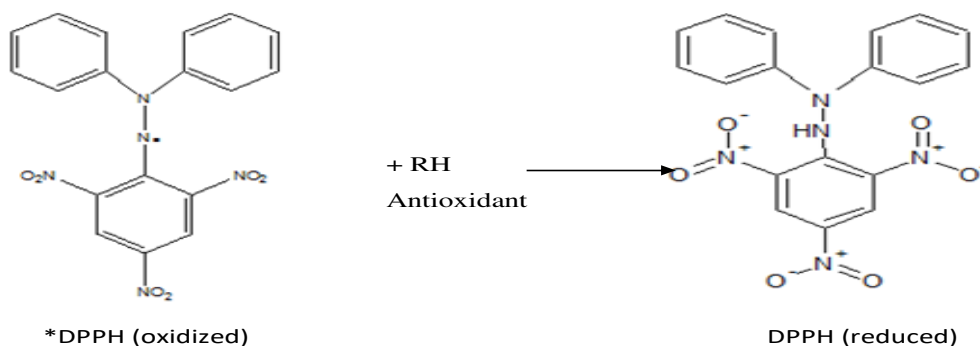
2.2.11. *In vitro* antioxidant activity study of rosuvastatin and its complexes

In vitro antioxidative abilities of drugs and drug complexes were screened in terms of DPPH free radical scavenging activity.

2.2.11.1. DPPH free radical scavenging property

Antioxidant activity of drugs and drug complexes was measured by a method described by Braca *et al.* (2001) which is developed upon the ability of the sample to reduce the stable 1,1-diphenyl-2-picrylhydrazyl (DPPH) free radical.

2.0 mL of stock methanolic solution of drug and drug complexes were serially diluted to different concentrations and then 3.0 mL of methanolic solution of DPPH (20 $\mu\text{g/mL}$) was added. The antioxidant property was determined from the bleaching of purple colored methanolic solution of DPPH radical by the drug and the drug complexes, and the quantification of the amount of bleaching was done by UV spectrophotometer using *tert*-butyl-1-hydroxytoluene (BHT) as standard.



2.2.11.2. Preparation of standard for antioxidant activity determination

As positive control standard BHT (tert-butyl-1-hydroxytoluene) was used. A stock solution of 1000 $\mu\text{g/mL}$ was prepared by weighing BHT and dissolving in methanol. Serial dilution was performed from the stock to make a range of concentration from 500.0 $\mu\text{g/mL}$ to 0.977 $\mu\text{g/mL}$.

2.2.11.3. Preparation of test sample

Drug samples were weighted and dissolved in methanol to get a stock solution of 1000 $\mu\text{g/mL}$. After diluting serially, a range of concentration from 500.0 $\mu\text{g/mL}$ to 0.977 $\mu\text{g/mL}$ were collected in test tubes and marked accordingly.

2.2.11.4. Preparation of DPPH solution

DPPH was accurately weighed (20 mg) and 20.0 $\mu\text{g/mL}$ methanolic solution was prepared. By devising the solution in amber colored bottle was stored in dark area to prevent reduction.

2.2.11.5. Evaluation of antioxidant property

DPPH methanolic solution of 3.0 mL was mixed with 2.0 mL of sample (drug/control) at every concentration from 500 $\mu\text{g/mL}$ to 0.977 $\mu\text{g/mL}$. After 30 min incubation of test tubes at dark cabinet at laboratory temperature the reaction was completed and then absorbance was studied at 517 nm in UV spectrophotometer using methanol as blank (Figure 2.5). The percentage inhibitory property was calculated from the following equation:

$$\% \text{ of inhibition} = [(A_0 - A_1) / A_0] \times 100$$

Where, A_0 = absorbance of control, A_1 = absorbance of sample/standard

IC₅₀ value was determined from the equation of straight line obtained after plotting a graph of concentration (µg/mL) versus % inhibition.

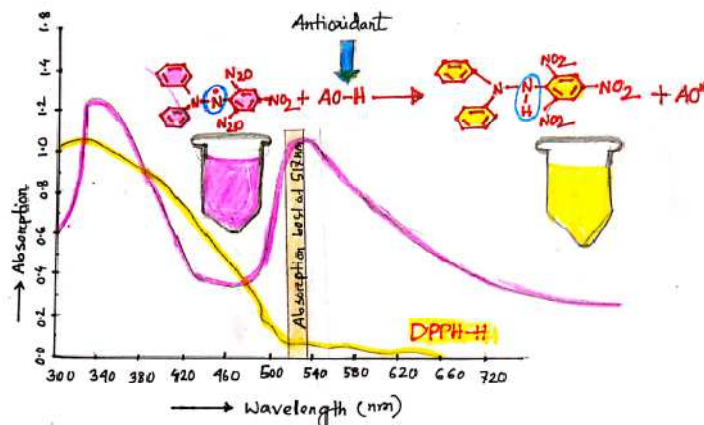


Figure 2.5. Antioxidant activity by DPPH assay.

2.2.12. Fluorescence quenching characteristics of drugs and drug-drug complexes

The fluorescence studies were conducted at three different temperatures 298 K, 308 K and 318 K that were maintained by using a circulating water bath. Different concentrations of aqueous drugs were 10 µM, 20 µM and 50 µM while BSA concentration was fixed at 10 µM. Solutions were made using pH 7.4 phosphate buffer. Most of the 295-400 nm range of fluorescence emission spectra were reported at 280 nm and 293 nm excitation wavelength. The test tubes having BSA solution and the drug/its complexes were heated minimum of 10 min before the fluorescence measurement (Tanwir *et al.*, 2012).

2.2.12.1. Quenching analysis by fluorescence spectrophotometer

In order to evaluate the quenching property, the fluorescence data can be elucidated from the Stern-Volmer equation (Lakowicz, 2006).

$$F_0/F = 1 - K_q c_0 [Q] = 1 + K_{SV} [Q]$$

Here, F_0 and F are the relative fluorescence intensities in the absence and presence of the quencher, respectively, K_{SV} is the Stern-Volmer dynamic quenching constant. $[Q]$ is the concentration of quencher, K_q is the biomolecular quenching rate constant, τ_0 is the average lifetime of the fluorophore in the excited state and usually for a protein it is 10^{-8} (Hu *et al.*, 2010; Lakowicz, 1999; Zhao *et al.*, 2010). From the values of K_q the formation of complex was further ascertained, $k_q = K_{SV} / \tau_0$

2.2.12.2. Evaluation of the binding constant and binding sites

The efficacy of the drugs as therapeutics is principally dependent upon their binding possibilities which further control the stability and toxicity of the drug during their use in treating a disease (Suryawanshi *et al.*, 2016). Moreover, for obtaining perceptions about the usual drug-protein interactions the study of drug-protein complex can be observed as an outstanding small project. To evaluate the binding interactions between antidiabetic-antihypertensive drugs and complexes with blood protein albumin, the values of binding constant were calculated from the fluorescence intensity data. When the drugs binds to a group of binding sites on a protein independently, then the amount of free drug and protein bounded drug is balanced by following the equation stated below (Zhao *et al.*, 2009):

$$\text{Log } (F_0-F)/F = \log K + n \log [Q]$$

Thus, the number of binding sites (n) and the binding constant (K) per BSA molecule may be determined, where F_0 , F and $[Q]$ values are same as those in the Stern-Volmer equation. A plot of $\log [(F_0-F)/F]$ versus $\log [Q]$ displays a straight-line equation and whose slope gives equivalent value for n and intercept on the Y axis resemblances value of $\log K$.

2.2.12.3. Thermodynamic parameters and binding forces

Four types of usual interaction forces between a protein and small organic molecule (drug) are hydrophobic interaction, hydrogen bonding, vander Waals forces and lastly electrostatic interaction. Types of individual kinds of interactions are interpreted from the values and direction of thermodynamic parameters like ΔH (change in enthalpy) and ΔS (change in entropy) which have been characterized by Ross and Subramanian (1981). If $\Delta H > 0$ and $\Delta S > 0$, the interaction force employed may be the hydrophobic interaction. If $\Delta H < 0$ and $\Delta S < 0$, the associated drug protein binding forces may be hydrogen bonding or Vander Waals force driven. When $\Delta H < 0$ and $\Delta S > 0$ then in drug protein interaction electrostatic force plays major role. When a little of temperature is changed the ΔH can be considered as constant. Form the below Van't Hoff equation these thermodynamic values can be calculated:

$$\ln K_T = - (\Delta H/RT) + (\Delta S/R)$$

ΔS is the change in entropy, K is the binding constant at temperature T , and R is the gas constant. From the slope and intercept of the fitted curve of Stern-Volmer equation of

$\ln K_{sv}$ against $1/T$, both ΔH and ΔS were measured. From the slope of the Van't Hoff equation the enthalpy change (ΔH) was calculated. The free energy change (ΔG) is calculated using the equation stated below:

$$\Delta G = H - T\Delta S$$

The negative sign associated with the value of ΔG indicates the spontaneity of the drug-protein interaction.

Statistical Analysis

The data are expressed as mean \pm SD. Statistical analyses were performed using Microsoft-Excel 2007.

CHAPTER THREE

**RESULTS AND
DISCUSSION**

CHAPTER THREE

RESULTS AND DISCUSSION

3.1. OLMESARTAN MEDOXOMIL AND THREE ANTIDIABETIC DRUGS COMPLEXATION: SYNTHESIS, CHARACTERIZATION AND EVALUATION OF BIOLOGICAL ACTIVITY

Three new complexes were synthesized as olmesartan-dapagliflozin (OD), olmesartan-vildagliptin (OV) and olmesartan-metformin (OM). The complexes were assessed with different R_f values on TLC plate and new peak patterns of FT-IR and NMR spectra. Melting point determination and TGA analysis reflected the thermal stability and thermochemical characteristics of the synthesized complexes. The binding constant and binding points were determined by calculating the Stern-Volmer constant at different temperatures (298 K, 308 K and 318 K) at pH 7.4. Characterization and investigation of interactions of BSA- standard drug and BSA- drug complexes were covered. Moreover, thermodynamic properties such as change of enthalpy (ΔH), entropy (ΔS) and free energy (ΔG) were estimated to evaluate the type of binding energies. Moreover, anti-diabetic activity (*in vivo*), biochemical study of serum and histopathological study of hepatic and nephritic tissues of the newly formed complexes were carried out.

3.1.1. TLC characterization of the drug complexes

Crystalline and amorphous complexes were formed during the complexation. To compare the R_f values of the complexes with their precursor ligands (drugs) TLC tests were performed in the solvent system of MeOH-CHCl₃ at a ratio of 40:60. There were found five prominent spots of the complexes having different R_f values from their precursor drugs (Table 3.1). The spots of the complexes indicated the formation of different complex compounds which might be new.

Table 3.1. R_f values of precursor drugs and their complexes.

Item	Mobile phase	R_f value
Olmesartan medoxomil		0.8
Dapagliflozin		0.6
Vildagliptin	MeOH-CHCl ₃ (40:60)	0.9
Metformin HCl		0.3
OD complex		0.7
OV complex		0.5
OM complex		0.3

3.1.2. Analysis of parent drugs and drug complexes by HPLC

After complexation reactions the washed products and the precursor drugs were subjected to analysis by HPLC. The chromatographic analyses were carried out on a C18 analytical column (5 μ m particle size, 25 mm x 46 mm id) using the mobile phase comprising of a mixture of acetonitrile and 15 mM phosphate buffer in the ratio of 60:40 v/v in isocratic mode. The eluate was monitored at 254 nm and the R_t (retention times) were obtained at 3.59 min, 3.80 min, 3.21 min, 2.50 min for olmesartan medoxomil, dapagliflozin, vildagliptin and metformin, respectively. On the other hand, R_t of the synthesized complexes were found at 2.87 min, 2.90 min and 3.30 min for OD, OV and OM, respectively. The chromatograms are shown in Figures 3.1-3.3.

From the HPLC chromatograms it was obviously clear that the complex OD was different from the precursor drugs olmesartan medoxomil and dapagliflozin (Figure 3.1); OV was different from the precursor drugs olmesartan medoxomil and vildagliptin (Figure 3.2), and OM was also different from olmesartan medoxomil and metformin (Figure 3.3). These phenomena indicated that the formation of the complexes which might be new.

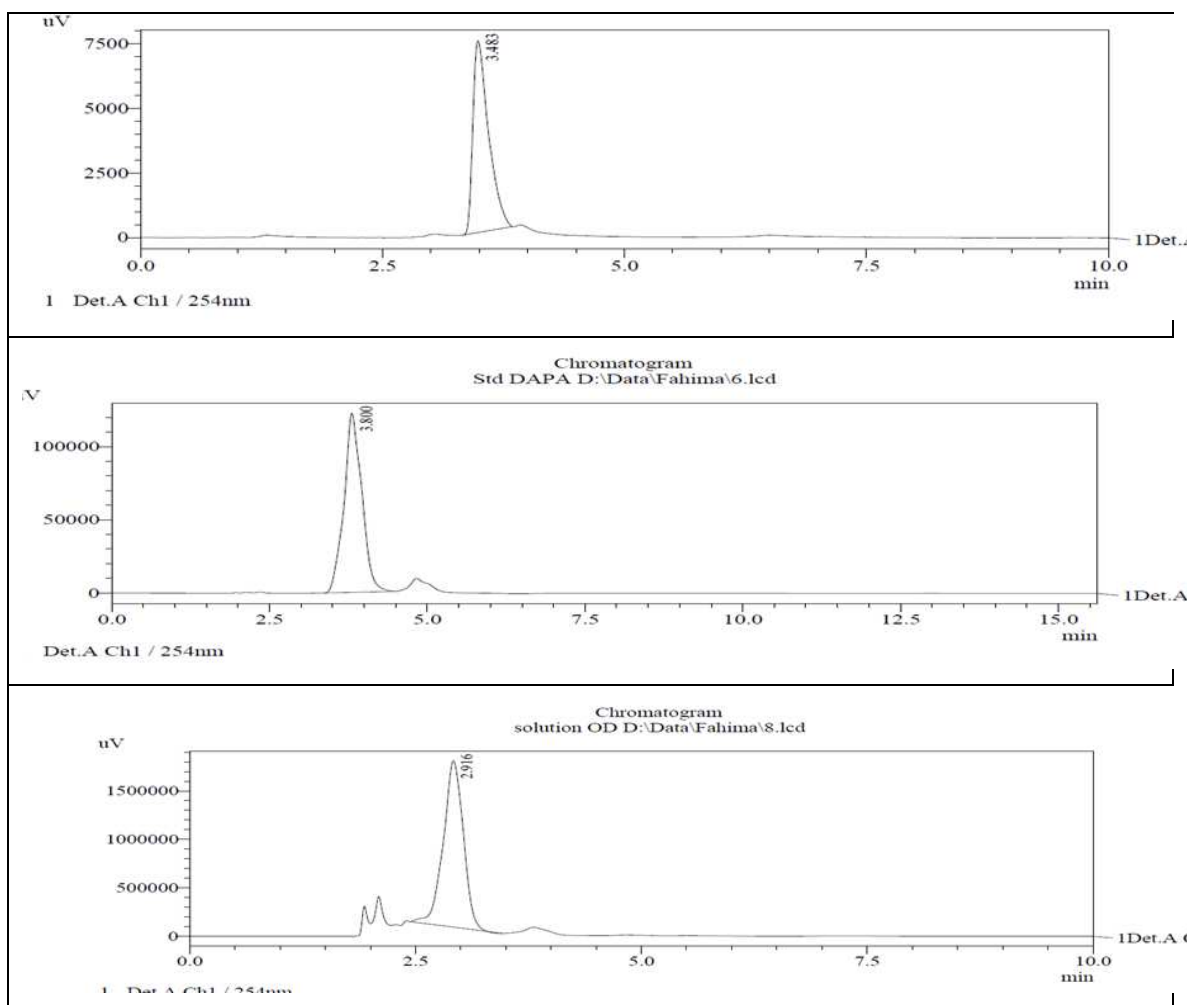


Figure 3.1. HPLC chromatograms of O, D and OD.

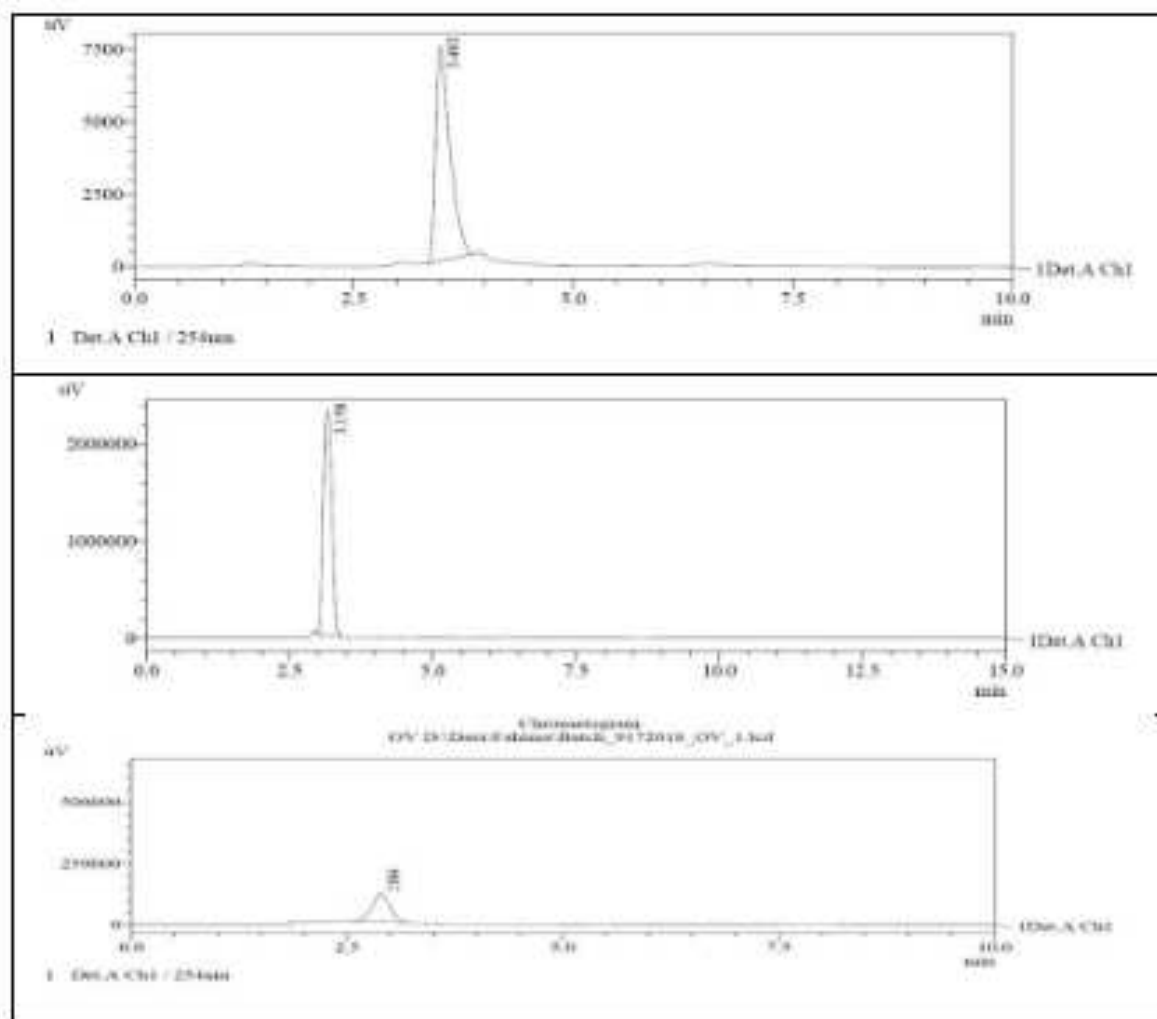
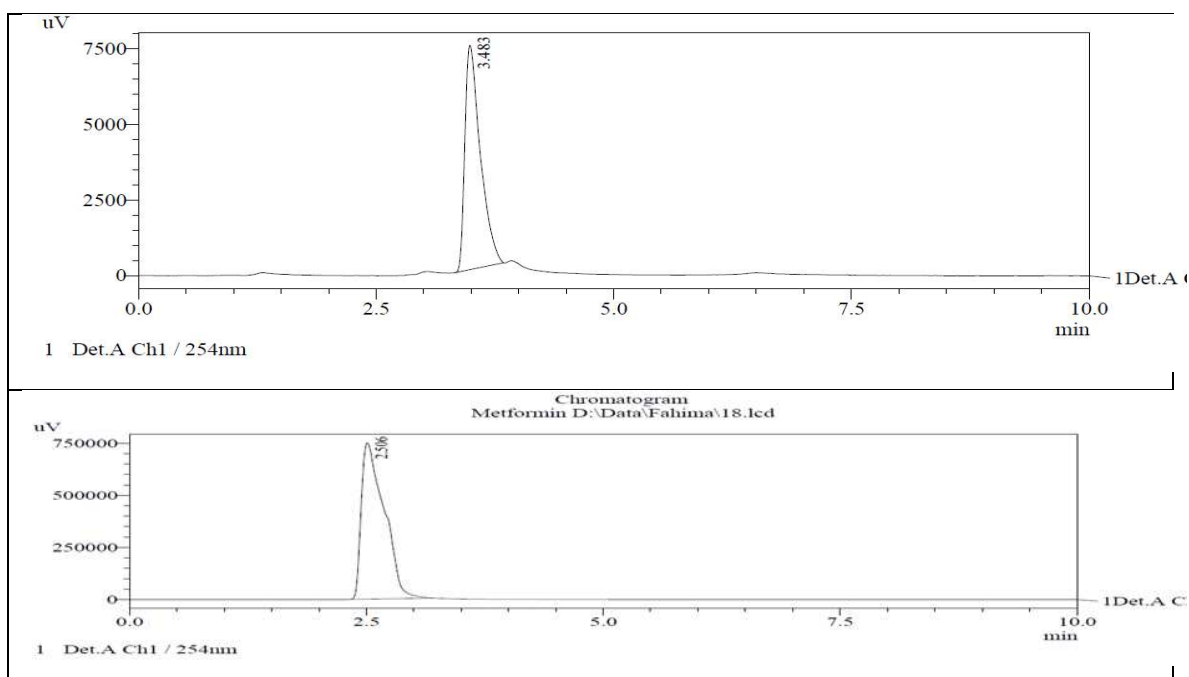


Figure 3.2. HPLC chromatograms of O, V and OV.



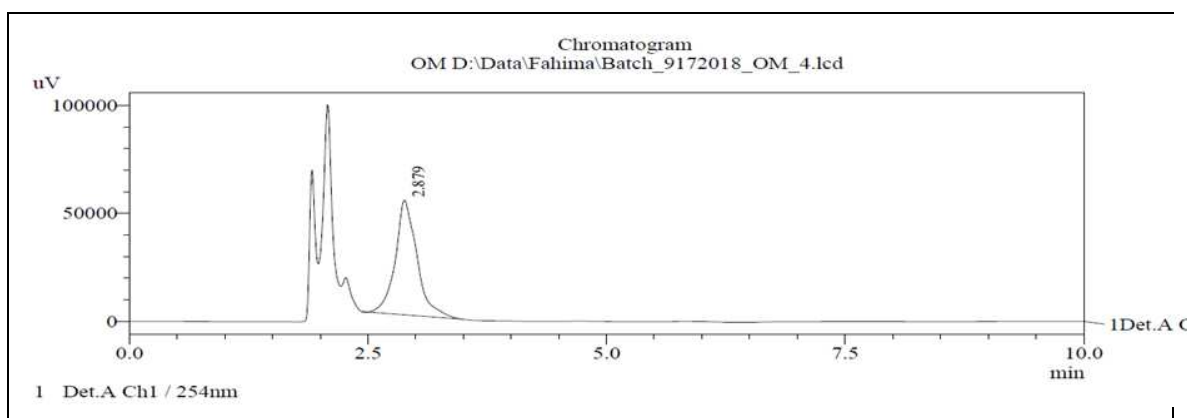


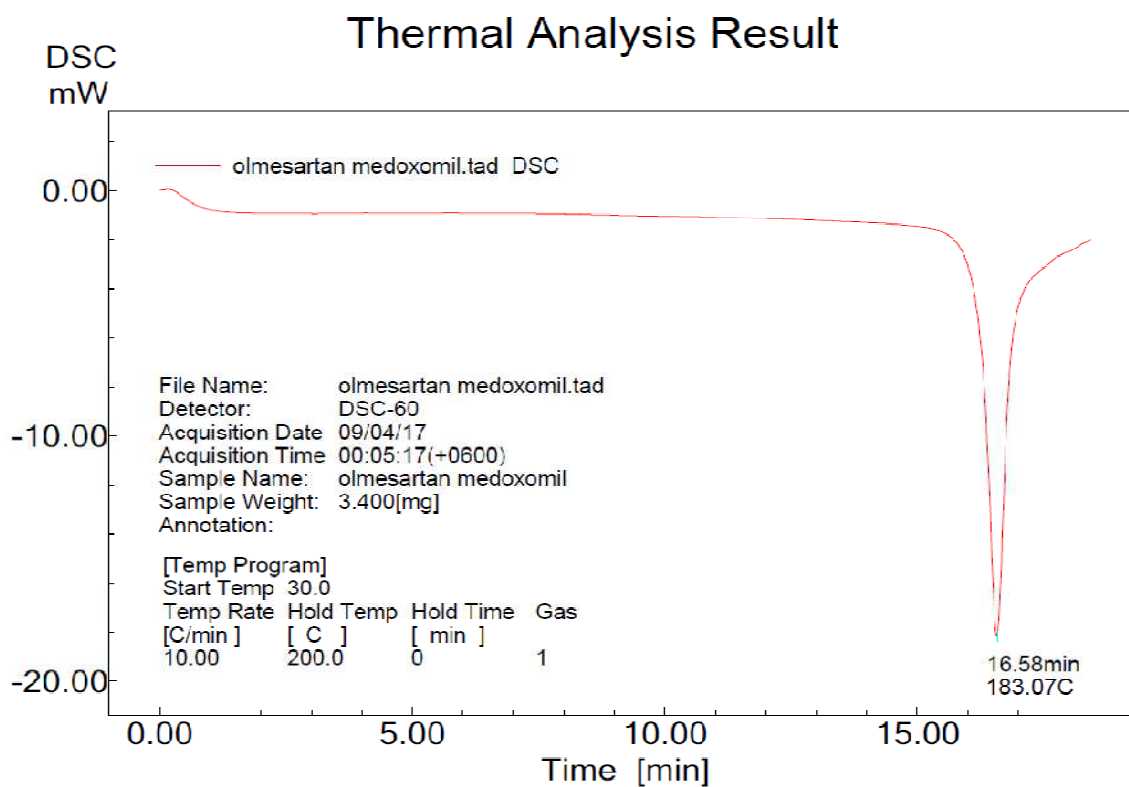
Figure 3.3. HPLC chromatograms of O, M and OM.

3.1.3. Analysis of parent drugs and drug complexes by DSC

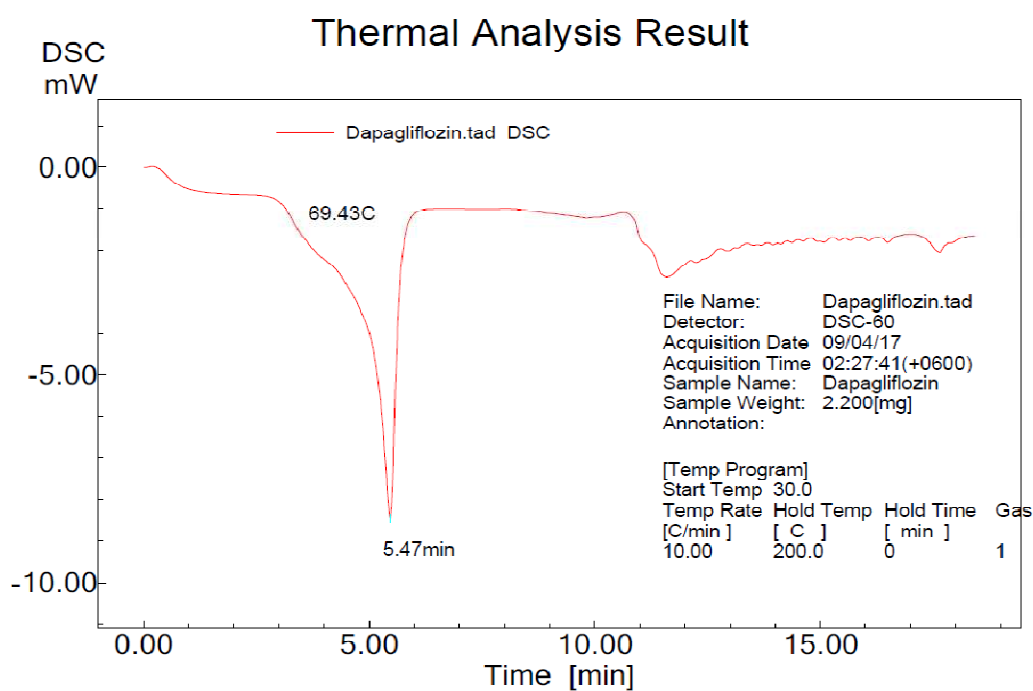
In DSC thermograms olmesartan medoxomil exhibited melting endotherms at 183.07 °C, dapagliflozin at 69.43 °C, vildagliptin at 151.64 °C and metformin at 232.30 °C which are shown in Table 3.2 and in Figure 3.4.

Table 3.2. Melting points from DSC thermograms.

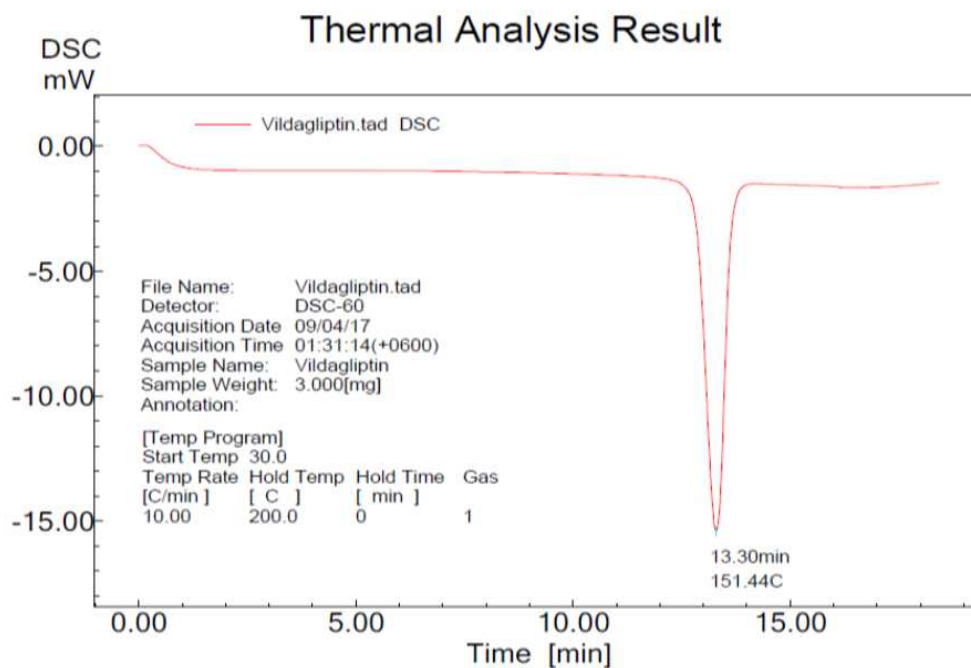
Sample	Melting endotherms
Olmesartan medoxomil	183.07 °C
Dapagliflozin	69.43 °C
Vildagliptin	151.44 °C
Metformin HCl	232.30 °C
OD	96.69 °C
OV	111.97 °C
OM	121.39 °C



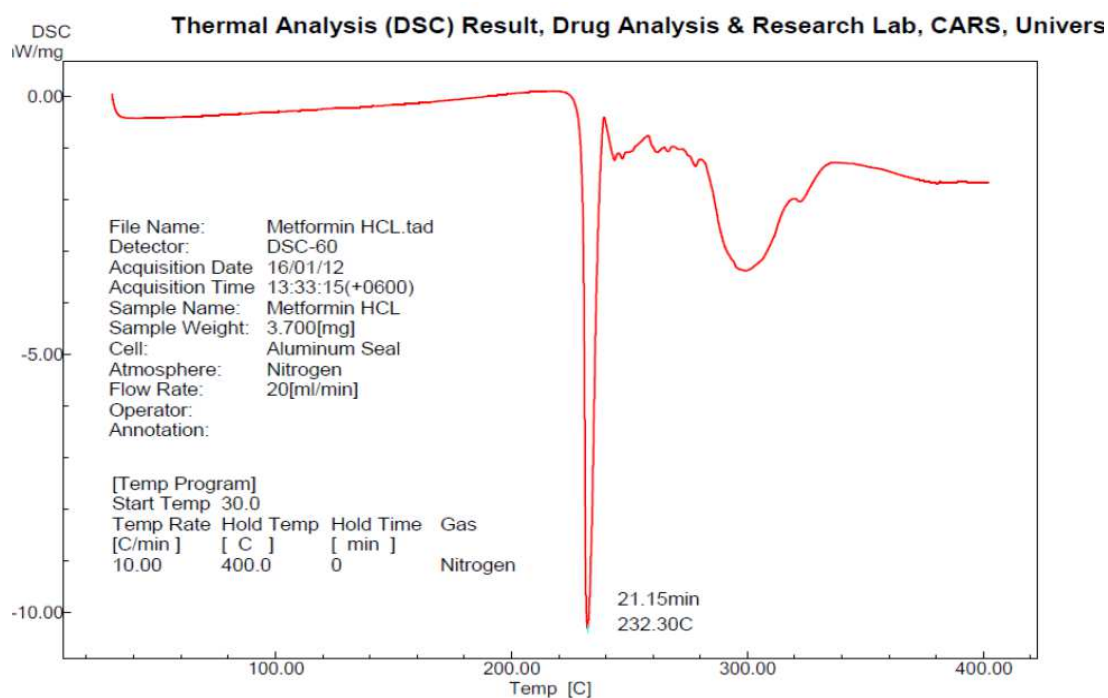
(1) DSC thermogram of olmesartan medoxomil.



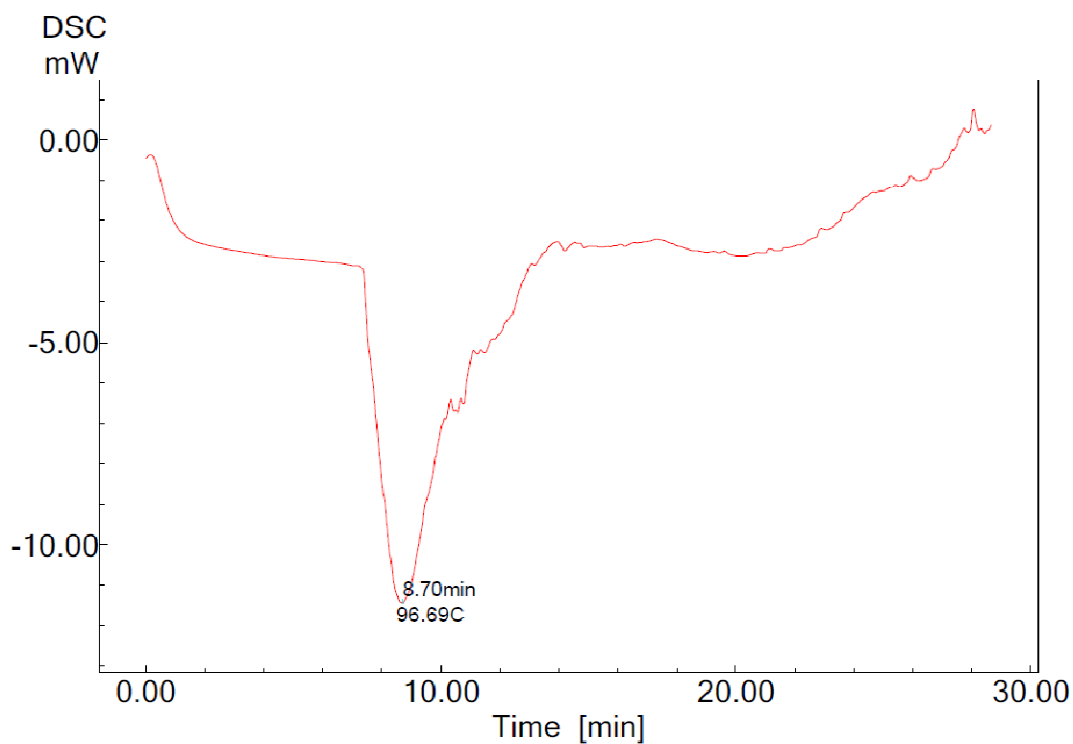
(2) DSC thermogram of dapagliflozin.



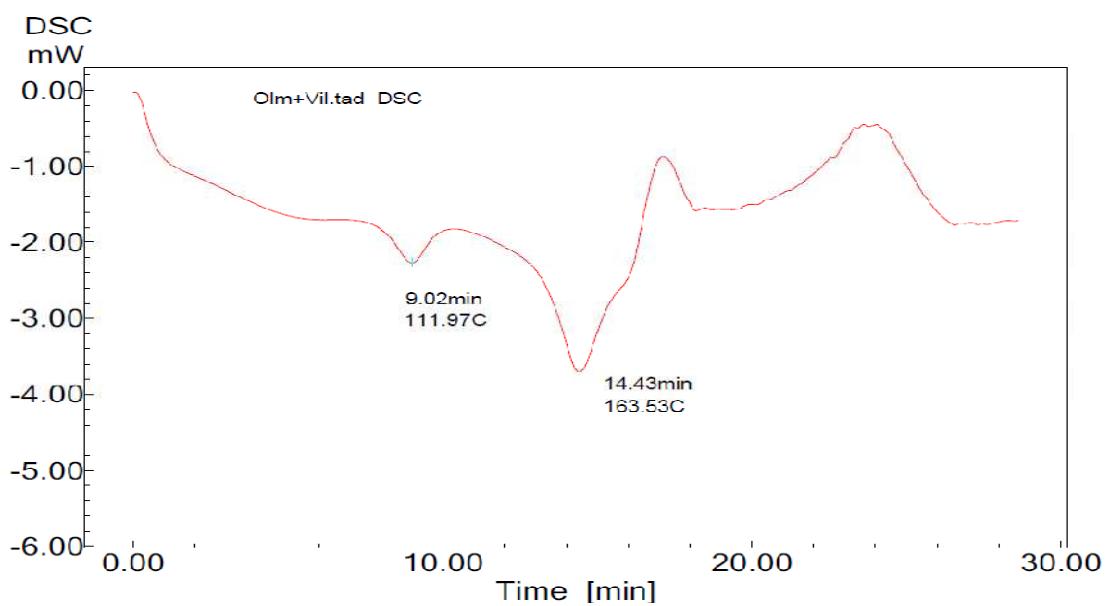
(3) DSC thermogram of vildagliptin.



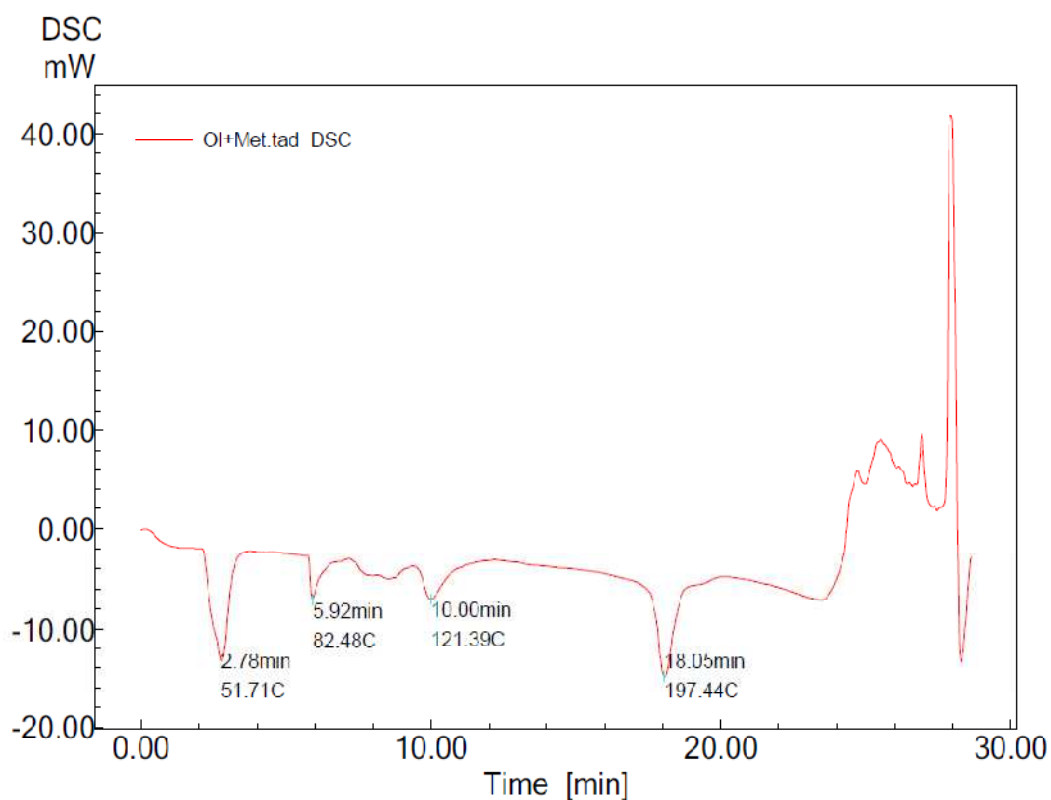
(4) DSC thermogram of metformin HCL.



(5) DSC thermogram of complex OD.



(6) DSC thermogram of complex OV.



(7) DSC thermogram of complex OM.

Figure 3.4. DSC thermograms of drugs: (1) olmesartan medoxomil, (2) dapagliflozin, (3) vildagliptin, (4) metformin, (5) OD, (6) OV and (7) OM.

The formed complex OD displayed an endothermic peak at 96.69 °C and this peak is found different from the peaks displayed by the parent precursor drugs viz. olmesartan medoxomil (183.07 °C) and dapagliflozin (69.43 °C) suggesting a new formation of complex. Similarly, other two new complexes OV and OM also gave endothermic peaks at 111.97 °C and 198.01 °C, respectively which were also different from their precursor drugs olmesartan, vildagliptin and metformin. These differences in DSC findings further recommended the evolution of new complexes as OV and OM (Figure 3.5).

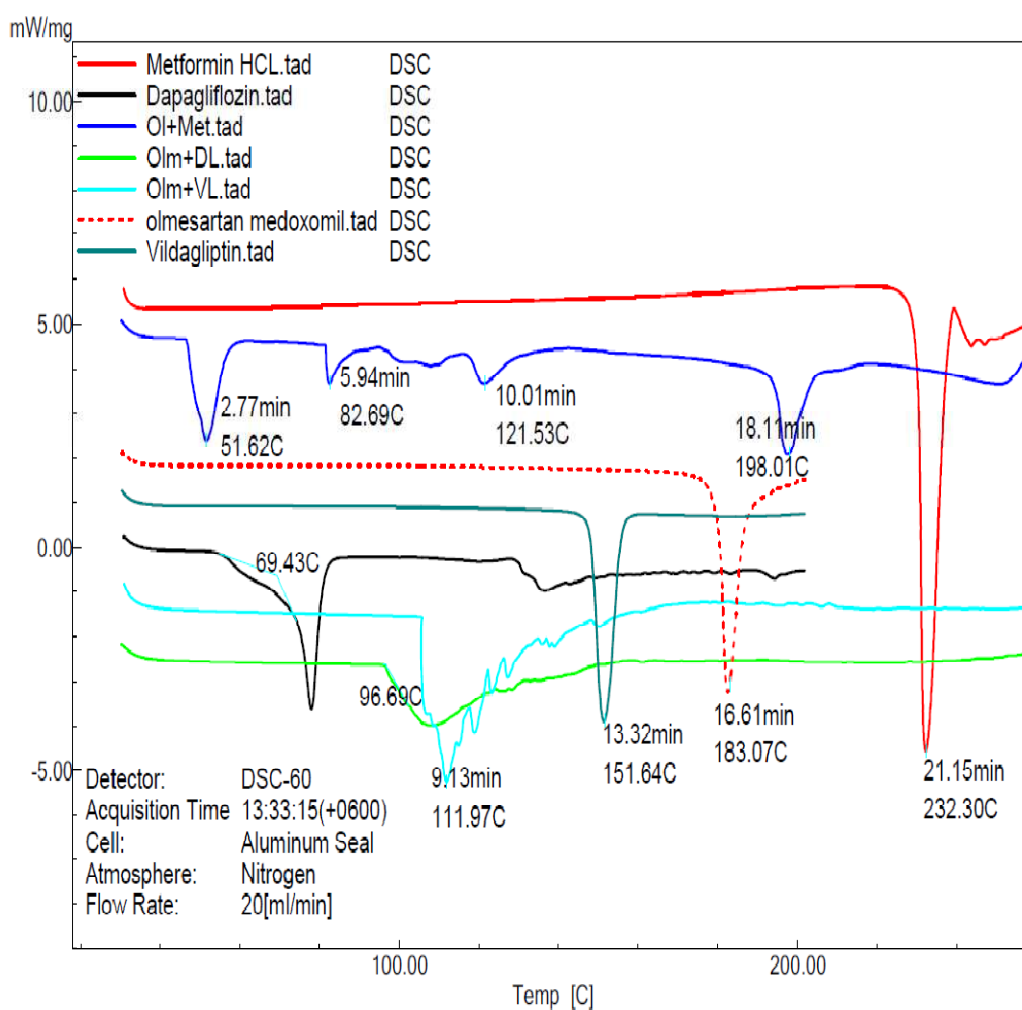


Figure 3.5. Overlaid DSC thermograms of olmesartan medoxomil, dapagliflozin, vildagliptin, metformin HCl and the newly formed complexes viz. OD, OV and OM.

3.1.4. Determination of melting point

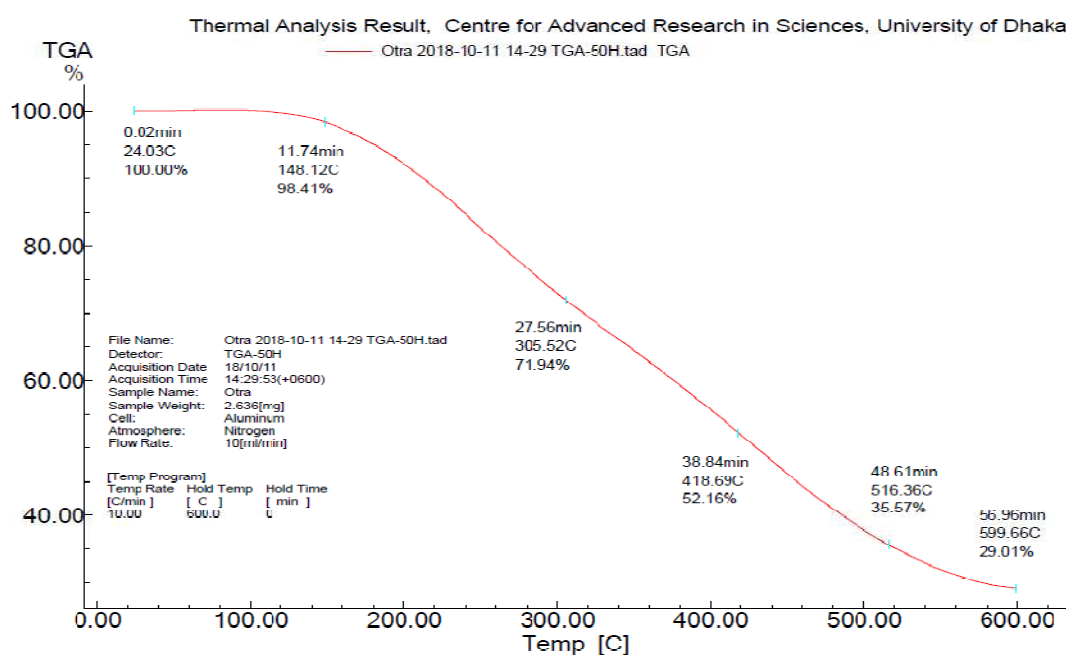
The melting points of the complexes were found to be lower than that of precursor drugs, reflecting formation of different compounds from the precursor drugs and their thermal stability (Table 3.3).

Table 3.3. Melting points of olmesartan and three antidiabetic drugs and their complexes, OD, OV and OM.

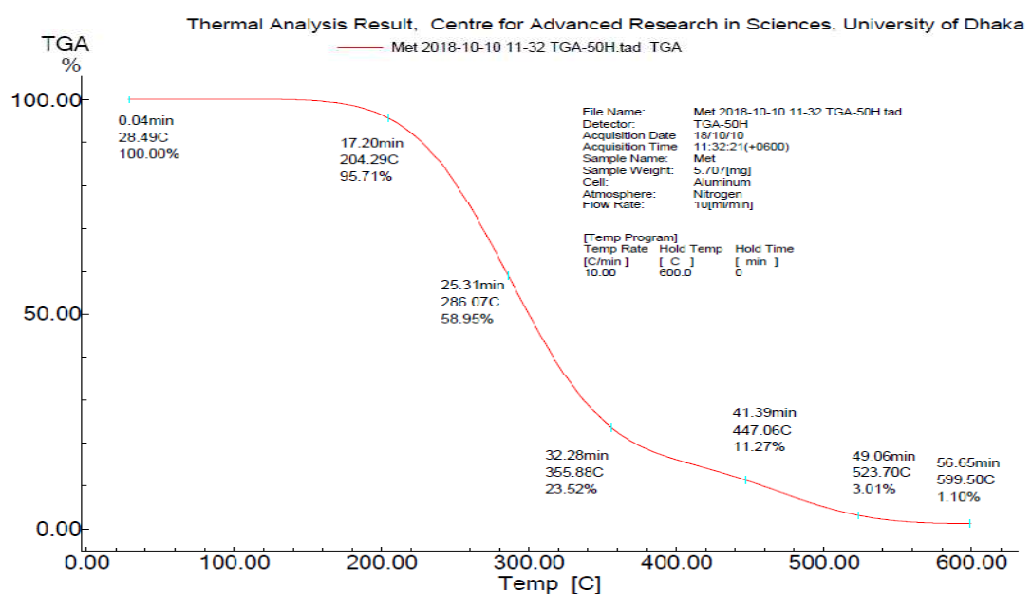
Sample	Melting point (°C)
Olmesartan	175-180 °C
Dapagliflozin	80-85 °C
Vildagliptin	150-154 °C
Metformin	221-225 °C
OD	80-85 °C
OV	100-105 °C
OM	68-72 °C

3.1.5. Analysis of parent drugs and drug complexes by TGA

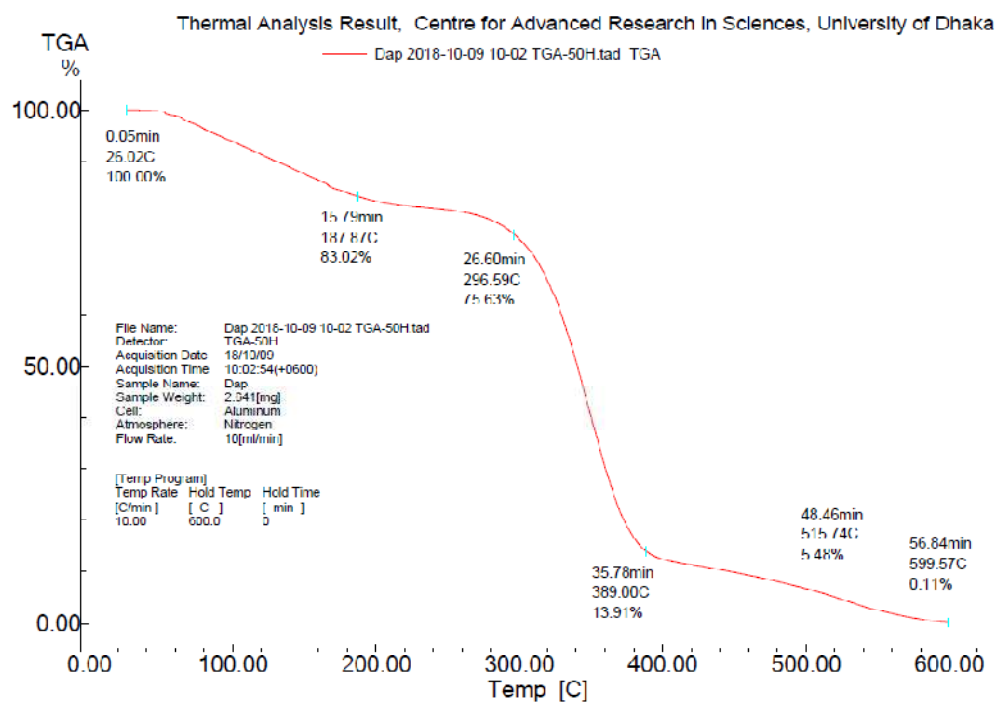
TGA thermograms were assayed from the reactant drugs and their complexes. The pure drugs and the newly formed drug complexes showed different fragmentation patterns with the increase in temperature suggesting the molecular structural differences (Figure 3.6).



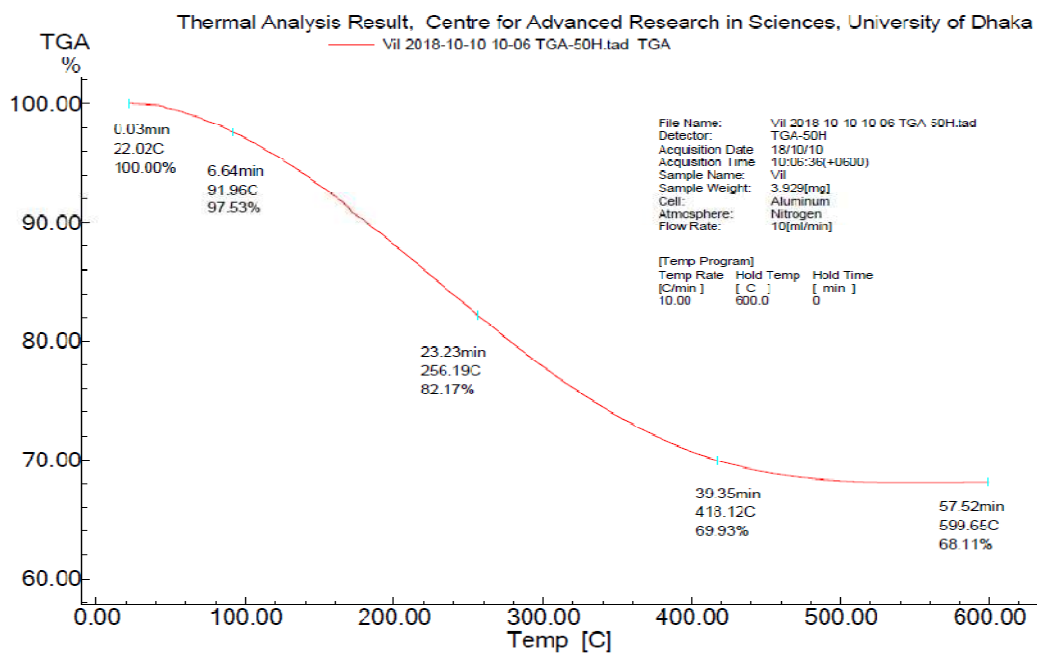
(1) TGA thermogram of olmesartan medoxomil.



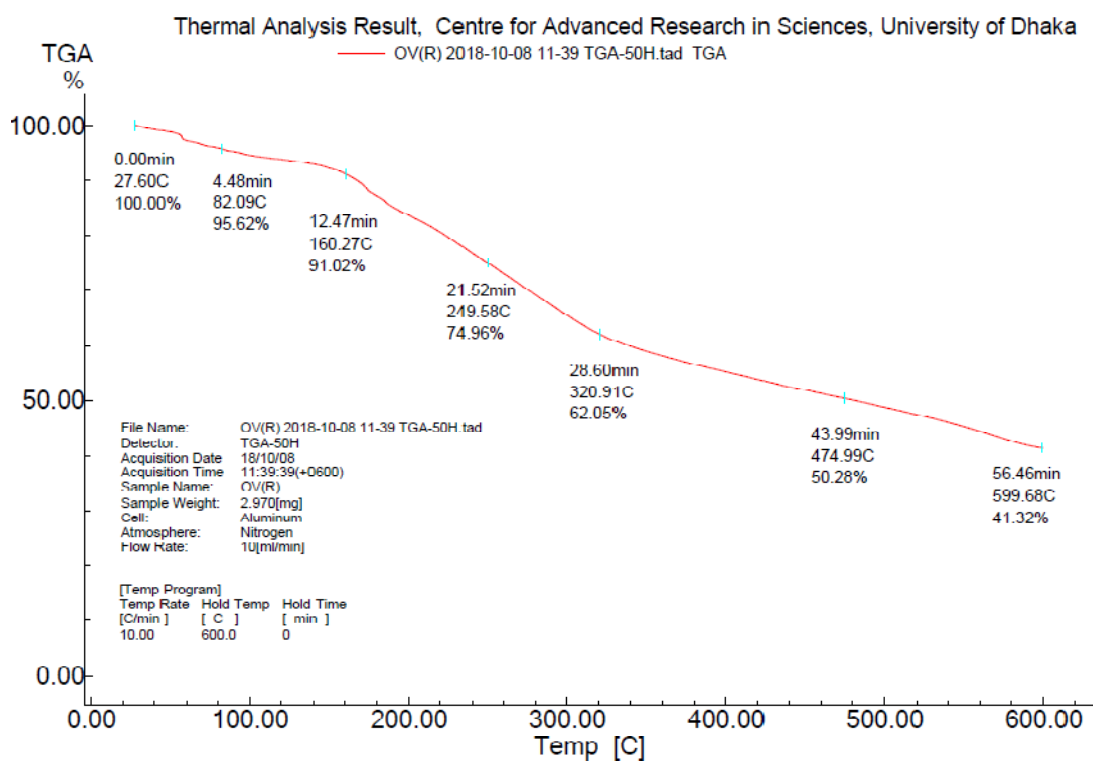
(2) TGA thermogram of the drug metformin HCl.



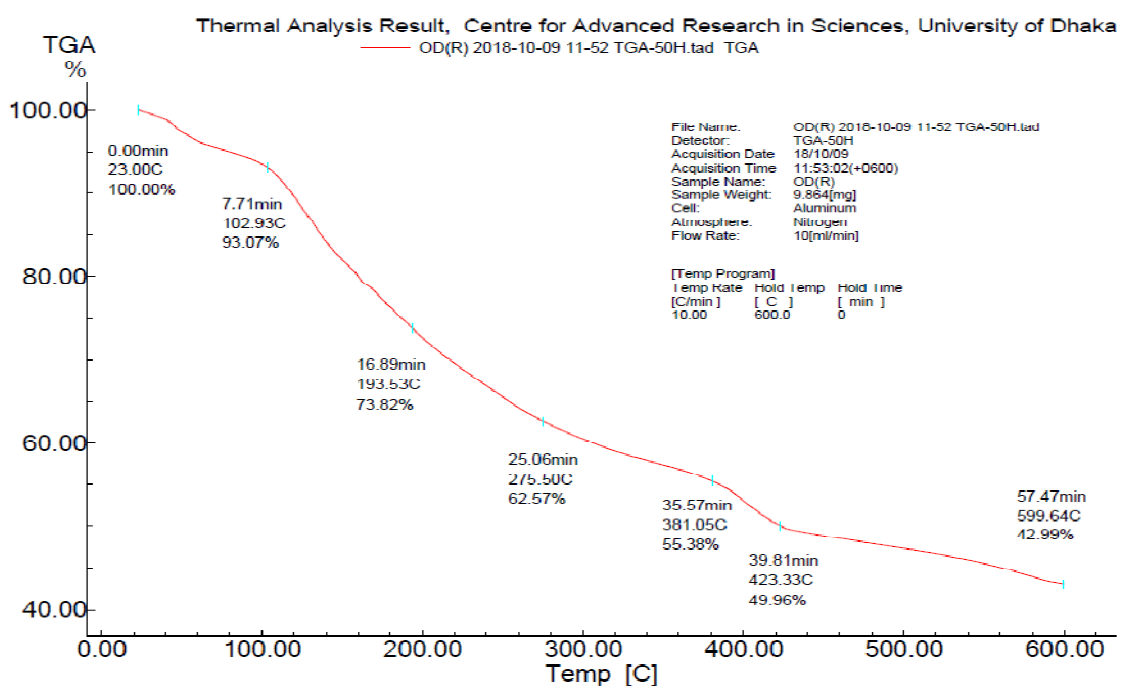
(3) TGA thermogram of the drug dapagliflozin.



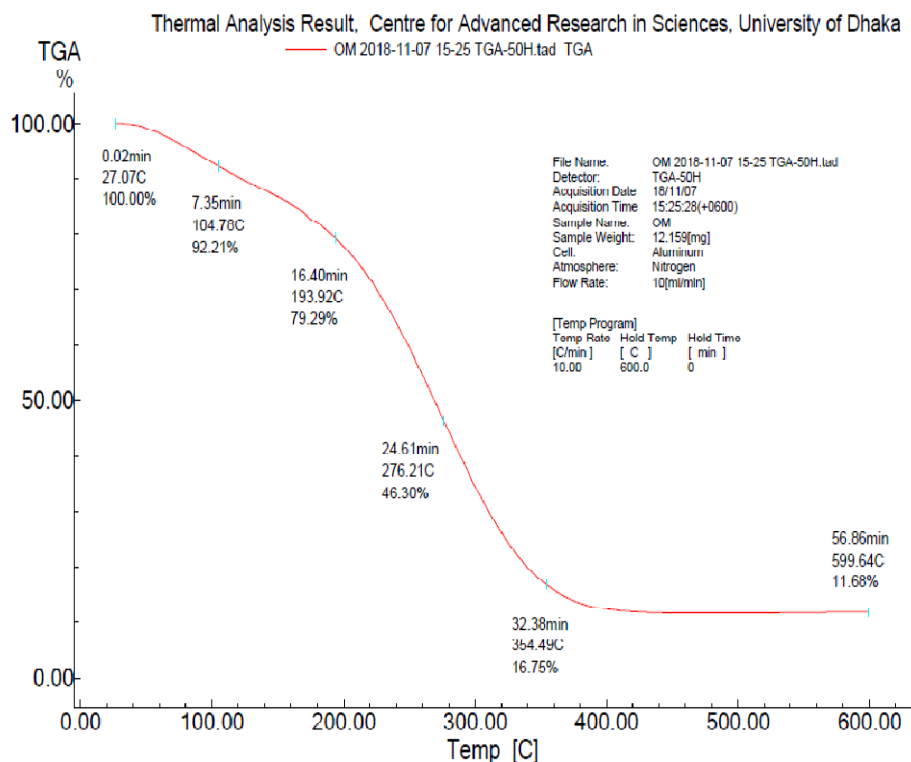
(4) TGA thermogram of the drug vildagliptin.



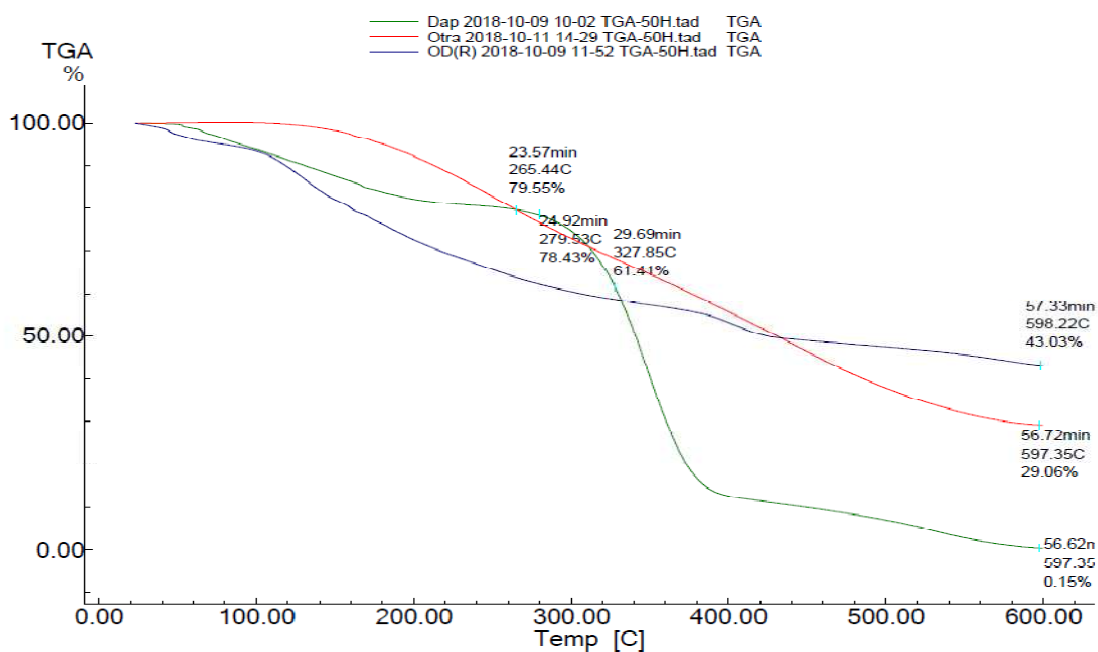
(5) TGA thermogram of the drug complex OV.



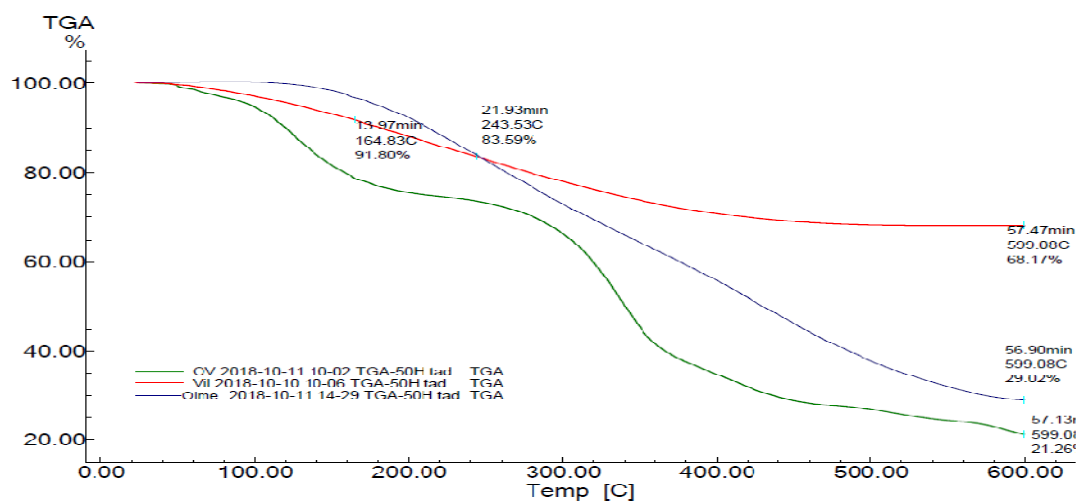
(6) TGA thermogram of the drug complex OD.



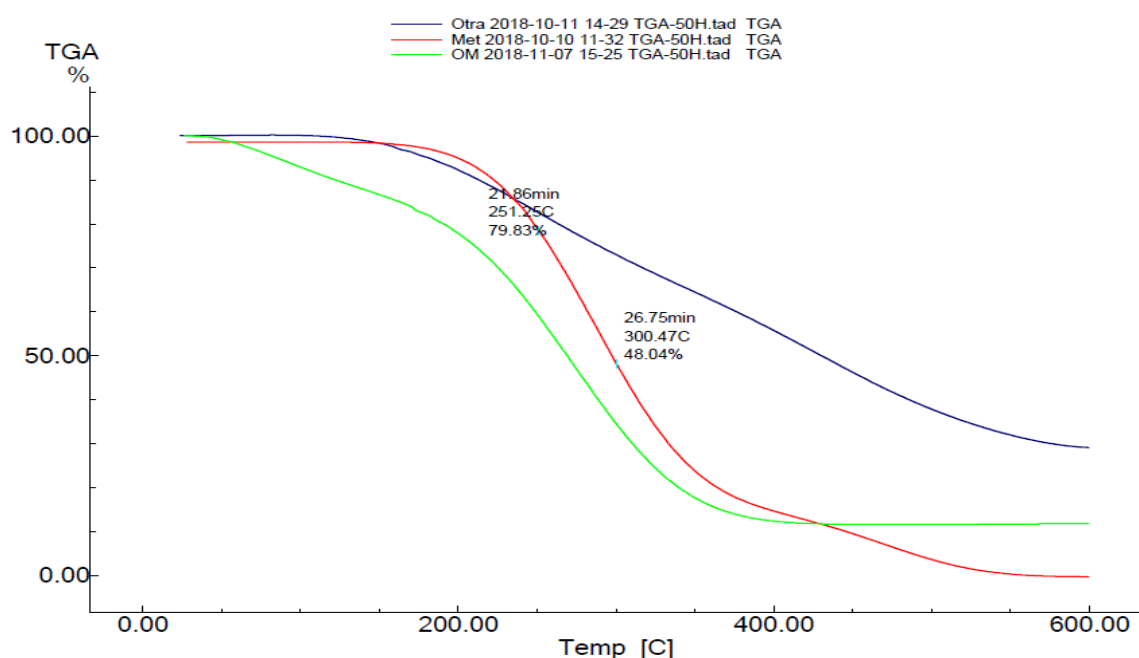
(7) TGA thermogram of the drug complex OM.



(8) Overlaid TGA thermograms of dapagliflozin, olmesartan and the complex OD.



(9) Overlaid TGA thermograms of vildagliptin, olmesartan and the complex OV.



(10) Overlaid TGA thermograms of metformin, olmesartan and the complex OM.

Figure 3.6. TGA thermograms of pure drugs, drug complexes:(1) olmesartan medoxomil, (2) metformin HCl, (3) dapagliflozin, (4) vildagliptin, (5) OD, (6) OV, (7) OM, (8) Overlaid thermograms of dapagliflozin, olmesartan and the complex OD, (9) Overlaid thermograms of vildagliptin, olmesartan and the complex OV, (10) Overlaid thermograms of metformin, olmesartan and the complex OM.

The overlaid TGA thermograms are shown in Figure 3.7 which revealed the different break down patterns of the newly formed complexes.

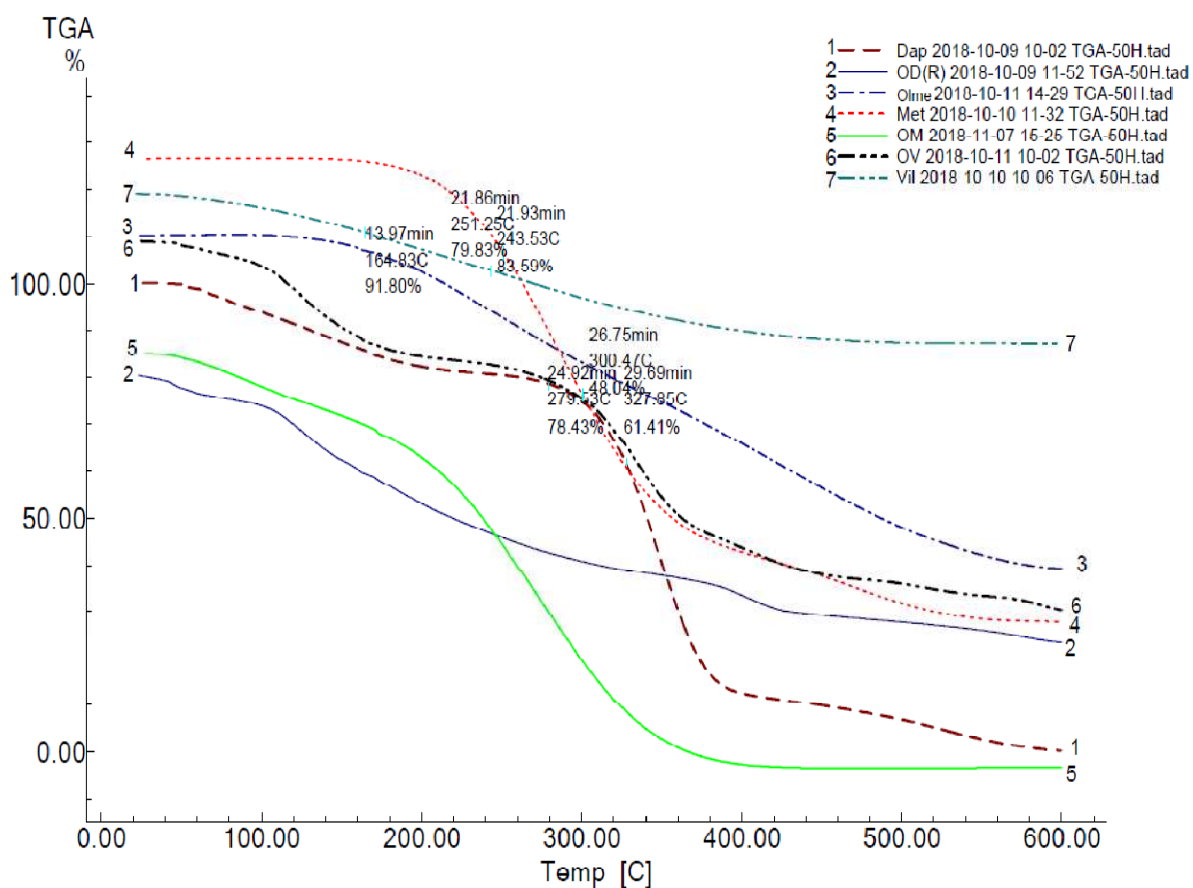


Figure 3.7. Overlaid TGA thermograms of precursor drugs and their complexes.

Olmesartan medoxomil might be fragmented as shown in Figure 3.8 which was also described by Shankar *et al.* (2014). In the TGA thermogram, the drug olmesartanmedoxomil showed 20.17% degradation at 243.53 °C which corresponds to the first step release of medoxomil group from the drug molecule (i.e m/e 558.22 to m/e 444.23) (Figure 3.7). This fragmentation pattern indicated the single entity of the drug.

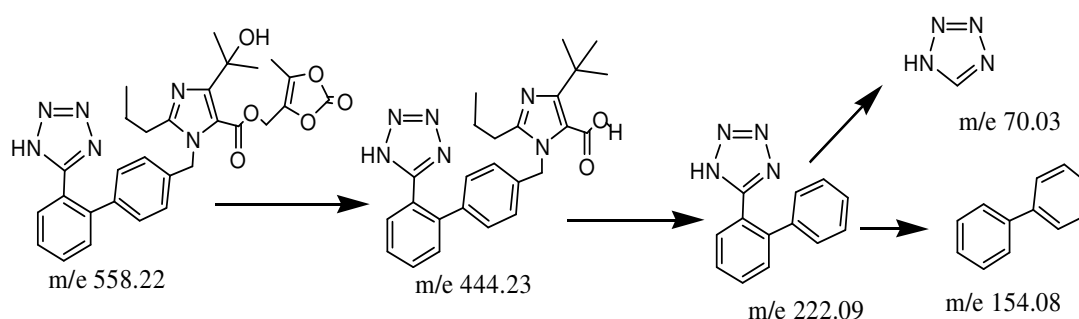


Figure 3.8. Degradation pattern of olmesartan medoxomil.

TGA thermogram also showed 21.57% and 38.59% decomposition of dapagliflozin at 279.53 °C and 327.85 °C, respectively (Figure 3.9) which also previously described by Amit *et al.* (2005).

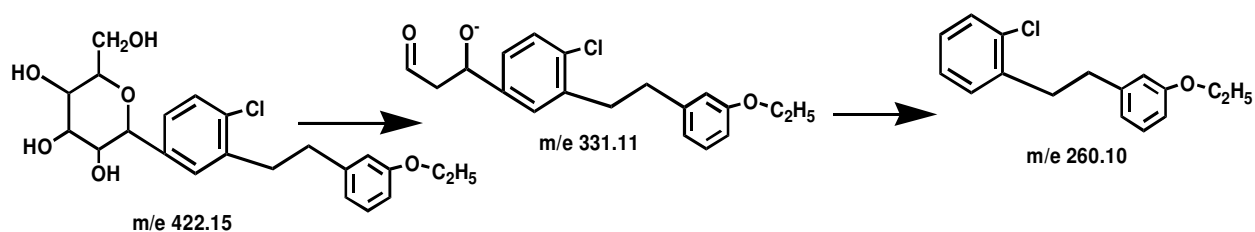


Figure 3.9. Degradation pattern of dapagliflozin.

In TGA thermogram the fragmentation pattern of vildagliptin was also found as 8.18% at 164.83 °C and 16.41% at 243.53 °C which shown in Figure 3.10. This pattern also supported by Neeraj *et al.* (2016).

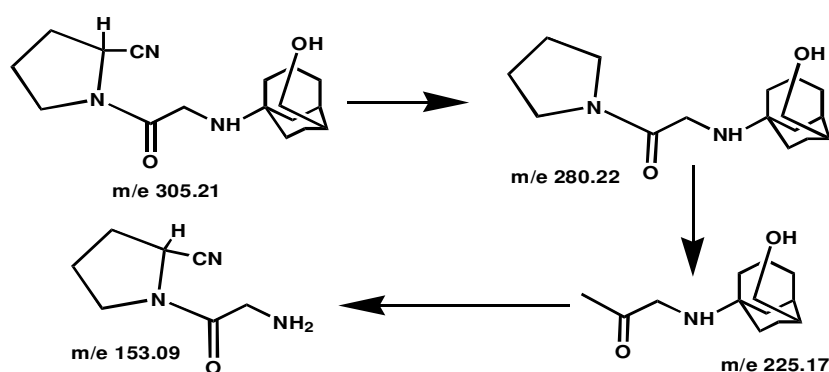


Figure 3.10. Fragmentation pattern of vildagliptin.

Like above mentioned drugs metformin HCl also decomposed 20.08% at 251.25 °C by removal of HCl molecule, and 51.96% fragmentation occurred at 300.47 °C by removal of secondary amide (-NH₂-NH) group which was published by Agarwal *et al.*, (2010) and are shown in Figure 3.11.

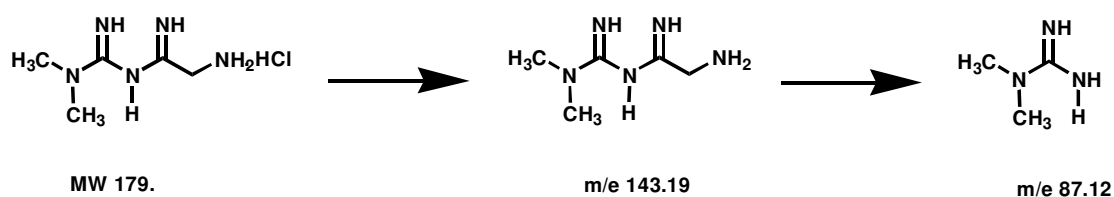


Figure 3.11. Decomposition pattern of metformin HCl.

After drug-drug complexation, the formed compounds also exhibited decomposition patterns which were different from their precursor drugs. The TGA thermogram of the complex OD showed the decomposition at 423.92 °C (50.10%) and 598.22 °C (56.97%) which were found to be different from the parent drugs olmesartan and dapagliflozin. It might be the formation of a different compound OD (Figure 3.7).

Like OD, drug complex OM also exhibited different decomposition patterns than olmesartanmedoxomil and metformin. The 25.31% and 81.32% decompositions of OM occurred at 211.31 °C and 592.70 °C, respectively which were found to be different than that of olmesartan medoxomil and metformin (Figure 3.7) indicating the formation of a new complex.

The drug complex OV also decomposed at 183.59 °C, 300.86 °C and 599 °C by 23.46%, 33.84% and 78.74%, respectively. These decomposition patterns were found to be different from olmesartan medoxomil and vildagliptin indicating the synthesized new molecule as OV (Figure 3.7).The percentage of degradation at different temperature for Olmesartan, dapagliflozin, vildagliptin, metformin, OD, OV and OM is compiled in Table 3.4.

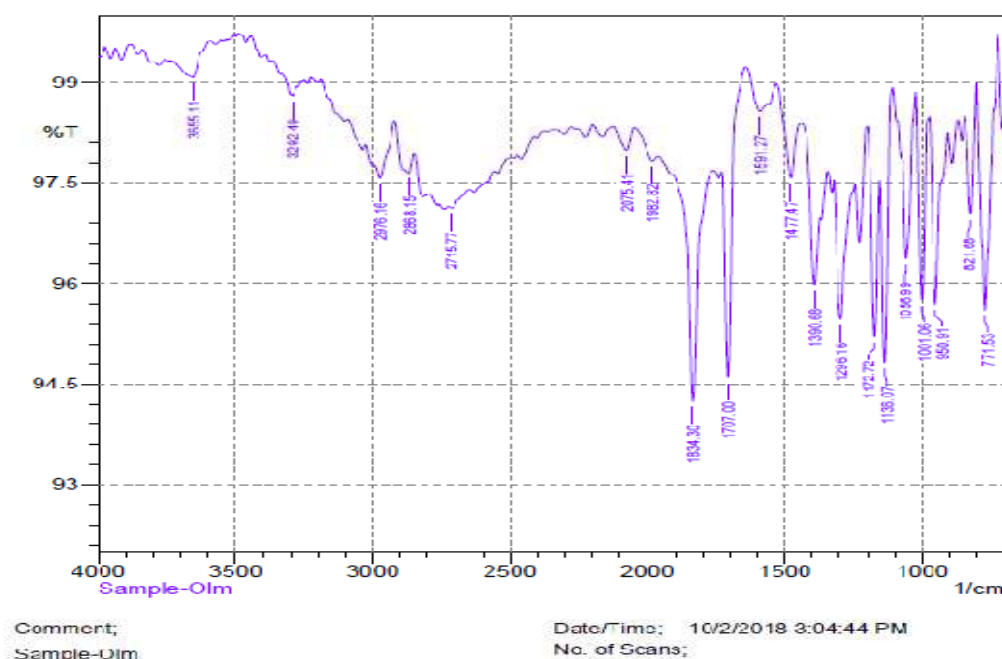
Table 3.4. Percent (%) degradation of drugs and drug complexes from TGA thermograms.

Sample	% degradation with increasing temperature				
	(i)	(ii)	(iii)	(iv)	(v)
Olmesartan	0 at 26.02°C	20.17 at 243.53 °C	48.21 at 418.69°C	64.38 at 516.36°C	71.09 at 599.66°C
Dapagliflozin	0 at 26.02 °C	21.57 at 279.53 °C	38.59 at 327.85 °C	86 at 389.0 °C	99.89 at 599.57 °C
Vildagliptin	0 at 22.02 °C	8.18 at 164.83 °C	16.41 at 243.53 °C	30 at 418.12 °C	31 at 599.65 °C
Metformin	0 at 28.49 °C	20.08 at 251.25 °C	51.96 at 300.47 °C	89.73 at 447.06 °C	98.90 at 599.50 °C
OD	0 at 23.0 °C	7 at 102.93 °C	46.53 at 275.50 °C	50.10 at 423.92 °C	56.97 at 598.22 °C
OV	0 at 27.60 °C	23.46 at 183.59 °C	33.84 at 300.86 °C	49.82 at 474.99 °C	78.74 at 599 °C
OM	0 at 27.07 °C	25.31 at 211.31 °C	63.70 at 276.21 °C	81.32 at 592.70 °C	88.42 at 599.64 °C

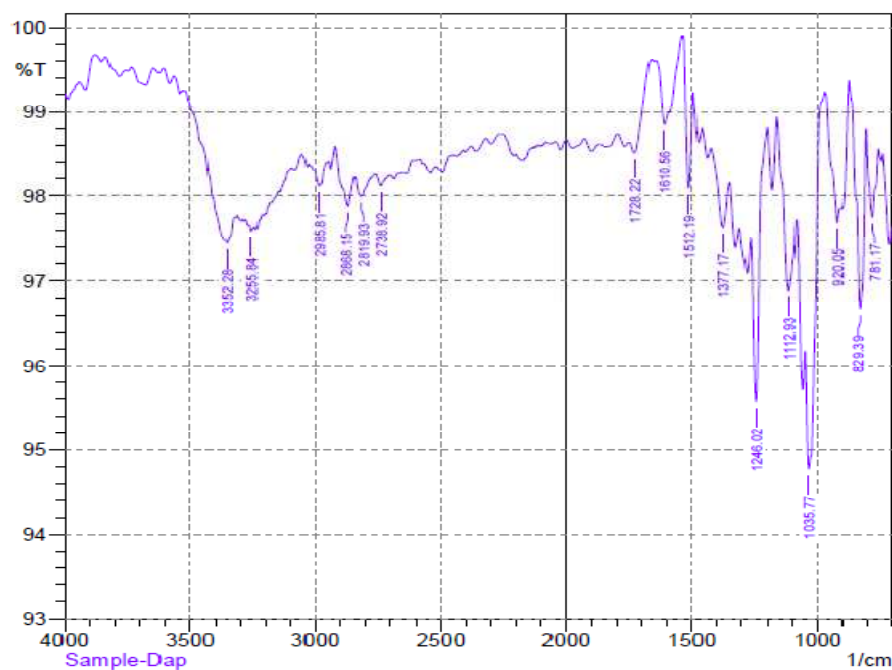
3.1.6. Analysis of drugs and drug complexes by FT-IR

Specific functional group of organic molecules can be determined from the spectra of FT-IR. If the IR spectra of two or more compounds become identical, it indicates the same compounds.

Likewise, any change or disappearance of signals indicates the different molecule(s). After drug-drug interactions the complexes were subjected to IR analysis and the spectra were found to be different in comparison to their precursor drugs indicating the formation of different molecules. The peaks obtained at 3655.11 cm^{-1} , 3352.28 cm^{-1} , 3741 cm^{-1} in the FT-IR spectra of olmesartan medoxomil, dapagliflozin, vildagliptin, respectively indicated the presence of the OH group stretching. But the above mentioned stretching peaks of OH group were disappeared from the spectra of FT-IR of OD and OV. On the other hand, characteristic single peak at 3410.15 cm^{-1} and 3414 cm^{-1} were obtained in the IR spectra of OD and OV, respectively. Similarly, characteristic stretching peak for -NH_2 group of metformin shifted from 3742.93 cm^{-1} to 3232.75 cm^{-1} in the spectrum of OM (Figure 3.12) which indicated the formation of a complex between the two drugs (Aktar *et al.*, 2019).



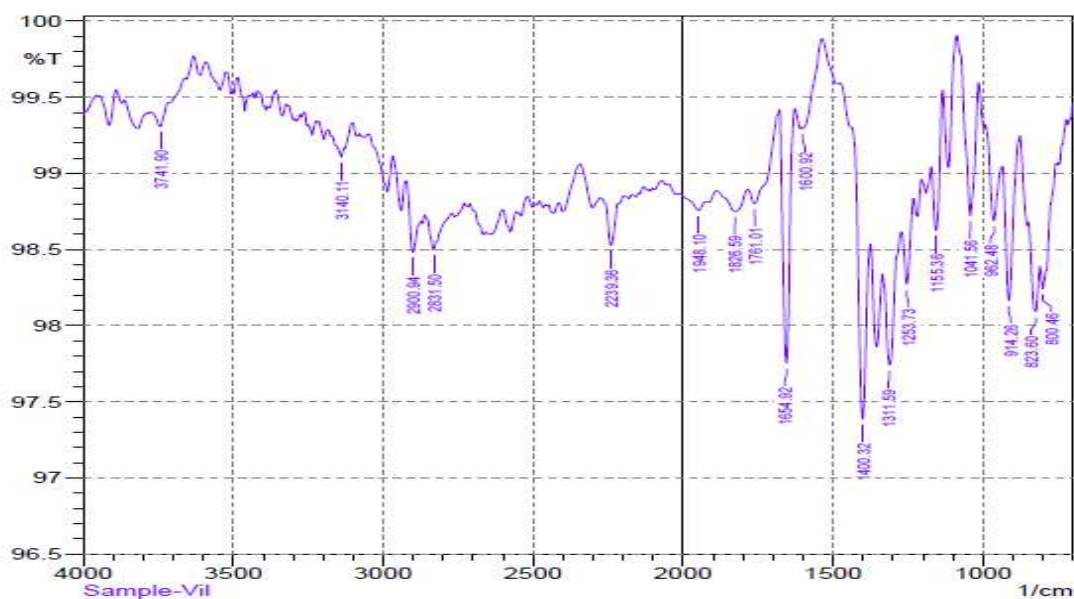
(1) FT-IR spectrum of the drug olmesartan medoxomil.



Comment;
Sample-Dap

Date/Time: 10/2/2018 3:11:33 PM
No. of Scans;

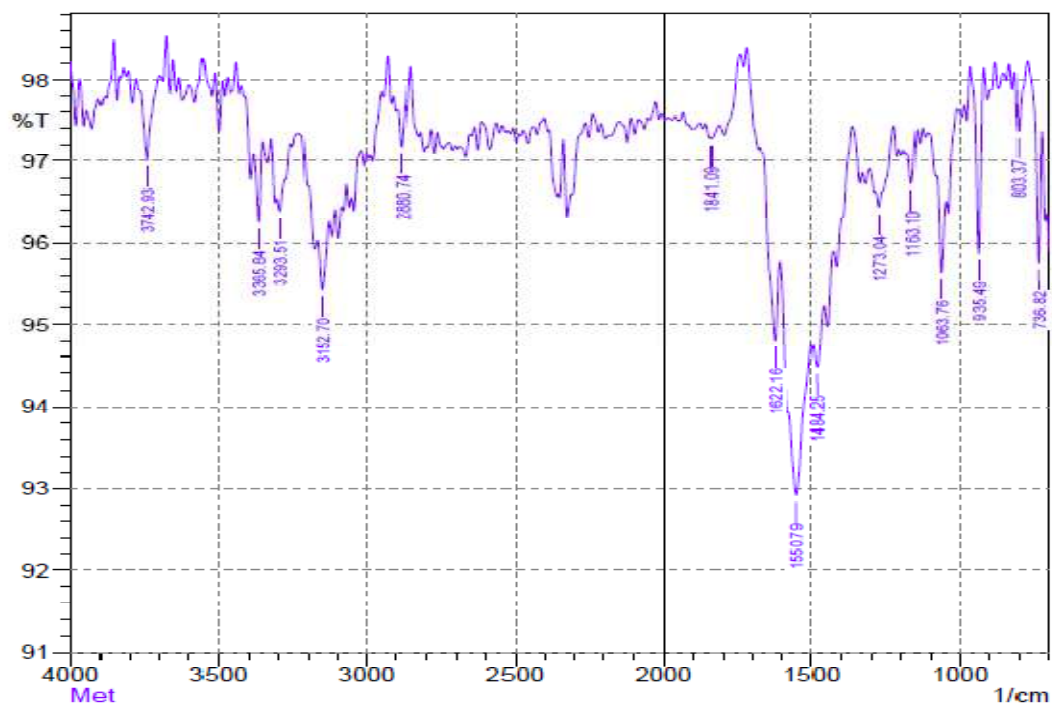
(2) FT-IR spectrum of dapagliflozin.



Comment;
Sample-Vil

Date/Time: 10/2/2018 2:55:02 PM
No. of Scans;

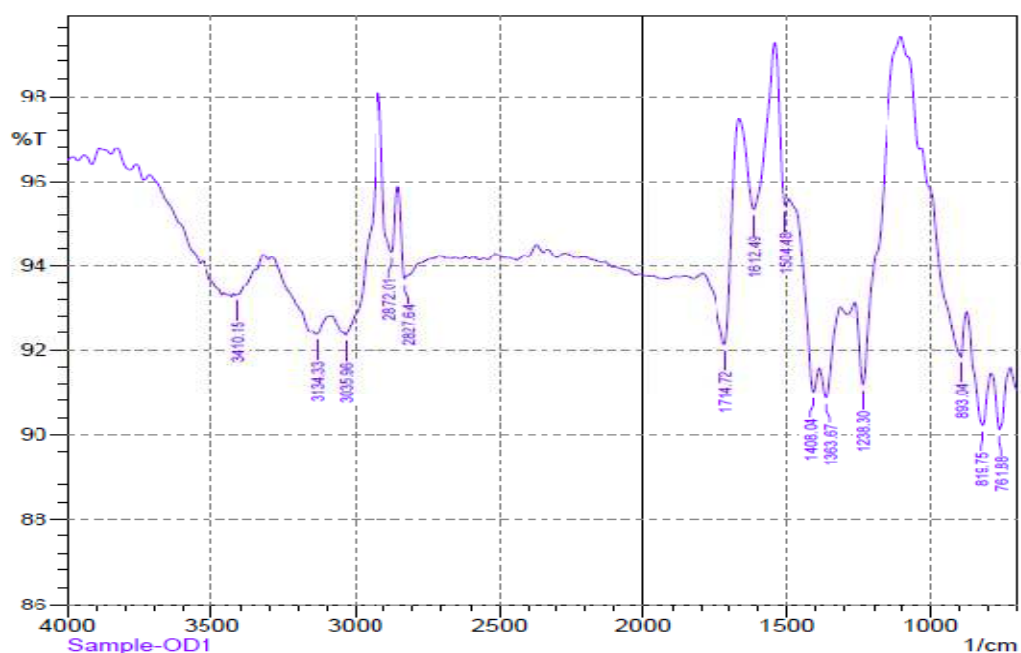
(3) FT-IR spectrum of vildagliptin.



Comment:
Met

Date/Time: 12/24/2018 12:13:11 PM
No. of Scans;

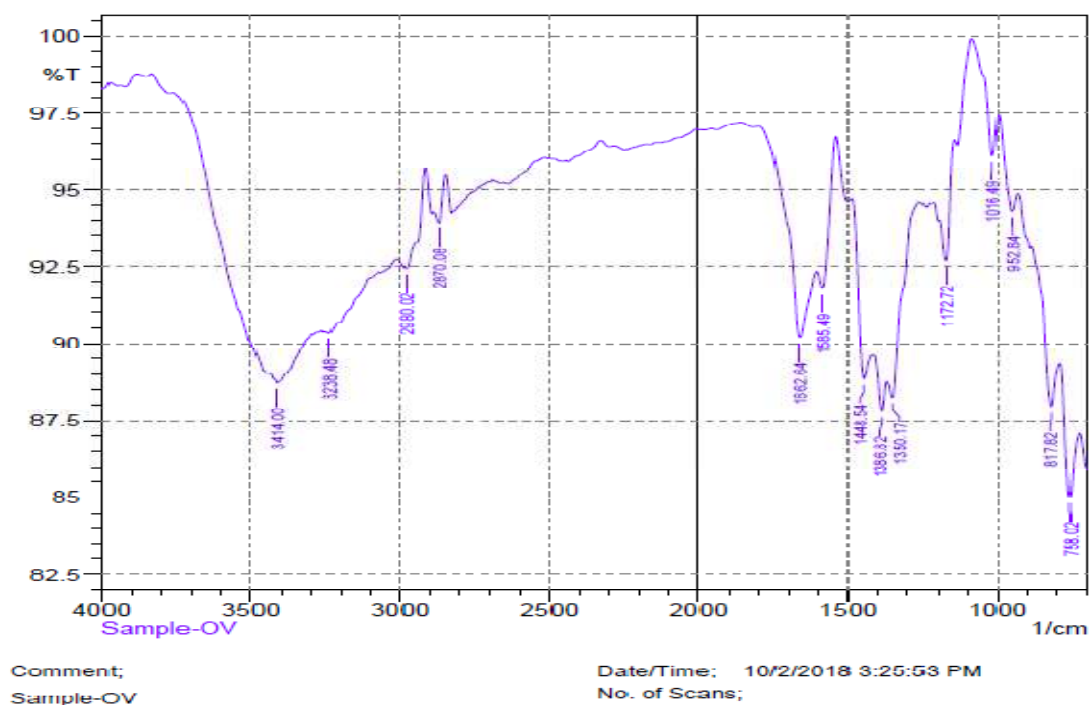
(4) FT-IR spectrum of metformin HCl.



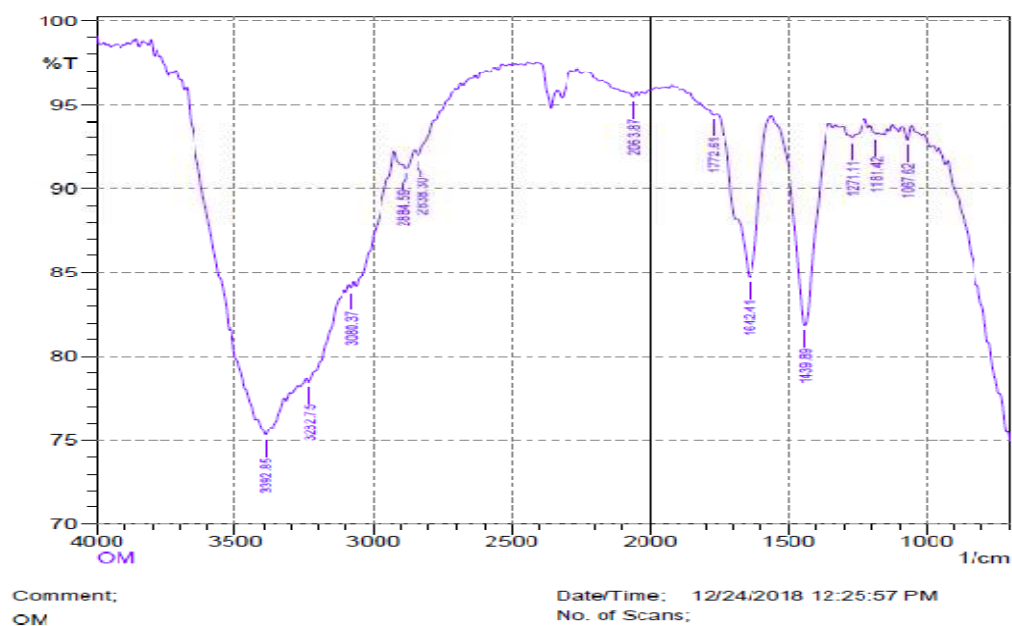
Comment:
Sample-OD1

Date/Time: 10/2/2018 3:32:39 PM
No. of Scans;

(5) FT-IR spectrum of complex OD.



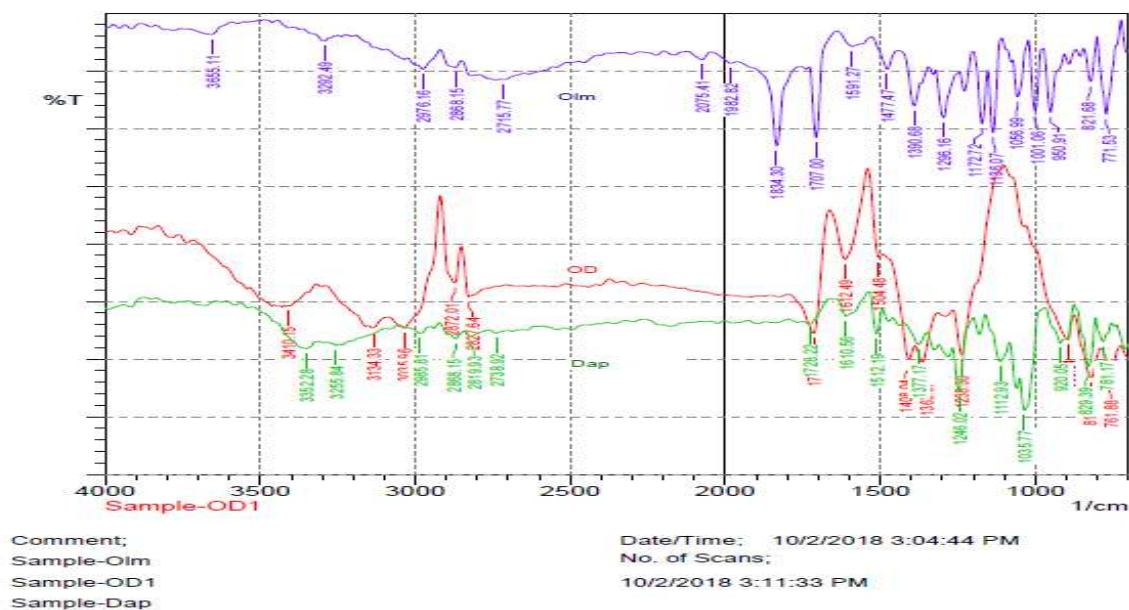
(6) FT-IR spectrum of complex OV.



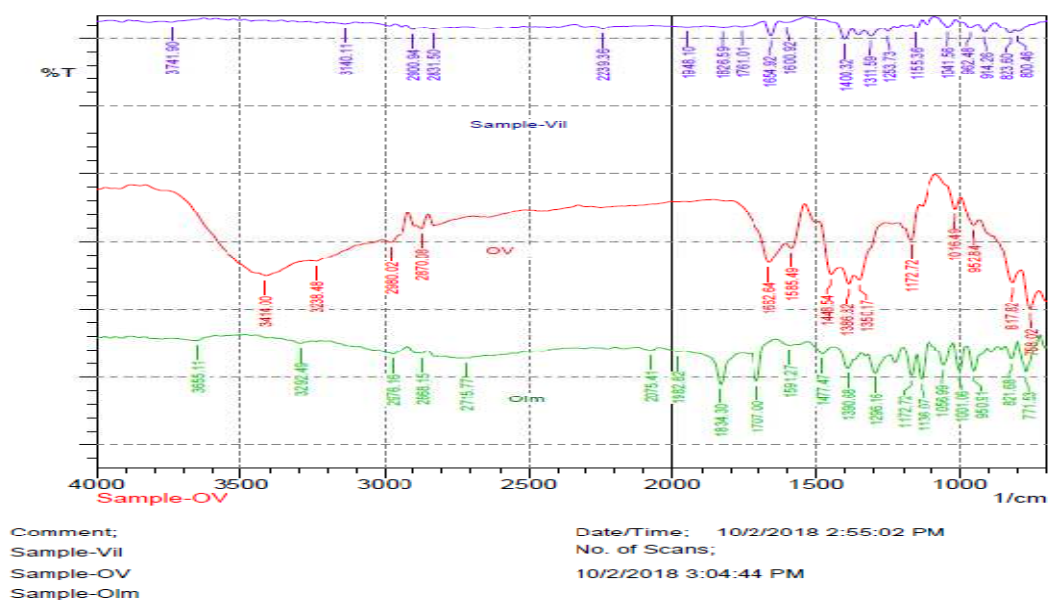
(7) FT-IR spectrum of complex OM.

Figure 3.12. FT-IR spectra of pure drugs and complexes: (1) olmesartan medoxomil, (2) dapagliflozin, (3) vildagliptin, (4) metformin HCl, (5) OD, (6) OV and (7) OM.

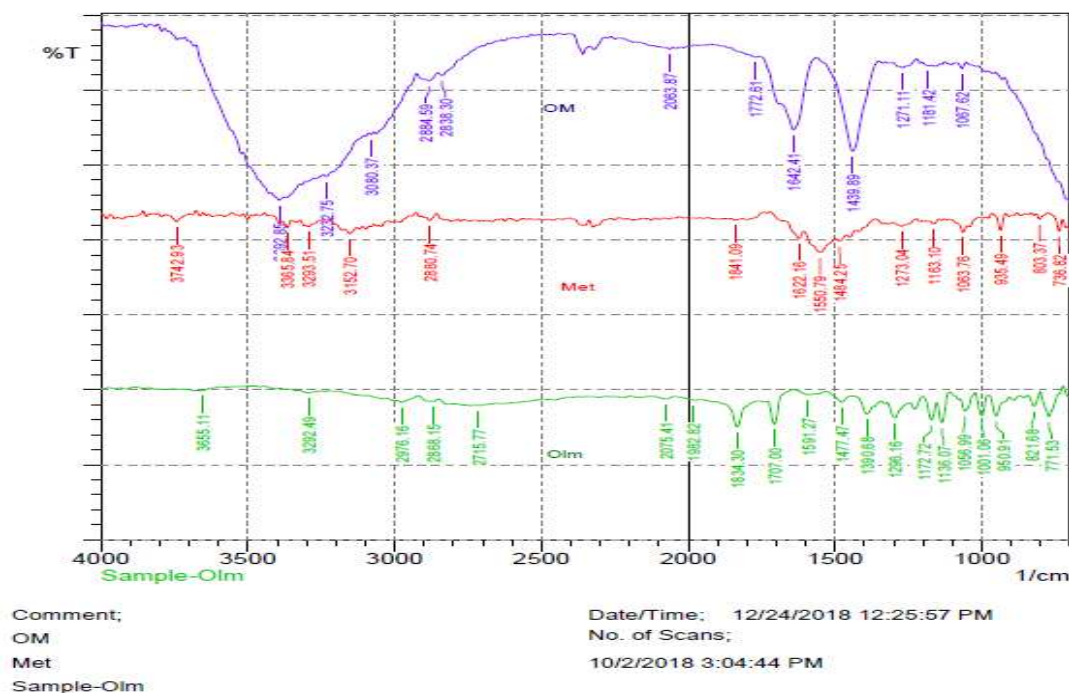
Overlaid FT-IR spectra implies the results in Figure 3.13.



(1) Overlaid FT-IR spectra of olmesartan medoxomil, dapagliflozin and complex OD.



(2) Overlaid FT-IR spectra of olmesartan medoxomil, vildagliptin and complex OV.



(3) Overlaid FT-IR spectra of olmesartan medoxomil, metformin and complex OM.

Figure 3.13. Overlaid FT-IR spectra of olmesartanmedoxomil and its complexes: (1) olmesartan medoxomil, dapagliflozin and complex OD, (2) olmesartan medoxomil, vildagliptin and complex OV, (3) olmesartan medoxomil, metformin and complex OM.

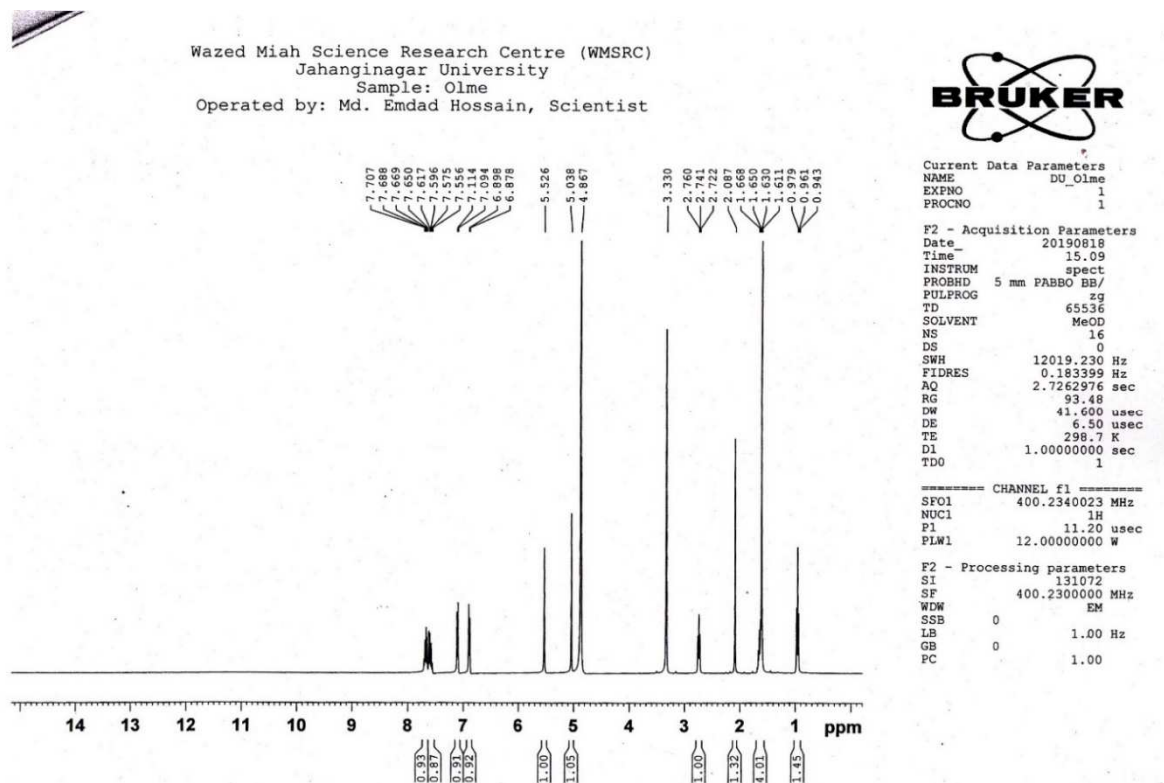
3.1.7. ^1H NMR spectra of parent drug and drug complexes

No attempt was taken for in-depth analysis of the spectral data. The main objective of acquiring the ^1H NMR spectra of the drugs and complexes was to see the differences in the spectral patterns between the parent drug(s) and the corresponding synthesized complex(es). Careful analysis of the ^1H NMR spectra demonstrated that differences could be seen between the spectra of the parent drug and synthesized complex. This was only to show that complexes were formed which was further supported by TLC, TGA, DSC and FTIR analyses.

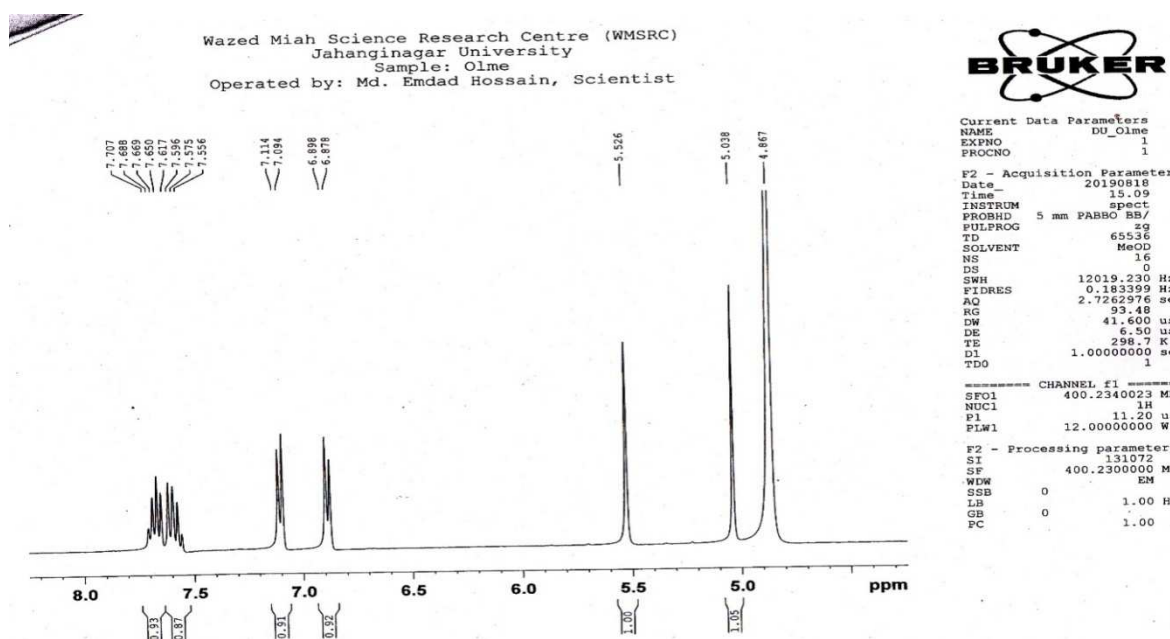
^1H NMR of the reference drugs, drug-drug solid mixture interaction without solvent and the newly synthesized drug complexes were recorded to compare if complexation happened or not. The newly formed drug complexes were found impure with unreacted individual drugs.

So, to study the detailed structure of the new complexes further purifications have been suggested. In (Figure 3.14.) the ^1H NMR spectra of olmesartan medoxomil,

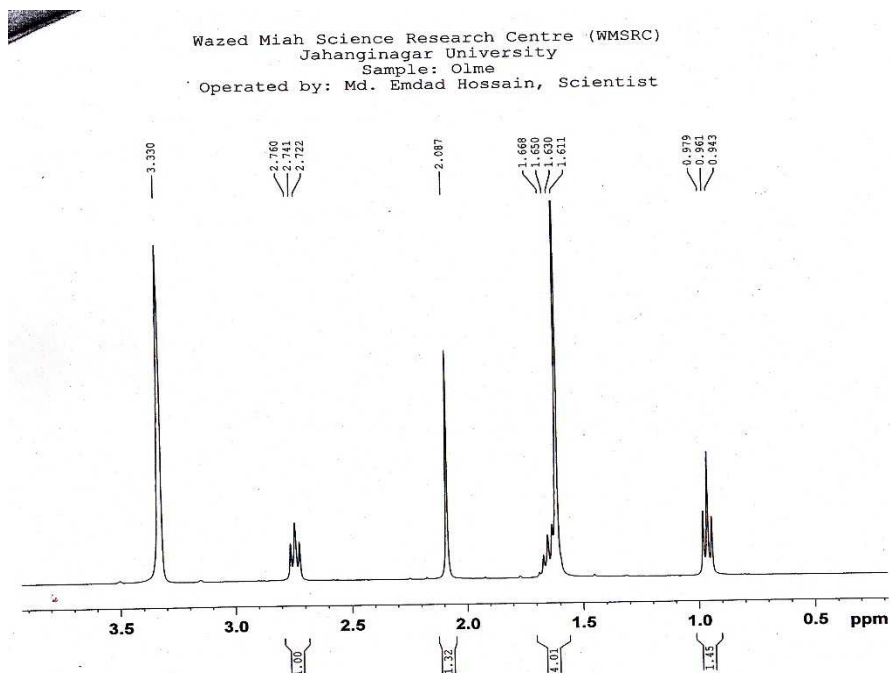
dapagliflozin, their unreacted mixture and the new complex OD have been shown. ^1H NMR spectrum of olmesartan medoxomil, vildagliptin, their unreacted mixture and the new complex OV have been shown in Figure 3.15. In Figure 3.16, the ^1H NMR spectra of olmesartan medoxomil, metformin, their unreacted mixture and their new complex OM have been shown.



(1) NMR of olmesartan medoxomil.

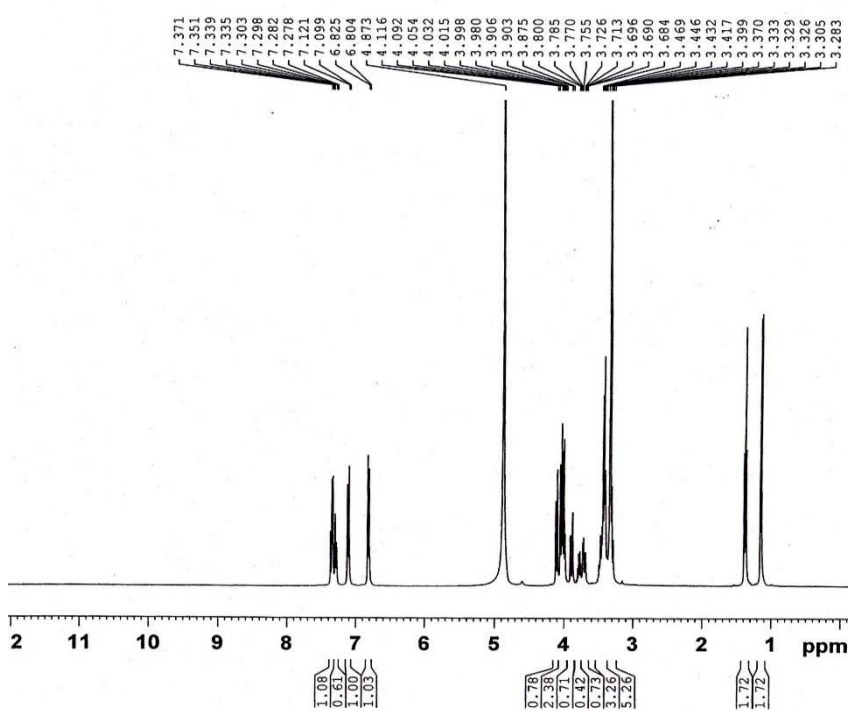


(2) NMR of olmesartan medoxomil.



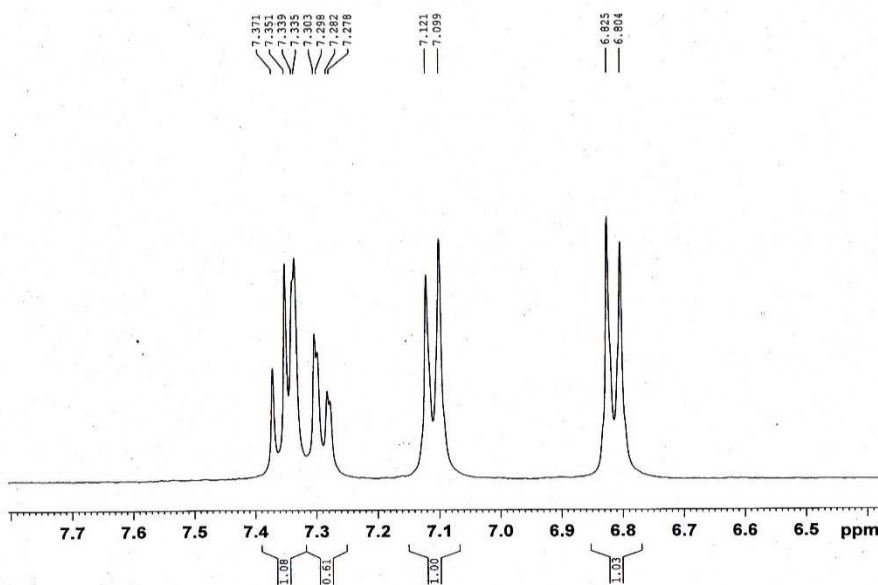
(3) NMR of olmesartan medoxomil.

Wazed Miah Science Research Centre (WMSRC)
Jahangirnagar University
Sample: Dapa
Operated by: Md. Emdad Hossain, Scientist



(4) NMR of dapagliflozin.

Wazed Miah Science Research Centre (WMSRC)
 Jahanginagar University
 Sample: Dapa
 Operated by: Md. Emdad Hossain, Scientist



Current Data Parameters
 NAME DU_Dapa
 EXPNO 1
 PROCNO 1

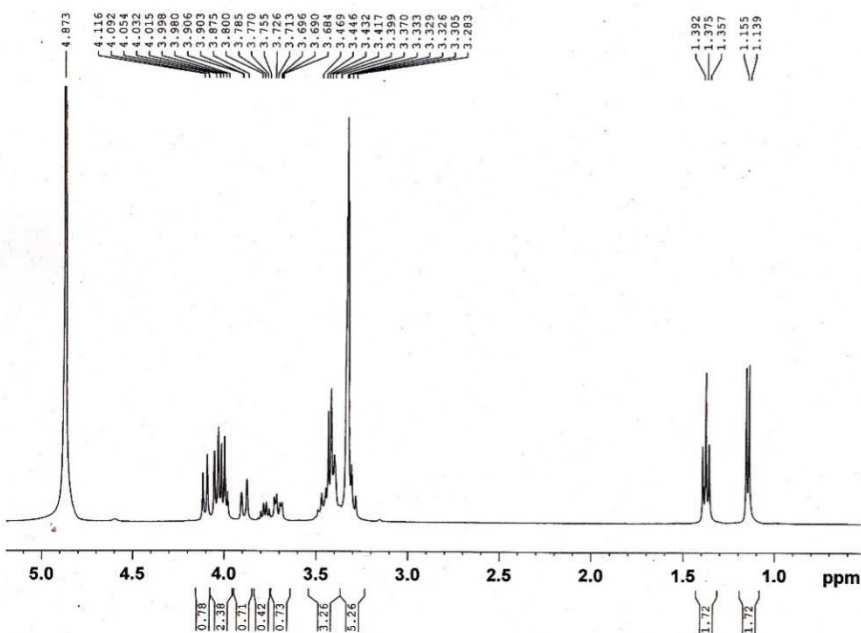
F2 - Acquisition Parameters
 Date_ 20190818
 Time 15.04
 INSTRUM spect
 PROBHD 5 mm PABBO BB/
 PULPROG zg
 TD 65536
 SOLVENT MeOD
 NS 16
 DS 0
 SWH 12019.230 Hz
 FIDRES 0.183399 Hz
 AQ 2.7262976 sec
 RG 133.94
 DW 41.600 usec
 DE 6.50 usec
 TE 298.5 K
 D1 1.00000000 sec
 TDO 1

===== CHANNEL f1 =====
 SF01 400.2340023 MHz
 NUC1 1H
 P1 11.20 usec
 PLW1 12.00000000 W

F2 - Processing parameters
 SI 131072
 SF 400.2300000 MHz
 WDW EM
 SSB 0
 LB 1.00 Hz
 GB 0
 PC 1.00

(5) NMR of dapagliflozin.

Wazed Miah Science Research Centre (WMSRC)
 Jahanginagar University
 Sample: Dapa
 Operated by: Md. Emdad Hossain, Scientist



Current Data Parameters
 NAME DU_Dapa
 EXPNO 1
 PROCNO 1

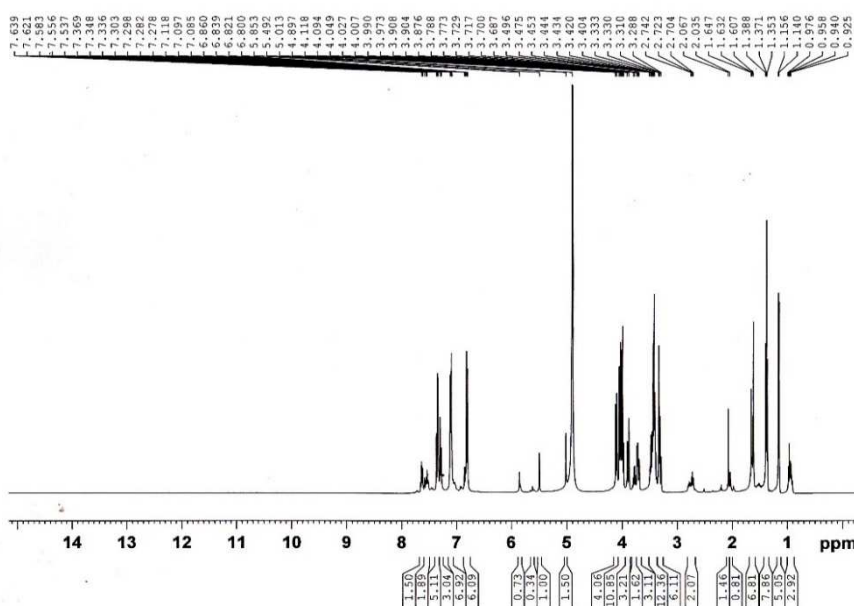
F2 - Acquisition Parameters
 Date_ 20190818
 Time 15.04
 INSTRUM spect
 PROBHD 5 mm PABBO BB/
 PULPROG zg
 TD 65536
 SOLVENT MeOD
 NS 16
 DS 0
 SWH 12019.230 Hz
 FIDRES 0.183399 Hz
 AQ 2.7262976 sec
 RG 133.94
 DW 41.600 usec
 DE 6.50 usec
 TE 298.5 K
 D1 1.00000000 sec
 TDO 1

===== CHANNEL f1 =====
 SF01 400.2340023 MHz
 NUC1 1H
 P1 11.20 usec
 PLW1 12.00000000 W

F2 - Processing parameters
 SI 131072
 SF 400.2300000 MHz
 WDW EM
 SSB 0
 LB 1.00 Hz
 GB 0
 PC 1.00

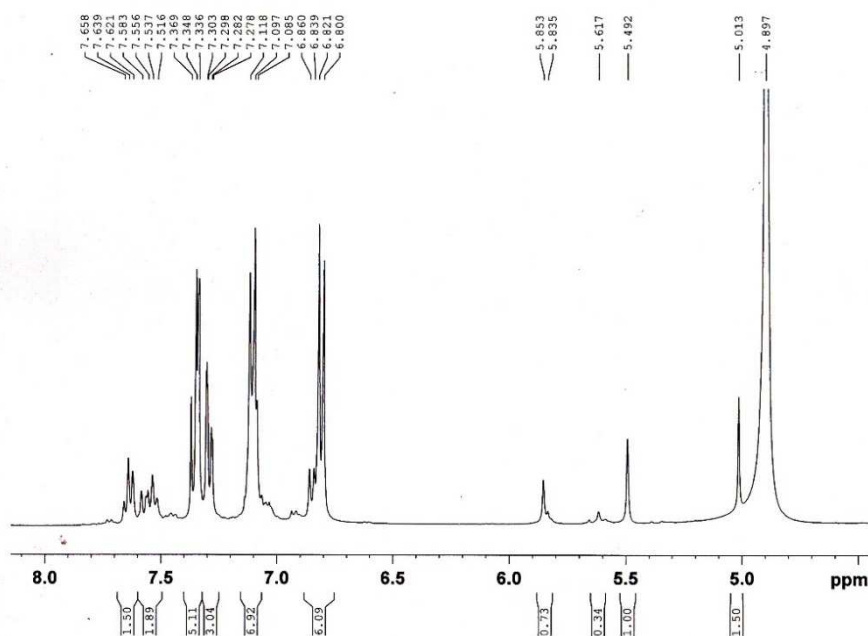
(6) NMR of dapagliflozin.

Wazed Miah Science Research Centre (WMSRC)
Jahangirnagar University
Sample: OD
Operated by: Md. Emdad Hossain, Scientist



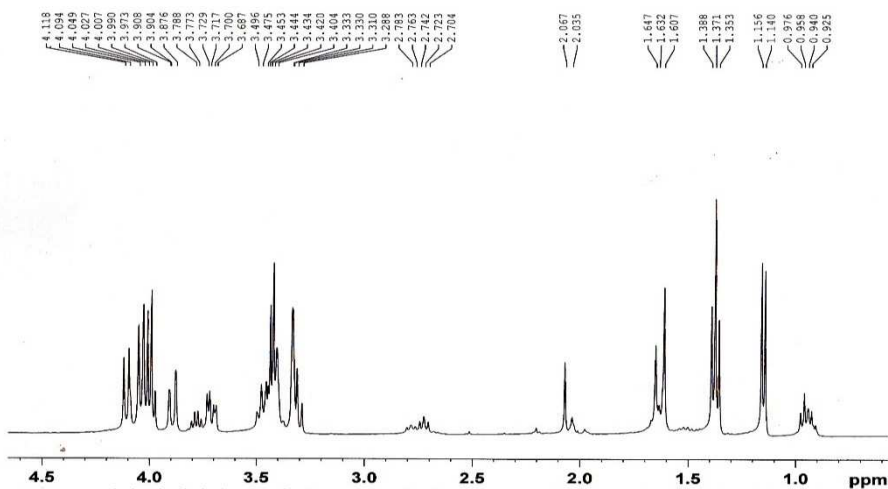
(7) NMR of complex OD.

Wazed Miah Science Research Centre (WMSRC)
Jahangirnagar University
Sample: OD
Operated by: Md. Emdad Hossain, Scientist



(8) NMR of complex OD.

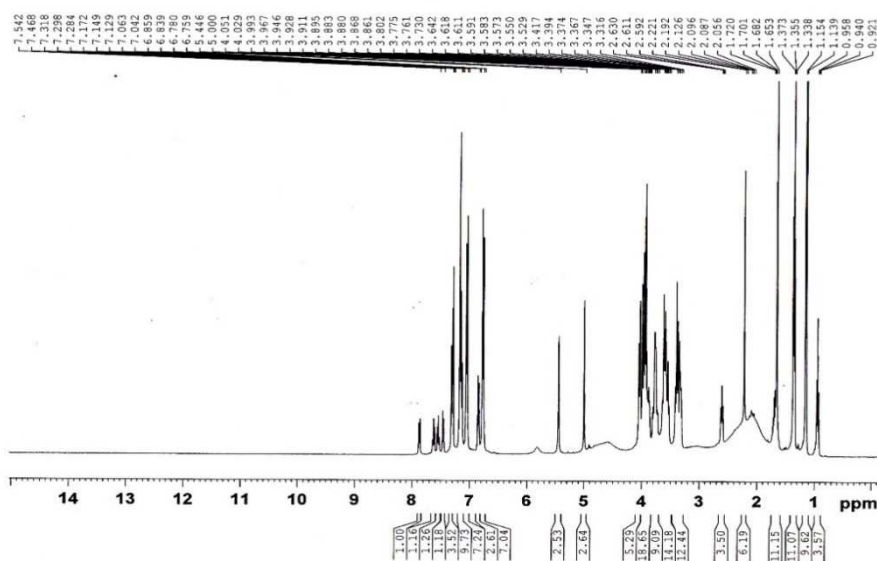
Wazed Miah Science Research Centre (WMSRC)
 Jahangirnagar University
 Sample: OD
 Operated by: Md. Emdad Hossain, Scientist



Current Data Parameters
 NAME DU_OD
 EXPNO 1
 PROCNO 1
 F2 - Acquisition Parameter
 Date 20191022
 Time 12.37
 INSTRUM spect
 PROBHD 5 mm PABBO BB/
 PULPROG zg
 TD 65536
 SOLVENT MeOH
 NS 16
 DS 0
 SWH 12019.230 Hz
 FIDRES 0.183399 Hz
 AQ 2.7262976 Hz
 RG 58.24
 DW 41.600 us
 DE 6.50 us
 TE 297.0 K
 D1 1.00000000 sec
 TDO 1
 ===== CHANNEL f1 =====
 SFO1 400.2340023 MHz
 NUC1 1H
 P1 11.20 us
 PLW1 12.00000000 W
 F2 - Processing parameters
 SI 131072
 SF 400.2300000 MHz
 WDW EM
 SSB 0
 LB 1.00 Hz
 GB 0
 PC 1.00

(9) NMR of complex OD.

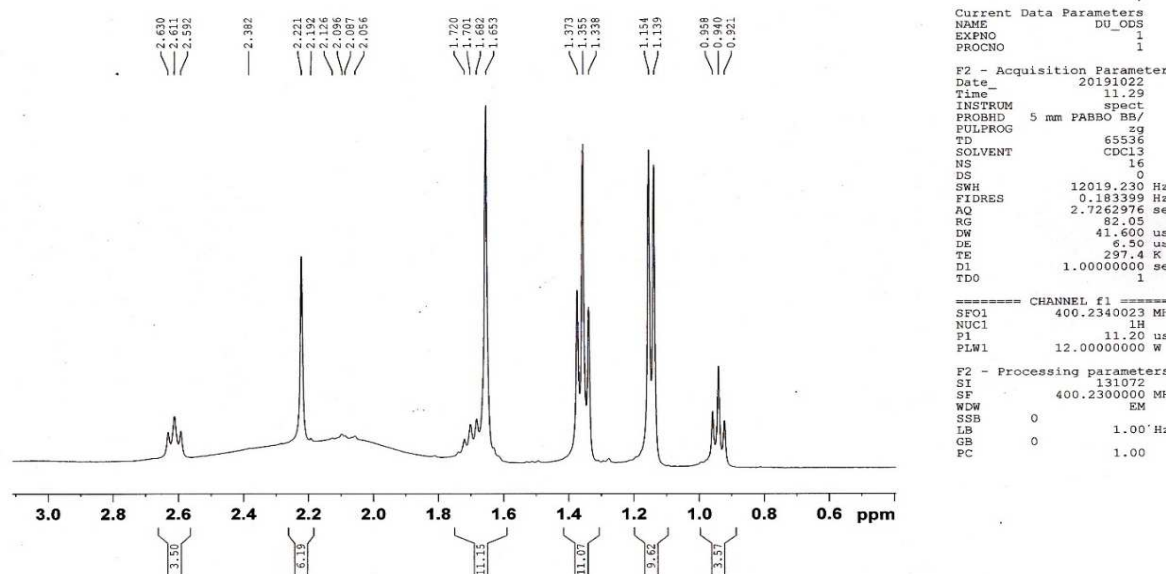
Wazed Miah Science Research Centre (WMSRC)
 Jahangirnagar University
 Sample: ODS
 Operated by: Md. Emdad Hossain, Scientist



Current Data Parameters
 NAME DU_ODS
 EXPNO 1
 PROCNO 1
 F2 - Acquisition Parameters
 Date 20191022
 Time 11.29
 INSTRUM spect
 PROBHD 5 mm PABBO BB/
 PULPROG zg
 TD 65536
 SOLVENT CDC13
 NS 16
 DS 0
 SWH 12019.230 Hz
 FIDRES 0.183399 Hz
 AQ 2.7262976 sec
 RG 82.05
 DW 41.600 usec
 DE 6.50 usec
 TE 297.4 K
 D1 1.00000000 sec
 TDO 1
 ===== CHANNEL f1 =====
 SFO1 400.2340023 MHz
 NUC1 1H
 P1 11.20 usec
 PLW1 12.00000000 W
 F2 - Processing parameters
 SI 131072
 SF 400.2300000 MHz
 WDW EM
 SSB 0
 LB 1.00 Hz
 GB 0
 PC 1.00

(10) NMR of unreacted solid mixture of olmesartan and dapagliflozin.

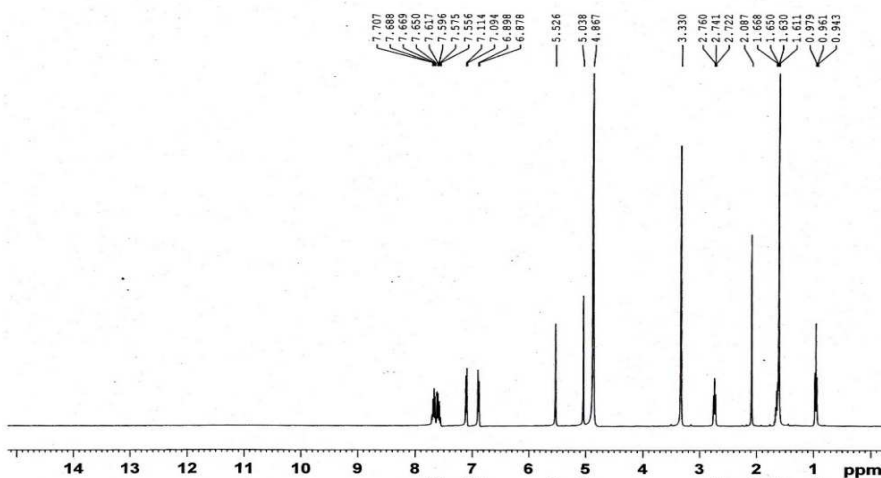
Wazed Miah Science Research Centre (WMSRC)
 Jahangirnagar University
 Sample: ODS
 Operated by: Md. Emdad Hossain, Scientist



(11) NMR of unreacted solid mixture of olmesartan and dapagliflozin.

Figure 3.14. NMR spectra of olmesartanmedoxomil (1-3), dapagliflozin (4-6), reacted complex OD (7-9) and unreacted solid mixture of olmesartanmedoxomil and dapagliflozin (10-11).

Wazed Miah Science Research Centre (WMSRC)
Jahangirnagar University
Sample: Olme
Operated by: Md. Emdad Hossain, Scientist



Current Data Parameters
NAME DU_Olme
EXPNO 1
PROCNO 1

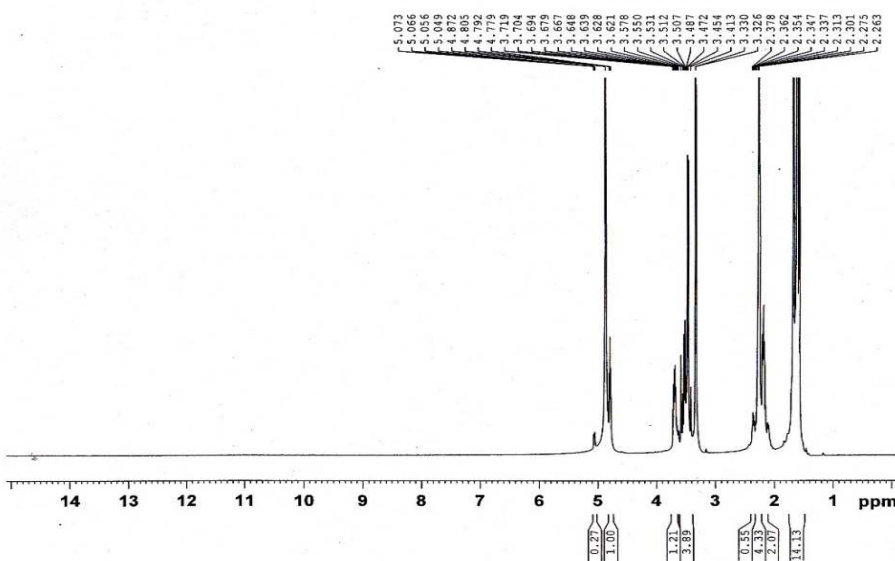
F2 - Acquisition Parameters
Date_ 20190818
Time 15.09
INSTRUM spect
PROBHD 5 mm PABBO BB/
PULPROG zg
TD 65536
SOLVENT MeOD
NS 16
DS 0
SWH 12019.230 Hz
FIDRES 0.183399 Hz
AQ 2.7262976 sec
RG 93.48
DE 41.600 use
TE 298.7 K
D1 1.00000000 sec
TDO 1

CHANNEL f1
SF01 400.2340023 MHz
NUC1 1H
P1 11.20 use
PLW1 12.00000000 W

F2 - Processing parameters
SI 131072
SF 400.2300000 MHz
WDW EM
SSB 0
LB 1.00 Hz
GB 0
PC 1.00

(12) NMR of olmesartan medoxomil.

Wazed Miah Science Research Centre (WMSRC)
Jahangirnagar University
Sample: Vilda
Operated by: Md. Emdad Hossain, Scientist



Current Data Parameters
NAME DU_Vilda
EXPNO 1
PROCNO 1

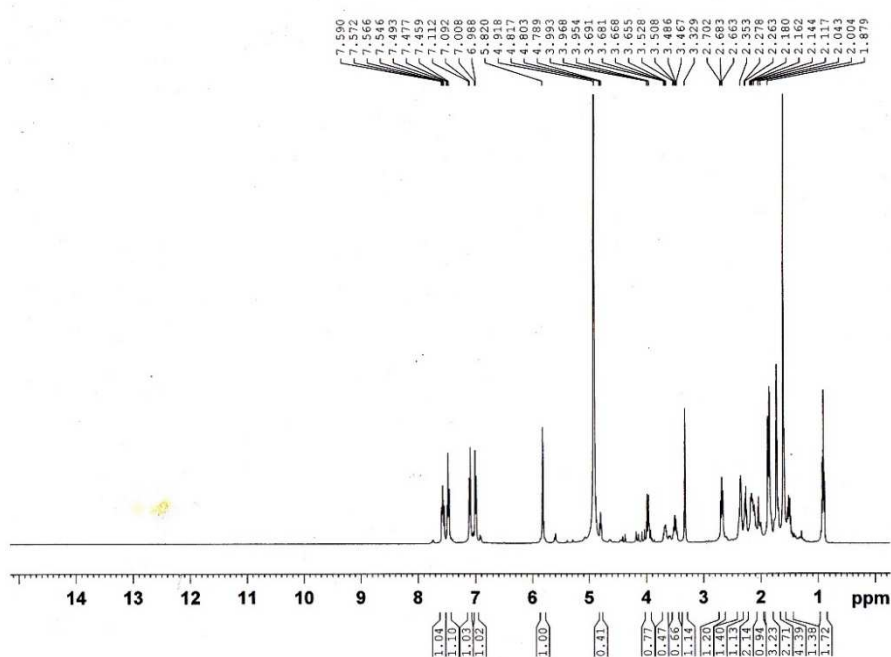
F2 - Acquisition Parameters
Date_ 20190818
Time 14.52
INSTRUM spect
PROBHD 5 mm PABBO BB/
PULPROG zg
TD 65536
SOLVENT MeOD
NS 16
DS 0
SWH 12019.230 Hz
FIDRES 0.183399 Hz
AQ 2.7262976 sec
RG 133.94
DE 41.600 Hz
TE 298.5 K
D1 1.00000000 sec
TDO 1

CHANNEL f1
SF01 400.2340023 MHz
NUC1 1H
P1 11.20 use
PLW1 12.00000000 W

F2 - Processing parameters
SI 131072
SF 400.2300000 MHz
WDW EM
SSB 0
LB 1.00 Hz
GB 0
PC 1.00

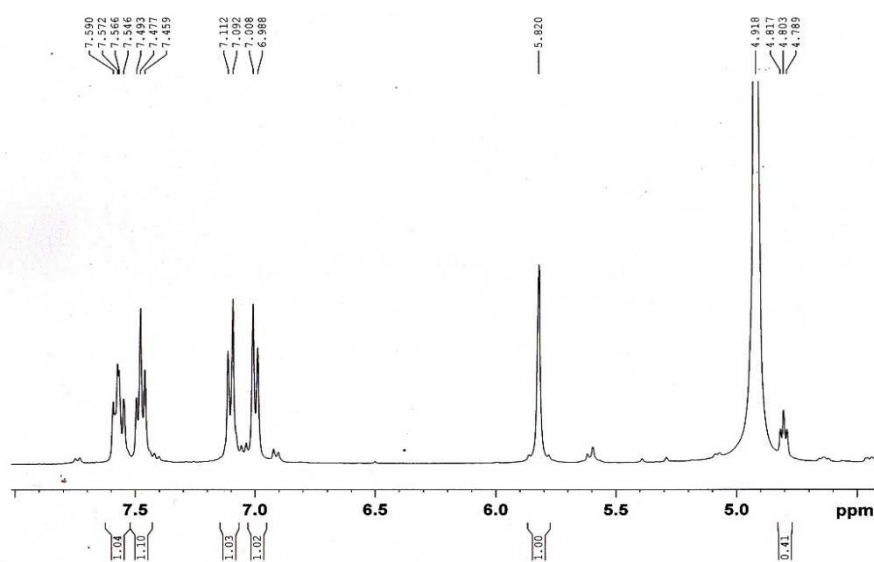
(13) NMR of vildagliptin.

Wazed Miah Science Research Centre (WMSRC)
 Jahanginagar University
 Sample: OV
 Operated by: Md. Emdad Hossain, Scientist



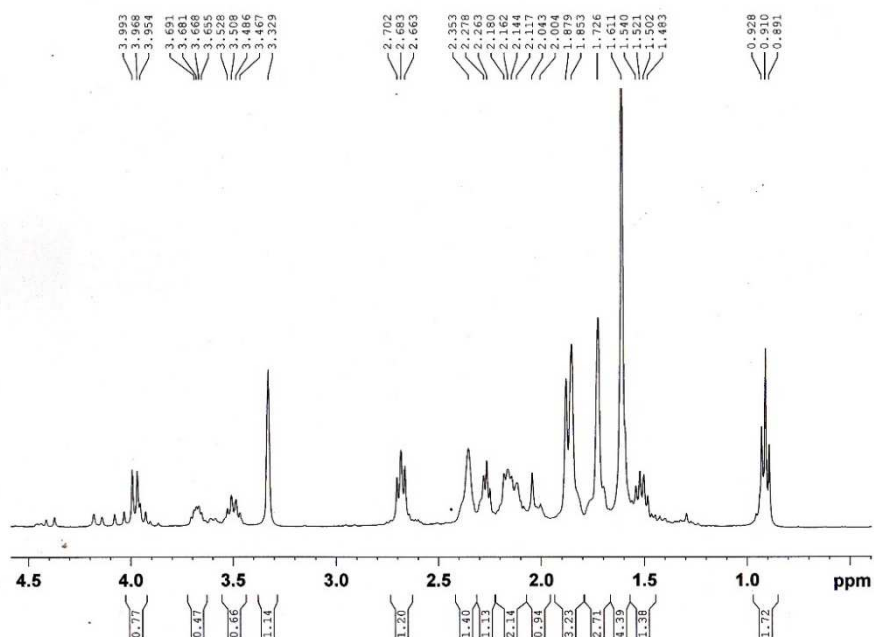
(14) NMR of complex OV.

Wazed Miah Science Research Centre (WMSRC)
 Jahanginagar University
 Sample: OV
 Operated by: Md. Emdad Hossain, Scientist



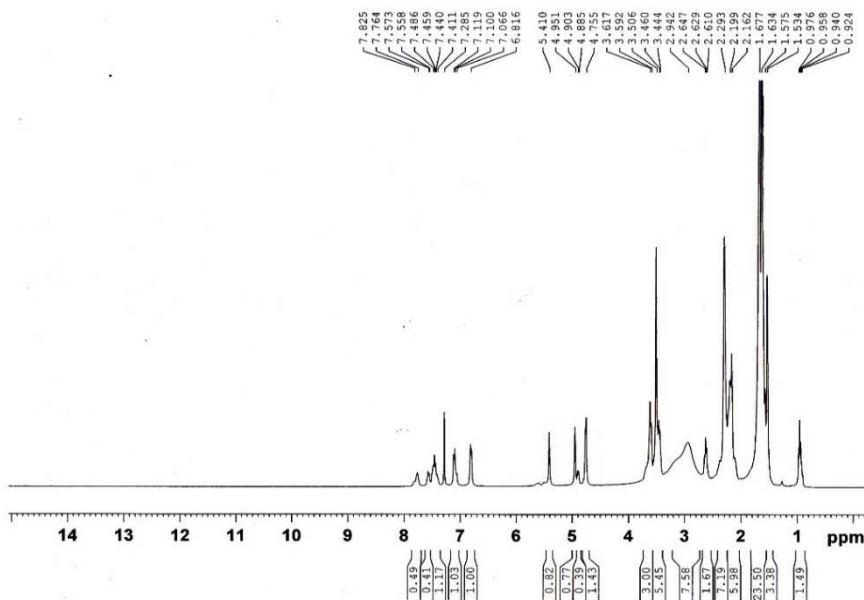
(15) NMR of complex OV.

Wazed Miah Science Research Centre (WMSRC)
 Jahanginagar University
 Sample: OV
 Operated by: Md. Emdad Hossain, Scientist

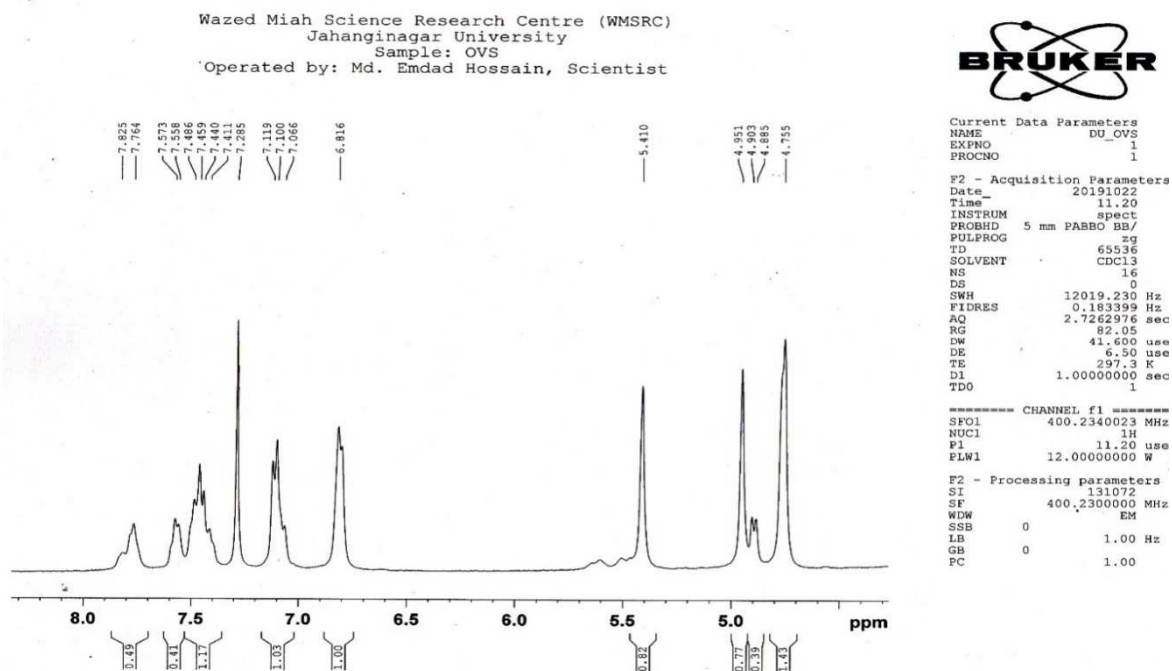


(16) NMR of complex OV.

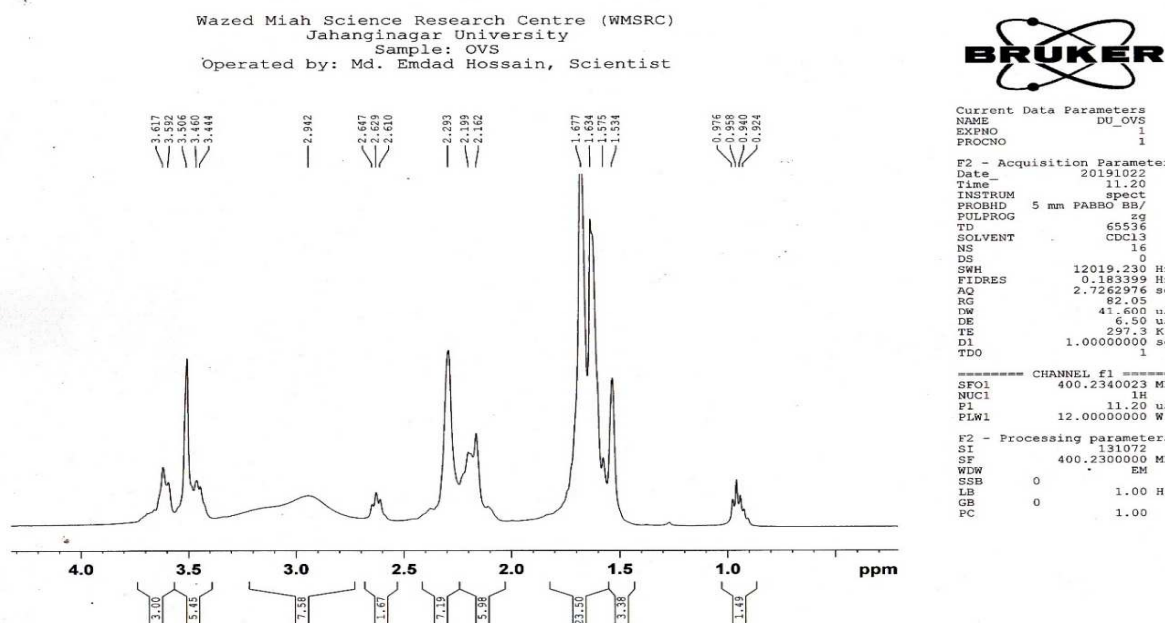
Wazed Miah Science Research Centre (WMSRC)
 Jahanginagar University
 Sample: OVS
 Operated by: Md. Emdad Hossain, Scientist



(17) NMR of solid mixture of unreacted olmesartan and vildagliptin.



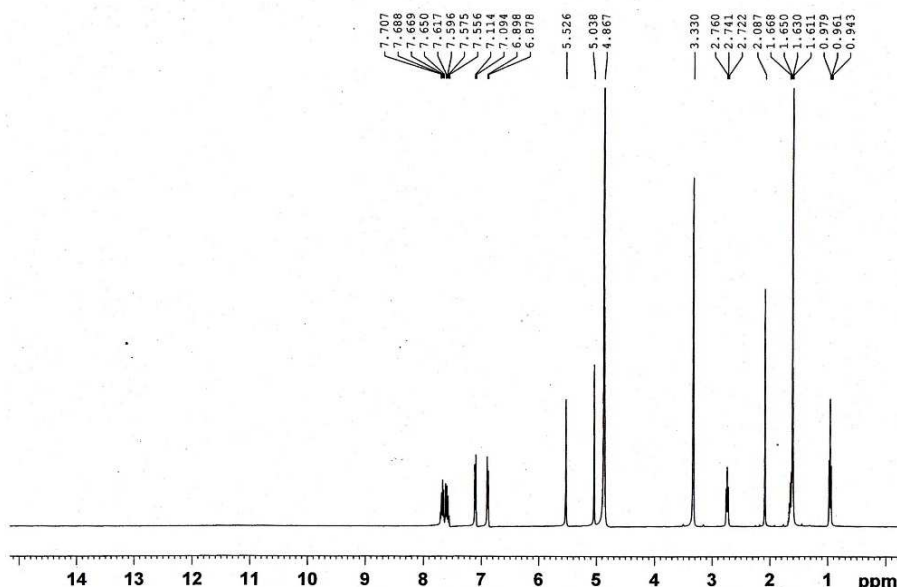
(18) NMR of solid mixture of unreacted olmesartan and vildagliptin.



(19) NMR of solid mixture of unreacted olmesartan and vildagliptin.

Figure 3.15. NMR spectra of olmesartan medoxomil (12), vildagliptin (13), reacted complex OV (14-16) and unreacted solid mixture of olmesartan medoxomil, vildagliptin (17-19).

Wazed Miah Science Research Centre (WMSRC)
Jahangirnagar University
Sample: Olme
Operated by: Md. Emdad Hossain, Scientist



Current Data Parameters
NAME DU_Olme
EXPNO 1
PROCNO 1

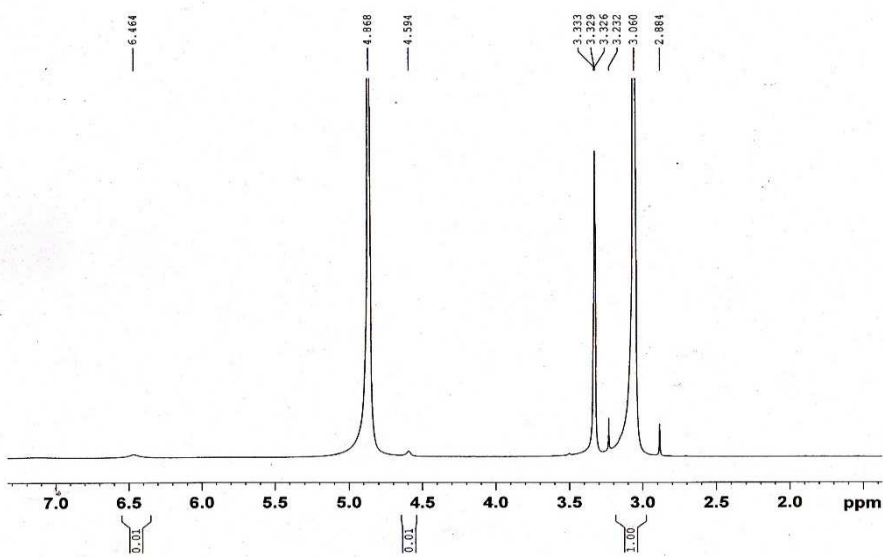
F2 - Acquisition Parameters
Date_ 20190818
Time 15.09
INSTRUM spect
PROBHD 5 mm PABBO BB/
PULPROG zg
TD 65536
SOLVENT MeOD
NS 16
DS 0
SWH 12019.230 Hz
FIDRES 0.183399 Hz
AQ 2.7262976 sec
RG 93.48
DW 41.600 usec
DE 6.50 usec
TE 298.7 K
D1 1.00000000 sec
TDO 1

----- CHANNEL f1 -----
SF01 400.2340023 MHz
NUC1 1H
P1 11.20 usec
PLW1 12.00000000 W

F2 - Processing parameters
SI 131072
SF 400.2300000 MHz
WDW EM
SSB 0
LB 1.00 Hz
GB 0
PC 1.00

(20) NMR of olmesartan medoxomil.

Wazed Miah Science Research Centre (WMSRC)
Jahangirnagar University
Sample: Met
Operated by: Md. Emdad Hossain, Scientist



Current Data Parameters
NAME DU_Met
EXPNO 1
PROCNO 1

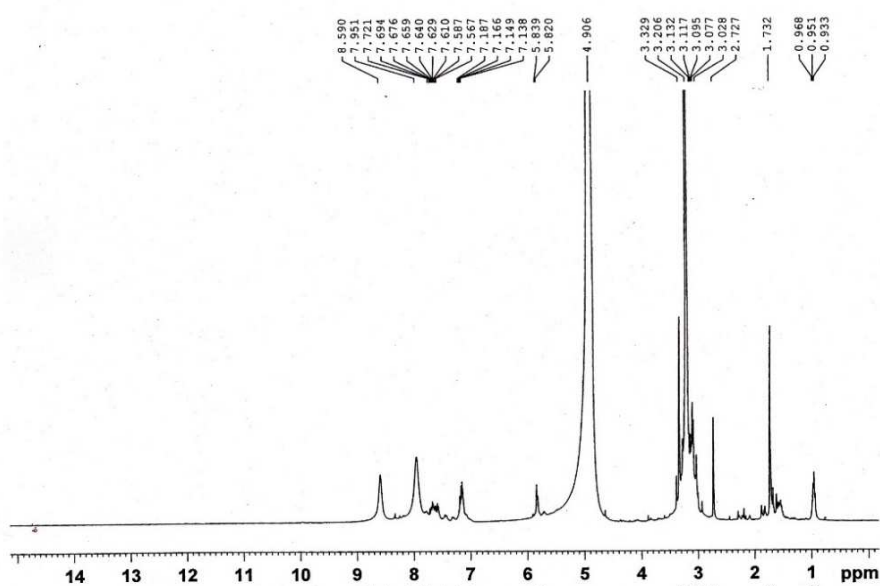
F2 - Acquisition Parameters
Date_ 20190818
Time 14.59
INSTRUM spect
PROBHD 5 mm PABBO BB/
PULPROG zg
TD 65536
SOLVENT MeOD
NS 16
DS 0
SWH 12019.230 Hz
FIDRES 0.183399 Hz
AQ 2.7262976 sec
RG 93.48
DW 41.600 usec
DE 6.50 usec
TE 298.5 K
D1 1.00000000 sec
TDO 1

----- CHANNEL f1 -----
SF01 400.2340023 MHz
NUC1 1H
P1 11.20 usec
PLW1 12.00000000 W

F2 - Processing parameters
SI 131072
SF 400.2300000 MHz
WDW EM
SSB 0
LB 1.00 Hz
GB 0
PC 1.00

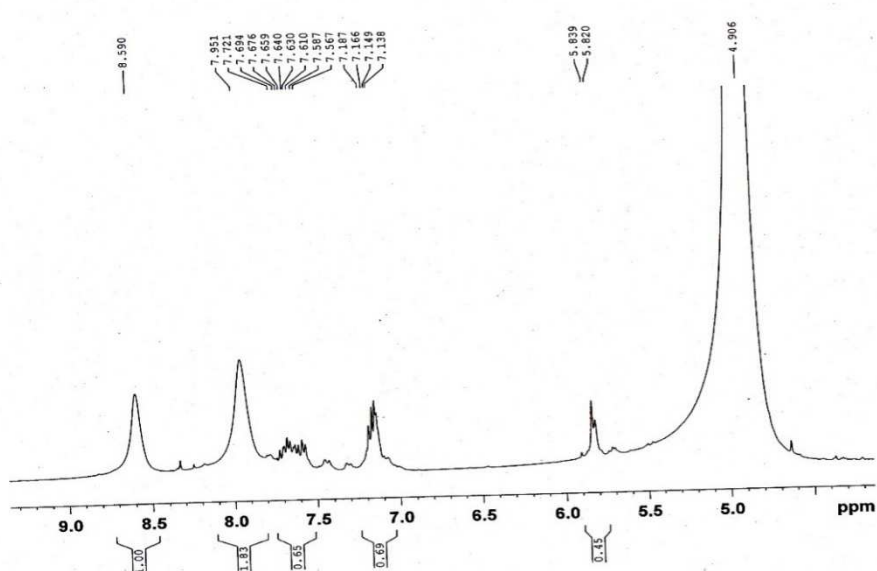
(21) NMR of metformin HCl.

Wazed Miah Science Research Centre (WMSRC)
 Jahangirnagar University
 Sample: Met+Olme
 Operated by: Md. Emdad Hossain, Scientist

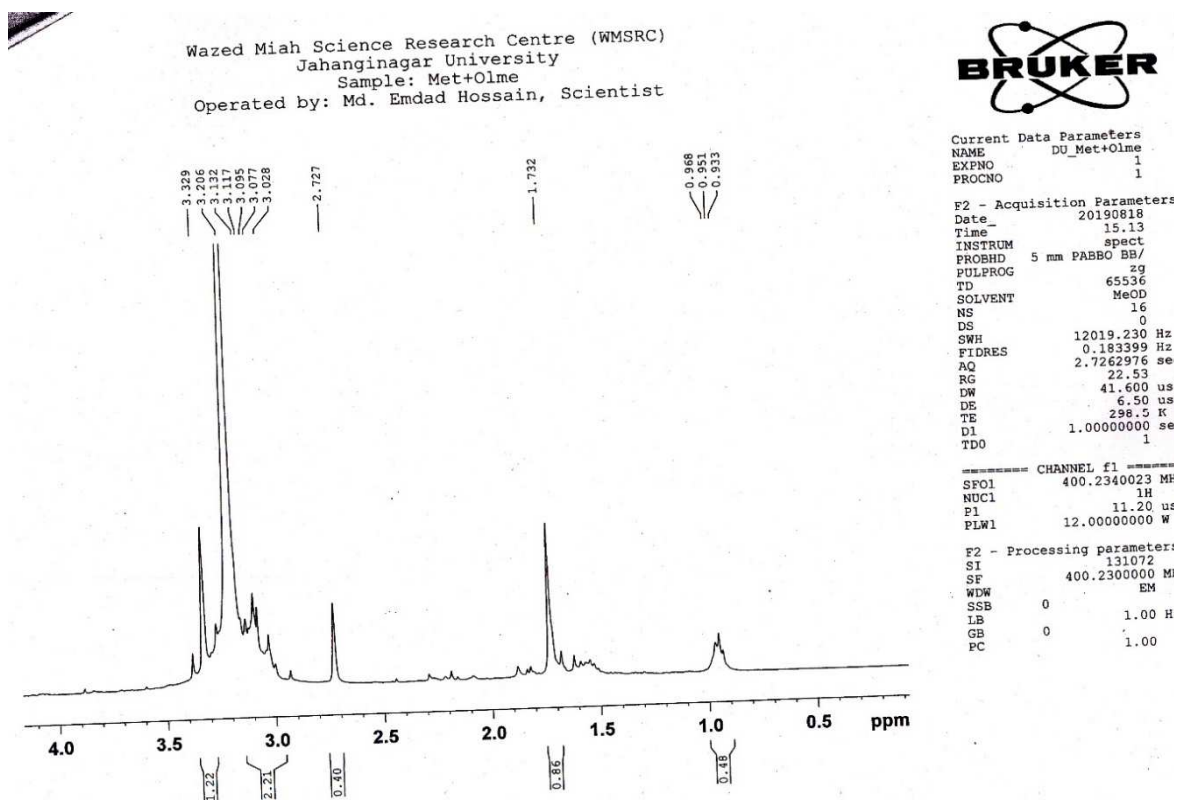


(22) NMR of complex OM.

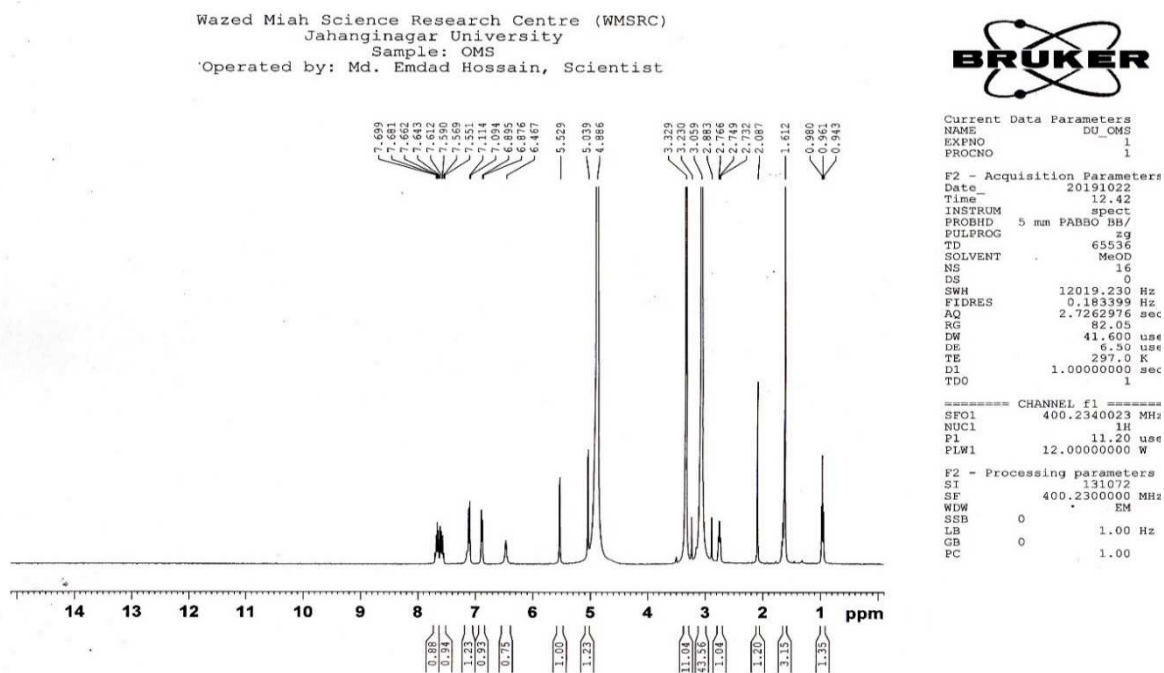
Wazed Miah Science Research Centre (WMSRC)
 Jahangirnagar University
 Sample: Met+Olme
 Operated by: Md. Emdad Hossain, Scientist



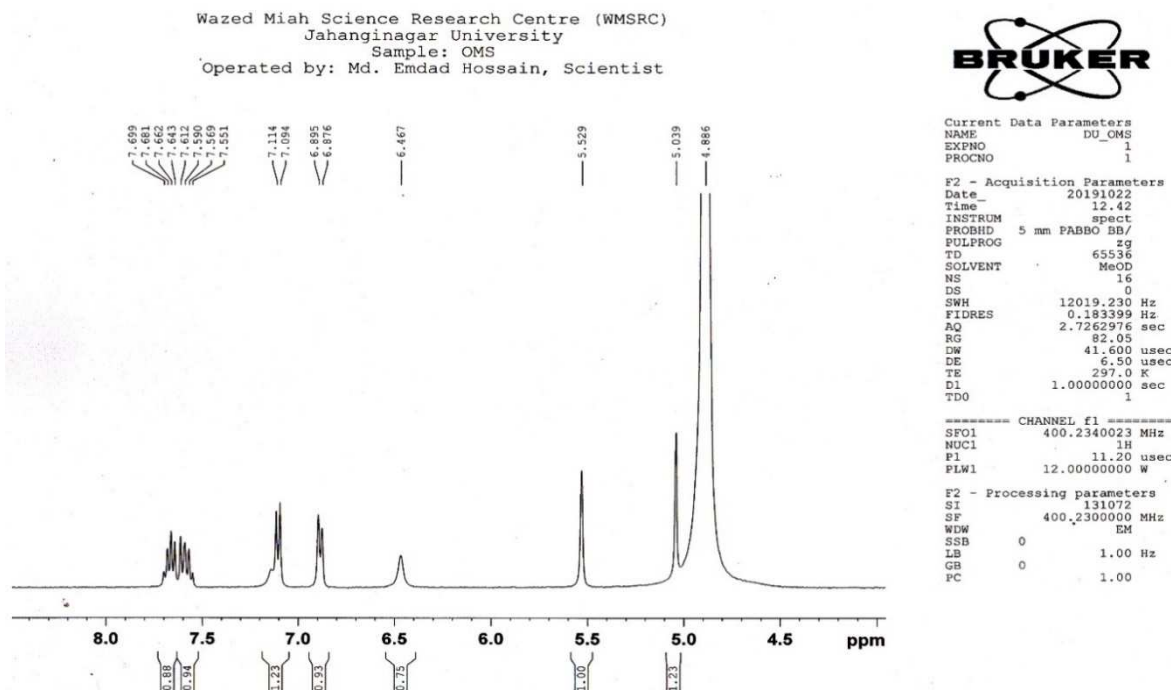
(23) NMR of complex OM.



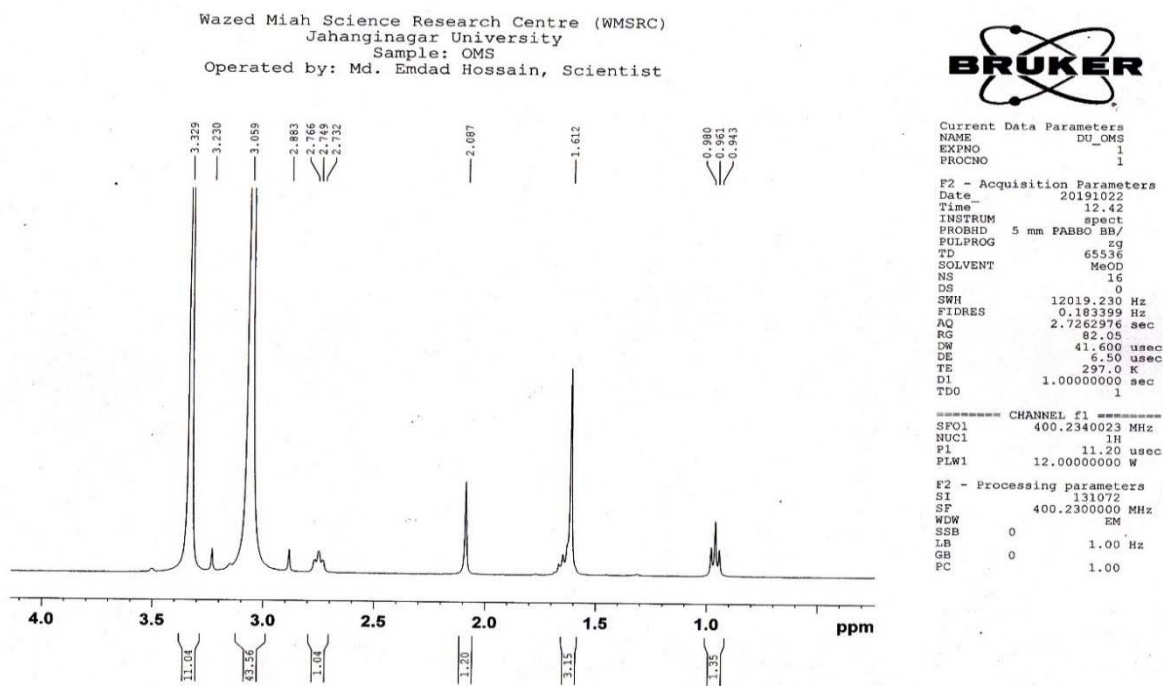
(24) NMR of complex OM.



(25) NMR of unreacted solid mixture of olmesatan medoxomil and metformin HCl.



(26) NMR of unreacted solid mixture of olmesatan medoxomil and metformin HCl.

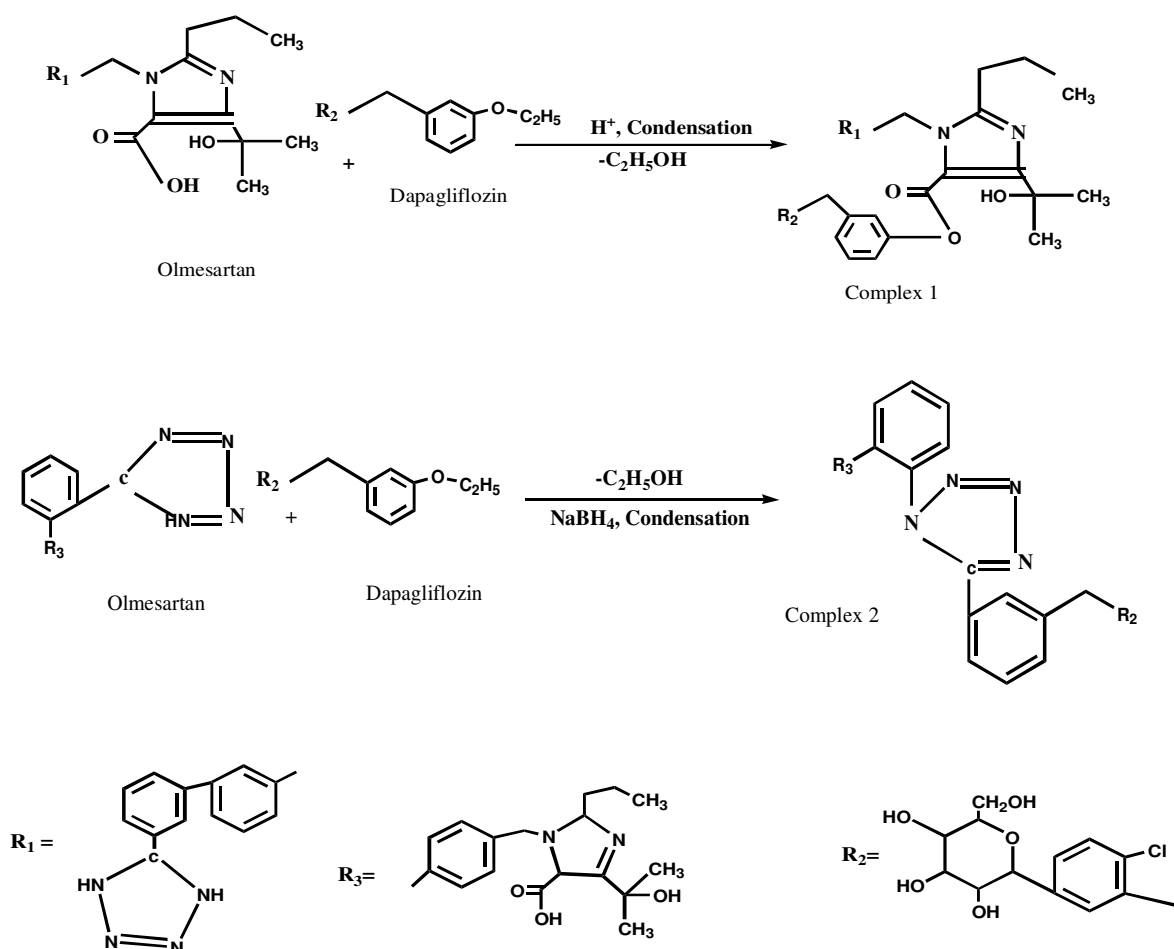
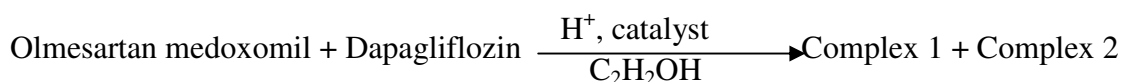


(27) NMR of unreacted solid mixture of olmesatan medoxomil and metformin HCl.

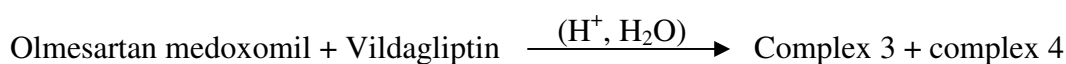
Figure 3.16. NMR spectra of olmesatan medoxomil (20), metformin HCl (21), complex OM (22-24) and unreacted solid mixture of olmesatan medoxomil and metformin HCl (25-27).

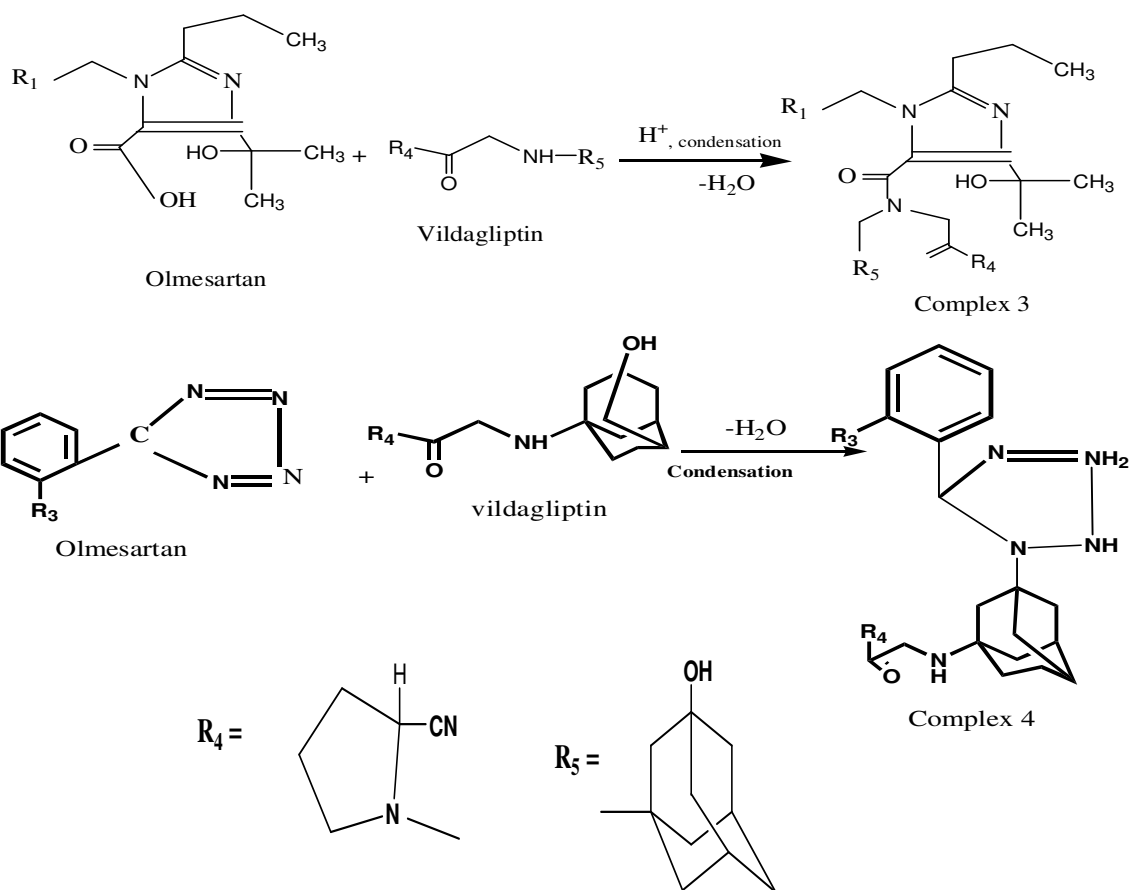
3.1.8. Postulation of the complex formation

The syntheses of complexes are postulated according to the following reaction. In this postulation olmesartan medoxomil and dapagliflozin interacted by condensation reaction to produce complex 1 and complex 2 which were assumed to be under suitable condition (Dams *et al.*, 2015).



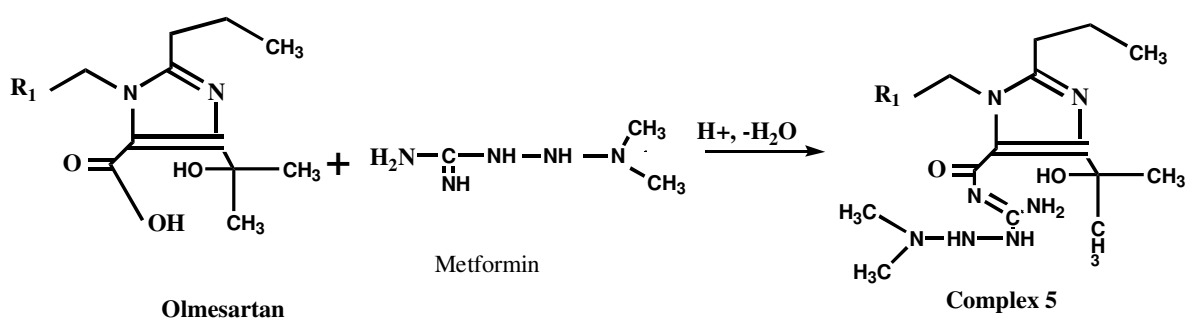
According to Neeraj *et al.* (2016), olmesartan medoxomil and vildagliptin reacted with each other and released a water molecule in presence of acid to form new complexes which are shown as follows;





During the reaction of olmesartan and metformin one molecule of water was depleted from the condensation complex. This reaction was supported by TGA which was shown as below;

Olmesartan medoxomil + Metformin \longrightarrow Complex 5



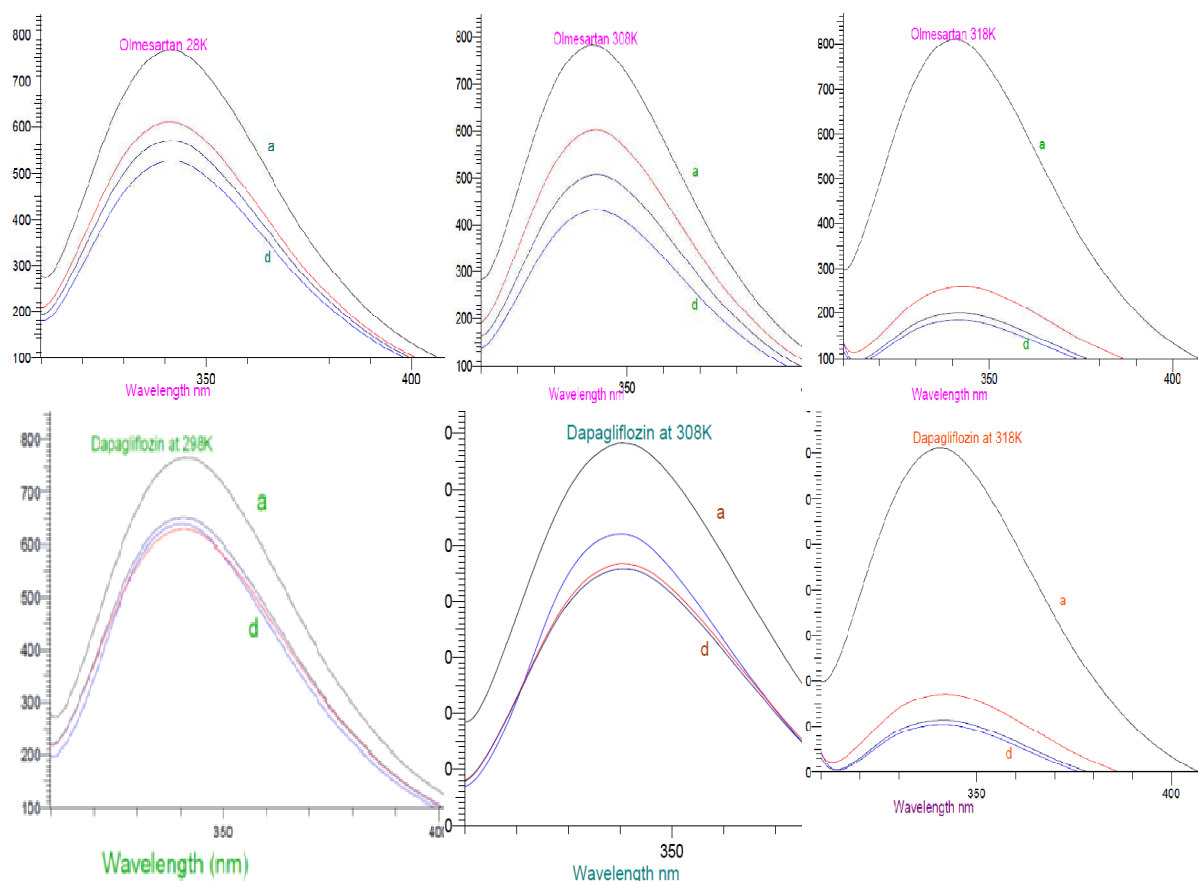
3.1.9. Fluorescence quenching studies

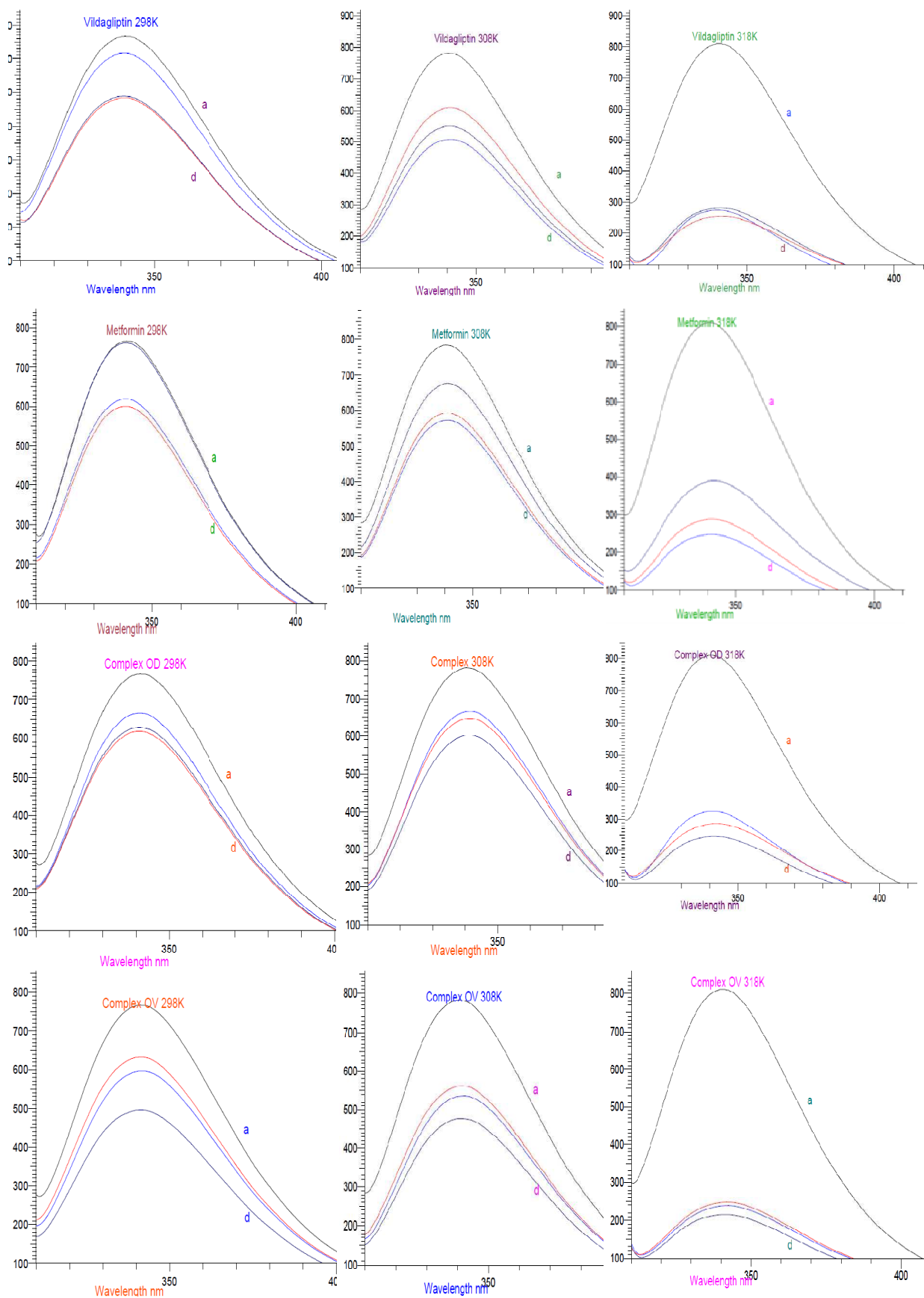
The tryptophan, tyrosine and phenyl alanine, components of BSA and known as fluorophores emit fluorescence when BSA is excited by a suitable wavelength. The fluorescence property of serum albumin is the combined contribution of both tryptophan and tyrosine when a 280 nm light excites the protein but at 293 nm wavelength only

contributes fluorescence come from tryptophan residue (Steinhardt *et al.*, 1971). When a comparison of fluorescence of BSA at 280 nm and 293 nm by a quencher (drug and drug complexes) is performed then it can help to observe the interaction procedure of the protein with respective analytes.

The graph of F_0/F against the concentration of quencher (drug) was drawn both at 280 nm and 293 nm excitation wavelength and at constant temperature of 298 K. The pattern of the fluorescence intensities at two different wavelengths found to be different. For the molecular interaction of tyrosine and tryptophan residues of BSA with drug the different fluorescence quenching of BSA were observed.

BSA fluorescence quenching spectra in presence of different concentration of drugs and their complexes were recorded at physiological conditions at three different temperatures and are depicted in Figure 3.17. The recorded spectra exhibited a single broad band centered around 340 nm. The spectra in presence of pure drugs or combination of drugs, i.e. the synthesized complexes individually generated a downward directed fluorescence at maximum emission wavelength. The peak shift phenomenon was not observed. The observations may suggest a ground-state formation of complex while interacting with BSA and drugs.





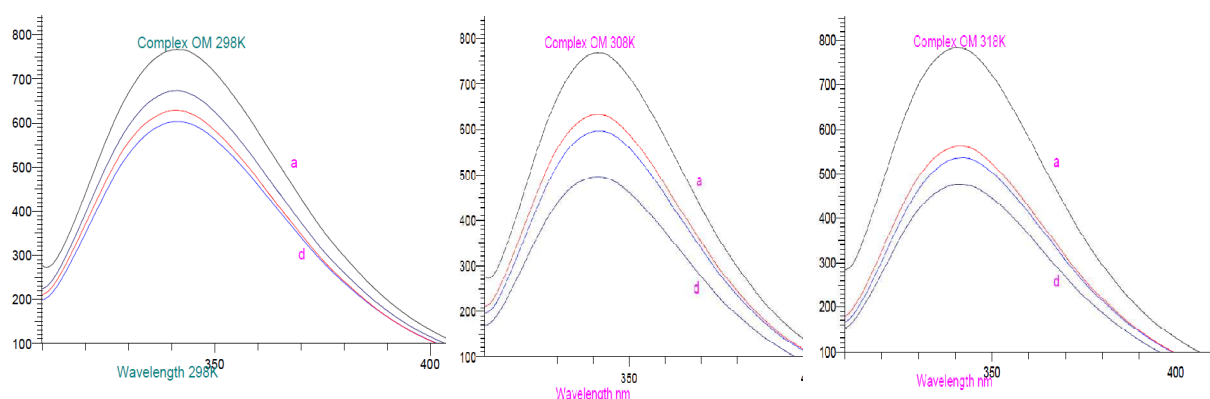
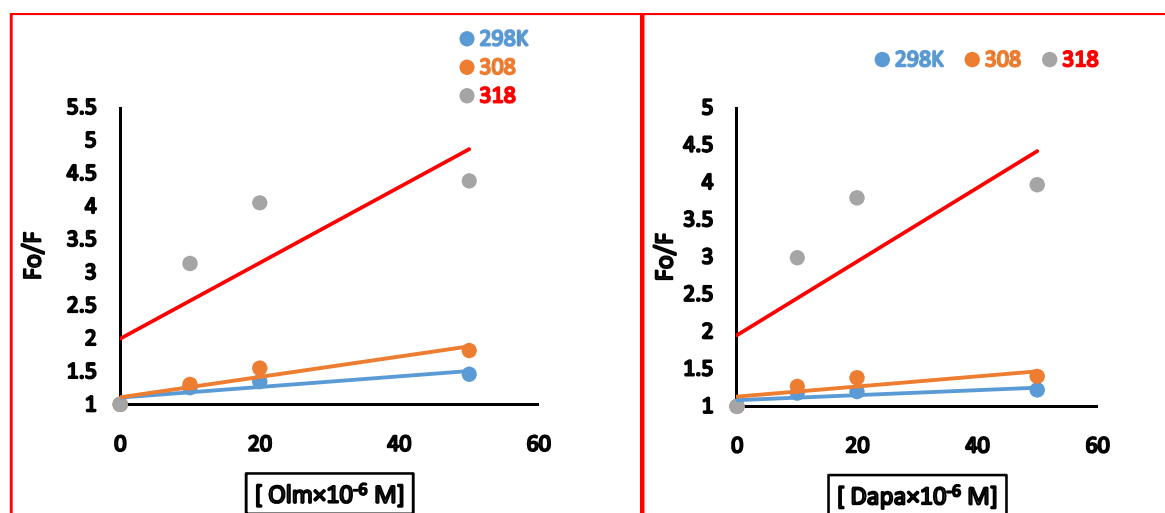


Figure 3.17. Emission spectra of BSA in presence of different concentration of olmesartan medoxomil, dapagliflozin, vildagliptin, metformin, complex OD, complex OV, complex OM, (T= 298K, 308K and 318K; $\lambda_{ex} = 280$ nm). $C(\text{BSA}) = 10 \times 10^{-6}$ mol L^{-1} , $C(\text{drugs/drug complexes}) (10^{-6}$ mol $L^{-1})$, curves a»d: 0, 10, 20 and 50 μM , respectively.

The Stern-Volmer plots of BSA quenching by Olmesartan, dapagliflozin, vildagliptin, metformin, OD complex, OV complex and OM complex at three different temperature are shown in Figure 3.18 and the corresponding Stern-Volmer quenching constants (K_{sv}) as well as rate constant (K_q) of quenching are also summarized in Table 3.5.



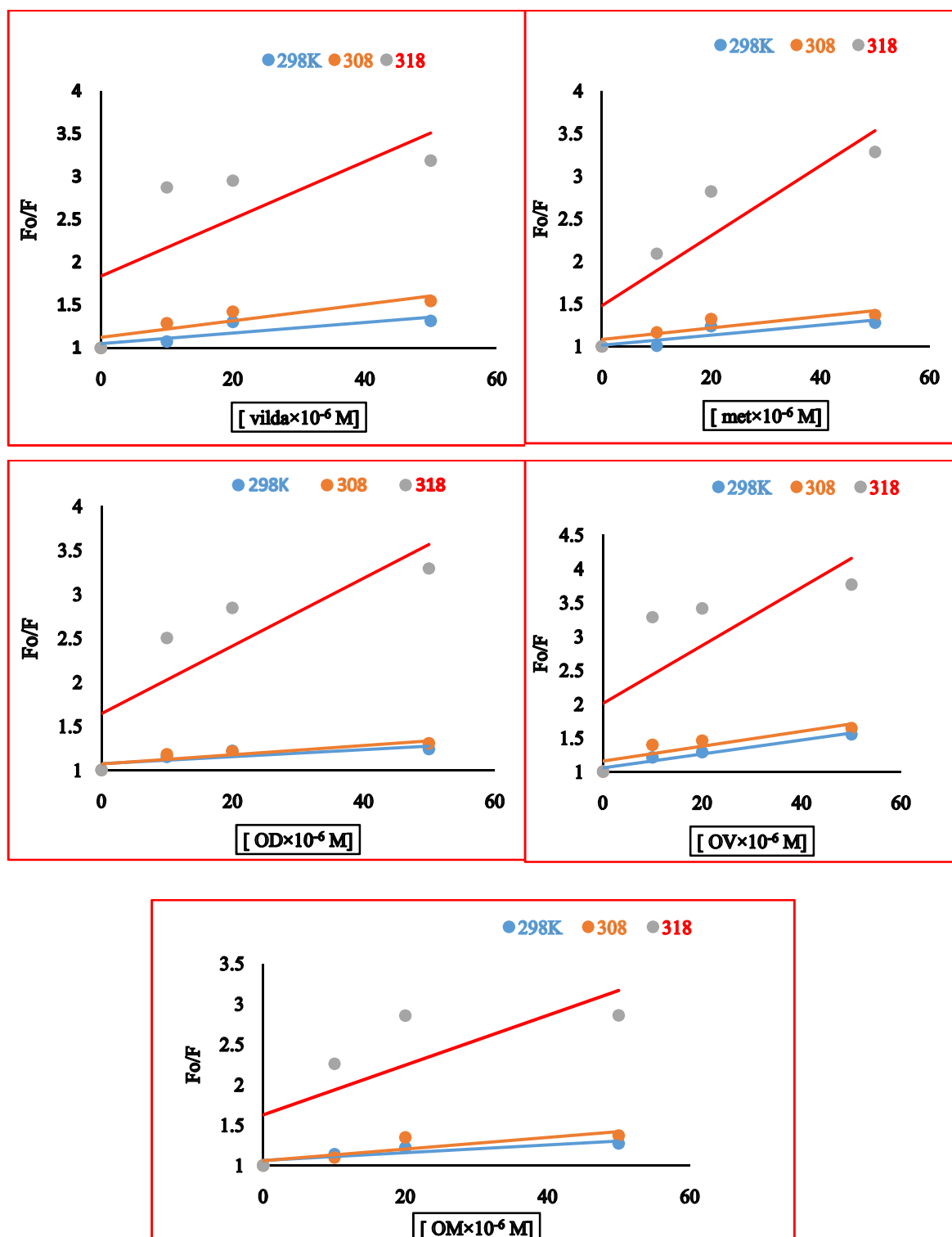


Figure 3.18. BSA quenching Stern-Volmer plots with increased concentrations of olmesartan, dapagliflozin, vildagliptin, metformin, complex OD, complex OV and complex OM at 298K, 308K and 318K.

As K_{sv} values increased with the increase in the temperature it can be assumed that these drugs and the newly formed complexes quench the BSA by dynamic quenching

mechanism. The energy of activation for quenching reaction was measured from the Arrhenius plot (Figure 3.19) and the values were listed in the Table no 3.5. The result revealed that the energy of activation for drug complexes was less than the energy of activation of their individual interactions which is also an indicator of the complexation between the drugs.

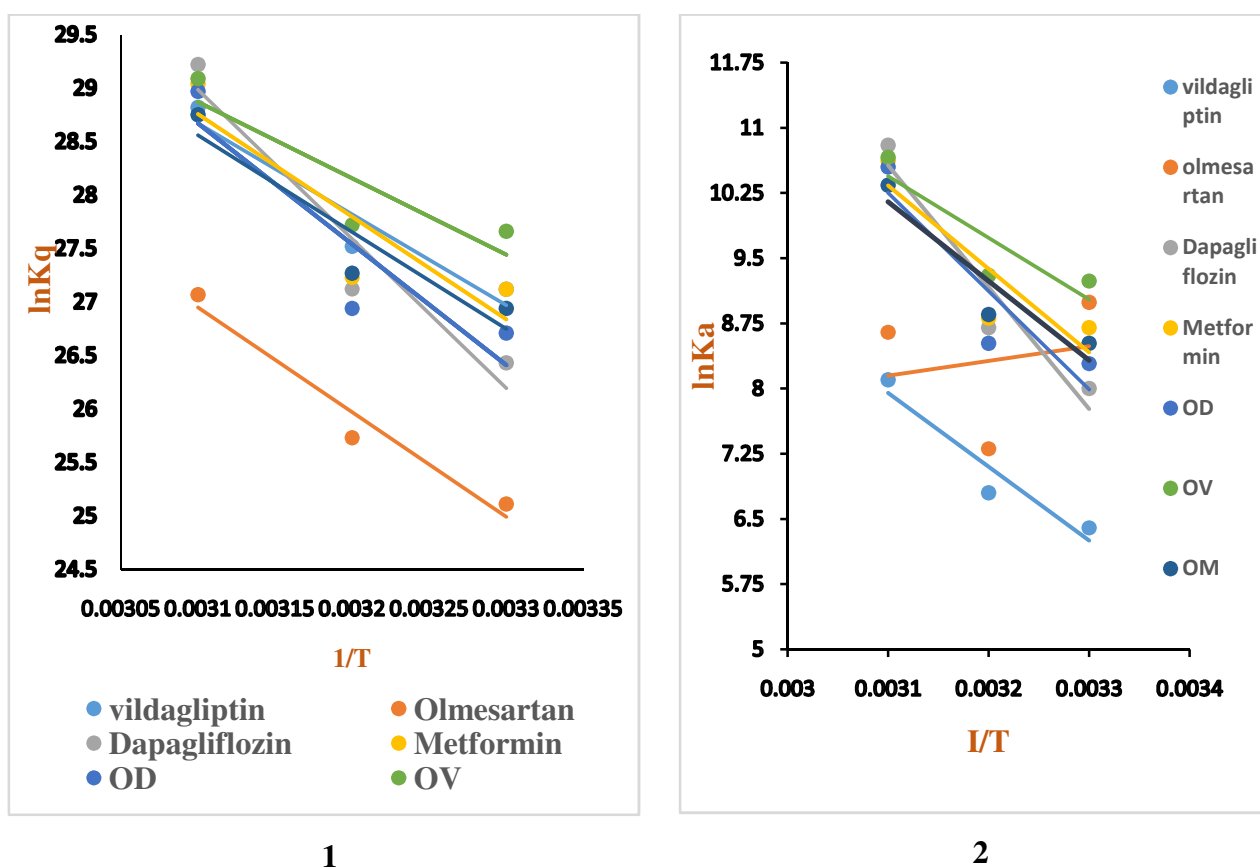


Figure 3.19. Arrhenius plot (1) and Van't Hoff plot (2), for interaction of BSA with olmesartan, dapagliflozin, vildagliptin, metformin, OD complex, OV complex and OM complex to determine the energy of activation of quenching process at pH 7.4, C (BSA) = $10.0 \times 10^{-6} \text{ mol.L}^{-1}$.

Table 3.5. Stern-Volmer quenching rate constant K_{sv} and K_q of the olmesartan-BSA, dapagliflozin-BSA, vildagliptin-BSA, metformin-BSA, OD-BSA, OV-BSA and OM-BSA system at different temperature at physiological pH.

System	T(K)	1/T(K ⁻¹)	$K_{sv} (\times 10^4 \text{L.mol}^{-1})$	$K_q (\times 10^{12} \text{L.mol}^{-1})$	Ea (KJ.mol ⁻¹)
Olmesartan-BSA	298	0.0034	0.8	0.8	-81.5
	308	0.0032	1.5	1.5	
	318	0.0031	5.7	5.7	
Dapagliflozin-BSA	298	0.0034	0.3	0.3	116
	308	0.0032	0.6	0.6	
	318	0.0031	4.9	4.9	
Vildagliptin-BSA	298	0.0034	0.6	0.6	70.69
	308	0.0032	0.9	0.9	
	318	0.0031	3.3	3.3	
Metformin-BSA	298	0.0034	0.6	0.6	79.83
	308	0.0032	0.67	0.67	
	318	0.0031	4.11	4.11	
OD-BSA	298	0.0034	0.4	0.4	93.97
	308	0.0032	0.5	0.5	
	318	0.0031	3.8	3.8	
OV-BSA	298	0.0034	1.03	1.03	59.46
	308	0.0032	1.09	1.09	
	318	0.0031	4.29	4.29	
OM-BSA	298	0.0034	0.5	0.5	75.26
	308	0.0032	0.7	0.7	
	318	0.0031	3.08	3.08	

3.1.9.1. Analysis of thermodynamic parameters and the binding forces

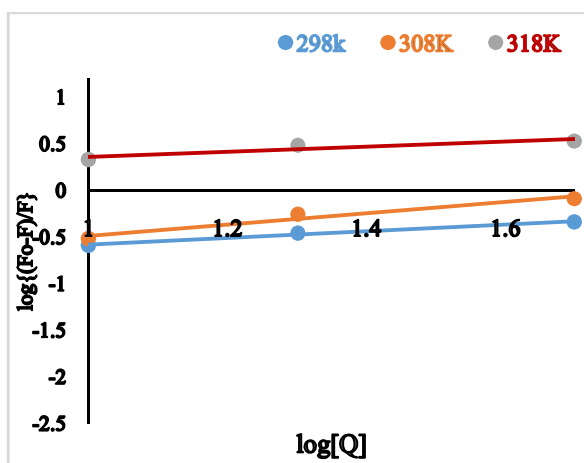
The linear Van't Hoff plot (Figure 3.19, Table 3.6) was used to determine the thermodynamic parameters at three different temperatures like as 298 K, 308 K and 318 K. These are calculated on the basis of binding constants. The negative ΔG value indicated the spontaneous interaction process. The positive ΔH and ΔS value indicated that the binding of dapagliflozin, vildagliptin, metformin, OD, OV and OM with BSA was predominantly by enthalpy driven where major interaction force was hydrophobic interaction. But in case of olmesartan medoxomil the negative ΔH value along with $\Delta S > 0$, suggested that only electrostatic force was responsible for the BSA quenching process.

Table 3.6. Thermodynamic parameters of drugs and newly synthesized drug complexes mediated BSA quenching at 298 K, 308 K and 318 K.

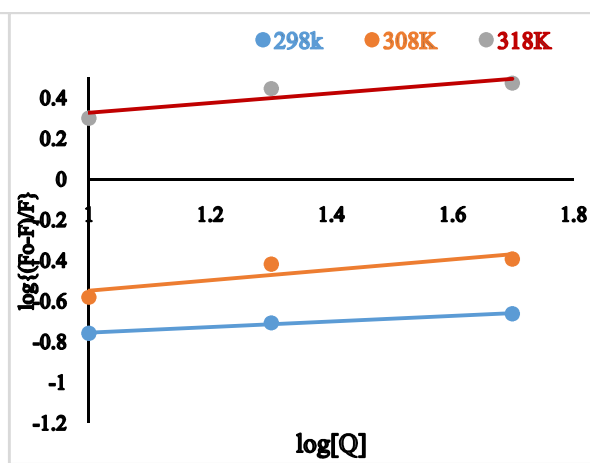
system	T(K)	1/T(K ⁻¹)	ΔH(KJ/mol)	ΔS(j/mol/K)	ΔG (KJ/mol)
Olmesartan-BSA	298	0.0033	-14.14	23.9	-7136.34
	308	0.0032			-7375.34
	318	0.0031			-7614.34
Dapagliflozin-BSA	298	0.0033	114.24	449	-133687.76
	308	0.0032			-138177.76
	318	0.0031			-142667.76
Vildagliptin-BSA	298	0.0033	70.686	285	-84859.314
	308	0.0032			-87709.314
	318	0.0031			-90559.314
Metformin-BSA	298	0.0033	79.83	333.55	-99318.07
	308	0.0032			-102653.57
	318	0.0031			-105989.07
OD-BSA	298	0.0033	93.98	377	-112252.02
	308	0.0032			-116022.02
	318	0.0031			-119792.02
OV-BSA	298	0.0033	59.04	270	-80400.96
	308	0.0032			-83100.96
	318	0.0031			-85800.96
OM-BSA	298	0.0033	75.68	320	-95284.32
	308	0.0032			-98484.32
	318	0.0031			-101684.32

3.1.9.2. Analysis of binding constants (n) and no of binding points (K_b)

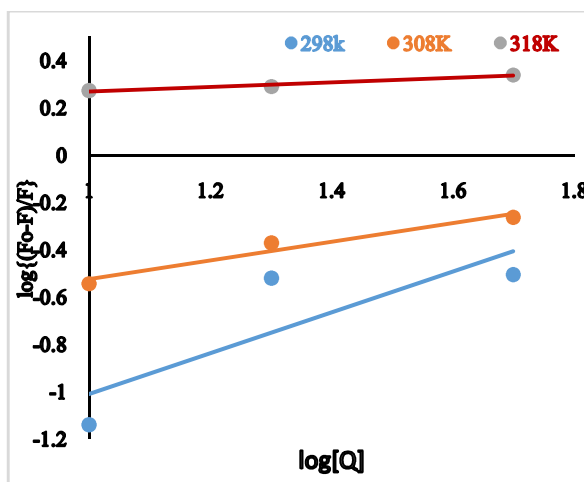
The No of binding sites (n) and binding constant (k_b) were determined from graphical calculation of the plot of log (F₀-F)/F vs log[Q] and the values are displayed in the Table 3.7, Figure 3.20. Except from metformin-BSA system, in all the interactions the K_b values were increased with increase in temperature. But the n value almost remains constant with the change in temperature, except metformin-BSA system and it was found to be almost 1 which also demonstrated towards 1:1 mole ratio interaction with BSA and drugs.



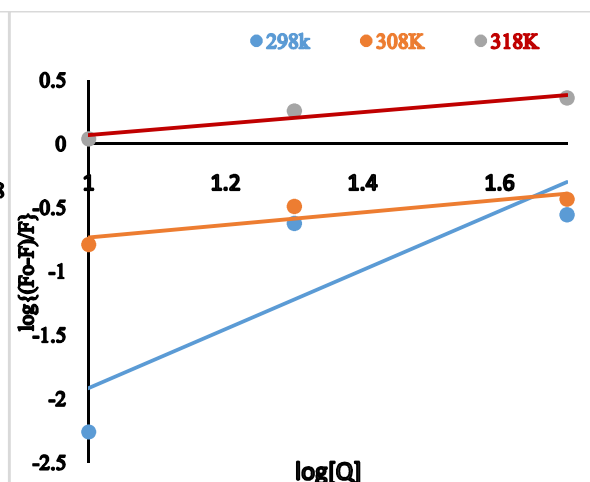
(1) Olmesartan-BSA



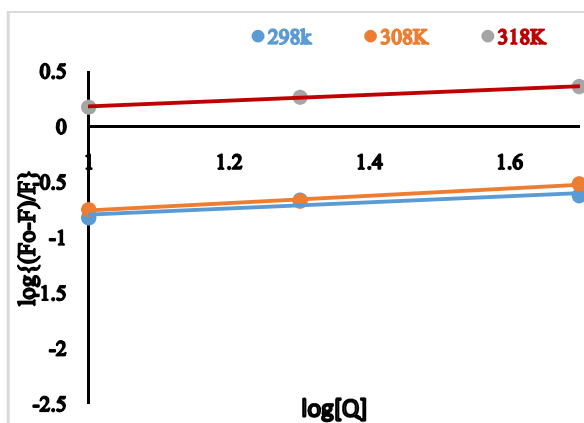
(2) Dapagliflozin-BSA



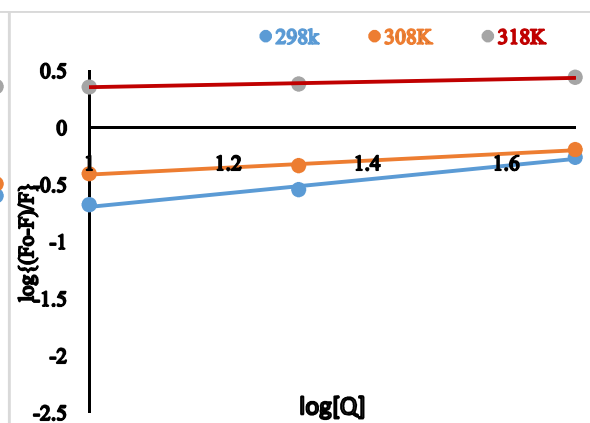
(3) vildagliptin-BSA



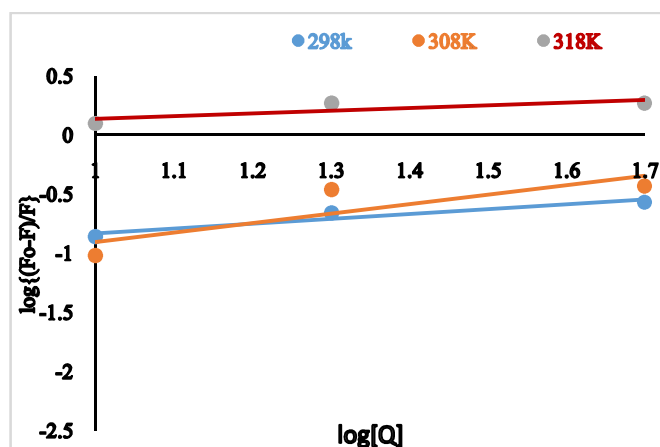
(4) Metformin-BSA



(5) OD-BSA



(6) OV-BSA



(7) OM-BSA

Figure 3.20. Log plot for determination of binding constant (K_b) and no of binding point (n) for different systems like (1) Olmesartan-BSA,(2) dapagliflozin-BSA,(3) Vildagliptin-BSA,(4) metformin-BSA,(5) OD-BSA,(6) OV-BSA and (7) OM-BSA at 298 K, 308 K and 318 K.

Table 3.7. Binding constant (K_b) and no of binding sites (n) of the pure drugs and drug complexes at three different temperatures like 298 K,308 K and 318 K.

Interaction system	pH	T(K)	K_b (L/mol)	n
Olmesartan-BSA	7.4	298	0.11	0.36
		308	0.08	0.61
		318	1.2	0.28
Dapagliflozin-BSA	7.4	298	0.13	0.136
		308	0.16	0.257
		318	1.22	0.239
Vildagliptin-BSA	7.4	298	0.133	0.8633
		308	0.121	0.393
		318	1.488	0.096
Metformin-BSA	7.4	298	5.86	2.31
		308	0.06	0.49
		318	0.42	0.45
OD-BSA	7.4	298	0.085	0.27
		308	0.082	0.33
		318	0.827	0.26
OV-BSA	7.4	298	0.051	0.601
		308	0.194	0.303
		318	1.715	0.121
OM-BSA	7.4	298	0.057	0.41
		308	0.02	0.801
		318	0.804	0.23

3.1.10. Analysis of blood glucose level in mice

Blood glucose levels for seven groups of mice were measured at every two days interval in fasting condition. The glucose levels in mmol/L were listed in Table 3.8.

Table 3.8. Fasting blood glucose level (mmol/L) of different group of mice at different days.

Group I (control)	SL	Before administra- -tion of alloxan	After administra- -tion of alloxan	Application of drugs						
				Day 2	Day 4	Day 6	Day 8	Day 10	Day 12	Day 14
	1	5.2								6.2
	2	5.1	ND	ND	ND	ND	ND	ND	ND	5.2
	3	6.1								5.1
	4	6.2								6.1
	5	6.1								6.2
Mean		5.74								5.76

ND= Not Detected

Group II (metformin)	SL	Before administra- -tion of alloxan	After administra- -tion of alloxan	Application of drugs						
				Day 2	Day 4	Day 6	Day 8	Day 10	Day 12	Day 14
	1	3.6	30.4	25.7	18.7	20.5	19.1	18	18.5	19.5
	2	3.4	32.1	32.1	19.8	19.7	19.5	19.2	19.1	18.9
	3	3.5	32	29	18.7	19.3	19.4	18.3	18.2	18.2
	4	3.6	31.6	24.8	23.5	22.4	22.2	21.8	20.7	19.8
	5	4.1	31.6	29.4	27.3	27.2	26.4	22.7	20.3	18.7
Mean		3.64	31.54							19.02

Group	SL	Before administration of alloxan	After administration of alloxan	Application of drugs						
				Day 2	Day 4	Day 6	Day 8	Day 10	Day 12	Day 14
Group IV (Dapagliflozin)	1	4.3	30.3	31.6	27.7	26.3	25.2	24.7	23.6	20.2
	2	4.4	29.6	16.5	12.5	12.3	12.2	11.9	10.3	10.2
	3	4.1	High	28.7	26.8	22.8	21.5	20.5	11.5	9.2
	4	3.8	29.6	7.4	High	26.4	17	High	30.2	17.6
	5	3.6	31.2	7.1	10.6	10.2	9	9.1	8.8	8.5
Mean		4.04	30.367							13.14
Group VI (Vildagliptin)	SL	Before administration of alloxan	After administration of alloxan	Application of drugs						Day 14
				Day 2	Day 4	Day 6	Day 8	Day 10	Day 12	
	1	4.7	31.4	28.3	26.6	20.4	19.9	18.7	18.6	15.2
	2	4.5	30.4	30.1	28.9	22.4	16.3	6.8	7.8	7
	3	4.9	31.5	26.7	High	22.6	21.7	19.3	18.7	18.7
	4	3.8	30.6	25.6	20.8	19.4	19.3	18.3	18.1	16.2
	5	4.1	31.1	31	27.9	22.9	20.5	20.3	20.1	18.5
Mean		4.4	31							15.12
Group XVI (OM)	SL	Before administration alloxan	After administration alloxan	Application of drugs						
				Day 2	Day 4	Day 6	Day 8	Day 10	Day 12	Day 14
	1	5.3	31.9	29.3	27.2	24.4	20.1	21.1	19.1	18.5
	2	6.1	High	24.6	23.9	30.2	27.6	24.5	20.2	19.3
	3	5.7	23.3	20.6	18.2	17.2	15.1	12.1	10.1	10
	4	4.1	30.1	28.2	23.5	22.6	21.5	19.8	18	19
	5	5	32.2	28.9	26.2	24.2	20.3	19.5	17.2	17
Mean		5.24	29.36						16.92	16.76

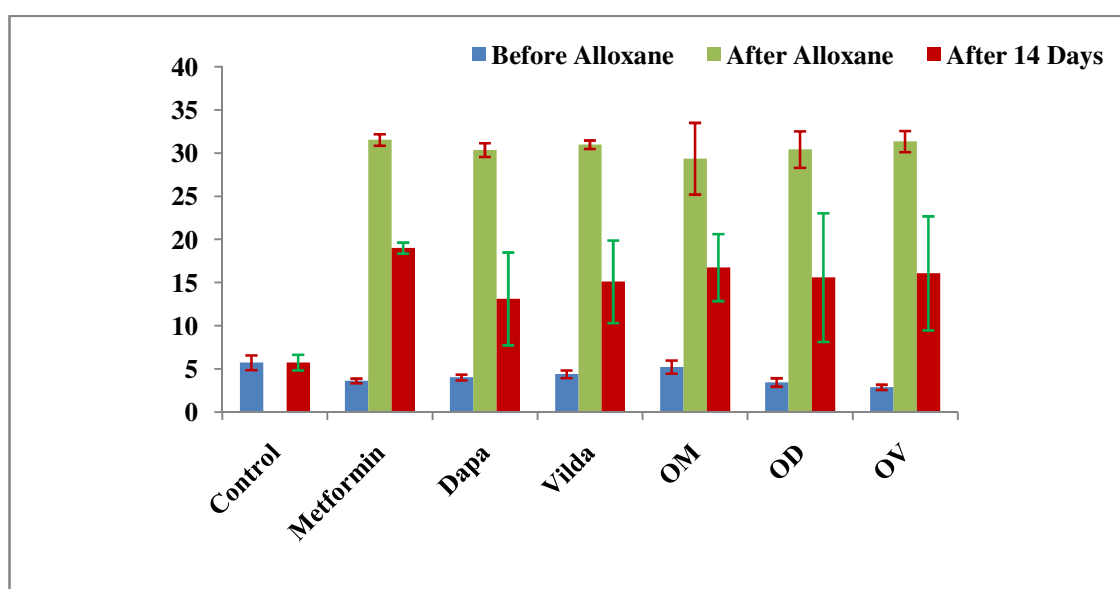
Group XIV (OD)	SL	Before admini stration of alloxan	After admini stration of alloxan	Application of drugs						
				Day 2	Day 4	Day 6	Day 8	Day 10	Day 12	Day 14
	1	3.1	32	30	28.5	21.5	14.4	12.2	12.8	27.7
	2	3.4	High	32	30.3	30.2	30.6	8.2	8.1	7.9
	3	2.8	29.9	29.8	29.4	26.2	21.8	20.2	18.5	15.3
	4	3.9	27.2	25.9	22.6	21.6	19.3	18.3	15.2	11.5
	5	4.1	32.6	32.3	32.3	D				
Mean		3.46	30.425							15.6

Group XV (OV)	SL	Before admini stration of alloxan	After administra tion of alloxan	Application of drugs						
				Day 2	Day 4	Day 6	Day 8	Day 10	Day 12	Day 14
	1	2.9	31.8	High	30	28.8	28.4	30.2	25	23.1
	2	2.7	32.6	25.2	23.1	27.4	15.3	12.2	10.2	10
	3	3.2	29.4	30.2	31.2	30.1	High	D		
	4	2.5	31.9	30.9	31.2	32.0	30.2	D		
	5	3.2	31.1	High	25.1	23.2	20.5	19.3	15.2	15.1
Mean		2.9	31.36							16.07

After 14 days of treatment the antidiabetic drugs metformin, dapagliflozin and vildagliptin reduced the blood sugar 39.70%, 56.73% and 51.22% respectively. While the newly synthesized complexes OM, OD and OV reduced the blood sugar by 42.95%, 50.50% and 48.66%, respectively. The results are demonstrated in Table 3.9 and Figure 3.21.

Table 3.9. Anti-diabetic activity of the pure drugs and drug complexes

Groups	Before Alloxan	SD	After Alloxan	SD	After 14 Days	SD (\pm)
Control	5.74	0.856154192			5.76	0.904434
Metformin	3.64	0.270185122	31.54	0.676757	19.02	0.637966
Dapagliflozin	4.04	0.336154726	30.37	0.802081	13.14	5.371964
Vildagliptin	4.4	0.447213595	31	0.484768	15.12	4.778807
OM	5.24	0.760263112	29.36	4.154816	16.76	3.881108
OD	3.46	0.484148737	30.425	2.114681	15.6	7.459893
OV	2.9	0.3082207	31.36	1.217785	16.07	6.603282

**Figure 3.21.** Antidiabetic activity of drug complexes OD, OV and OM in comparison to metformin, dapagliflozin and vildagliptin.

3.1.11. Histopathological study results of drugs and drug complexes

Hepatic and nephrotic tissues of pure dapagliflozin, vildagliptin and metformin HCl treated mice showed no remarkable changes. But OD complex treated mice liver tissue and OV complex treated kidney tissue showed moderate to severe dysplasia, respectively (Figure 3.22).

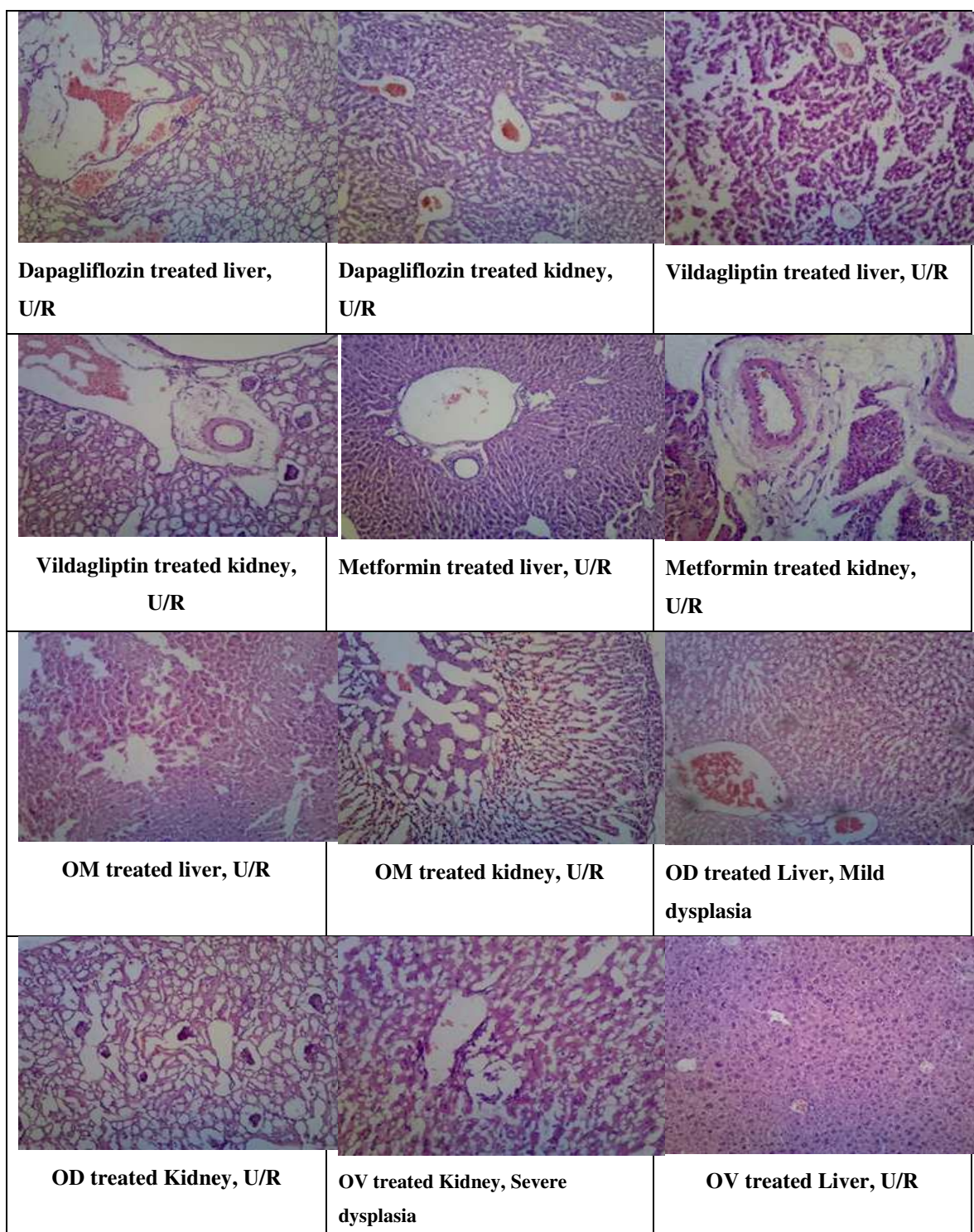


Figure 3.22. Histopathology of kidney and liver tissues of the experimental mice treated with dapagliflozin, vildagliptin, glimepiride, OD, OV and OM.

3.1.12. Serum creatinine analysis of drugs and complexes treated mice

In patients and in animal models the concentration of creatinine in serum is routinely employed as a simple substitute indicator for the glomerular filtration rate. The calculated creatinine values are listed in Table 3.10 and displayed in Figure 3.23. After

14 days of treatment the newly formed complexes OM, OD and OV increased the creatinine level compared to the antidiabetic drugs metformin, dapagliflozin and vildagliptin.

Table. 3.10. Serum creatinine level of mice groups treated with drugs and drug complexes.

Groups	Serum creatinine (mg/dL)	Serum creatinine (mg/dL)	Serum creatinine (mg/dL)	Average	SD
Control	4.7	3.57	3.13	3.8	0.8099
Metformin	3.58	3	3.56	3.38	0.3292
Dapagliflozi n	3.43	3.14	3.7	3.42	0.280
Vildagliptin	2.99	4.32	3.51	3.6	0.6702
OM	3.78	4.37	4.12	4.09	0.2961
OD	5.1	4.07	4.5	4.56	0.5173
OV	5.1	6.62	6.12	5.95	0.7747

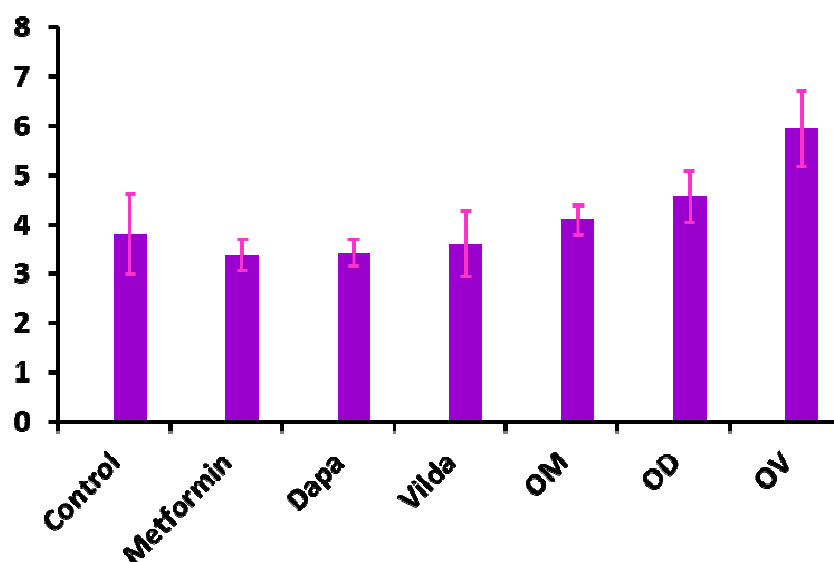


Figure 3.23. Serum creatinine level of mice groups treated with drugs and drug complexes.

3.1.13. Analysis of serum uric acid in mice treated with drugs and complexes

If serum uric acid level is ≤ 7.0 mg/dL, which is known as hyperuricemia, may cause gout, impaired renal uric acid excretion or produce both the problems in human body (Shoji *et al.*, 2004) Therefore the level of uric acid is a risk factor not only for arising gout but also the cardiovascular diseases, nephrolithiasis, diabetes, obesity and dyslipidemia (Fang and Alderman, 2000; Hayden and Tyagi, 2004; Nakagawa *et al.*, 2006).

Uric acid level was found elevated from the normal values and found 17.59, 10.06, 11.37, 16.84, 12.75, 15.64 and 17.81 mg/dL respectively for the control group, metformin, dapagliflozin, vildagliptin, OM, OD and OV treated mice group. The results are stated below in Table No. 3.11 and Figure No. 3.24.

Table 3.11. Serum Uric acid level after treatment with the drugs and drug complexes in different mice groups.

Groups	Serum uric acid (mg/dL)	SD
Control	17.59	1
Metformin	10.06	1.5
Dapagliflozin	11.37	1.2
Vildagliptin	16.84	1.6
OM	12.75	1.5
OD	15.64	1.7
OV	17.81	1.8

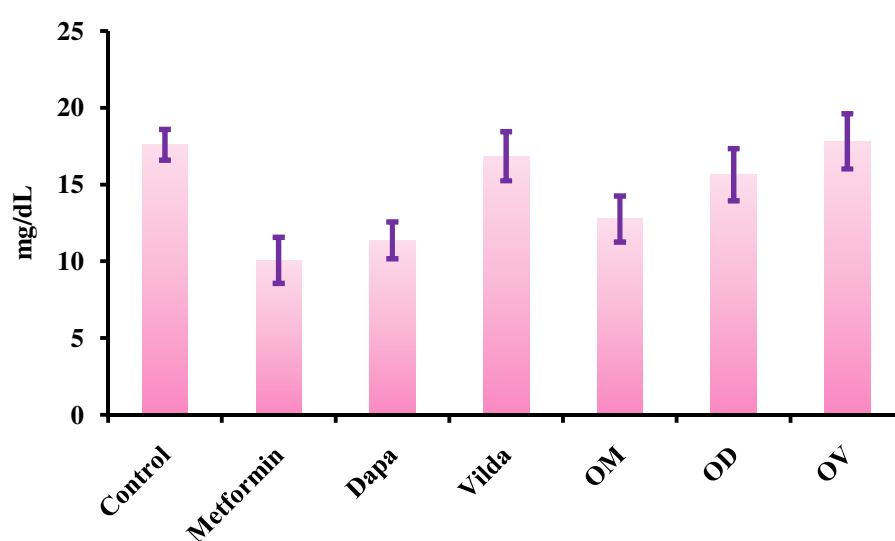


Figure 3.24. Serum uric acid levels in different mice treated with drug and drug complexes.

3.1.14. Serum SGPT and SGOT analysis in different mice groups

Due to damage of cells by oxidative stress SGPT and SGOT enzymes are activated in liver. The affected hepatocytes of liver excrete out SGPT and SGOT from liver cells into the bloodstream. The serum SGPT is an indicator of damaged liver. The serum SGOT level is also a marker of liver damage as well as other cell damage like muscles and heart.

The results of SGPT and SGOT levels in drugs treated mice group were displayed in Figure 3.25 and Table 3.12. The serum SGPT level for control, metformin, dapagliflozin, vildagliptin, complex OM, OD and OV treated mice were calculated as 23.85 U/L, 20.28 U/L, 21.02 U/L, 21.17 U/L, 17.35 U/L, 20.15 U/L and 27.78 U/L, respectively. Serum SGOT level in mice after treatment with drugs and drug complexes were found 21.23 U/L, 18.42 U/L, 17.24 U/L, 17.70 U/L, 15.54 U/L, 18.91 U/L and 25.67 U/L, respectively for control, metformin, dapagliflozin, vildagliptin, OM, OD and OV.

Table 3.12. Serum SGPT and SGOT level in mice after treatment with drug and drug-complexes.

Group	SGPT(U/L)	SD	SGOT(U/L)	SD
Control	23.8533	3.33	21.23	3.25
Metformin	20.2842	3.01	18.42	2.51
Dapagliflozin	21.0242	3.51	17.242	3.35
Vildagliptin	21.17	2.91	17.7	2.43
Complex OM	17.353	3.78	15.543	3.78
Complex OD	20.154	3.98	18.91	3.69
Complex OV	27.78	3.8	25.67	3.5

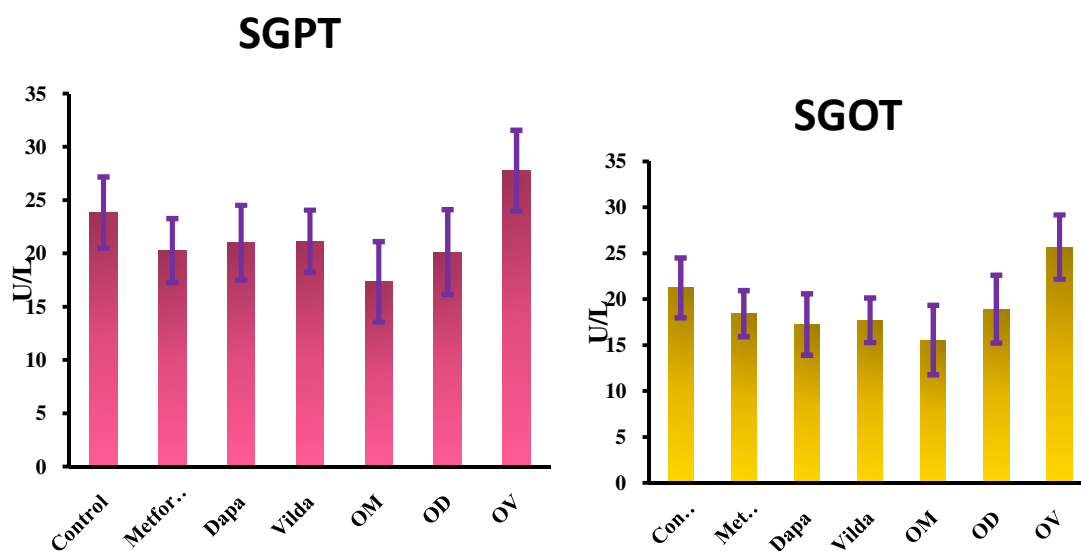


Figure 3.25. Serum SGPT and SGOT level of mice after treatment with drugs and drug complexes.

3.2. ROSUVASTATIN, PERINDOPRIL ERBUMINE AND VILDAGLIPTIN COMPLEXATION: SYNTHESIS, CHARACTERIZATION AND ASSESSMENT OF BIOLOGICAL ACTIVITY

The synthesis of complexes of rosuvastatin with perindopril erbumine and vildagliptin, called rosuvastatin-perindopril complex (PR), rosuvastatin-vildagliptin complex (RV) and perindopril-vildagliptin complex (PV) were done by co-evaporation technique. The complexation was evaluated with new peak patterns in FT-IR spectra and different R_f values over TLC plate. TGA analysis and melting point determination revealed the thermal stability and thermochemical characteristics of the synthesized complexes. Their protein binding characteristics using BSA was carried out by fluorescence quenching strategy. The binding phenomena were evaluated by estimating the Stern-Volmer constant, binding points determinations at the temperature of 298 K, 308 K and 318 K at pH 7.4 (physiological pH). Characterization and evaluation of BSA-Standard drug and BSA-Drug complexes interactions were done. Moreover, various thermodynamic points e.g. enthalpy change (ΔH), entropy change (ΔS) and free energy evolution (ΔG) were calculated to assess the properties of the binding energies. Finally, *in vivo* lipid lowering activity, *in vitro* thrombolytic, membrane stabilizing and antioxidant activities were evaluated.

3.2.1. TLC characterization of drugs and drug complexes

TLC assays of drugs and their complexes were carried out on plates (precoated TLC plate, F₂₅₄) using methanol and dichloromethane in the ratio of 20:80 as mobile phase in order to identify the formation of complex. The R_f values were found as mentioned in the Table 3.13.

Table 3.13. R_f values of rosuvastatin, perindopril, vildagliptin and their complexes.

Item	R_f Value
Rosuvastatin	0.8
Perindopril erbumine	0.6
Vildagliptin	0.5
RP complex	0.35
RV complex	0.4
PV complex	0.75

3.2.2. Analysis of melting points of drugs and drug complexes

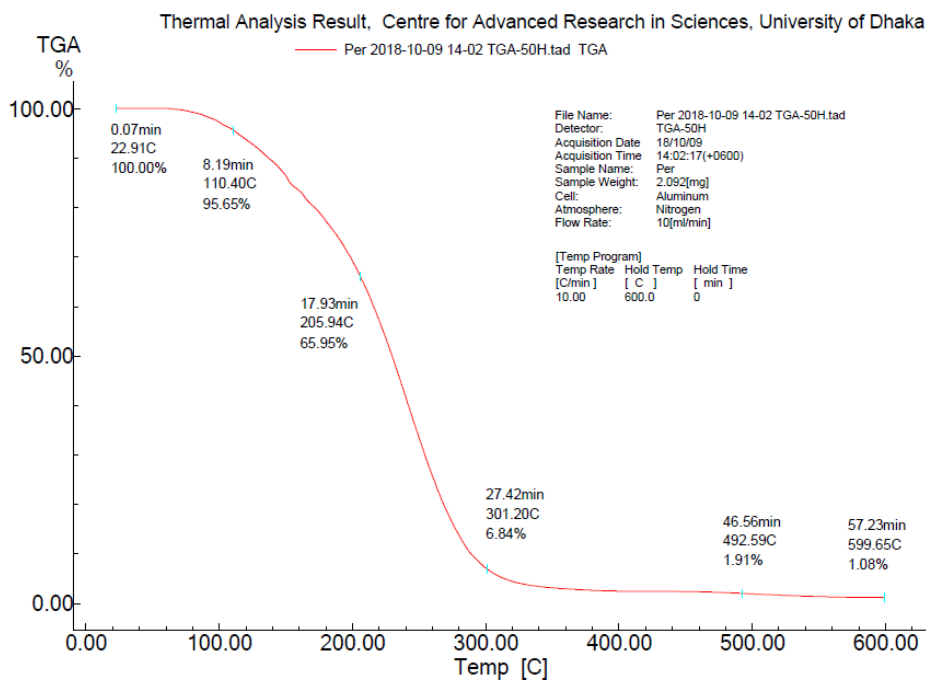
The melting points of the complexes were found to be different than that of their parent drugs. Rosuvastatin and vildagliptin showed their melting point at 156-160 °C and 145-150 °C, respectively while the RV complex melted at 110-115 °C. Similarly, perindopril gave melting point at 126-130 °C while the drug complexes PV and PR exhibited the melting points at 115-118 °C, 55-60 °C, respectively (Table 3.14).

Table 3.14. Different melting points of the drugs rosuvastatin, perindopril, vildagliptin and the newly formed complexes PR, RV and PV.

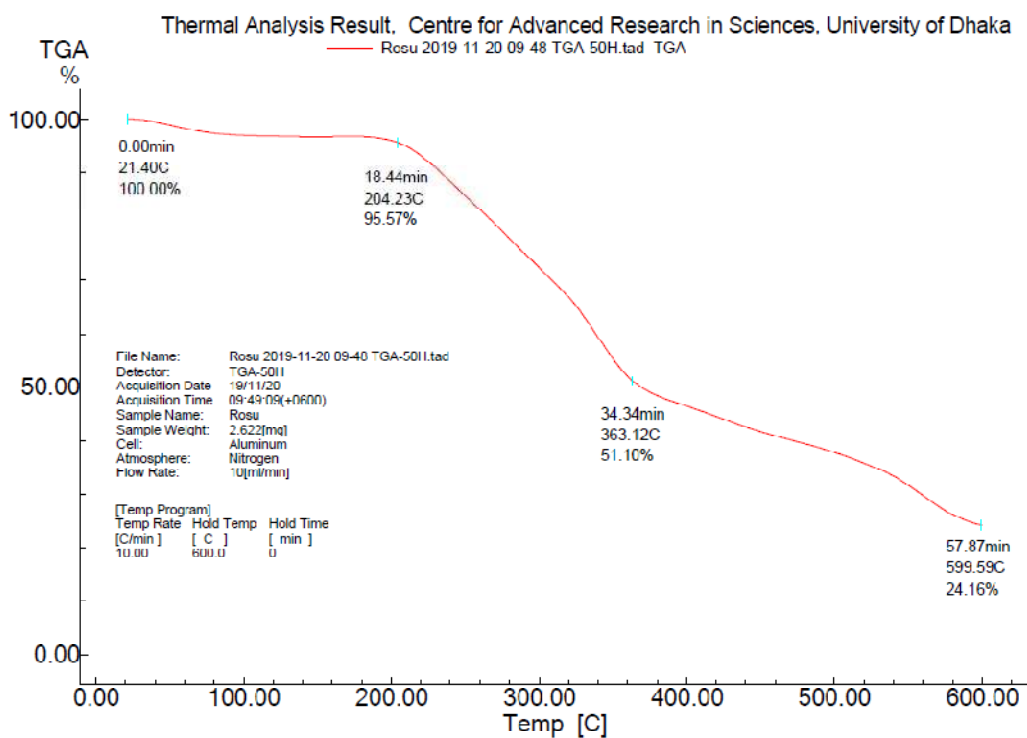
Item	Melting point
Rosuvastatin	156-160 °C
Perindopril erbumine	126-130 °C
Vildagliptin	145-150 °C
PR complex	55-60 °C
RV complex	110-115 °C
PV complex	115-118 °C

3.2.3. TGA thermogram analysis of parent drugs and drug complexes

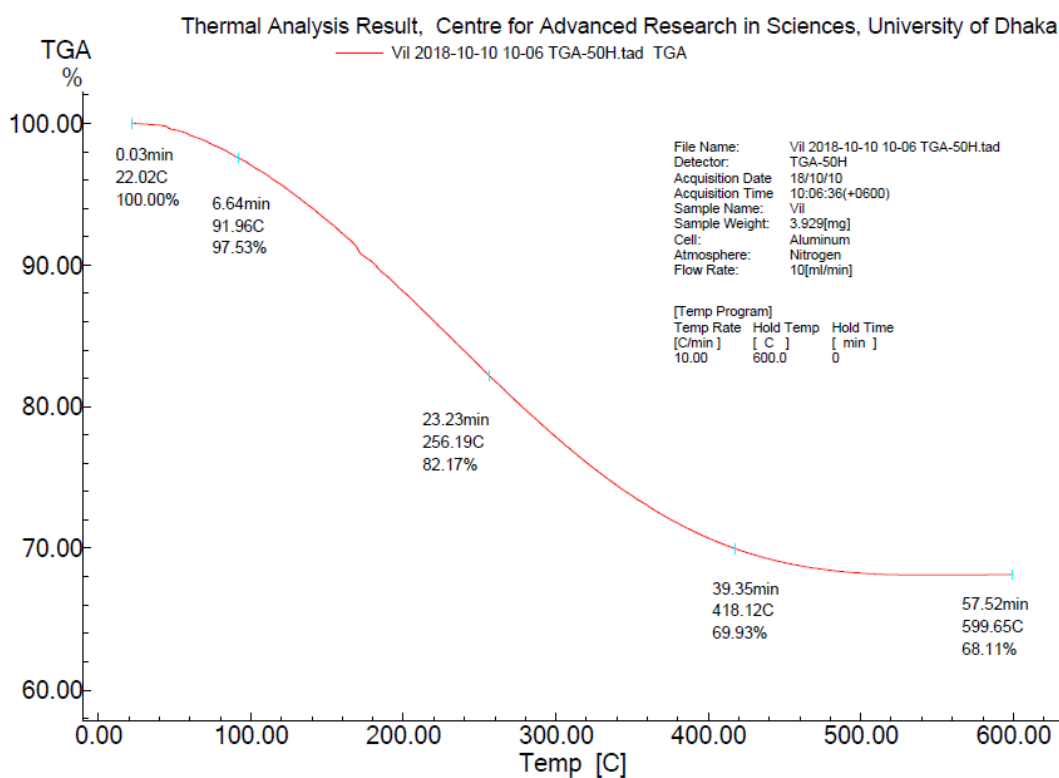
TGA thermograms were recorded for parent drugs and the formed complexes and have been shown in Figure 3.26.



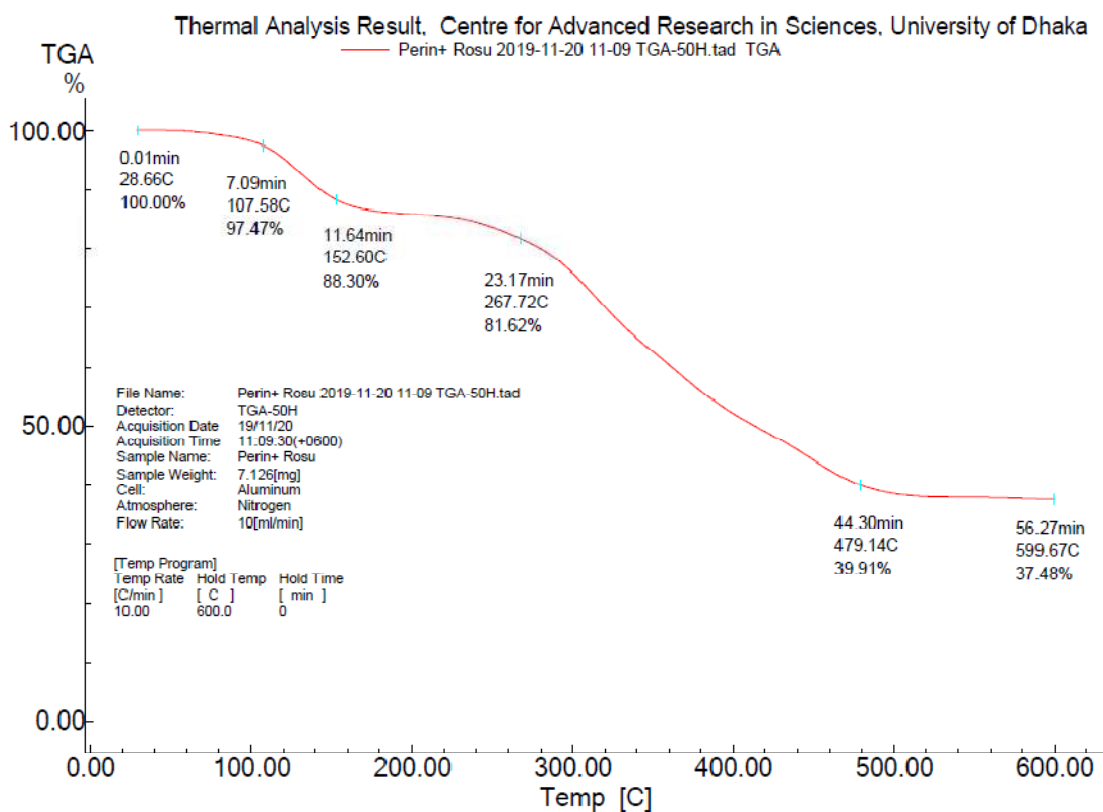
(1) TGA thermogram of perindopril erbumine.



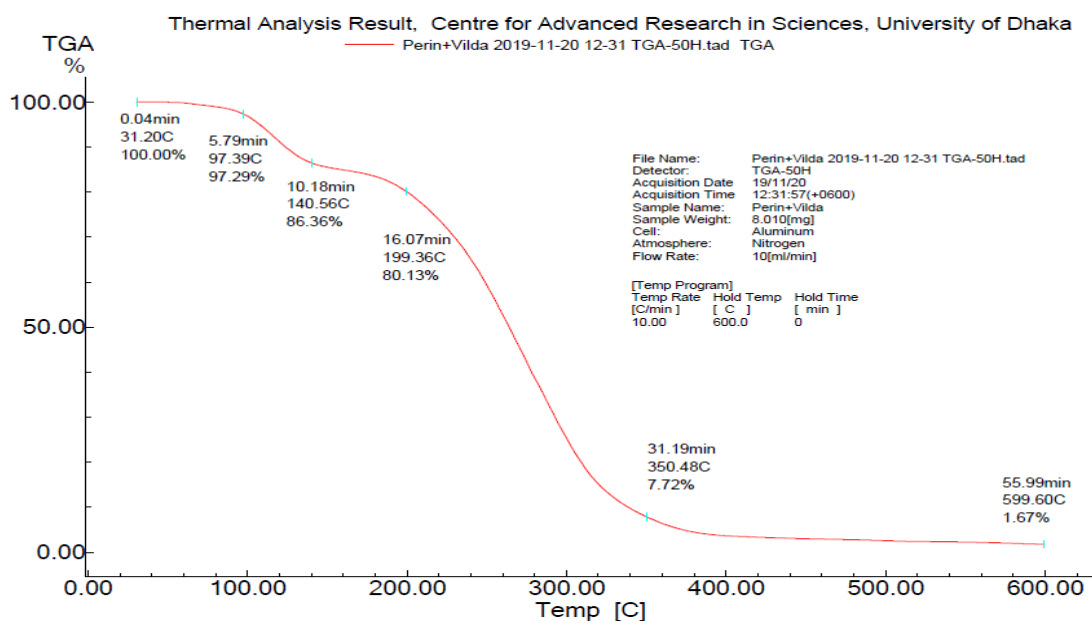
(2) TGA thermogram of rosuvastatin.



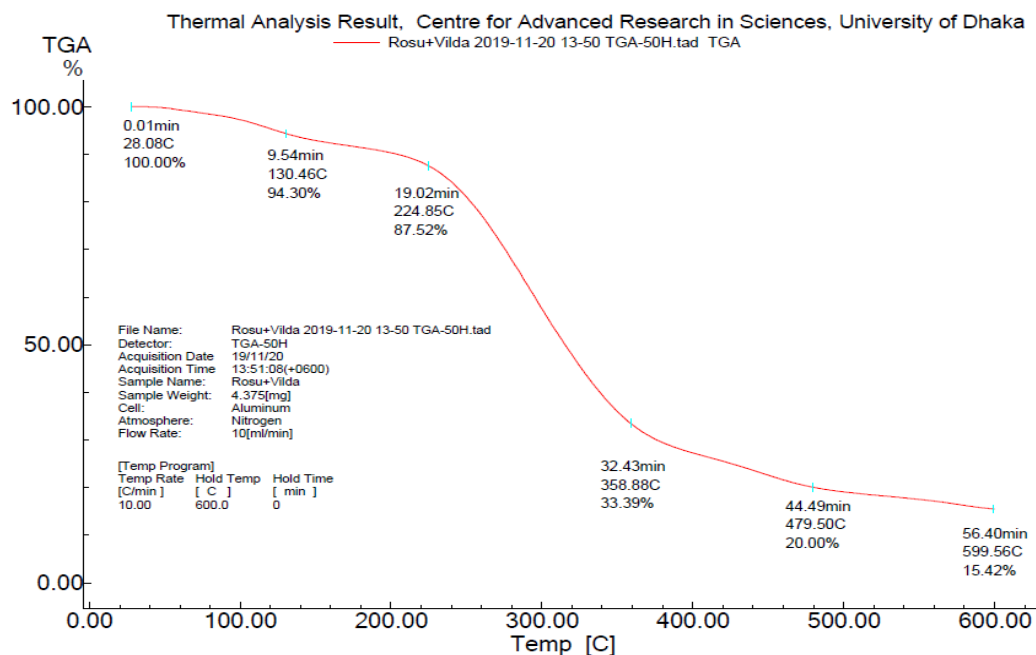
(3) TGA thermogram of vildagliptin.



(4) TGA thermogram of complex PR.



(5) TGA thermogram of the drug complex PV.

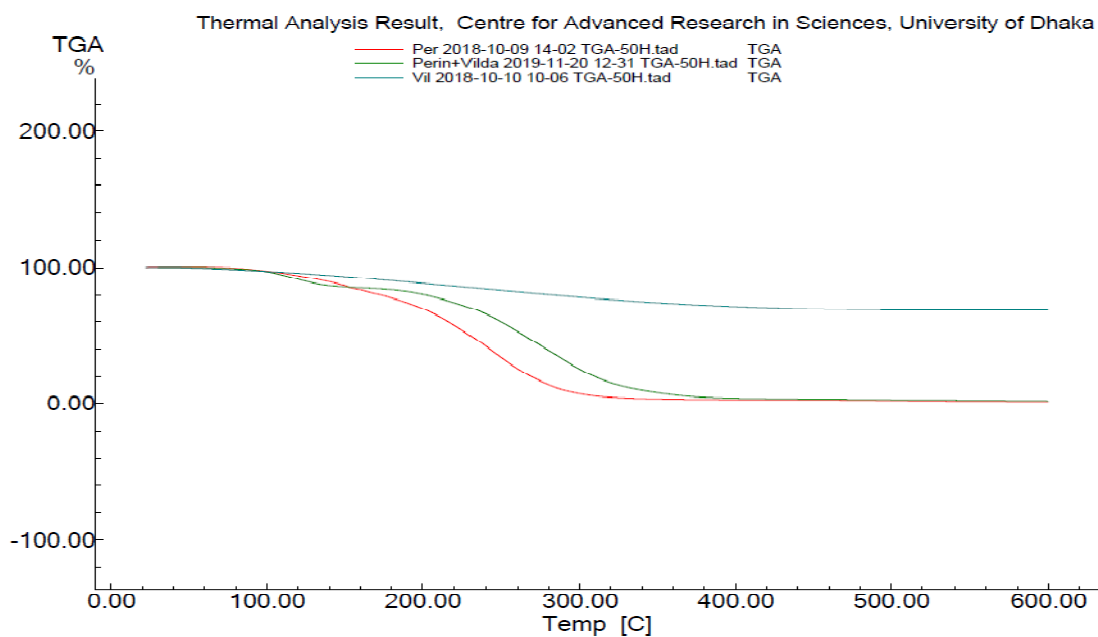


(6) TGA thermogram of the drug complex RV.

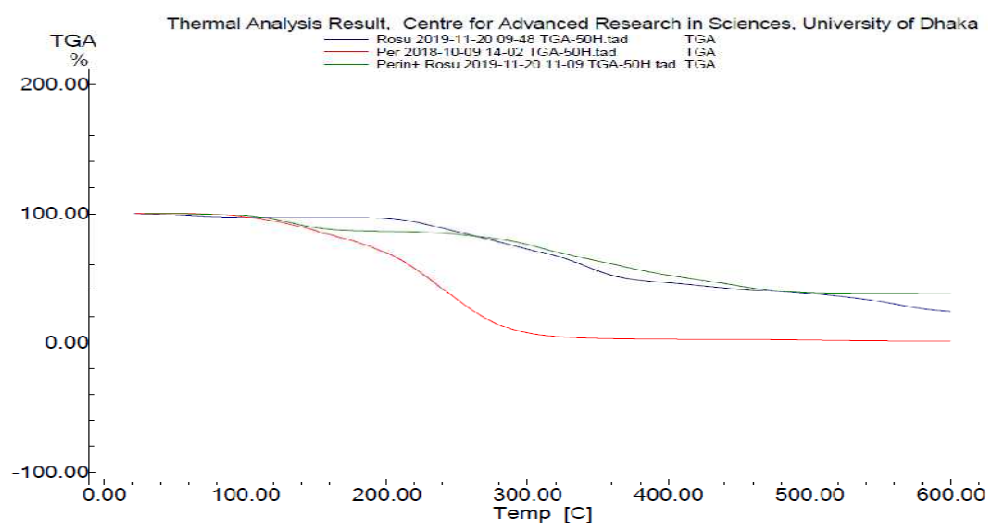
Figure 3.26. TGA thermograms of the drugs and newly formed drug complexes: (1) perindopril, (2) rosuvastatin, (3) vildagliptin, (4) drug complex PR, (5) drug complex PV, (6) drug complex RV.

In TGA perindopril produced 4.35% and 93.16% degradation at 110.40 °C and 301.20 °C, respectively. From the TGA of rosuvastatin, 4.43% and 75.84% degradation were observed at 204.23 °C and 599.59 °C, respectively. Vildagliptin also showed 2.47% and 30.07% degradation at 91.96 °C and 418.12 °C, respectively (Figure 3.26).

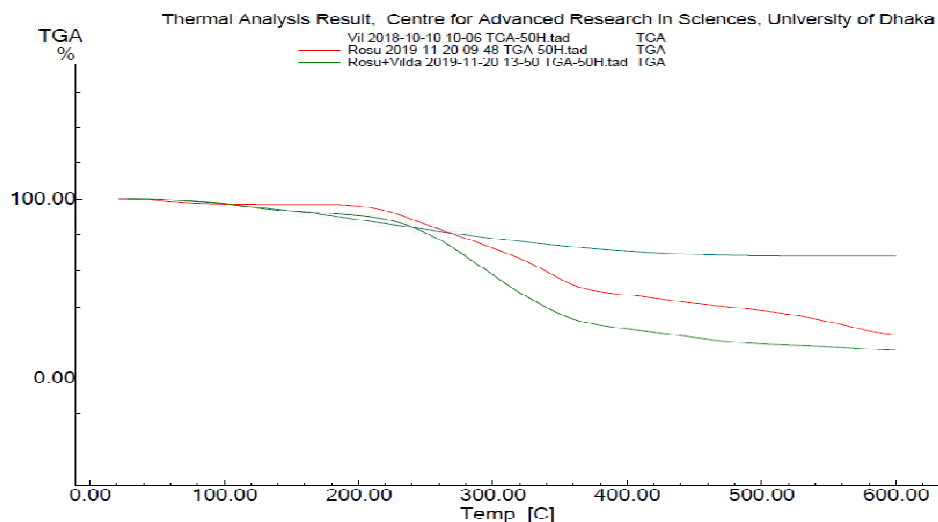
The overlaid TGA thermograms are given shown in Figure 3.27 which revealed different break down patterns of the newly formed drug complexes and the parent drug molecules.



(1) Overlaid TGA thermograms of perindopril, vildagliptin and the complex PV.



(2) Overlaid TGA thermograms of perindopril, rosuvastatin and the complex PR.



(3) Overlaid TGA thermograms of vildagliptin, rosuvastatin and the complex RV.

Figure 3.27. The three overlaid TGA thermograms of the drugs and newly formed drug complexes: (1) Overlaid TGA thermograms of perindopril, vildagliptin and the complex PV, (2) Overlaid TGA thermograms of perindopril, rosuvastatin and the complex PR and (3) Overlaid TGA thermograms of vildagliptin, rosuvastatin and the complex RV.

The TGA thermogram of PR revealed 11.7% and 60.09% degradation at corresponding temperature of 152.60 °C and 479.14 °C. The new complex PV gave 13.61% and 19.87% degradation at the temperatures of 140.56 °C and 199.36 °C, respectively. From the TGA thermogram of RV the 5.7% degradation was found at 130.46 °C and 12.48% at 224.85 °C. The drug complexes showed different degradation patterns from their parent drug molecules (Table 3.15).

Table 3.15. Percent (%) degradation of pure drugs and drug complexes with increasing temperature from TGA thermograms.

Sample	% degradation with increasing temperature				
	(i)	(ii)	(iii)	(iv)	(v)
Perindopril (P)	0 at 22.91°C	4.35 at 110.40 °C	34.05 at 205.94 °C	93.16 at 301.20 °C	98.92 at 599.65°C
Rosuvastatin (R)	0 at 21.40 °C	4.43 at 204.25 °C	48.9 at 363.12 °C	48.9 at 363.12 °C	75.84 at 599.59 °C
Vildagliptin (V)	0 at 22.02 °C	2.47 at 91.96 °C	17.83 at 252.19 °C	30.07 at 418.12 °C	31.89 at 599.65 °C
PR complex	0 at 28.66 °C	2.6 at 107.58 °C	11.7 at 152.60 °C	18.38 at 267.72 °C	62.52 at 599.67 °C
PV complex	0 at 31.20 °C	2.71 at 97.39 °C	13.61 at 140.56 °C	92.28 at 350.48 °C	98.33 at 599.60 °C
RV complex	0 at 28.08 °C	5.7 at 130.46 °C	12.48 at 224.85 °C	66.61 at 358.88 °C	84.58 at 599.56 °C

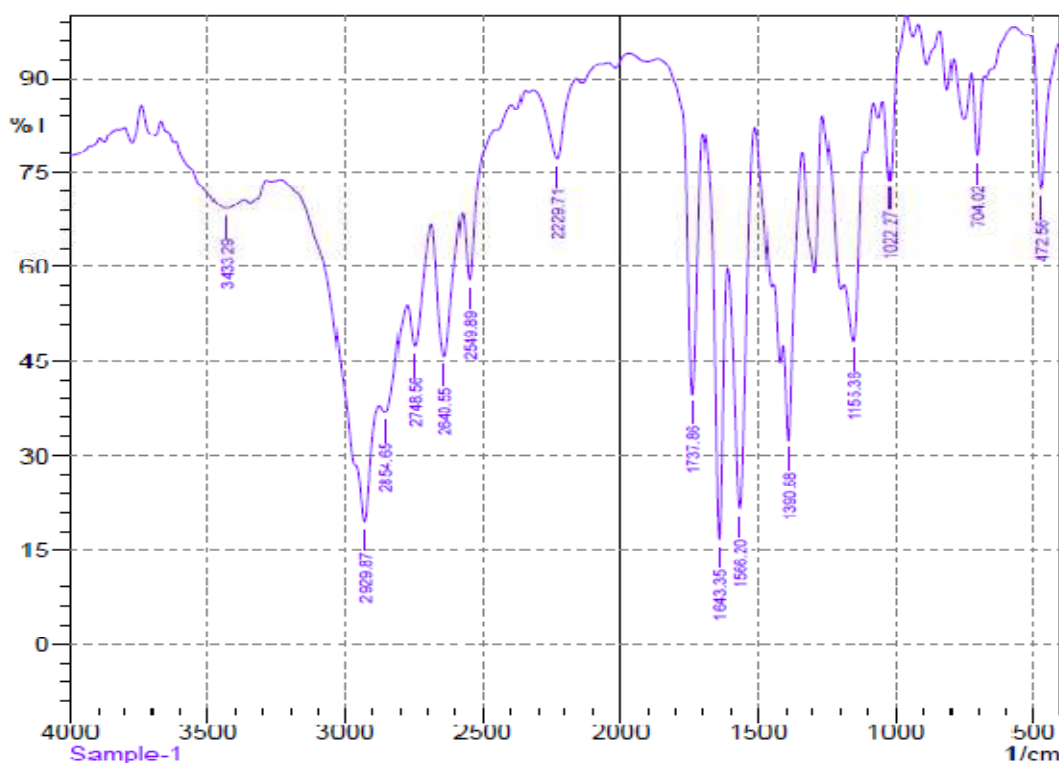
3.2.4. FT-IR spectra analysis of drugs and drugs complexes

Wave number of 2929.87 cm^{-1} in the IR spectrum of perindopril erbumine revealed the presence of C-H stretching. The peak at 1737.86 cm^{-1} indicated the presence of C=O stretching, the wave number 1643.35 cm^{-1} directed the appearance of N-H bending, peak at 1566.20 cm^{-1} indicated the presence of aromatic C=C and the C-H scissoring and bending was indicated by the presence of peak at 1390.68 cm^{-1} (Asadullah *et al.*, 2014; Ratnaparkhi, 2012).

FT-IR spectrum of rosuvastatin showed a broad region of band which was found from 3625 cm^{-1} to 3200 cm^{-1} which indicated the presence of hydroxyl group (OH). Carbonyl group showed a characteristics band at 1546.9 cm^{-1} . However, bands for the OH group and -CO group were found to be overlapped at the region of $3625\text{--}3200\text{ cm}^{-1}$. Beside this broad band, a peak was observed at 2968.45 cm^{-1} which was characteristics for olefinic C-H of heptanoic chain and C-H group showed a sharp band at 1546.91 cm^{-1} . Characteristics bands for sulfoxide group appeared at 1382.96 cm^{-1} and 1153.43 cm^{-1} , respectively (Tabassum *et al.*, 2016).

In the FT-IR spectrum of vildagliptin, the major peaks were found at $3011\text{--}3370\text{ cm}^{-1}$ and OH and N-H stretching vibrations was assigned to 3294.42 cm^{-1} . The prominent peak at 2916.37 cm^{-1} was assigned to nitrile group. The bands at 1658.78 and

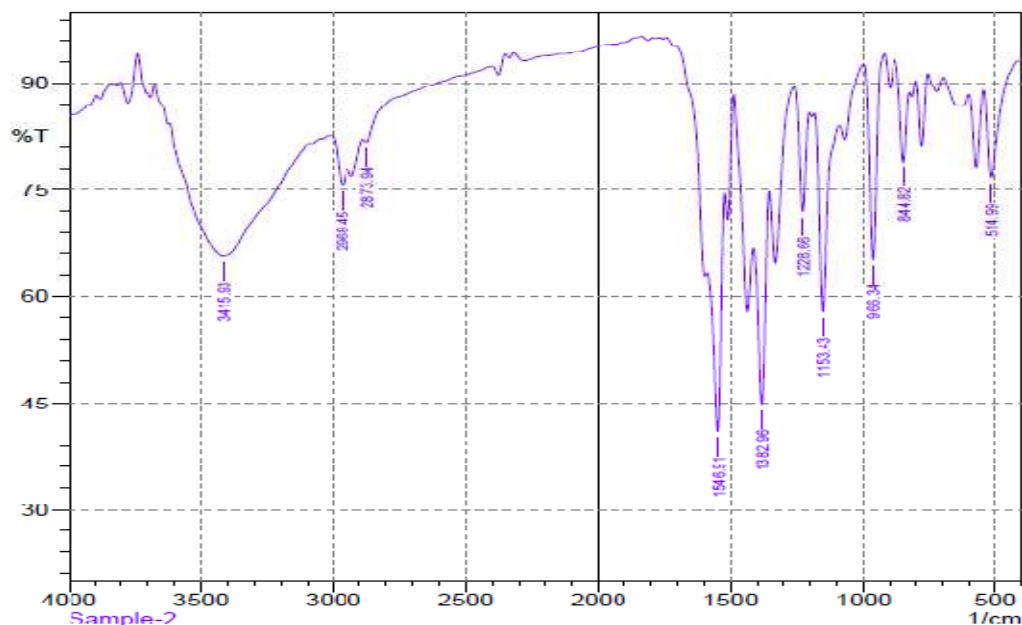
1309.67 cm^{-1} were obtained for amide C=O and C–N stretching (Naik and Waghulde, 2018). The FT-IR spectra are shown in Figure 3.28.



Comment;
Sample-1

Date/Time: 11/11/2020 11:01:07 AM
No. of Scans,

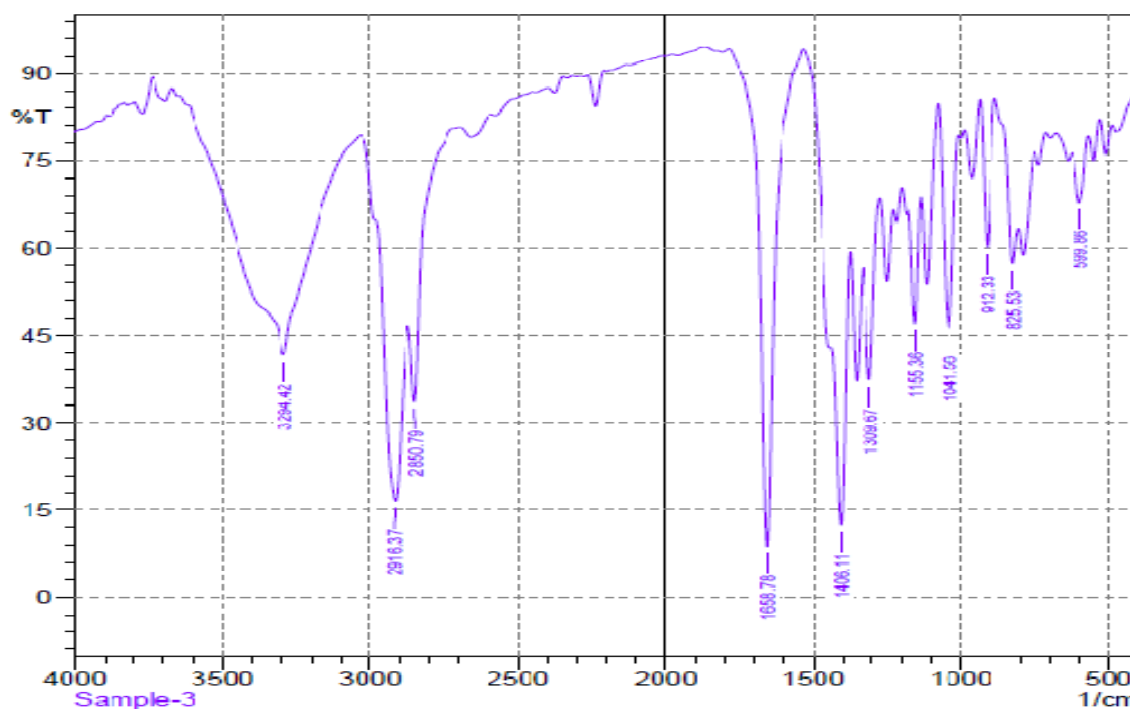
(1) FT-IR spectrum of perindopril erbumine.



Comment;
Sample-2

Date/Time: 11/11/2020 11:07:36 AM
No. of Scans;

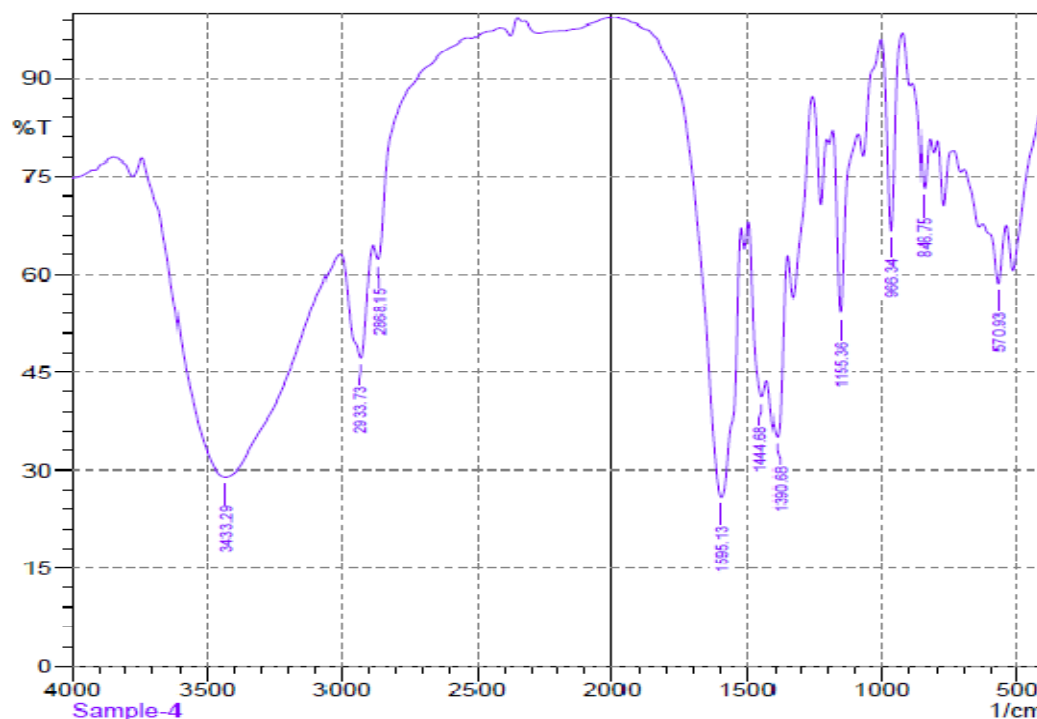
(2) FT-IR spectrum of rosuvastatin.



Comment;
Sample-3

Date/Time: 11/11/2020 11:29:41 AM
No. of Scans;

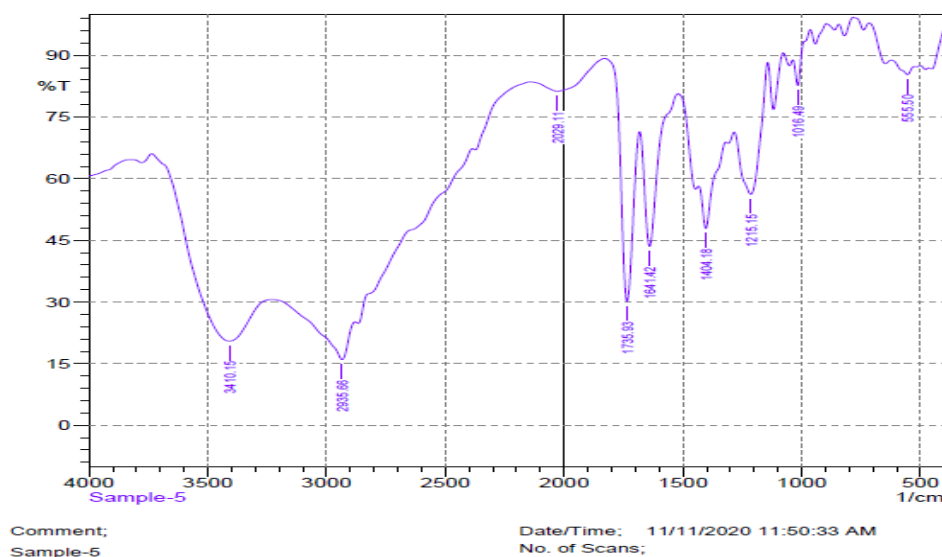
(3) FT-IR spectrum of vildagliptin.



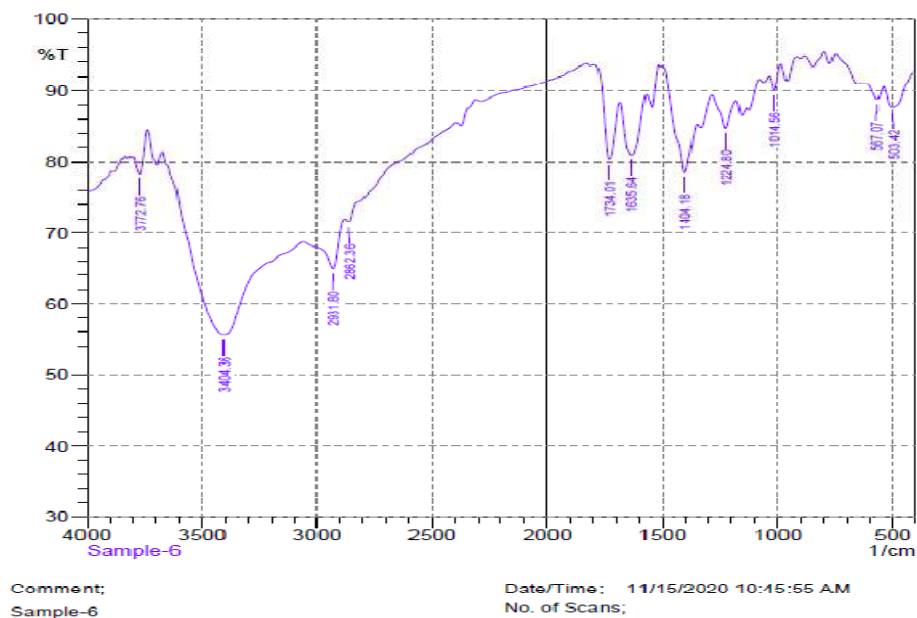
Comment;
Sample-4

Date/Time: 11/11/2020 11:37:27 AM
No. of Scans;

(4) FT-IR spectrum of the drug complex PR.



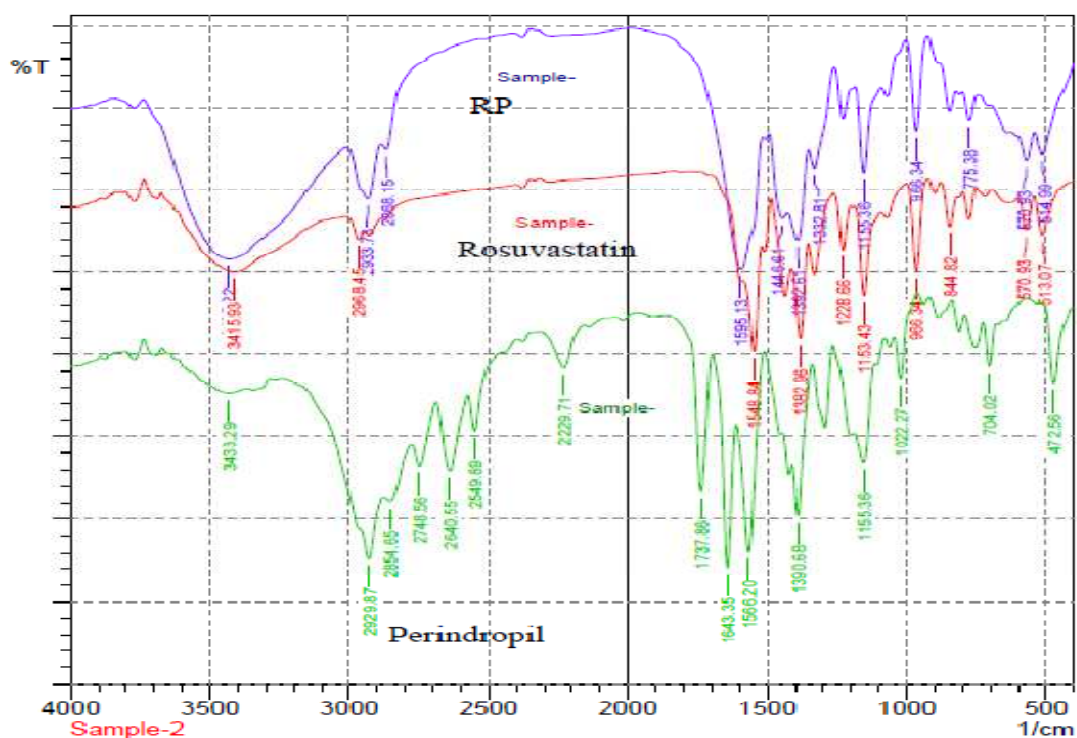
(5) FT-IR spectrum of the drug complex PV.



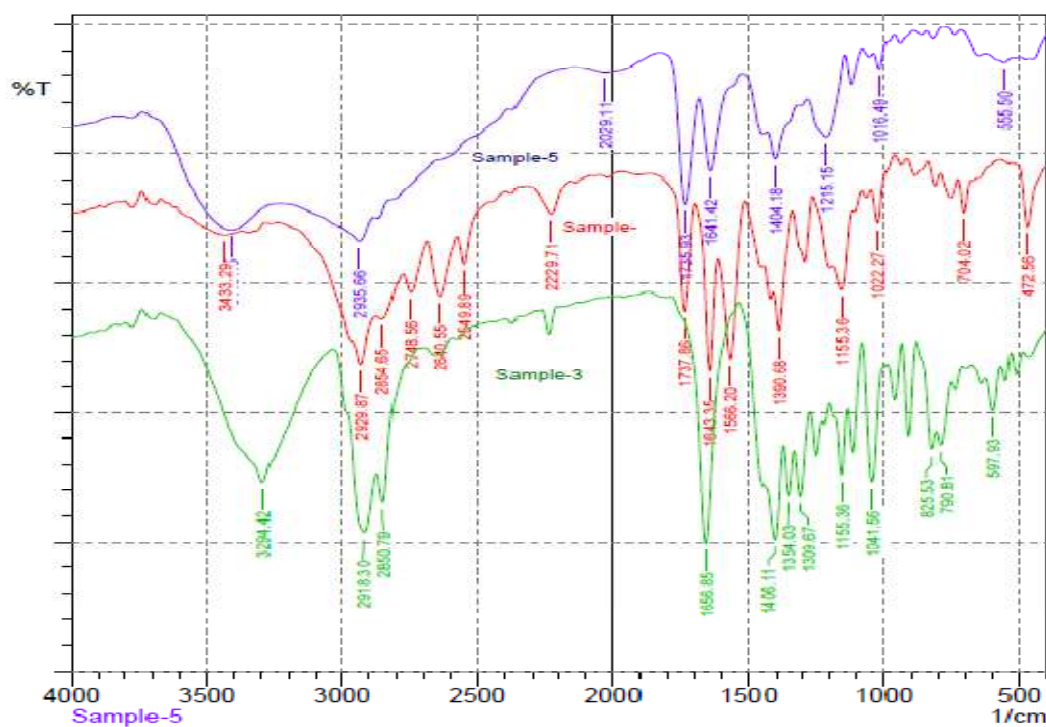
(6) FT-IR spectrum of the drug complex RV.

Figure 3.28. FT-IR spectra of the drugs and drugs complexes: (1) perindropil erbumine, (2) rosuvastatin, (3) vildagliptin, (4) drug complex PR, (5) drug complex PV and (6) drug complex RV.

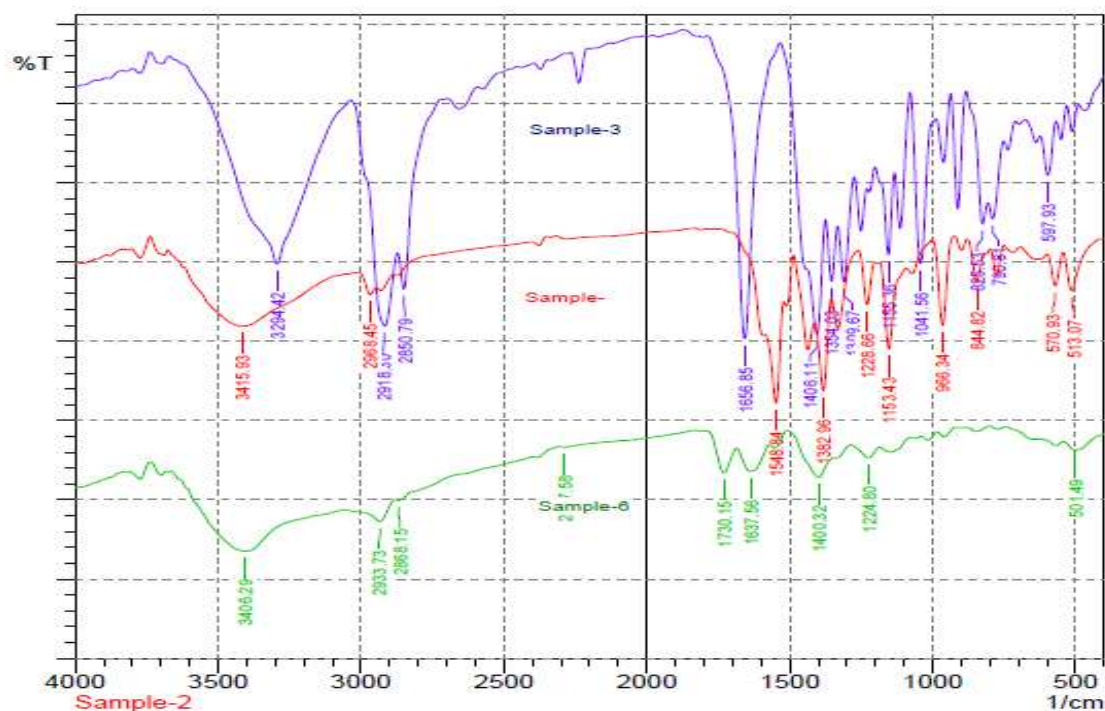
The overlaid FT-IR spectra are shown below in the Figure 3.29. The patterns of bands of the drug complexes are different from the parent drugs.



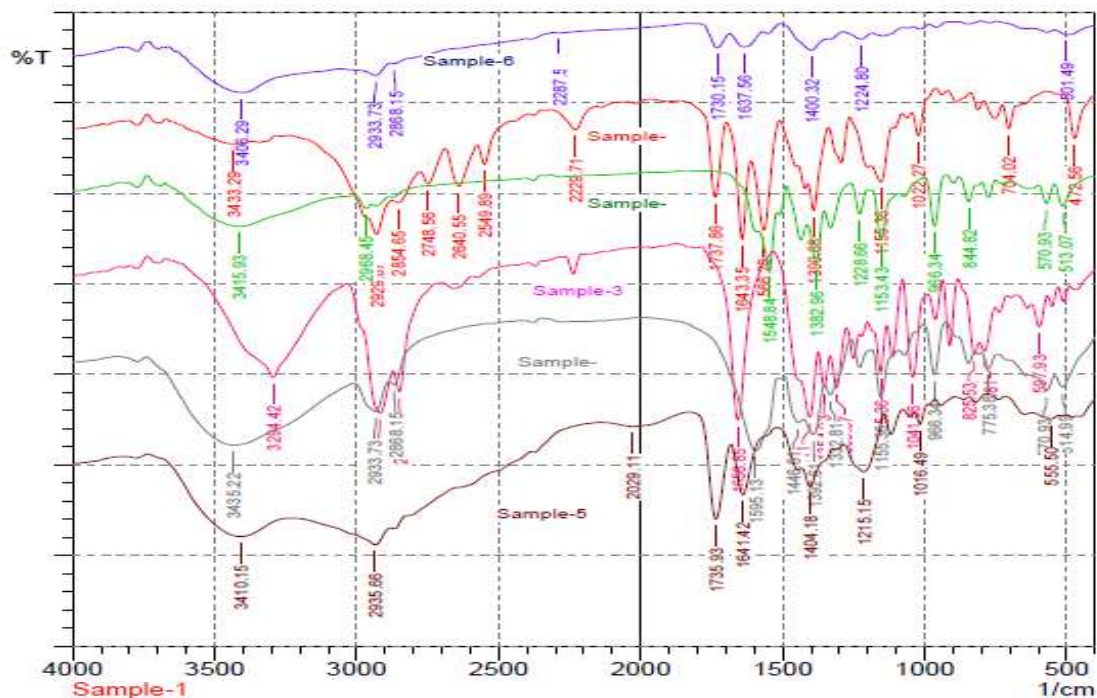
(1) Overlaid FT-IR spectra of perindopril, rosuvastatin and the drug complex PR.



(2) Overlaid FT-IR spectra of perindopril, vildagliptin and their complex PV.



(3) Overlaid FT-IR spectra of rosuvastatin, vildagliptin and the drug complex RV.



(4) Overlaid FT-IR spectra of perindopril, rosuvastatin, vildagliptin, PR, PV and RV.

Figure 3.29. Overlaid FT-IR spectra of: (1) perindopril, rosuvastatin the drug complex PR; (2) perindopril, vildagliptin and their complex PV; (3) rosuvastatin, vildagliptin and their complex RV; (4) perindopril, rosuvastatin, vildagliptin, PR, PV and RV.

3.2.5. *In vivo* study: Assessment of hypolipidemic activity of rosuvastatin and its complexes

Hyperlipidemia is one of the chief causes of cardiovascular diseases (CVDs) and it is responsible for 1/3 of total deaths worldwide (Ginghina *et al.*, 2011; Jorgensen *et al.*, 2013). Hyperlipidemia is characterized as an elevation of serum lipids, including triglycerides, cholesterol, cholesterol esters and phospholipids and/or plasma lipoprotein including very low density lipoprotein and reduced high-density lipoprotein levels (Jeyabalan and Palayan, 2009; Mishra *et al.*, 2011). Hypercholesterolemia and hypertriglyceridemia are two major reasons of atherosclerosis which have close association with ischemic heart disease (IHD) (Brouwers *et al.*, 2012), a leading cause of mortality. Moreover, increased level of plasma cholesterol accounts for about four million deaths in a year (Kumar *et al.*, 2012). In atherosclerosis, the arterial wall becomes narrowing by deposition of cholesterol and the arteries become harden. Hyperlipidemia stabilizes atherosclerosis and atherosclerosis-mediated disorders, e.g. coronary, cerebrovascular and peripheral vascular diseases (Wells *et al.*, 2007). Hyperlipidemia causes increased oxidative stress leading to increased oxygen free radical production that initiates atherosclerosis and associated CVDs by oxidative modifications of low density lipoproteins. Oxidative modifications in low-density lipoproteins play significant roles in the initiation and progression of atherosclerosis and associated cardiovascular diseases (Mishra *et al.*, 2011).

In the assessment of hypolipidemic activity of three drugs complexes PR, PV and RV we used rosuvastatin as standard and the study was conducted in rabbit model. The new complexes exhibited promising activity compared to the standard as shown in Table 3.16.

Table 3.16. Level of HDL, cholesterol, triglycerides, LDL cholesterol, VLDL cholesterol and non HDL cholesterol of different groups of rabbits treated with drugs.

Groups of rabbits	HDL mg/dL	Cholesterol mg/dL	Triglycerides mg/dL	LDL cholesterol mg/dL	VLDL cholesterol mg/dL	NonHDL cholesterol mg/dL
Control	12.48± 2.3	211.37± 10.13	2.52± 0.70	198.25± 10.71	1.0±0.98	198.75± 10.45
Oil feeding	43.97± 1.2	190.71± 8.10	239.10± 43.16	110.75± 10.28	35.75±4.33	146.75± 8.70
Rosuvastatin	30.34± 2.01	144.8±9.12	280.13±40.25	87.0±12.10	37.0±3.23	114.0±9.23
PR	28.33± 2.5	139.92±8.23	210.1±38.34	81.0±10.12	30.0±2.12	112.0±8.79
RV	34.9± 2.7	172.35±10.12	152.01±41.45	111.0±10.11	27.0±3.32	137±8.32
PV	49.44± 2.3	143.68±9.32	179.99±37.65	69.0±10.65	26.0±4.13	94.0±10.45

The complex PR decreased cholesterol, triglycerides, LDL cholesterol, non HDL cholesterol to 139.92±8.23 mg/dL, 210.1±38.34 mg/dL, 81.0±10.12 mg/dL, 30.0±2.12 mg/dL and 112.0±8.79 mg/dL, respectively while the standard drug rosuvastatin reduced the level to 144.8±9.12 mg/dL, 280.13±40.25 mg/dL, 87.0±12.10 mg/dL, 37.0±3.23 mg/dL and 114.0±9.23 mg/dL, respectively. Rosuvastatin as well as three newly formed complexes PR, RV, PV increased the HDL cholesterol level to 30.34± 2.01 mg/dL, 28.33± 2.5 mg/dL, 34.9± 2.7 mg/dL and 49.44± 2.3 mg/dL in comparison to the control group rabbits (12.48± 2.3 mg/dL). The complex RV also decreased cholesterol, triglycerides, LDL cholesterol, VLDL cholesterol, non HDL cholesterol compared to the standard drug rosuvastatin viz. 172.35±10.12 mg/dL, 152.01±41.45 mg/dL, 111.0±10.11 mg/dL, 27.0±3.32 mg/dL and 137±8.32 mg/dL, respectively. The promising complex PV reduced the LDL and VLDL to 69.0±10.65 mg/dL and 26.0±4.13 mg/dL, respectively where the standard drug rosuvastatin reduced the levels to 87.0±12.10 mg/dL and 37.0±3.23 mg/dL, respectively. The results are shown in Figure 3.30.

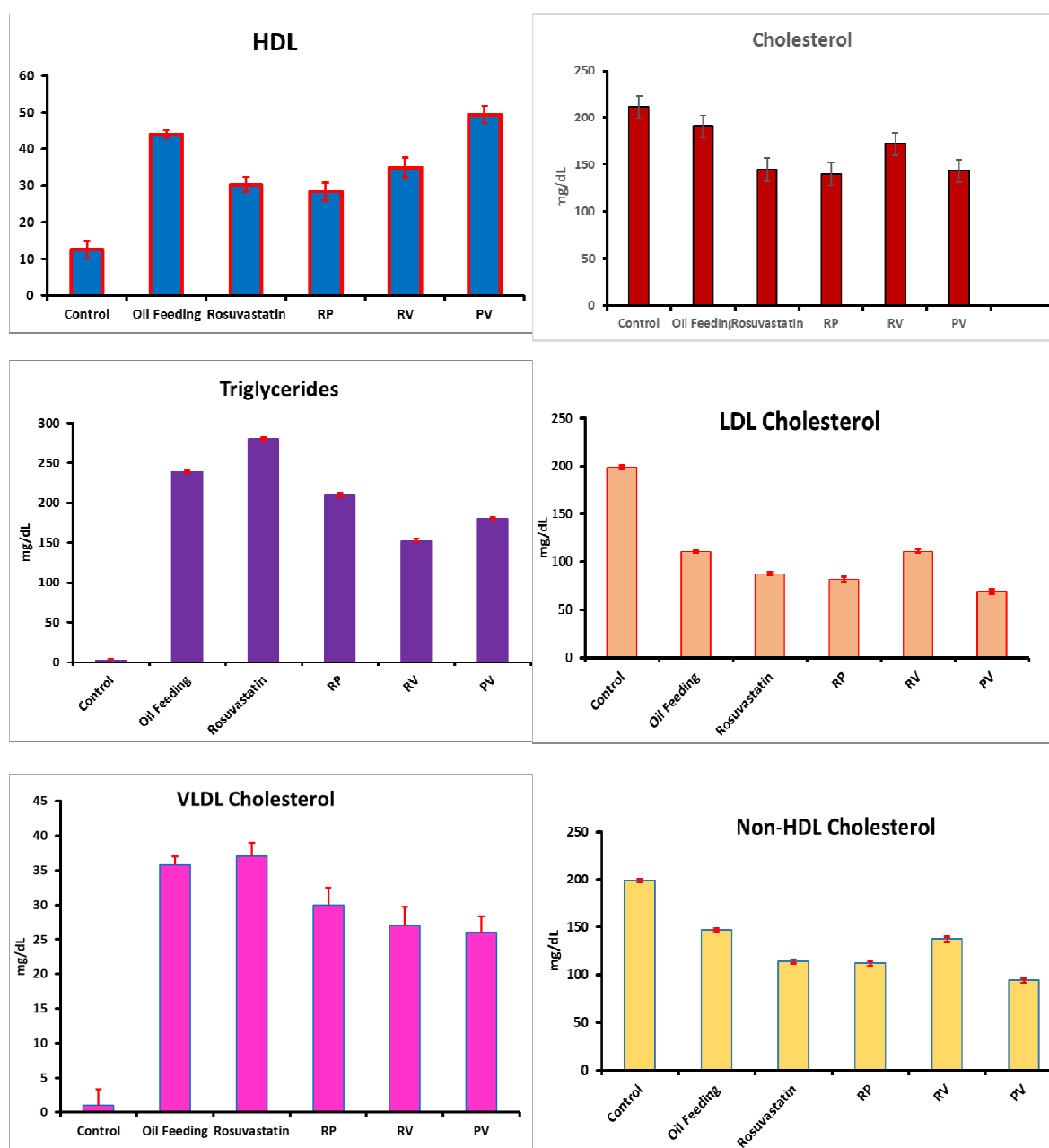


Figure 3.30. Comparison of levels of HDL, cholesterol, triglycerides, LDL cholesterol, VLDL cholesterol and non HDL cholesterol of different groups of drugs treated rabbits.

3.2.6. *In vitro* study: Determination of thrombolytic activity of drugs and drugs complexes

Newly synthesized drugs were evaluated for thrombolytic activity assay using streptokinase as standard. The standard exhibited 65.99 ± 2.65 % lysis of clot after addition to the clot and subsequent 90 minutes of incubation. Among the complexes, the RV demonstrated the highest thrombolytic activity (29.52 ± 09 %) (Table 3.17 and Figure 3.31).

Table 3.17. Thrombolytic activity of rosuvastatin and newly formed drug complexes PR, PV and RV.

Sample	W1	W2	W3	W4	W5	% clot lysis	Average	SD
Rosuvastatin	4806.5	5472.3	5350.5	121.8	665.8	18.2938	18.21	0.08
	4807.1	5471.8	5350.2	120.9	666.4	18.1423		
	4806.8	5472.1	5349.6	121.2	665.9	18.2009		
PR	5086.3	5406.4	5322.1	84.3	320.1	26.3355	26.39	0.06
	5085.8	5405.9	5321.7	84.7	320.2	26.4522		
	5086.4	5406.2	5322.3	84.5	320.3	26.3815		
PV	4854.6	5162.7	5098.1	64.6	308.1	20.9672	20.96	0.09
	4854.65	5162.57	5098.65	64.34	308.23	20.874		
	4854.89	5162.65	5098.78	64.98	308.78	21.0441		
RV	4860.9	5258.6	5141.6	117.0	397.7	29.4192	29.52	0.09
	4860.89	5258.57	5141.98	117.67	397.87	29.575		
	4860.79	5258.89	5141.76	117.45	397.34	29.5591		
Blank	4763.5	5142.6	5135.6	7.0	379.1	1.84648	1.87	0.02
	4763.58	5142.58	5135.59	7.17	379.26	1.89052		
	4763.63	5142.68	5135.87	7.12	379.16	1.87784		
SK	0.888	1.526	1.13	0.4	0.6	66.6667	65.99	2.65
	0.879	1.601	1.17	0.41	0.65	63.0769		
	0.869	1.519	1.14	0.43	0.63	68.254		

Here, W_1 = wt of vial alone, W_2 = wt of clot containing vial, W_3 = wt of clot containing vial after lysis, W_4 = wt of released clot, W_5 = wt of clot.

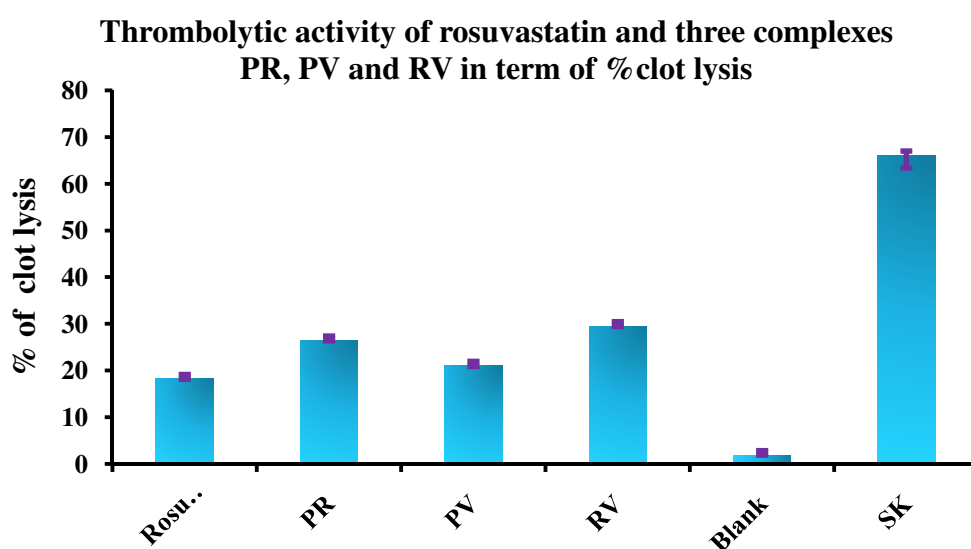


Figure 3.31. Thrombolytic activity exhibited by rosuvastatin, PR, PV and RV in a way of % of clot lysis.

3.2.7. *In vitro* study: Membrane stabilizing activity assay

To estimate the possibility to prevent RBC lysis induced by solution of hypotones rosuvastatin and the complexes were analyzed. The active rosuvastatin inhibited 39.92% hemolysis of RBC followed by the complex RV (35.18%). The reference standard, acetyl salicylic acid (0.1 mg/mL standard) showed 58.83% inhibition of hemolysis of RBC in hypotonic solution (Table 3.18 and Figure 3.32).

Table 3.18. Membrane stabilizing activity of the drug rosuvastatin, drug complex PR, PV and RV in terms of % of inhibition of hemolysis of RBCs in hypotonic solution.

Sample	Conc. (mg/mL)	Absorbance	% of inhibition by hypotonic solution
Control	2	1.518	-
Rosuvastatin	2	0.912	39.92
PR	2	1.115	26.55
PV	2	1.223	19.43
RV	2	0.984	35.18
Acetyl salicylic acid	0.1	0.625	58.83

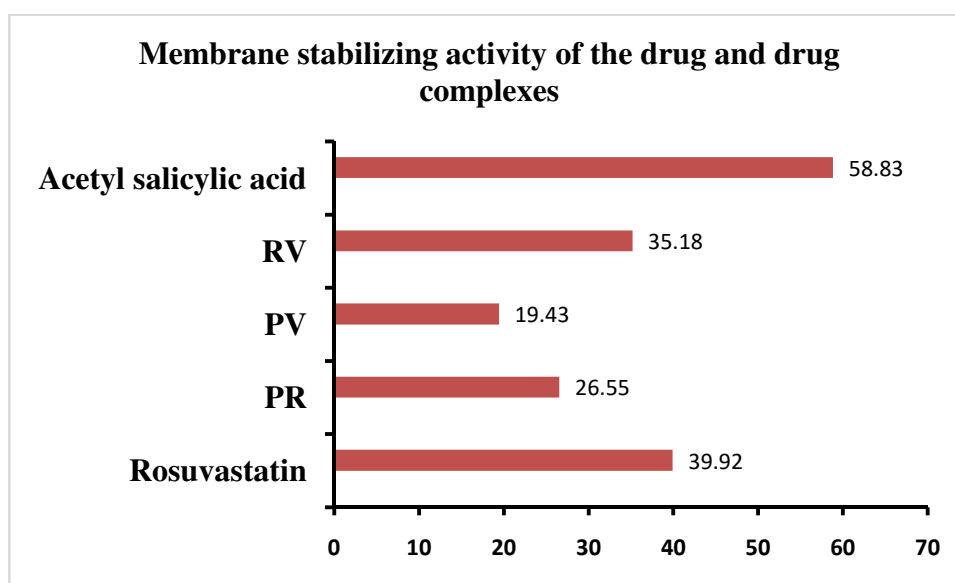


Figure 3.32. Membrane stabilizing activity of the drug rosuvastatin, drug complex PR, PV and RV in terms of % of inhibition of hemolysis of RBCs in hypotonic solution.

3.2.8. *In vitro* study of antioxidant activity

IC₅₀ values of antioxidant activity in DPPH technique were measured and ranged from (30.05 μg/mL) to (176.7 μg/mL). Among all samples the greater IC₅₀ value was given by PV (67.71 μg/mL) followed by RV (56.83 μg/mL), PR (54.79 μg/mL) and rosuvastatin

(131.6 $\mu\text{g/mL}$). The results of antioxidant activity were enlisted in Tables 3.19, 3.20, 3.21, 3.22, 3.23, 3.24 and in Figures 3.33 to 3.38.

Table 3.19. Antioxidant activity of rosuvastatin and the complexes PR, PV and RV.

Sample code	IC ₅₀ $\mu\text{g/ml}$
BHT	30.6
Rosuvastatin	131.6
PR	54.79
PV	67.71
RV	56.83

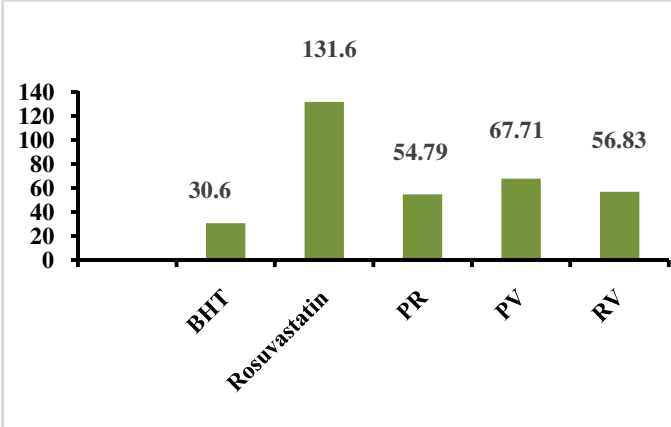


Figure 3.33. IC₅₀ values of BHT, rosuvastatin and three drug complexes.

Table 3.20. IC₅₀ values of tert-butyl-1-hydroxytoluene (BHT).

Absorbance of blank	Conc. ($\mu\text{g/mL}$)	Absorbance of the BHT	% inhibition	IC ₅₀
0.329	500	0.035	89.36	30.60
	250	0.062	81.16	
	125	0.096	70.82	
	62.5	0.141	57.14	
	31.25	0.181	44.98	
	15.63	0.215	34.65	
	7.813	0.237	27.96	
	3.906	0.256	22.19	
	1.953	0.271	17.63	
	0.977	0.29	11.85	

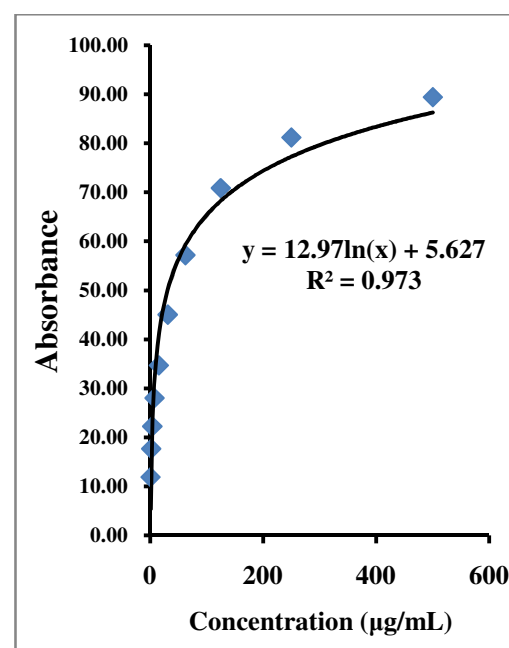
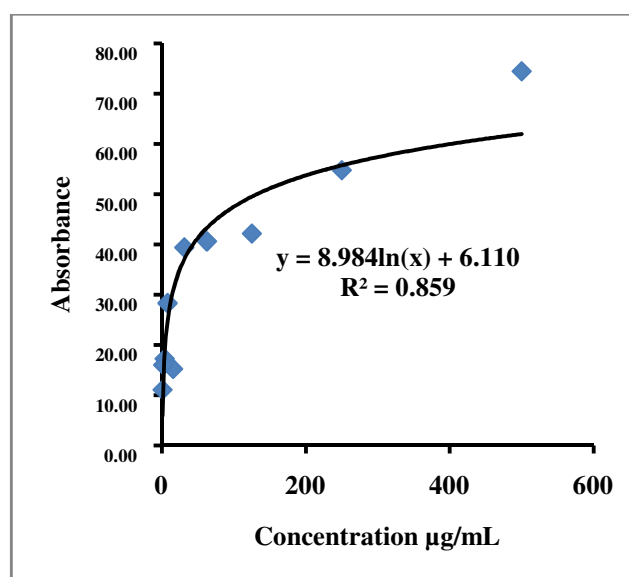


Table 3.21. IC₅₀ value of the standard drug rosuvastatin.

Absorbance of the blank	Conc. (µg/mL)	Absorbance of Rosuvastatin	% inhibition	IC ₅₀
0.325	500	0.083	74.46	131.6
	250	0.147	54.77	
	125	0.188	42.15	
	62.5	0.193	40.62	
	31.25	0.197	39.38	
	15.625	0.195	15.23	
	7.813	0.233	28.31	
	3.906	0.269	17.23	
	1.953	0.273	16.00	
	0.977	0.289	11.08	

**Figure 3.35.** IC₅₀ value of the standard drug rosuvastatin.**Table 3.22.** IC₅₀ values of the new drug complex PR.

Absorbance of the blank	Conc. (µg/mL)	Absorbance of PR	% inhibition	IC ₅₀
0.325	500	0.099	69.54	54.79
	250	0.108	66.77	
	125	0.135	58.46	
	62.5	0.164	49.54	
	31.25	0.179	44.92	
	15.625	0.197	39.38	
	7.813	0.219	32.62	
	3.906	0.253	22.15	
	1.953	0.274	15.69	
	0.977	0.280	13.85	

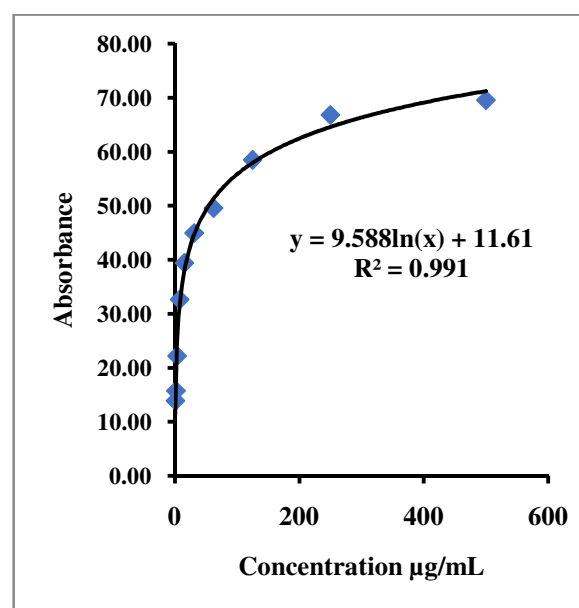
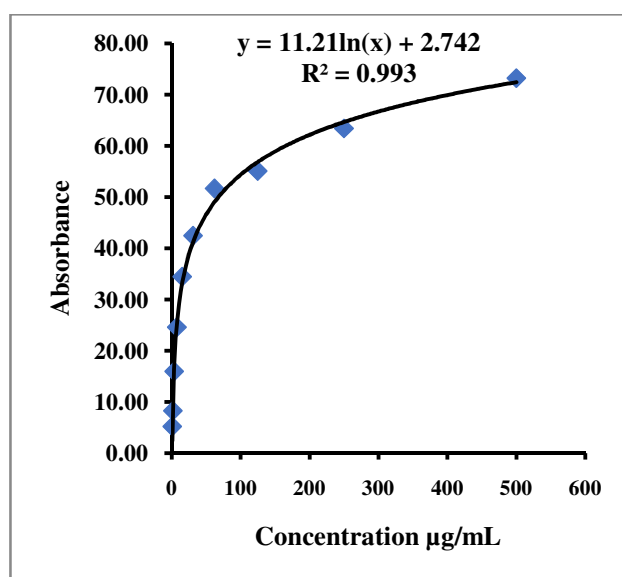
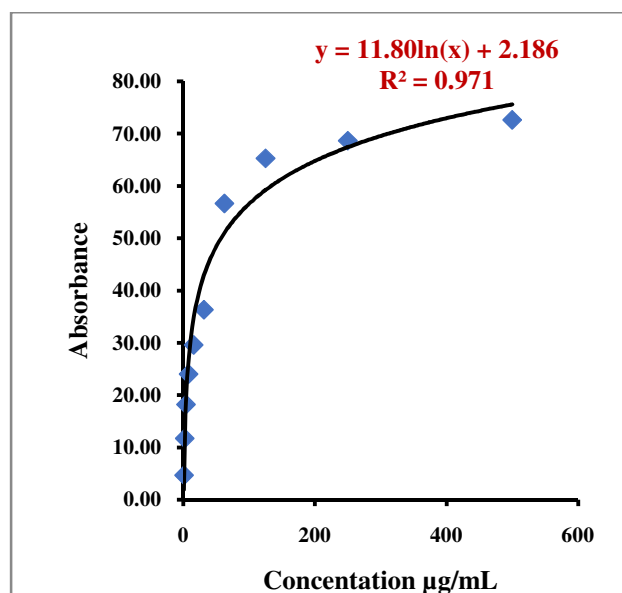
**Figure 3.36.** IC₅₀ value of the new drug complex PR.

Table 3.23. IC₅₀ value of the new drug complex PV.

Absorbance of the blank	Conc. (µg/mL)	Absorbance of PV	% inhibition	IC ₅₀
0.325	500	0.087	73.23	67.71
	250	0.119	63.38	
	125	0.146	55.08	
	62.5	0.157	51.69	
	31.25	0.187	42.46	
	15.625	0.213	34.46	
	7.813	0.245	24.62	
	3.906	0.273	16.00	
	1.953	0.298	8.31	
	0.977	0.308	5.23	

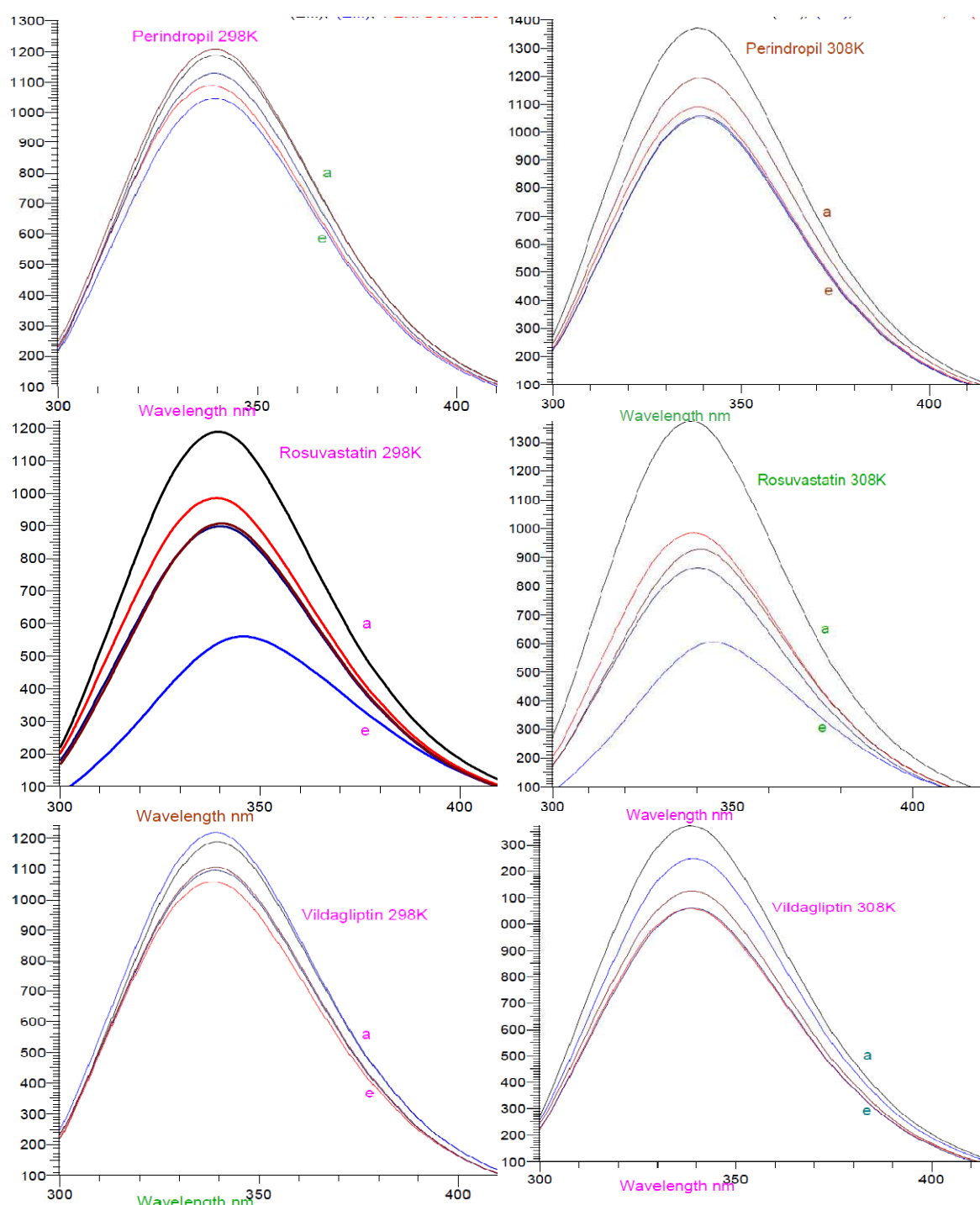
**Figure 3.37.** IC₅₀ value of the new drug complex PV.**Table 3.24.** IC₅₀ values of the new drug complex RV.

Absorbance of the blank	Conc. (µg/mL)	Absorbance of the RV	% inhibition	IC ₅₀
0.325	500	0.089	72.62	56.83
	250	0.102	68.62	
	125	0.113	65.23	
	62.5	0.141	56.62	
	31.25	0.207	36.31	
	15.63	0.229	29.54	
	7.813	0.247	24.00	
	3.906	0.266	18.15	
	1.953	0.287	11.69	
	0.977	0.310	4.62	

**Figure 3.38.** IC₅₀ value of the new drug complex RV.

3.2.9. Analyses of fluorescence quenching by perindopril, rosuvastatin, vildagliptin, and three drug complexes PR, PV and RV

The spectra of fluorescence quenching for BSA-drug and BSA-drug complex interaction were measured under physiological conditions at 280 nm at 298 K and 308 K which are shown in Figure 3.39. The spectra in presence of pure drugs or synthesized new complexes created a reduction in fluorescence intensity at 280 nm excitation wavelength. The study suggested the interaction occurred between BSA-drug and BSA-drug complexes.



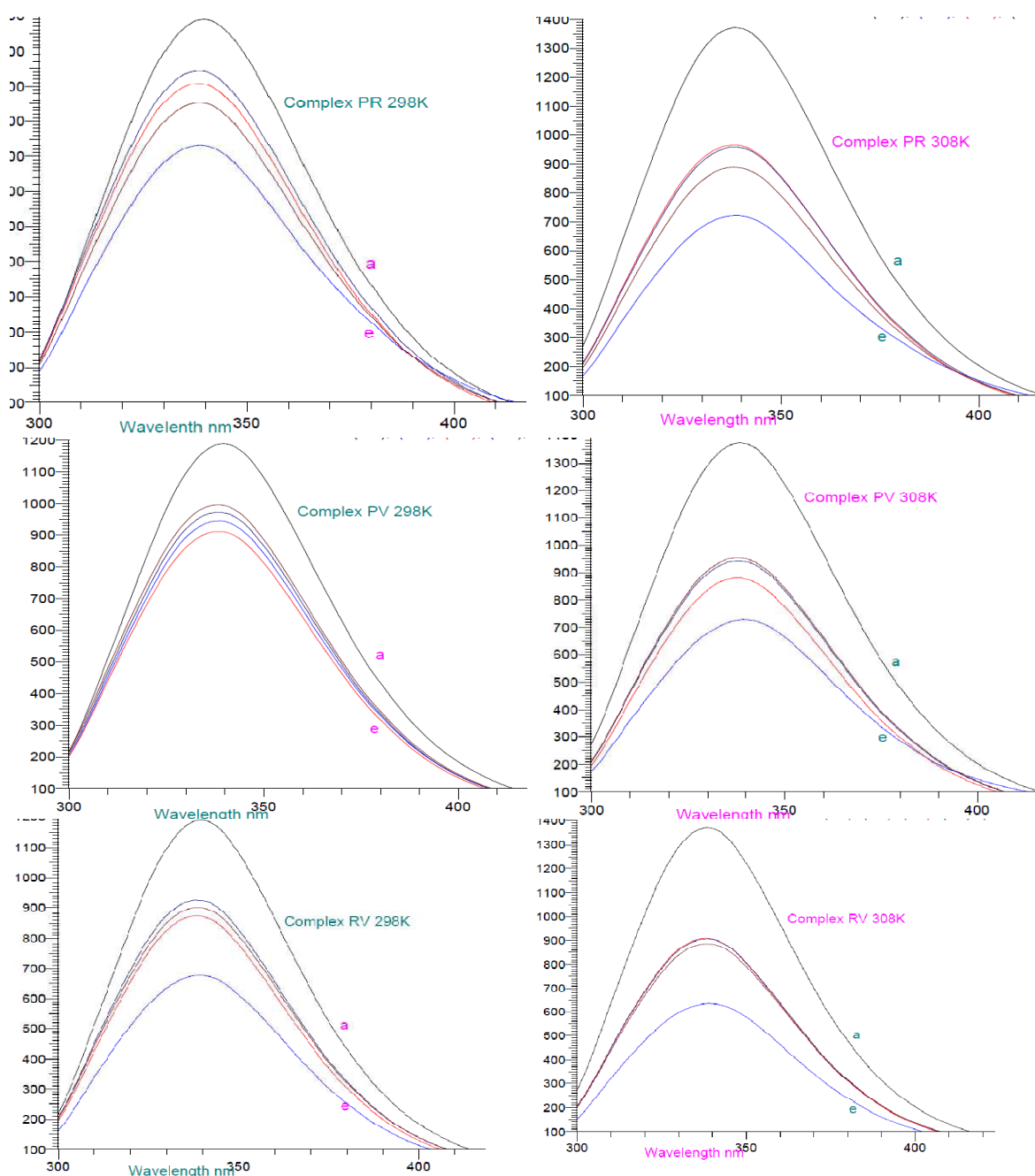


Figure 3.39. Fluorescence emission spectra of BSA in presence of different concentrations of perindopril, rosuvastatin, vildagliptin, complex PR, complex PV, complex RV, ($T = 298\text{ K}$ and 308 K ; $\lambda_{\text{ex}} = 280\text{ nm}$). $C(\text{BSA}) = 10 \times 10^{-6}\text{ mol L}^{-1}$, $C(\text{drugs/drug complexes}) (10^{-6}\text{ mol L}^{-1})$, curves a-e: 0, 5, 10, 20 and $50\text{ }\mu\text{M}$, respectively.

The Stern-Volmer plots for BSA quenching fluorescence by perindopril, rosuvastatin, vildagliptin, PR complex, PV complex and RV complex at two different temperatures were shown in Figure 3.41 and the corresponding Stern-Volmer quenching constants K_{sv} and quenching rate constant K_{q} were summarized in Table 3.25.

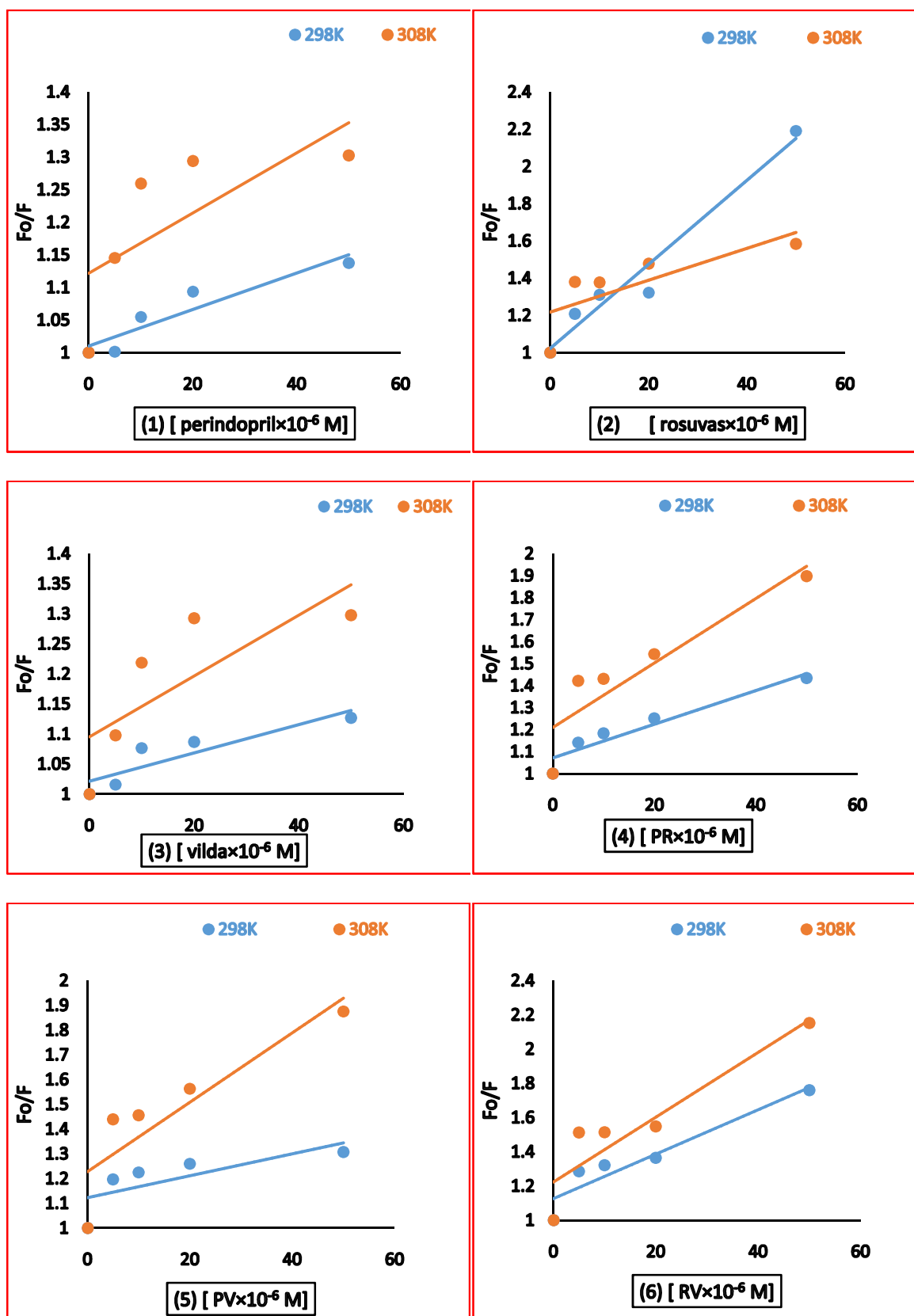


Figure 3.40. BSA quenching Stern-Volmer plots with increased concentration of (1) perindopril, (2) rosuvastatin, (3) vildagliptin, (4) complex PR, (5) complex PV and (6) complex RV at 298 K and 308 K.

With the increase in the temperature as K_{sv} values increased (except rosuvastatin-BSA and RV-BSA) it can be suggested that these drugs and the newly formed complexes reduced the fluorescence intensity of BSA by dynamic quenching mechanism. But in case of rosuvastatin-BSA and RV-BSA system K_{sv} values decreased with the increase in temperature, so the quenching might be happened by static mechanism. The activation energy of the quenching mechanism was calculated from the Arrhenius plot (Figure 3.42) and the values were listed in Table 3.25. It was evident that the activation energy of the complexes with BSA was less than the activation energy (except PV-BSA system) values of their individual interactions which is also an indicator of the complexation between the drugs.

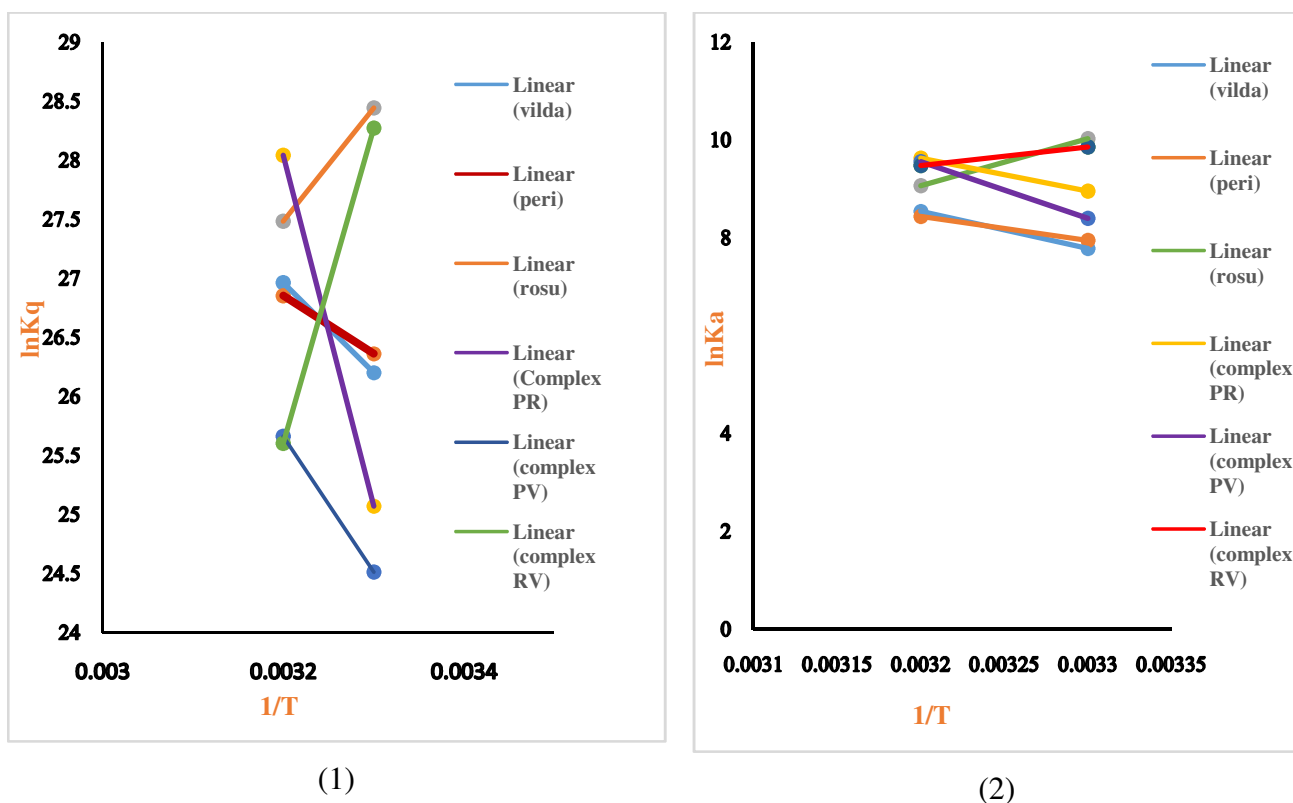


Figure 3.41. (1) Arrhenius plot, (2) Van't Hoff plot, after the interaction of BSA with perindopril, rosuvastatin, vildagliptin, PR complex, PV complex and RV complex, which help to measure activation energy for quenching at pH 7.4,

$$C(\text{BSA}) = 10.0 \times 10^{-6} \text{ mol.L}^{-1}$$

Table 3.25. Stern-Volmer quenching constants K_{sv} and quenching rate constants K_q of the perindopril-BSA, rosuvastatin-BSA, vildagliptin-BSA, PR-BSA, PV-BSA and RV-BSA system at different temperatures (at pH 7.4).

Interacting system	T(K)	1/T(K ⁻¹)	$K_{sv} (\times 10^4 \text{ Lmol}^{-1})$	$K_q (\times 10^{12} \text{ Lmol}^{-1} \text{ s}^{-1})$	$E_a (\text{KJmol}^{-1})$
Perindopril-BSA	298	0.0033	0.28	0.28	-40.75
	308	0.0032	0.46	0.46	
Rosuvastatin-BSA	298	0.0033	2.25	2.25	-79.83
	308	0.0032	0.86	0.86	
Vildagliptin-BSA	298	0.0033	0.24	0.24	-63.2
	308	0.0032	0.51	0.51	
Complex PR-BSA	298	0.0033	0.77	0.77	-246.99
	308	0.0032	1.5	1.5	
Complex PV-BSA	298	0.0033	0.44	0.44	95.63
	308	0.0032	1.4	1.4	
Complex RV-BSA	298	0.0033	1.89	1.89	-222.04
	308	0.0032	1.3	1.3	

3.2.9.1. Analyses of thermodynamic parameters and the binding forces

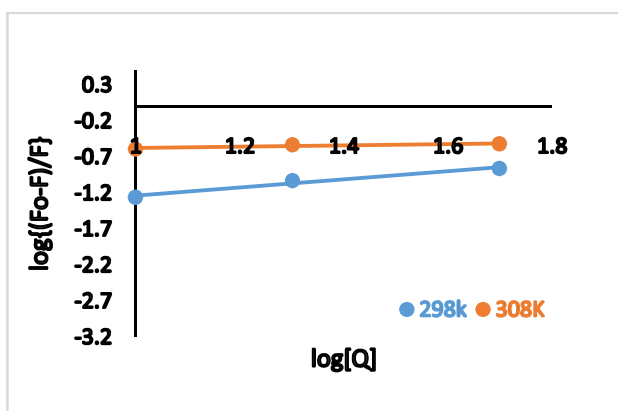
Thermodynamic parameters were calculated from the linear Van't Hoff plot (Figure 3.41, Table 3.26) at two different temperatures 298 K and 308 K. The negative ΔG value indicated the spontaneous interaction process. The positive ΔH and ΔS values indicated that the binding of perindopril, vildagliptin, PR, and PV with BSA was predominantly mediated by enthalpy where major interaction force was hydrophobic interaction. But in case of rosuvastatin and the complex RV the negative ΔH value along with $\Delta S < 0$ indicated towards that Vander Waals forces and H-bonds were principal interaction forces responsible for the BSA quenching process.

Table 3.26. Thermodynamic parameters of drugs and newly synthesized drug complexes mediated BSA quenching at 298 K and 308 K.

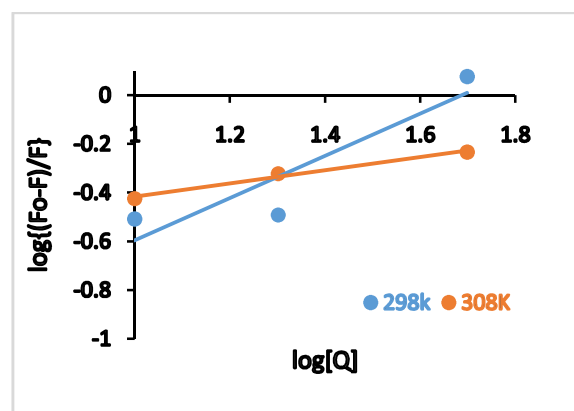
Interacting system	T(K)	1/T(K ⁻¹)	ΔH (KJmol ⁻¹)	ΔS (Jmol ⁻¹ K ⁻¹)	ΔG (KJmol ⁻¹)
Perindropil-BSA	298	0.0033	40.75	200.4	-59678.45
	308	0.0032			-61682.45
Rosuvastatin-BSA	298	0.0033	-79.88	-180.12	53595.88
	308	0.0032			55397.08
Vildagliptin-BSA	298	0.0033	63.2	273.22	-81356.36
	308	0.0032			-84088.56
Complex PR-BSA	298	0.0033	55.71	258	-76828.29
	308	0.0032			-79408.29
Complex PV-BSA	298	0.0033	96.45	388	-115527.55
	308	0.0032			-119407.55
Complex RV-BSA	298	0.0033	-31.6	-22.37	6634.66
	308	0.0032			6858.36

3.2.9.2. Analysis of binding constants (K_b) and no of binding points (n)

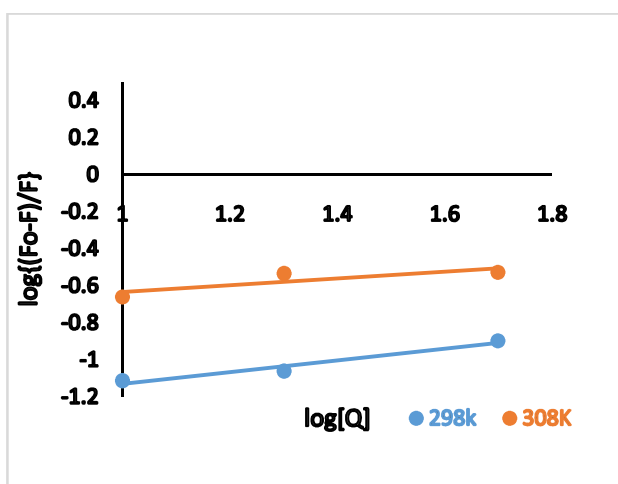
The number of binding sites (n) and binding constants (K_b) were calculated from the plot of $\log(F_0-F)/F$ vs $\log[Q]$ demonstrated in Figure 3.42 and these values are shown in the Table 3.27. Except from perindopril-BSA and vildagliptin-BSA systems, all the interactions the K_b values were increased with increase in temperature. But the n value almost remained constant with the change in temperature, and it was found to be almost 1 which also demonstrated towards 1:1 mole ratio interaction with BSA and drugs.



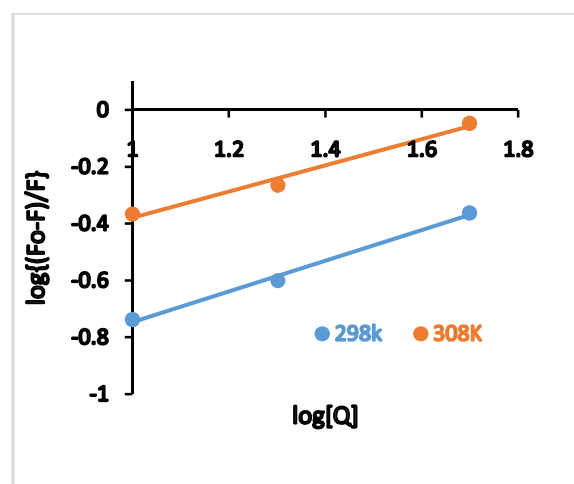
(1) Perindopril-BSA system



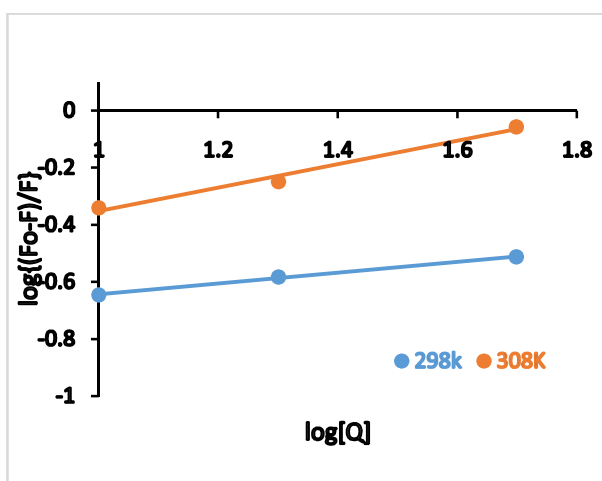
(2) Rosuvastatin-BSA system



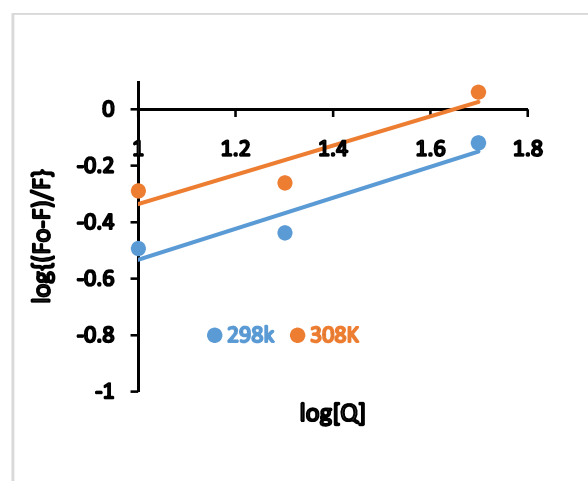
(3) Vildagliptin-BSA system



(4) PR-BSA system



(5) PV-BSA system



(6) RV-BSA system

Figure 3.42. Graphical log plot for determination of binding constant (K_b) and number of binding points (n) for (1) perindopril-BSA, (2) rosuvastatin-BSA, (3) vildagliptin-BSA, (4) PR-BSA, (5) PV-BSA and (6) RV-BSA at 298 K and 308 K.

Table 3.27. Binding constant (K_b) and number of binding sites (n) for the pure drugs and drug complexes at two different temperatures at 298 K and 308 K.

Interacting system	T(K)	1/T(K ⁻¹)	pH	K_b (Lmol ⁻¹)	n
Perindopril-BSA	298	0.0033	7.4	0.214	0.922
	308	0.0032		0.016	0.562
Rosuvastatin-BSA	298	0.0033	7.4	0.034	0.87
	308	0.0032		0.206	0.27
Vildagliptin-BSA	298	0.0033	7.4	0.036	0.316
	308	0.0032		0.153	0.181
Complex PR-BSA	298	0.0033	7.4	0.145	0.46
	308	0.0032		0.052	0.54
Complex PV-BSA	298	0.0033	7.4	0.146	0.19
	308	0.0032		0.173	0.41
Complex RV-BSA	298	0.0033	7.4	0.083	0.55
	308	0.0032		0.1403	0.52

3.3. COMPLEXATION OF CHROMIUM(III) WITH FOUR ANTIDIABETIC DRUGS: SYNTHESIS, CHARACTERIZATION AND ASSESSMENT OF BIOLOGICAL ACTIVITY

Four complexes of chromium(III) with the antidiabetic drugs metformin, dapagliflozin, vildagliptin and glimepiride were synthesized by the co-evaporation reaction followed by drying. Both crystalline and amorphous Cr-drug complexes were obtained. Four stable complexes of chromium(III)-metformin (Cr-metformin), chromium(III)-dapagliflozin (Cr-dapagliflozin), chromium(III)-vildagliptin (Cr-vildagliptin) and chromium(III)-glimepiride (Cr-glimepiride) were produced. The synthesized complexes were evaluated with different R_f values from Co-TLC, and different peak patterns in FT-IR and NMR spectra. By TGA analysis the thermal stability and thermochemical characteristics of the complexes were analyzed. Finally, evaluation of anti-diabetic activity (*in vivo*) and histopathological analyses of kidney and liver tissues were done.

3.3.1. TLC analysis of drugs and chromium complexes

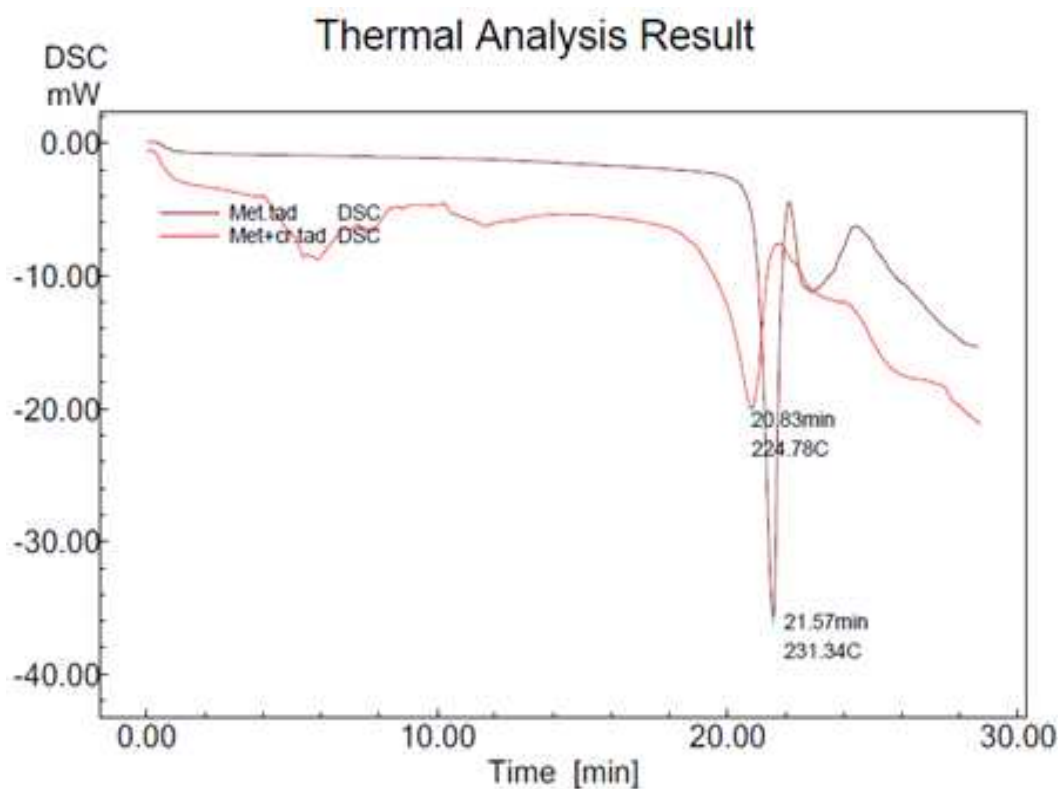
Co-TLC of all the Cr-drug complexes was carried out in methanol-dichloromethane as mobile phase in different ratio for different complex. From the metal drug complexes single spot were detected which were different from their precursor molecules. R_f values for the metal drug complexes and precursor drugs are mentioned in Table 3.28. Spots on TLC plates at different places from the spot of the parent drugs demonstrated the formation of new complexes.

Table 3.28. R_f values of drugs and the metal-drug complexes on F₂₅₄ TLC plate.

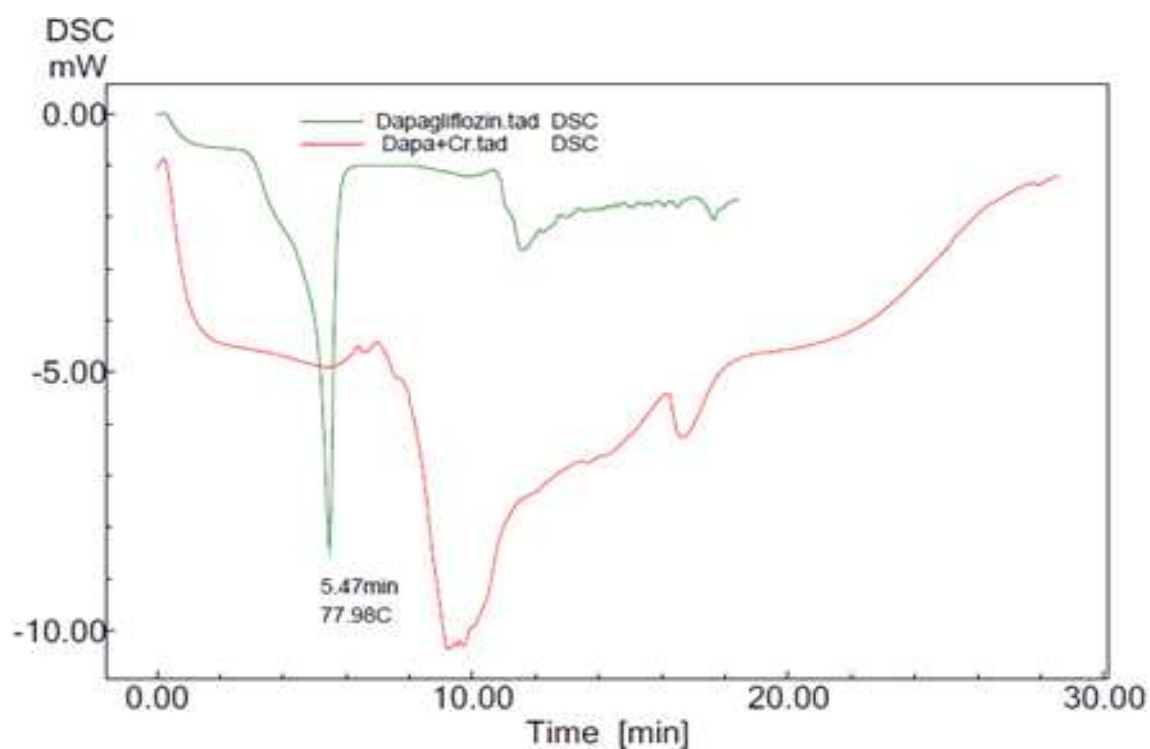
Item	Mobile phase	R_f value
Metformin HCl	Methanol/dichloromethane (3:7)	0.6
Cr-metformin complex		0.45
Dapagliflozin	Methanol/dichloromethane (8:2)	0.5
Cr-dapagliflozin complex		0.35
Vildagliptin	Methanol/dichloromethane (8:2)	0.4
Cr-vildagliptin complex		0.3
Glimepiride	Methanol/dichloromethane (2:8)	0.65
Cr-glimepiride complex		0.5

3.3.2. Analysis of drugs and drug chromium complexes by DSC

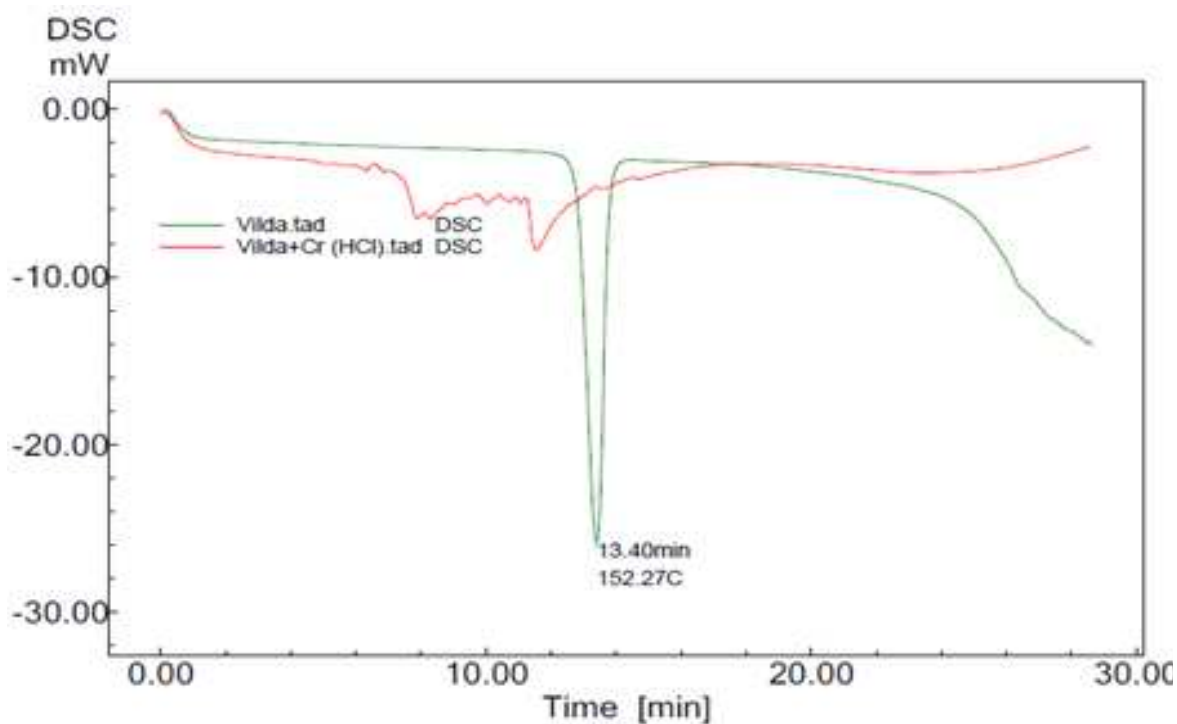
The phase changes of the pure anti-diabetic drugs and their Cr-complexes were analyzed by DSC method. Pure metformin showed melting endotherm at 231 °C and its Cr-complex appeared at 224 °C in [Figure 3.43 (1)]. Dapagliflozin exhibited melting endotherm at 77.98 °C while its Cr-complex showed different thermogram [Figure 3.43(2)]. In case of vildagliptin and glimepiride pure drugs gave melting endothermic points at 152 °C and 213 °C, respectively but their Cr-complexes showed different peaks from the parent drugs which revealed the formation of new complexes [Figure 3.43(3) and (4)].



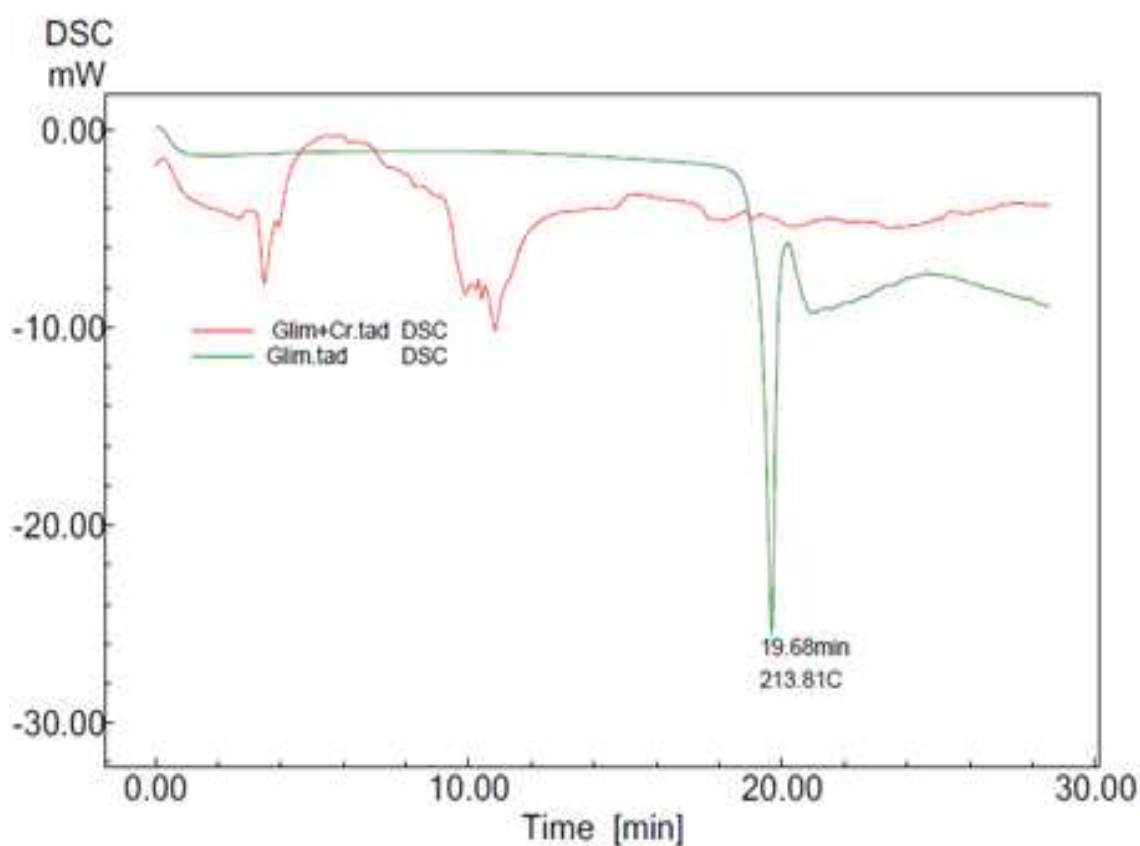
(1) Metformin and Cr-metformin complex.



(2) Dapagliflozin and Cr-dapagliflozin complex.



(3) Vildagliptin and Cr-vildagliptin complex.

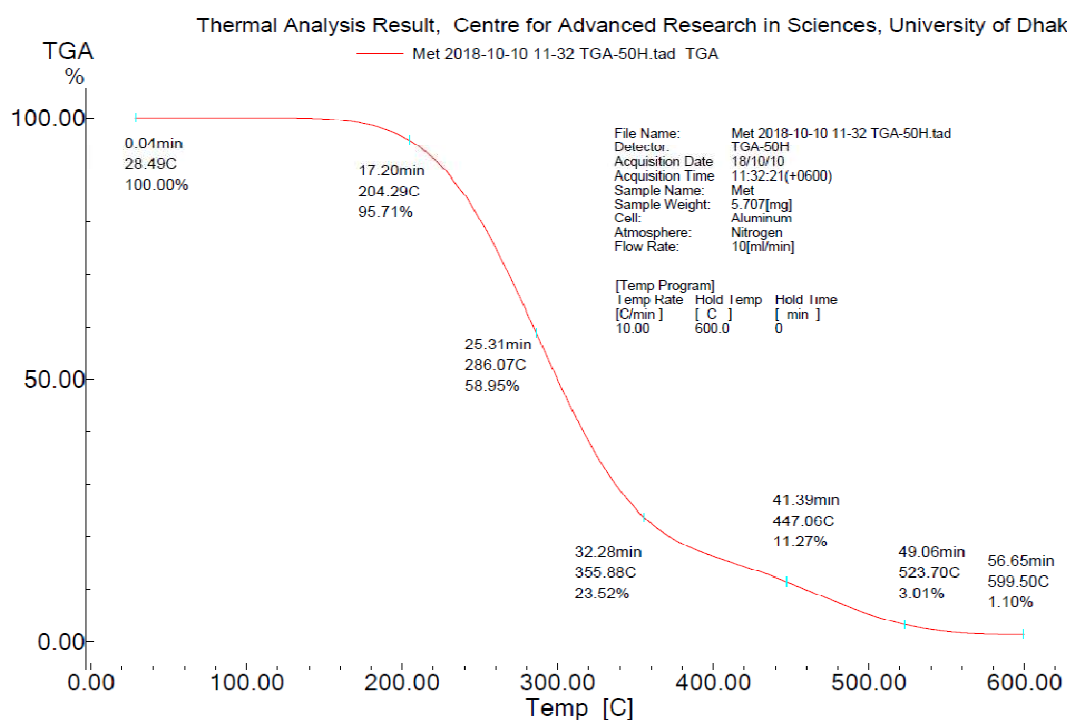


(4) Glimepiride and Cr-glimepiride complex.

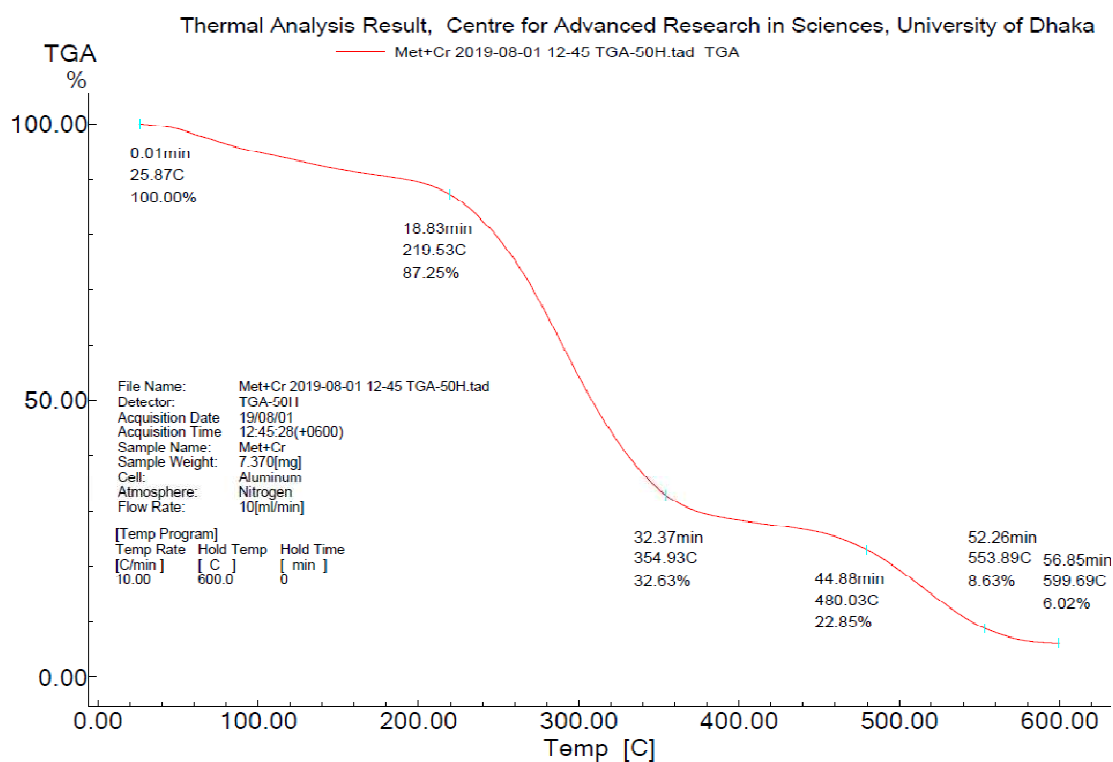
Figure 3.43. Overlaid DSC thermograms for (1) metformin and Cr-metformin complex, (2) dapagliflozin and Cr-dapagliflozin complex, (3) vildagliptin and Cr-vildagliptin complex and (4) glimepiride and Cr-glimepiride complex.

3.3.3. TGA analysis of drugs and chromium drug complexes

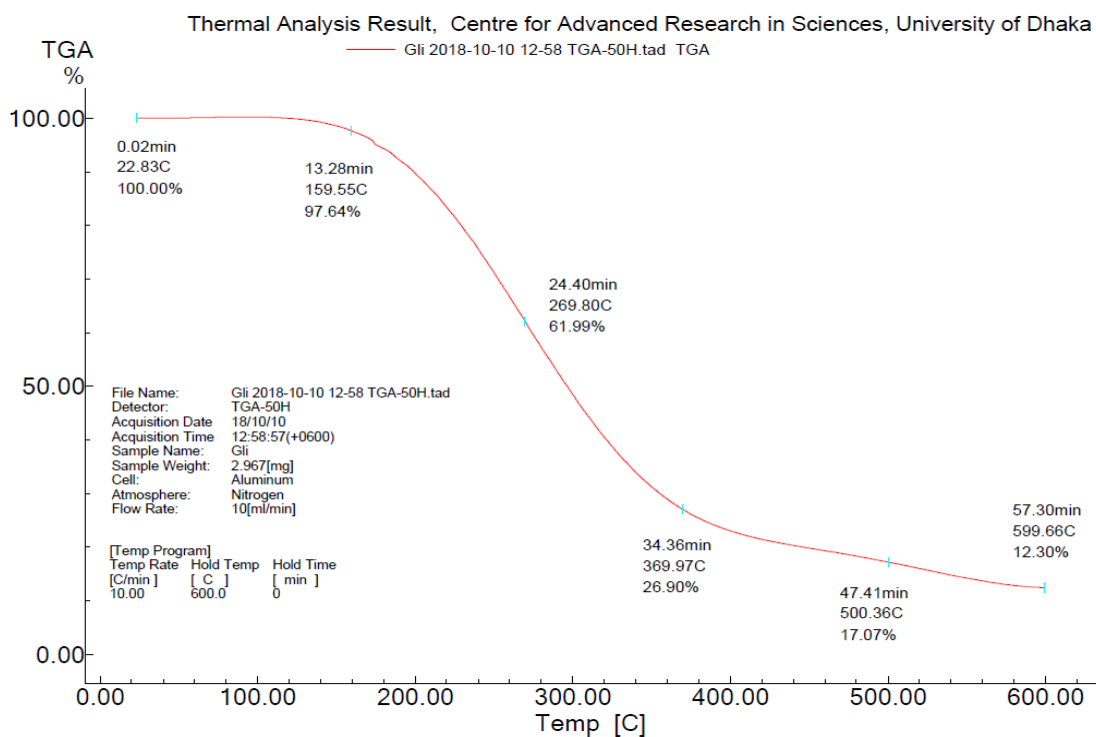
By thermogravimetric analysis the percentages of weight loss against rise in temperature for pure anti-diabetic drugs and their complexes were analyzed. For pure metformin degraded 4.29% at 205 °C. It also showed degradation by 88% at 356 °C probably due to removal of methyl groups. It further degraded by 97% at 599 °C, which may be resulted from the loss of amino groups. However, Cr-metformin complex showed different degradation pattern and results are shown in Figure 3.44 and Table 3.29.



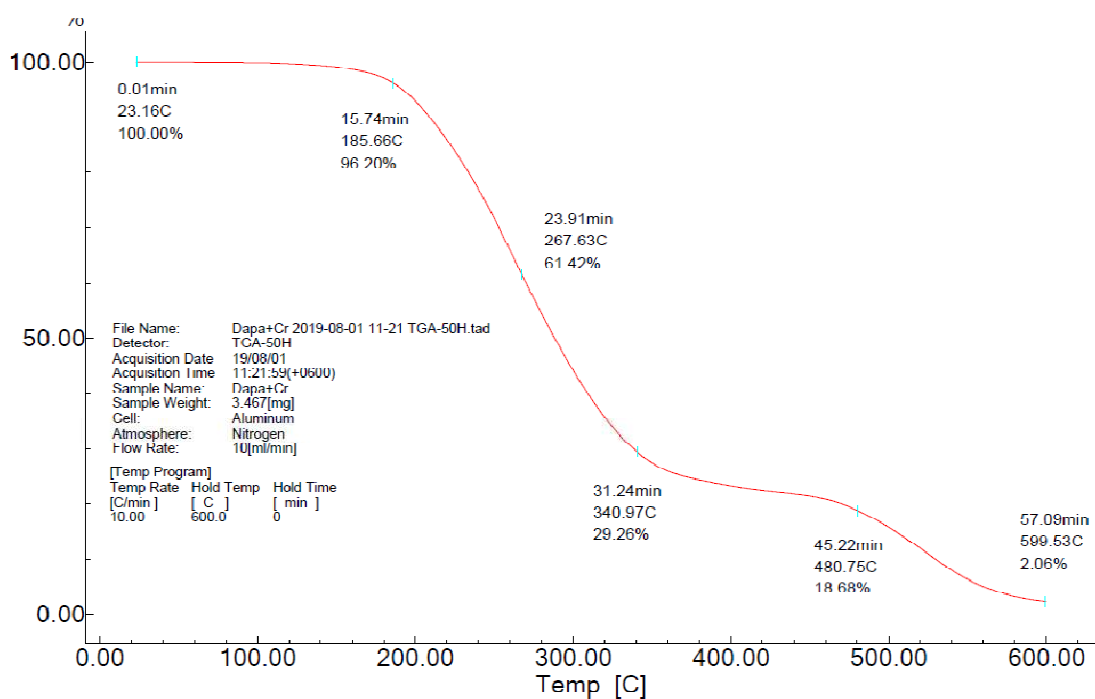
(1) TGA thermogram of metformin.



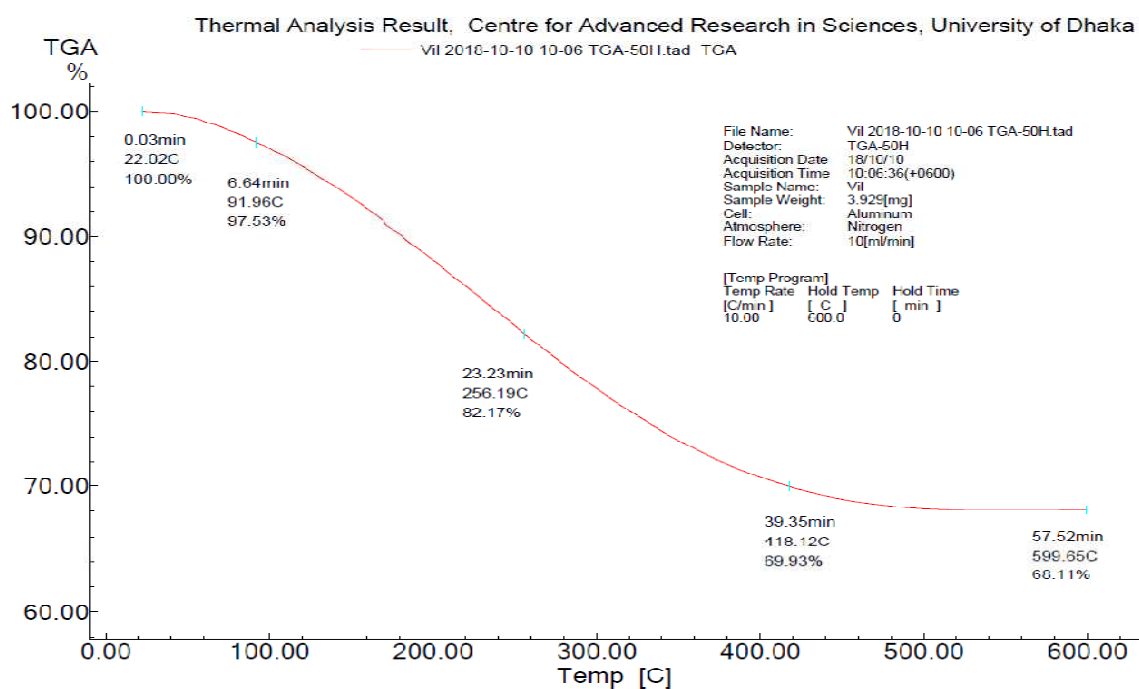
(2) TGA thermogram of Cr-metformin complex.



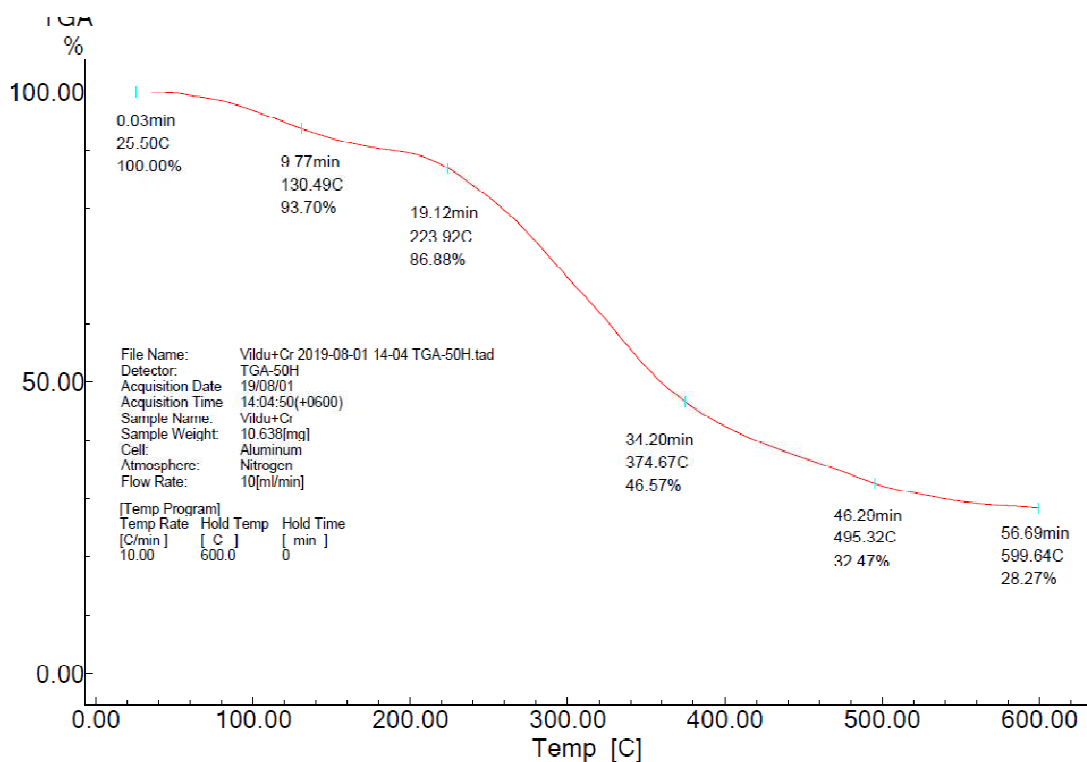
(3) TGA thermogram of glimepiride.



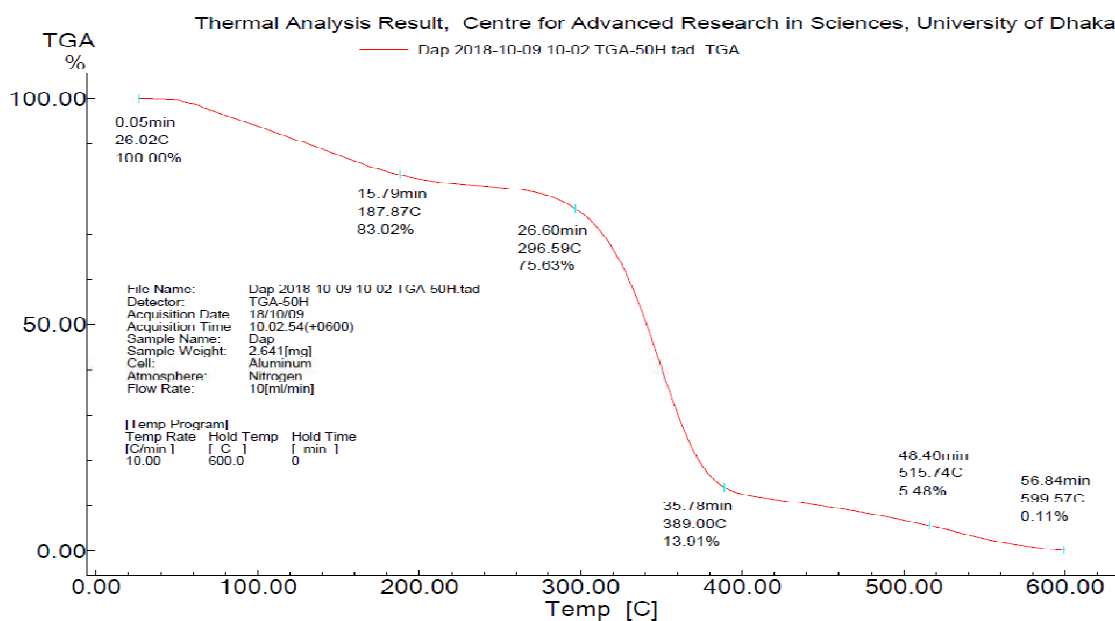
(4) TGA thermogram of Cr-glimepiride complex.



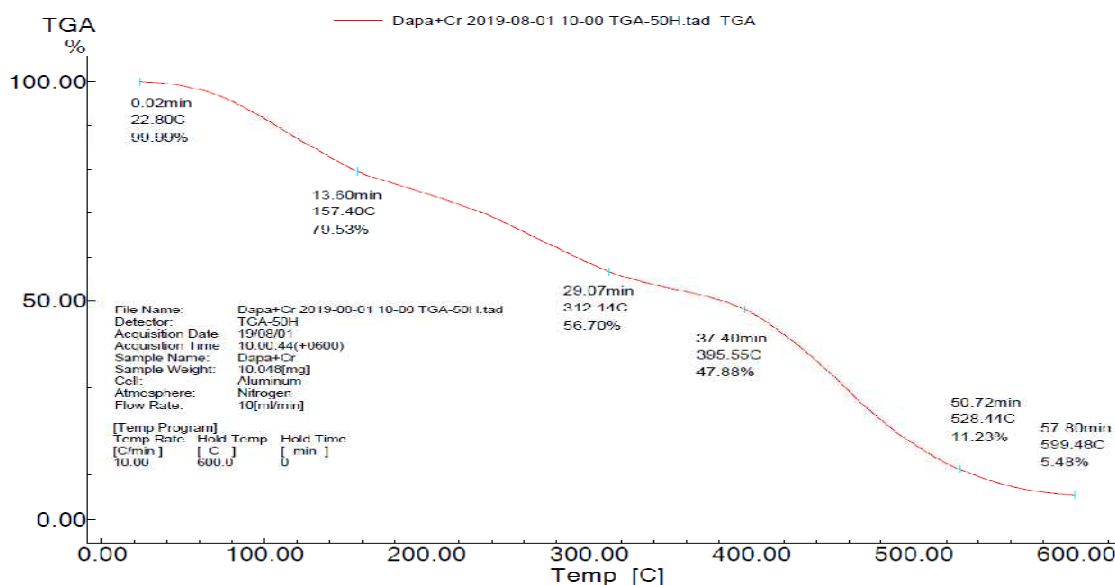
(5) TGA thermogram of vildagliptin.



(6) TGA thermogram of Cr-vildagliptin complex.



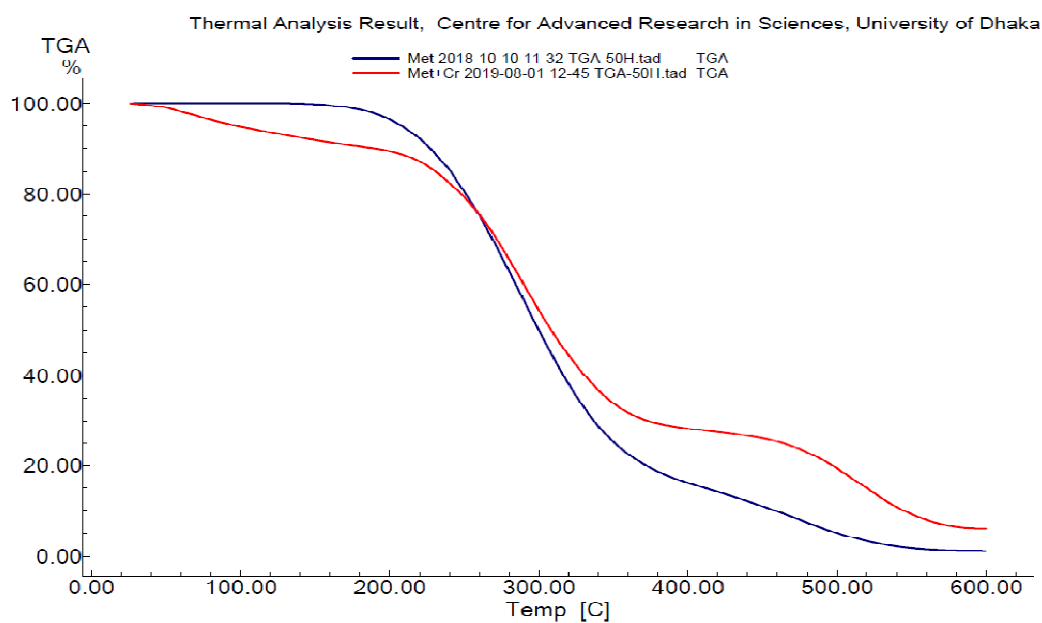
(7) TGA thermogram of dapagliflozin.



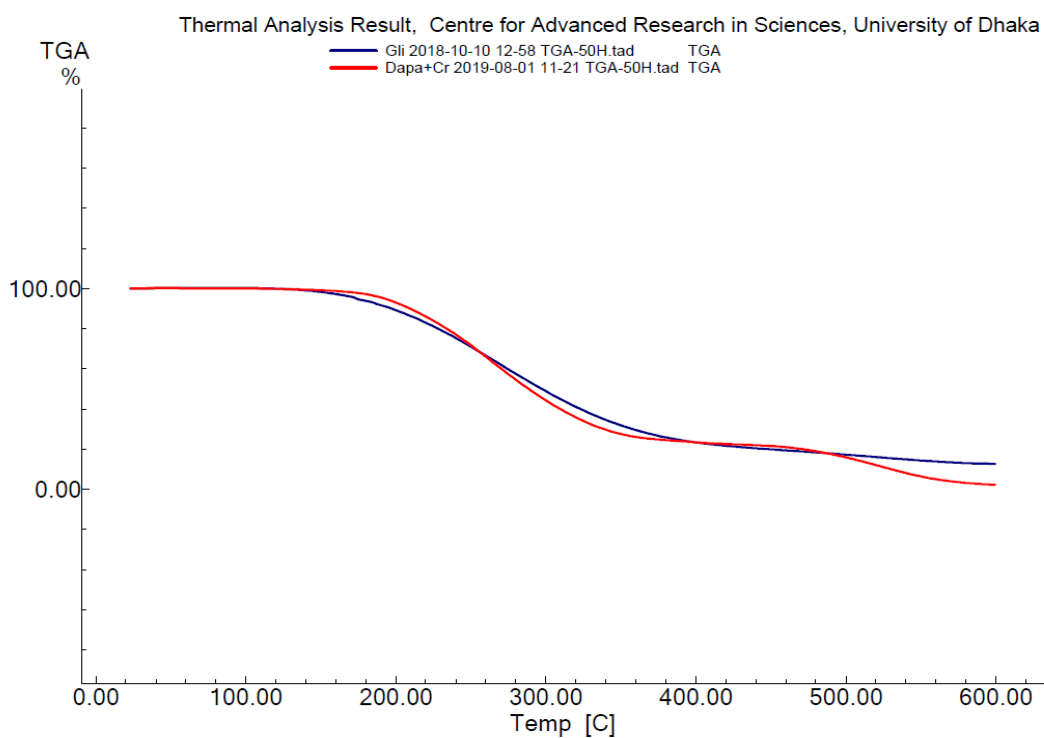
(8) TGA thermogram of Cr-dapagliflozin complex.

Figure 3.44. TGA thermograms: (1) metformin, (2) Cr-metformin complex, (3) glimepiride, (4) Cr-glimepiride complex, (5) vildagliptin, (6) Cr-vildagliptin complex, (7) dapagliflozin and (8) Cr-dapagliflozin complex.

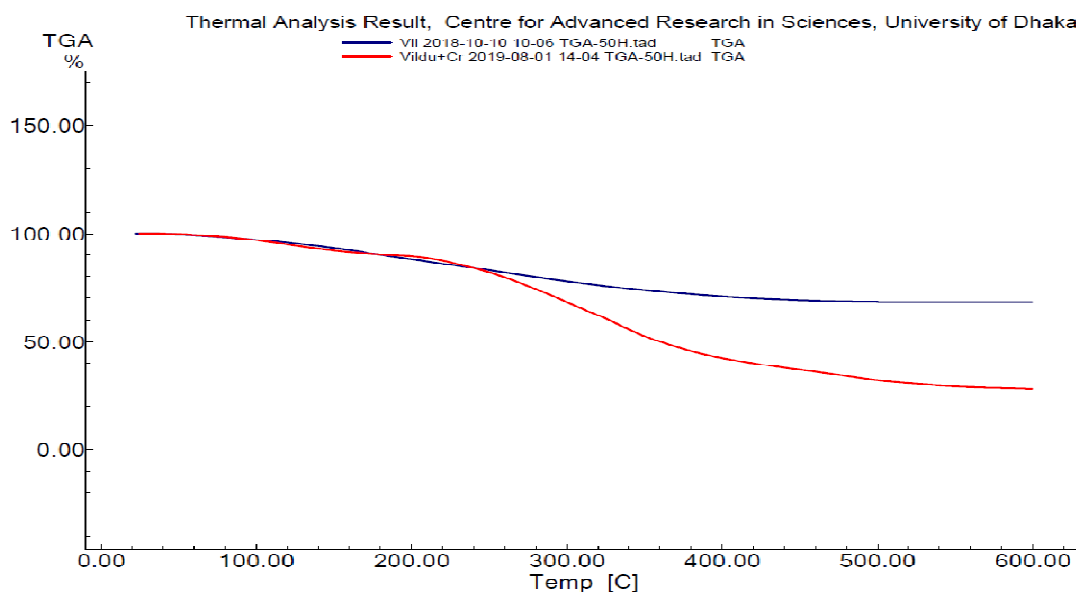
In the degradation pattern of pure dapagliflozin, it was found as 17% degradation at 189 °C, 86% at 389 °C and 94% at 516 °C, which may be due to releasing hydroxyl and methyl groups. Similarly, for vildagliptin and glimepiride and their Cr-complexes displayed different degradation pattern from pure drugs and the data are listed in Table 3.29 and Figure 3.44. The overlaid TGA thermograms are also displayed in Figure 3.45.



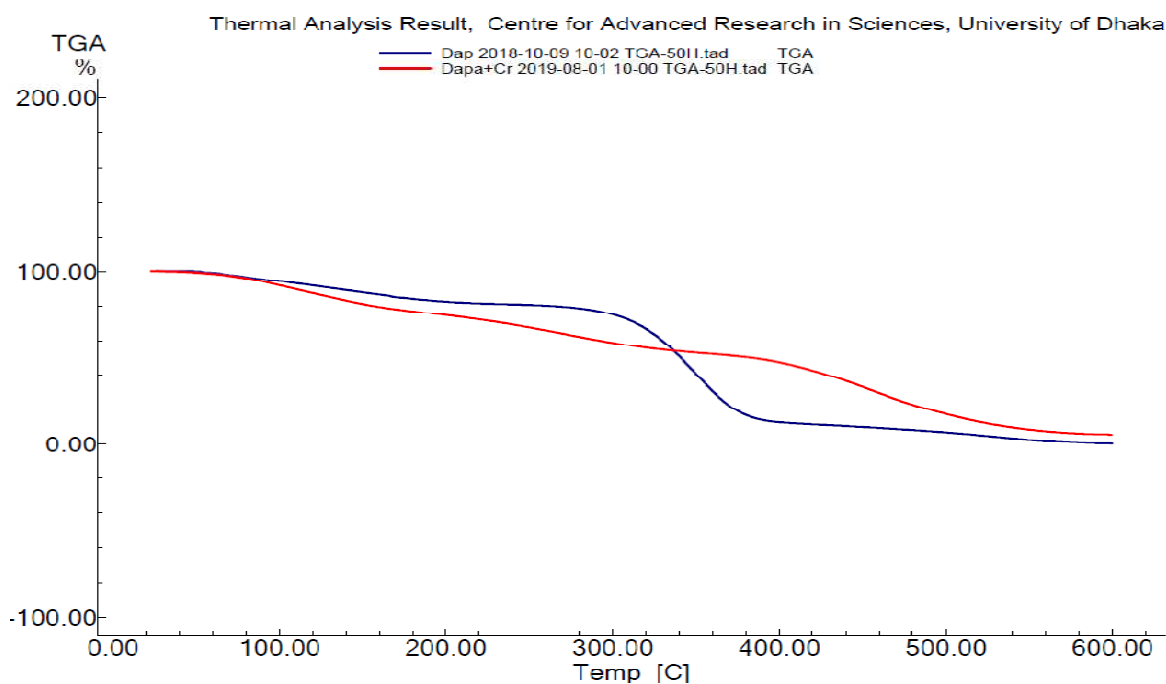
(1) Overlaid TGA thermogram of metformin and Cr-metformin complex.



(2) Overlaid TGA thermogram of glimepiride and Cr-glimepiride complex.



(3) Overlaid TGA thermogram of vildagliptin and Cr-vildagliptin complex.



(4) Overlaid TGA thermogram of dapagliflozin and Cr-dapagliflozin complex.

Figure 3.45. Overlaid TGA thermograms: (1) metformin and Cr-metformin complex, (2) glimepiride and Cr-glimepiride complex, (3) vildagliptin and Cr-vildagliptin complex and (4) dapagliflozin and Cr-dapagliflozin complex.

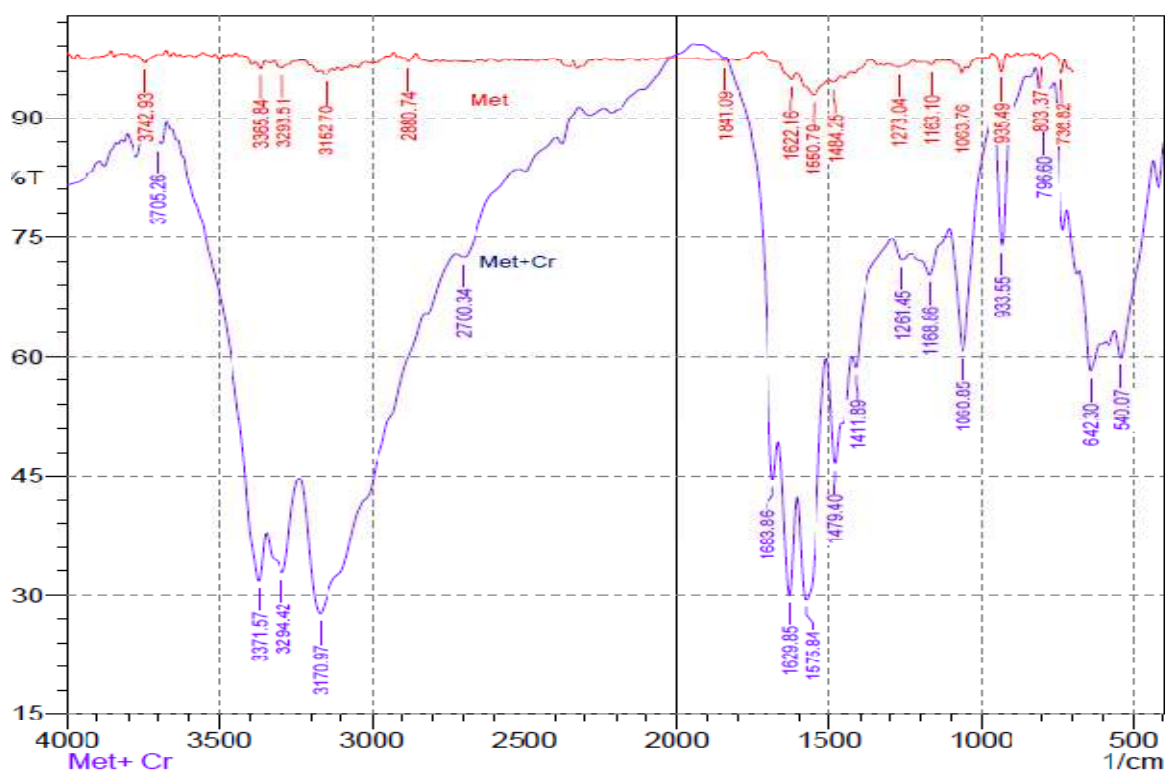
The percentage of degradation of metformin and Cr-metformin complex, glimepiride and Cr-glimepiride complex, vildagliptin and Cr-vildagliptin complex, dapagliflozin and Cr-dapagliflozin complex are listed in Table 3.29.

Table 3.29. Percent (%) degradation of pure drugs and metal drug complexes with increasing temperature from TGA thermograms.

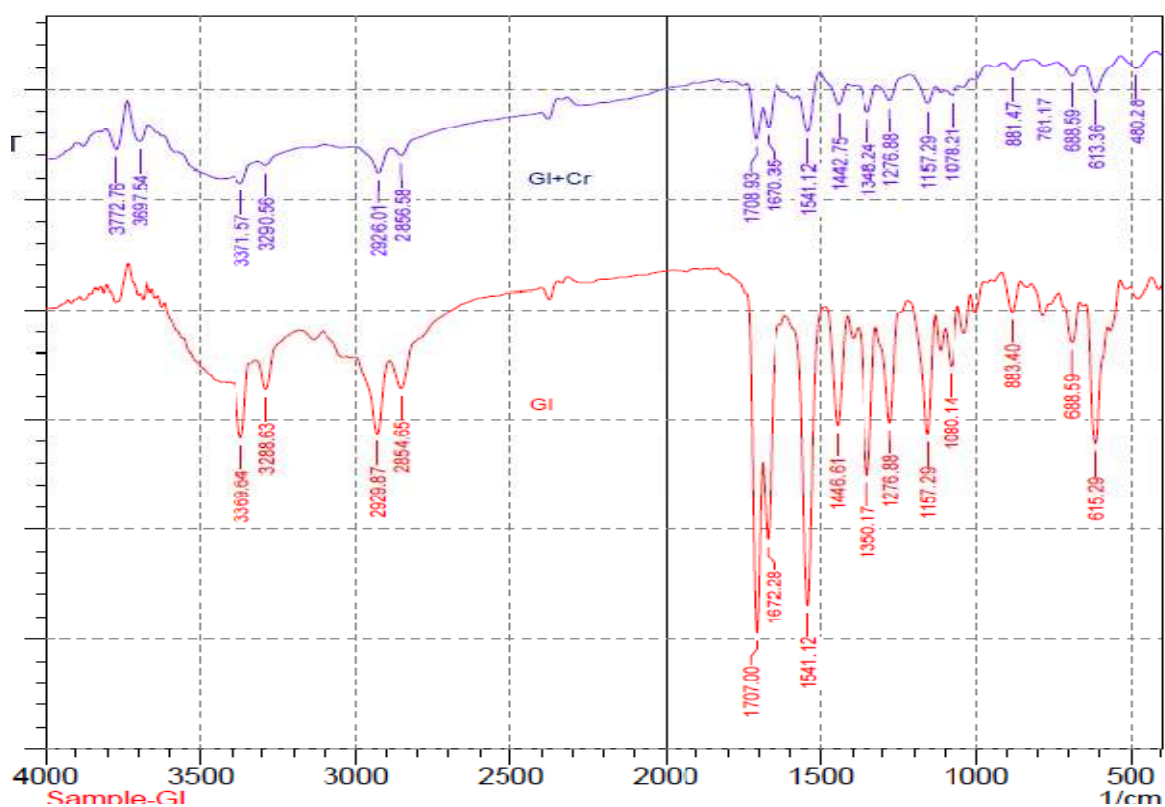
Sample	% Degradation with increasing temperature				
	(i)	(ii)	(iii)	(iv)	(v)
Metformin	0 at 28.49°C	4.29 at 204.29 °C	41.05 at 286.07 °C	76.48 at 355.88 °C	98.9 at 599.50°C
Cr-metformin	0 at 25.87 °C	21.75 at 219.53 °C	67.37 at 354.93 °C	77.15 at 480.85 °C	99.89 at 599.69 °C
Glimepiride	0 at 22.83 °C	2.36 at 164.83 °C	38.01 at 269.80 °C	73.1 at 369.97 °C	87.7 at 599.66 °C
Cr- glimepiride	0 at 23.16 °C	3.8 at 185.66 °C	38.58 at 267.63 °C	70.74 at 340.97 °C	97.94 at 599.53 °C
Vildagliptin	0 at 22.02 °C	2.47 at 91.96 °C	17.83 at 256.19° C	30.07 at 423.92 °C	31.89 at 599.65 °C
Cr- vildagliptin	0 at 25.50 °C	6.3 at 130.49 °C	53.43 at 374.67 °C	67.53 at 495.32 °C	71.73 at 599.64 °C
Dapagliflozin	0 at 26.02 °C	16.98 at 187.87 °C	24.37 at 296.59 °C	86.09 at 389.00 °C	99.89 at 599.57 °C
Cr- dapagliflozin	0 at 22.80 °C	20.47 at 157.40 °C	43.3 at 312.14 °C	52.11 at 395.55 °C	94.52 at 599.48 °C

3.3.4. FT-IR spectra analysis of drugs and chromium drug complexes

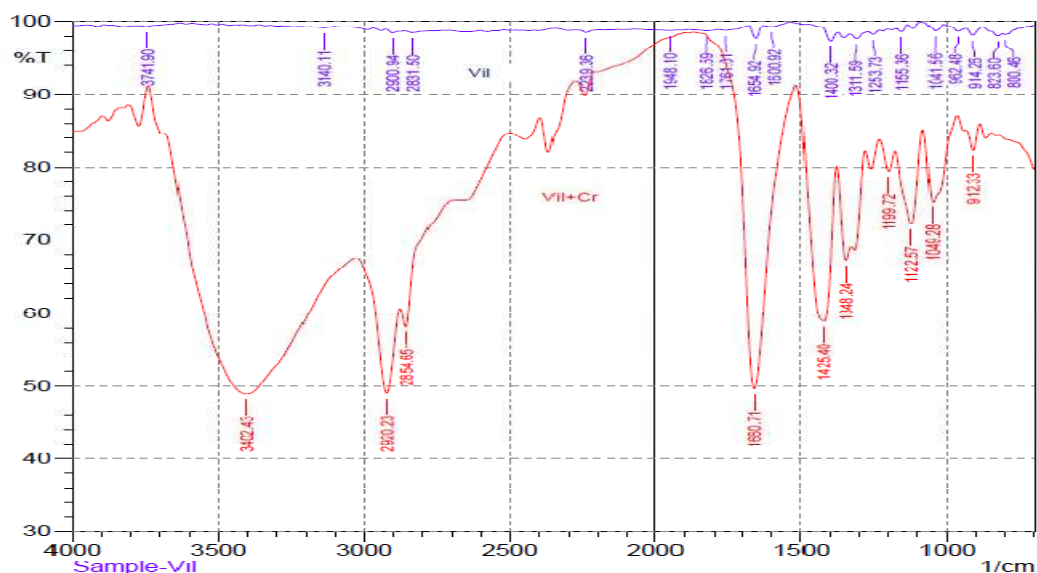
The FT-IR spectra were recorded to measure wavelength and intensity of the different functional groups of the drug molecule. The identification of specific types of molecular vibrations and stretching characteristics help to identify functional groups of new complexes. The FT-IR spectrum of pure drugs metformin, dapagliflozin, vildagliptin, glimepiride and their Cr-complexes are shown in Figure 3.46. If IR spectra of pure drugs and complexes are identical, it can be estimated that they are the same compounds. So, any appearance or absence or shifts of signals will be indicated as the presence of different compounds.



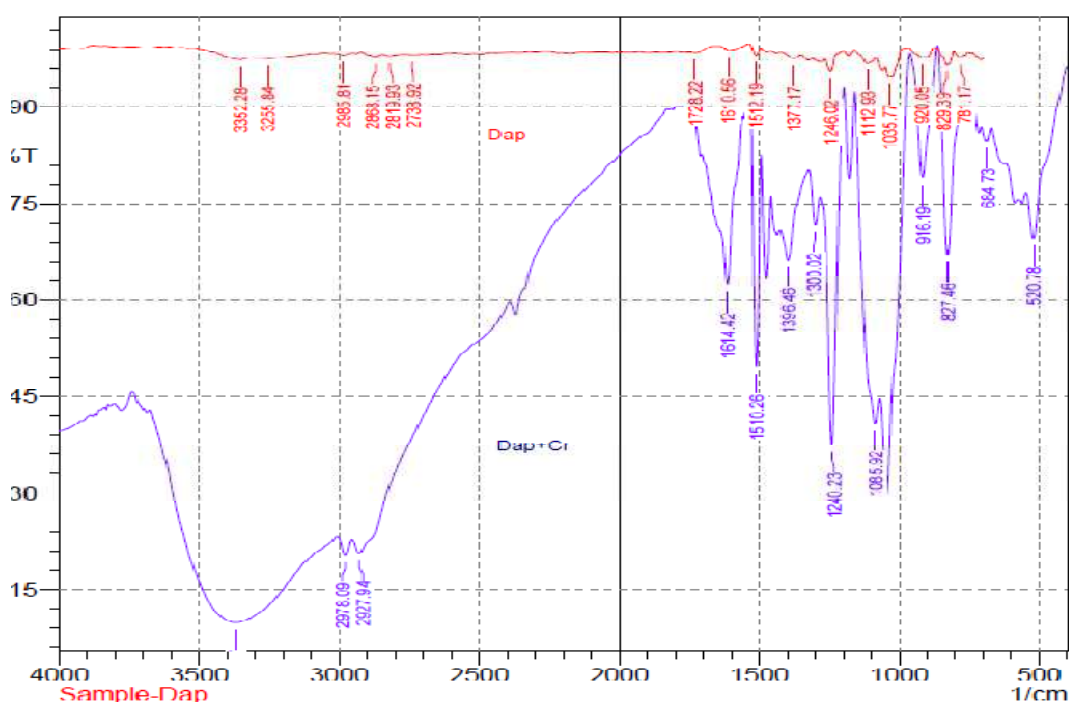
(1) FT-IR spectra of metformin and Pb-metformin complex.



(2) FT-IR spectra of glimepiride and Cr-glimepiride complex.



(3) FT-IR spectra of vildagliptin and Cr-vildagliptin complex.



(4) FT-IR spectra of dapagliflozin and Cr-dapagliflozin complex.

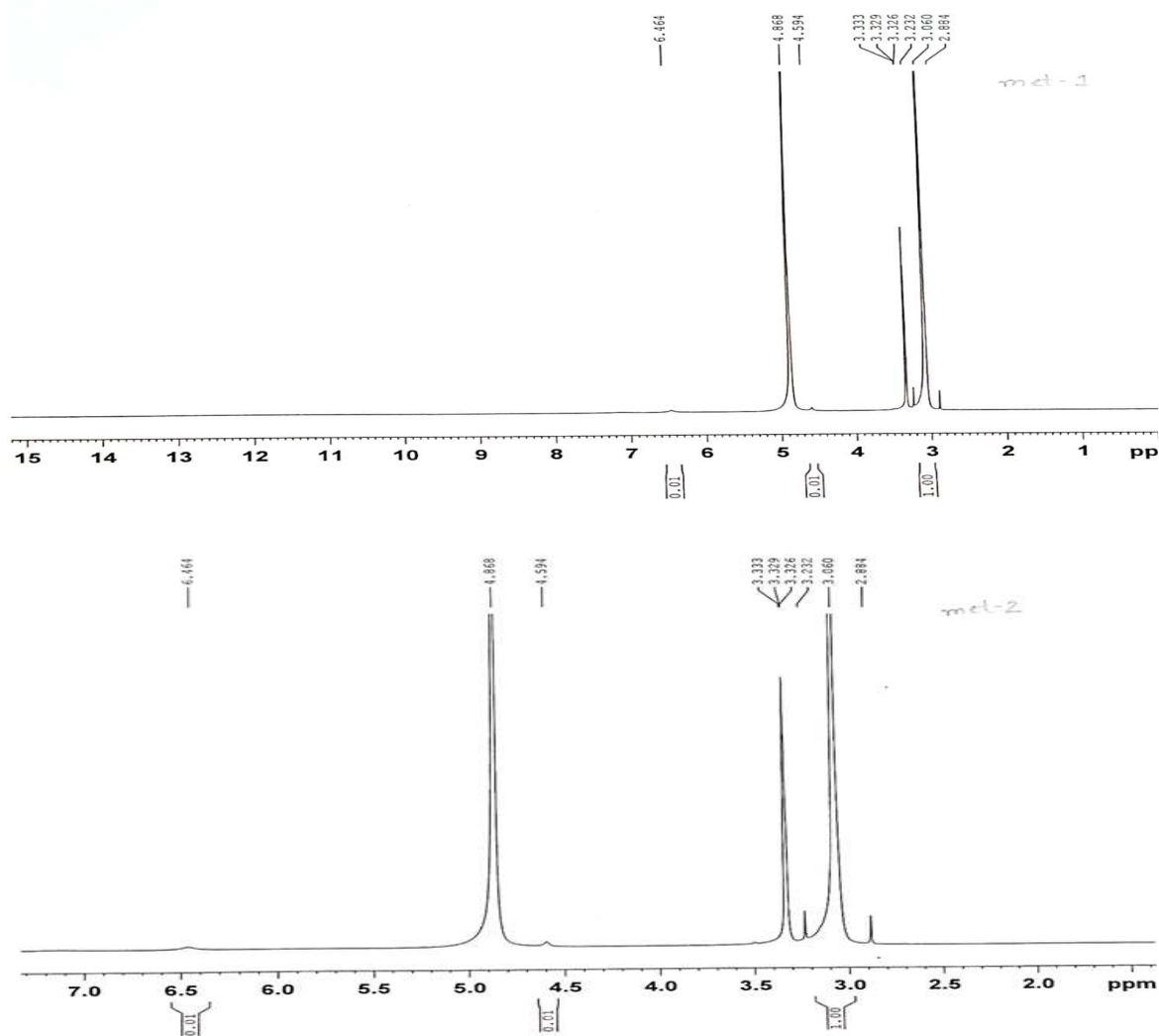
Figure 3.46. Overlaid IR spectra: (1) metformin and Cr-metformin complex, (2) glimepiride and Cr-glimepiride complex, (3) vildagliptin and Cr-vildagliptin complex and (4) dapagliflozin and Cr-dapagliflozin complex.

The -NH_2 group of metformin exhibited a stretching peak at 3742.93 cm^{-1} which was obtained in Cr-metformin in the downfield at 3706 cm^{-1} (Figure 3.46). Likewise, the characteristic peaks of OH stretching of dapagliflozin, vildagliptin and glimepiride observed at 3352.28 cm^{-1} , 3741 cm^{-1} , 3772 cm^{-1} , respectively which were missing in the IR spectra of Cr-drug complexes. A single broad signal was observed at 3390 cm^{-1} for

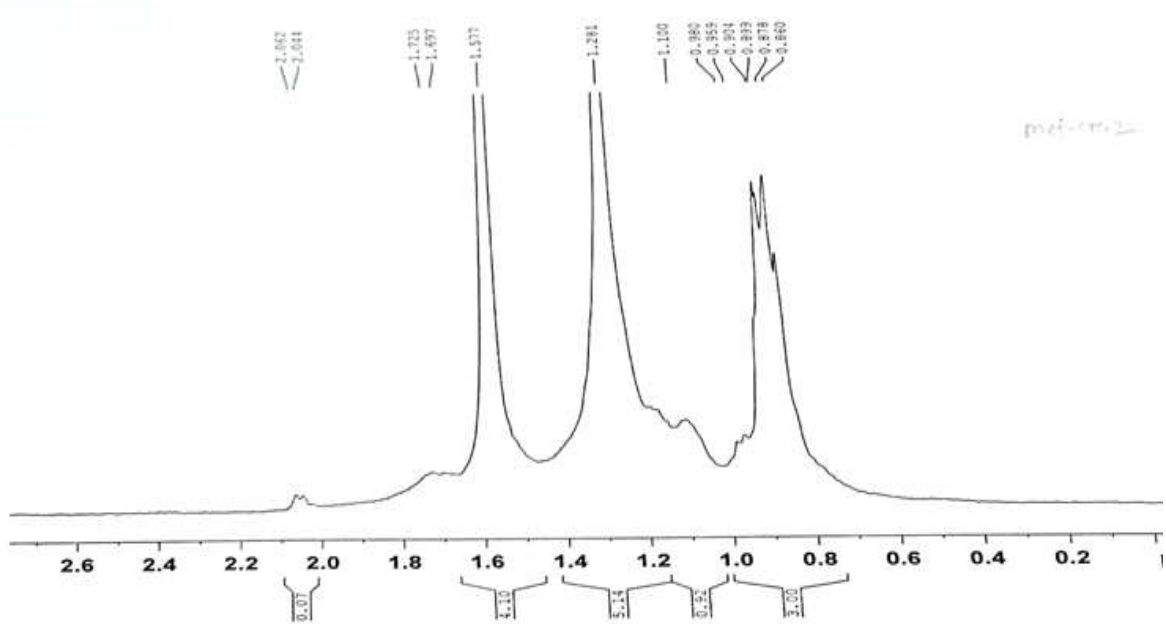
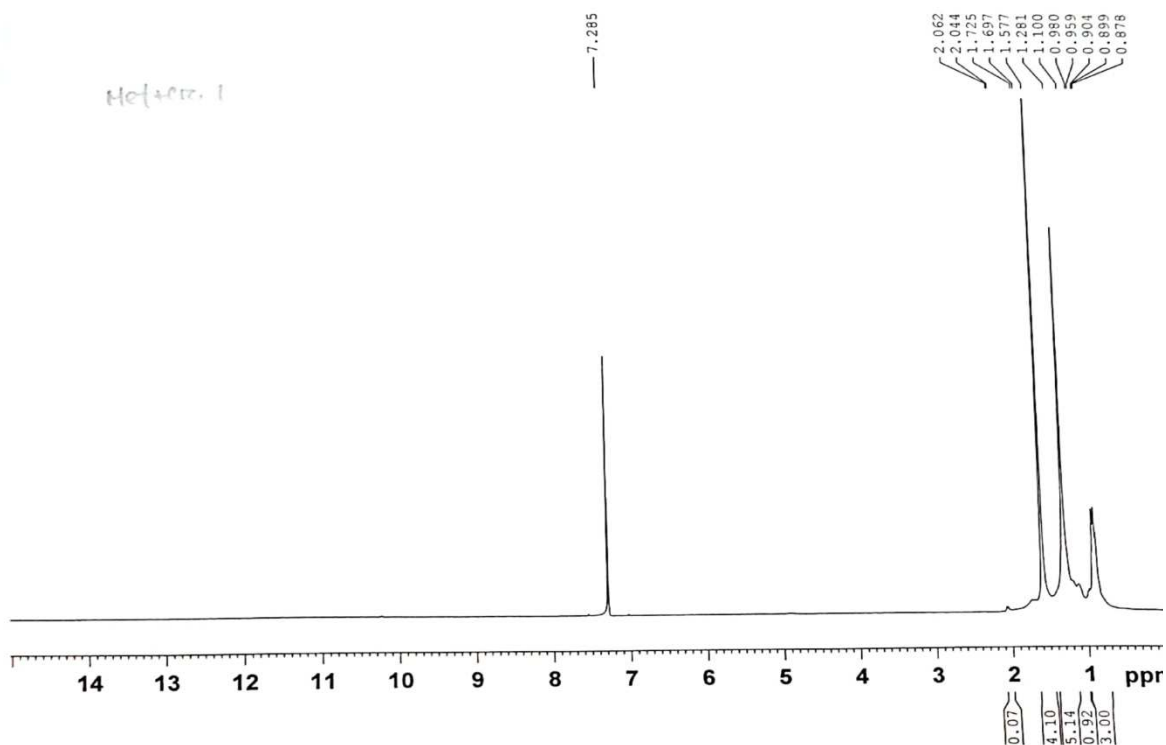
Cr- dapagliflozin and 3402.00 cm^{-1} for Cr-vildagliptin and 3569.54 cm^{-1} for Cr-glimepiride. These changes in the absorption characteristics in the IR spectra directed towards the complexation between the metal and the drugs.

3.3.5. ^1H NMR spectra analysis for drugs and chromium drug complexes

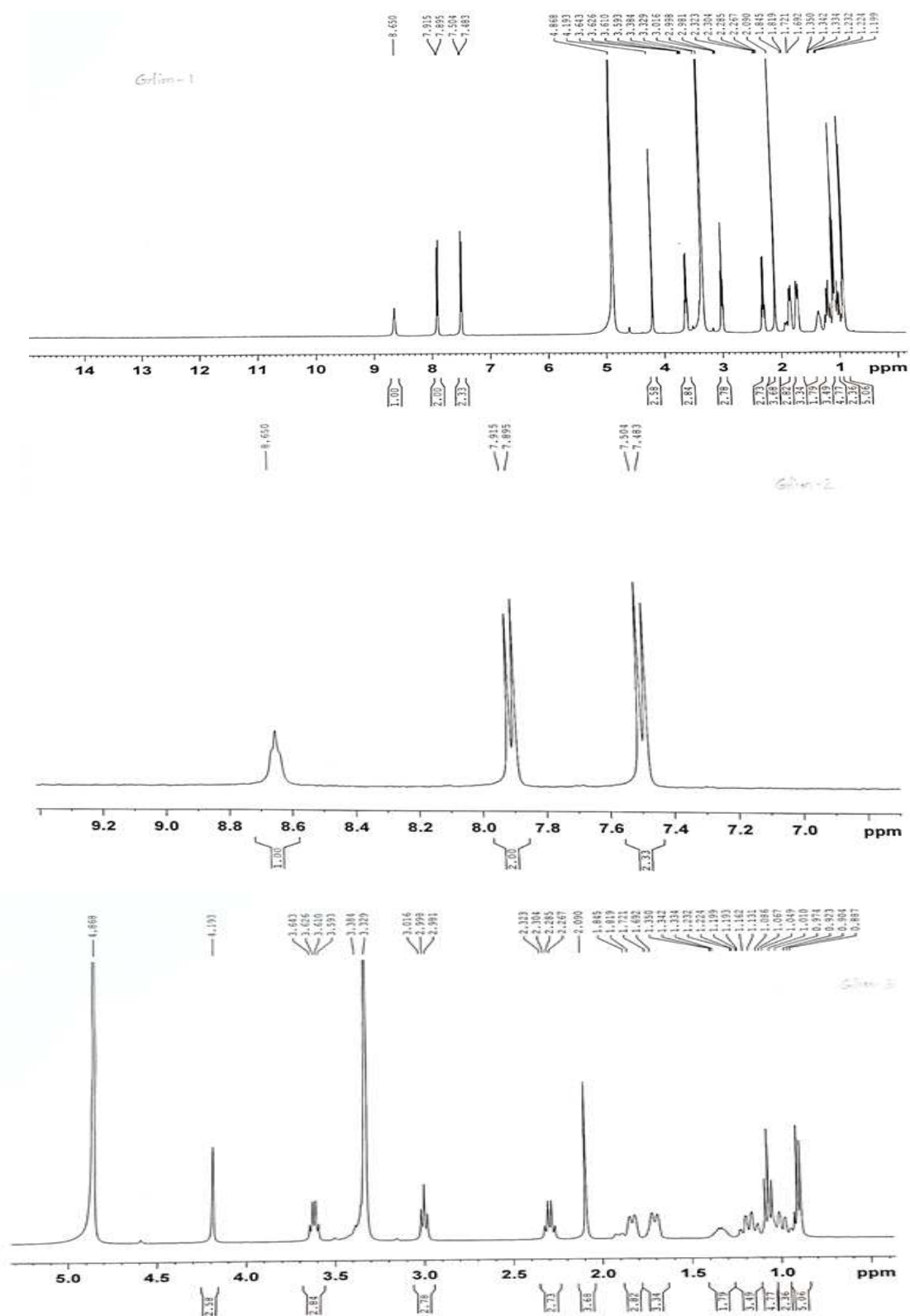
^1H NMR of the reference drugs and their chromium complexes were recorded to compare the peak pattern. For structure elucidation purification of the synthesized new drug complex was needed. Due to presence of mixture of unreacted and reacted drug structures elucidation was difficult. Further work is needed to explore the structures of the metal-drug complexes. The ^1H NMR spectra are shown in Figure 3.47.



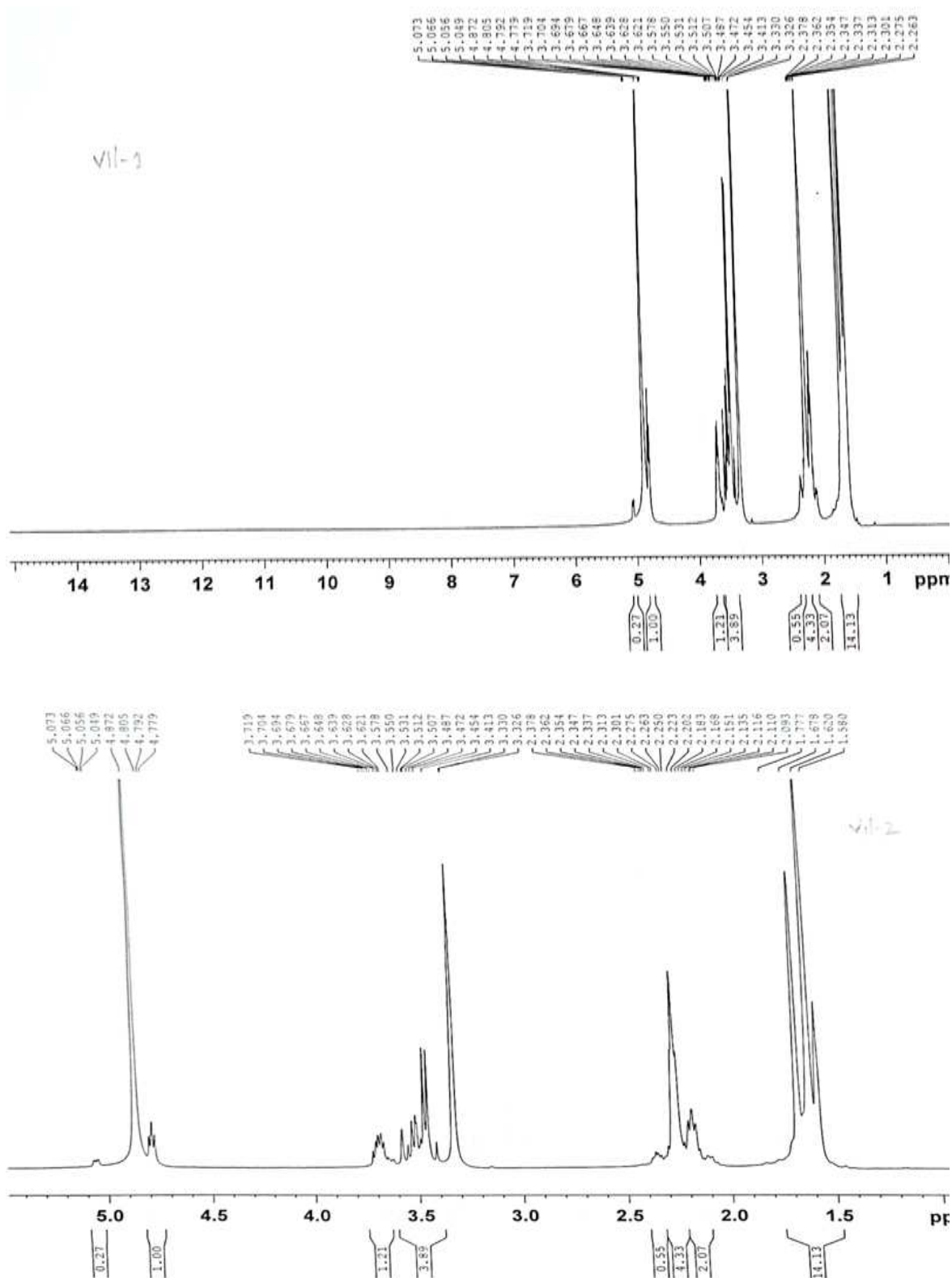
(1) NMR spectra of metformin.



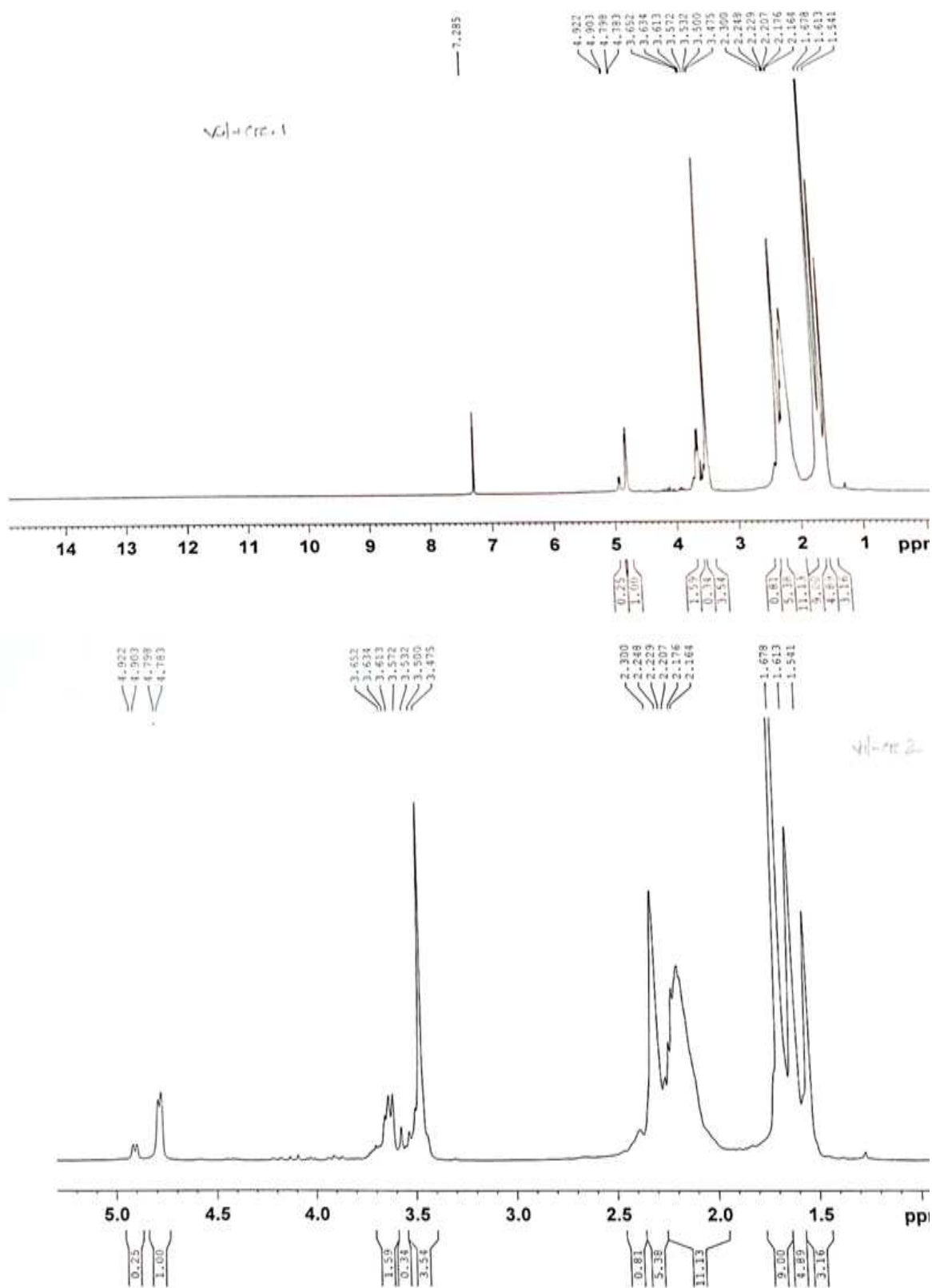
(2) NMR spectra of Cr-metformin.



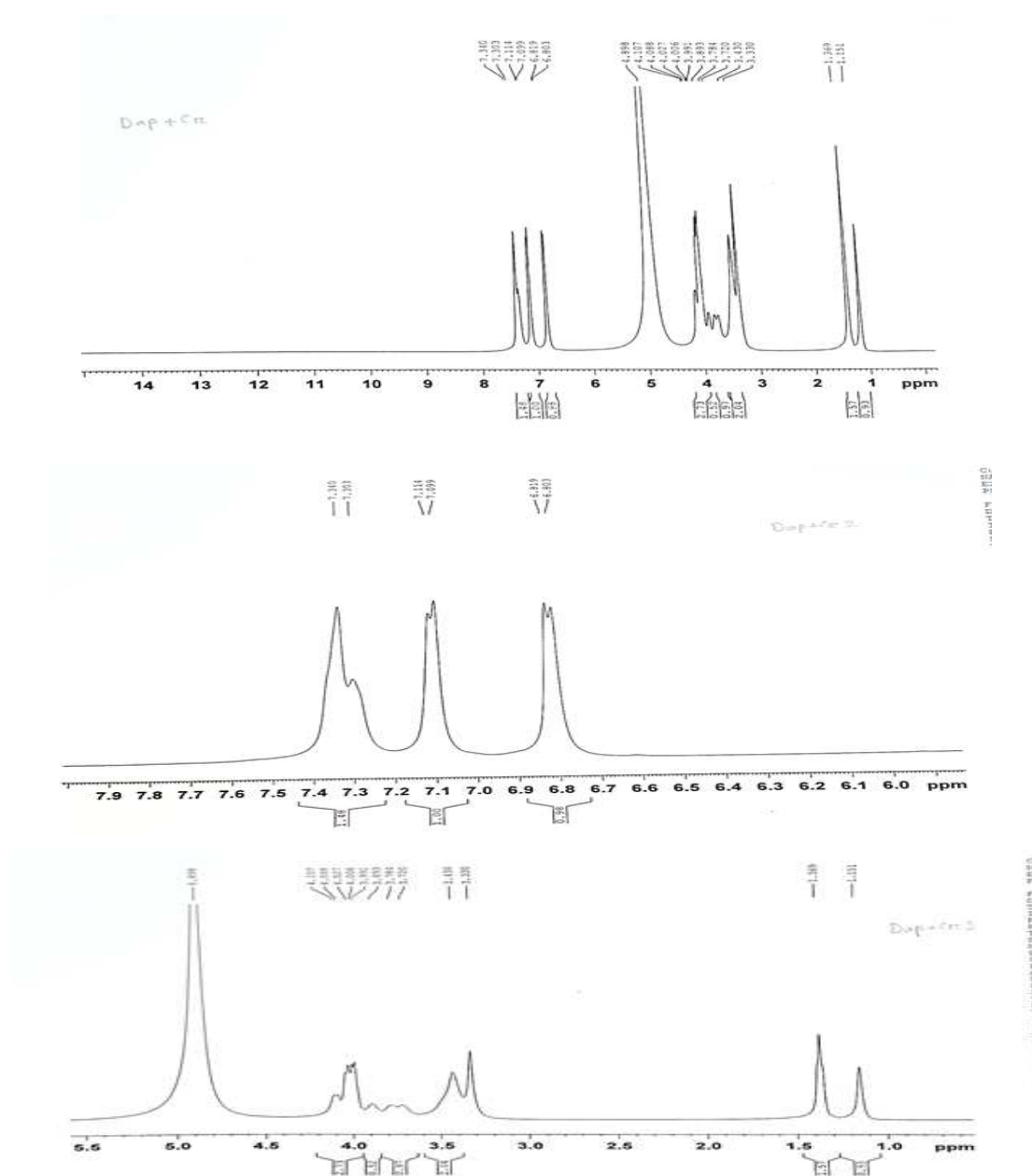
(3) NMR spectra of glimepiride.



(5) NMR spectra of vildagliptin.



(6) NMR spectra of Cr-vildagliptin complex.



(8) NMR spectra of Cr-dapagliflozin.

Figure 3.47. ^1H NMR spectra of: (1) metformin, (2) Cr-metformin, (3) glimepiride, (4) Cr-glimepiride, (5) vildagliptin, (6) Cr-vildagliptin, (7) dapagliflozin and (8) Cr-dapagliflozin.

3.3.6. Antidiabetic property of drugs and their Cr-complexes in mice

The Cr-complexes and standard anti-diabetic drugs were administered to mice which were induced hyperglycemic by injecting alloxan. The treatment significantly reduced the blood glucose level as compared to alloxan control mice which received distilled water and normal food and the results are shown in Table 3.30 and Figure 3.48. Among the four Cr-drug complexes Cr-dapa complex reduced blood glucose level significantly and it was found to be 64.20% more effective than standard dapagliflozin.

Table 3.30. *In vivo* antidiabetic property of antidiabetic drugs and their Cr-complexes in mice.

Drug and their complexes	Before Alloxan treatment (mmol/L)	After Alloxan treatment (mmol/L)	After 14 days of drug treatment (mmol/L)	Reduction of sugar level from corresponding drug (mmol/L)	% of reduction of sugar level from corresponding drug
Metformin	3.64	31.54	19.7		
Cr-Met	4.4	31	15.1	4.6	23.35025
Dapa	3.8	31.2	17.6		
Cr-Dapa	6.3	29.4	6.3	11.3	64.20455
Vilda	3.8	31.5	19.7		
Cr-Vilda	4.3	31.6	18.2	1.5	7.614213
Glim	5.4	31.2	11.6		
Cr-Glim	3.1	21.7	8.5	3.1	26.72414

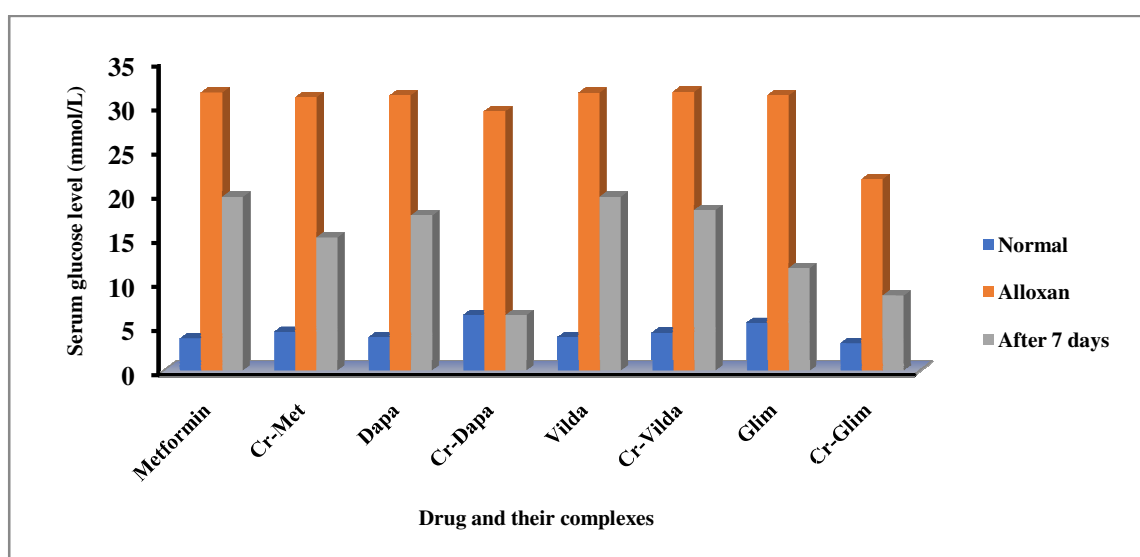
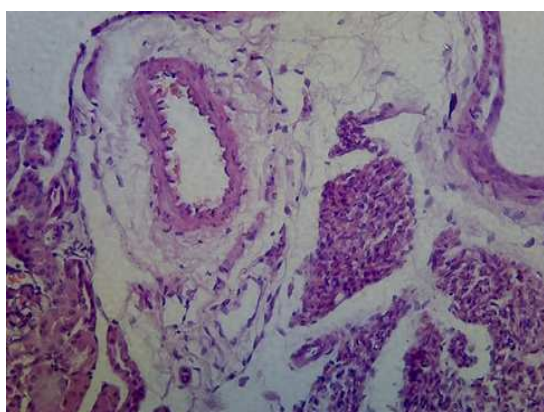


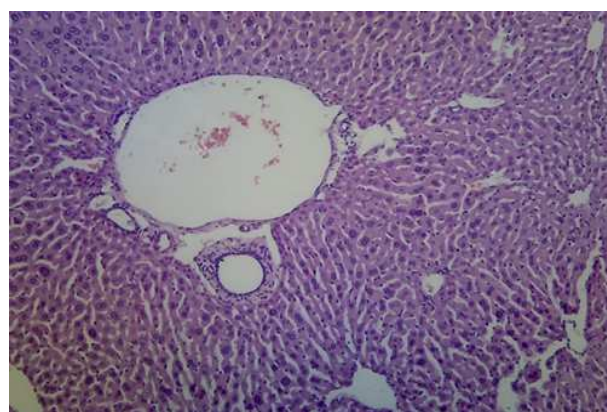
Figure 3.48. Graphical presentation of antidiabetic property of reference drugs and their Cr-complexes in mice model.

3.3.7. Histopathological studies of mice treated with chromium(III) drug complexes

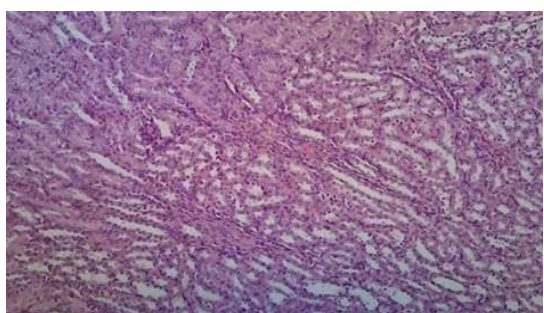
After the experimental period, all the mice were sacrificed, and the hepatic and nephrotic tissues were collected for histopathological studies. The experiment was conducted in Pathological Lab of Bangabandhu Sheikh Mujib Medical University (BSMMU), Dhaka. The results are shown in Figure 3.49. Metformin and Cr-metformin treated kidney and liver of mice remained in good condition. Same was found for glimepiride and Cr-glimepiride treated mice. Vildagliptin treatment showed no remarkable change in kidney and liver tissues of mice. But Cr-vildagliptin treatment caused moderate dysplasia in liver tissues of mice. Dapagliflozin treatment also showed no remarkable change in kidney and liver tissues of mice. But Cr-dapagliflozin treatment caused moderate dysplasia in liver tissues of mice.



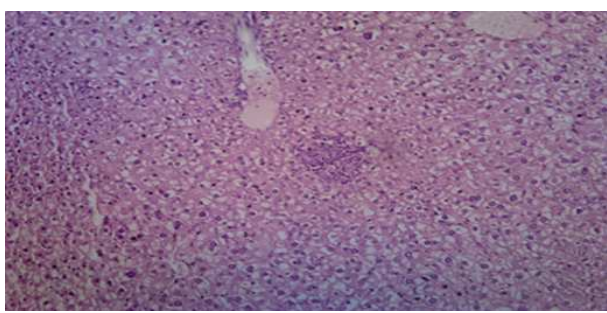
Metformin treated kidney, U/R



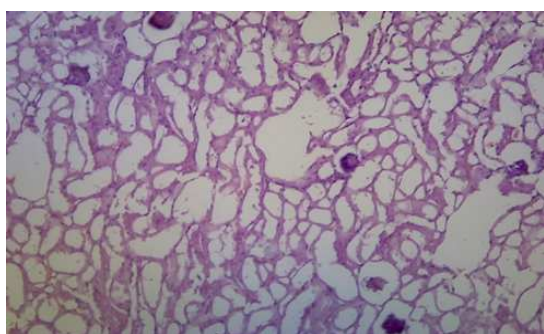
Metformin treated liver, U/R



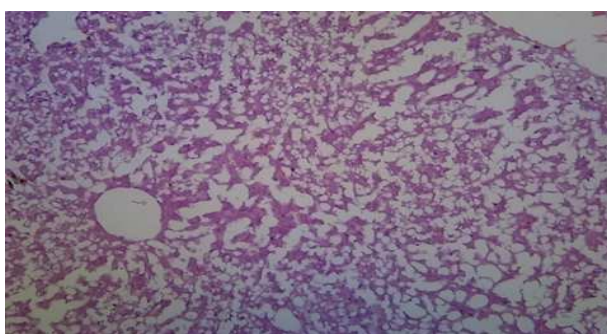
Cr-Metformin treated kidney, U/R



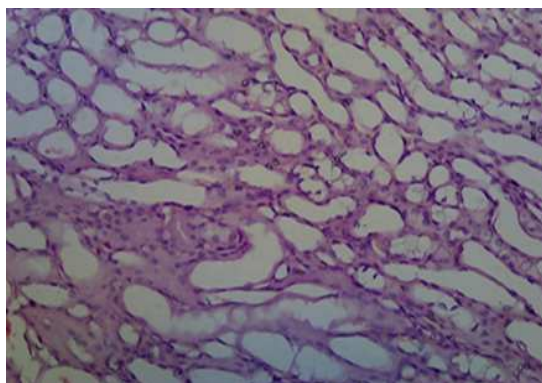
Cr-Metformin treated liver, U/R



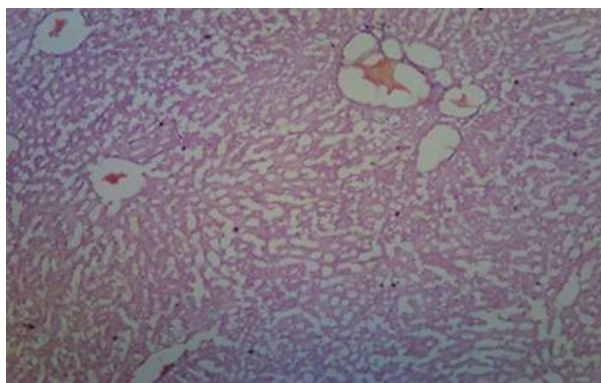
Glimepiride treated kidney, U/R



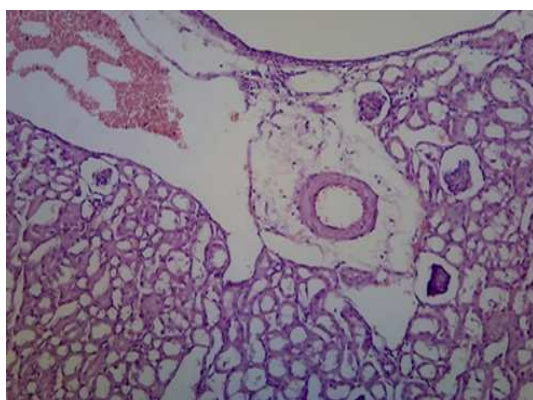
Glimepiride treated liver, U/R



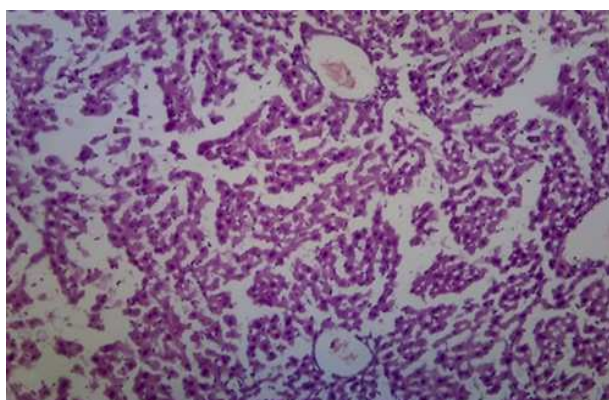
Cr-Glimepiride treated kidney, U/R



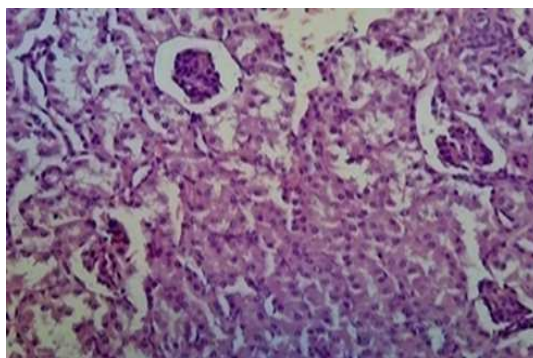
Cr-Glimepiride treated liver, U/R



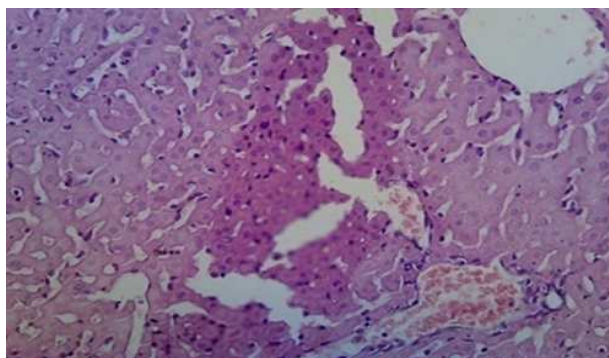
Vildagliptin treated kidney, U/R



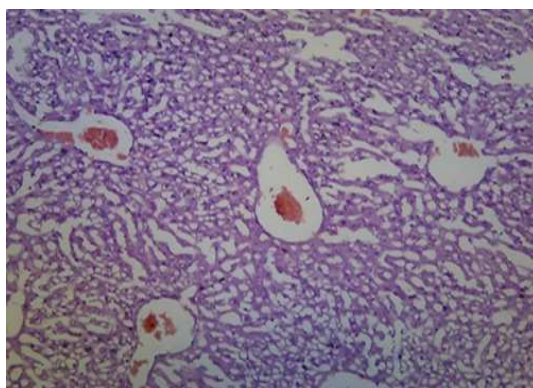
Vildagliptin treated liver, U/R



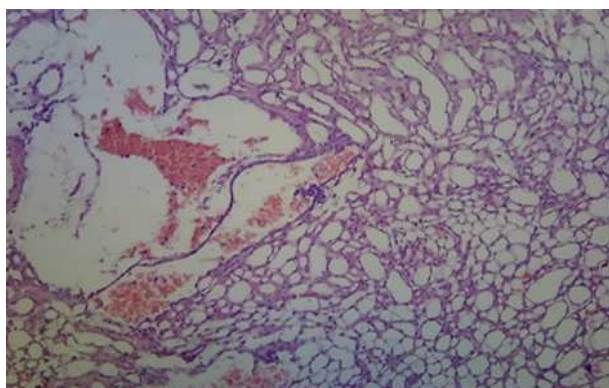
Cr-Vildagliptin treated kidney, U/R



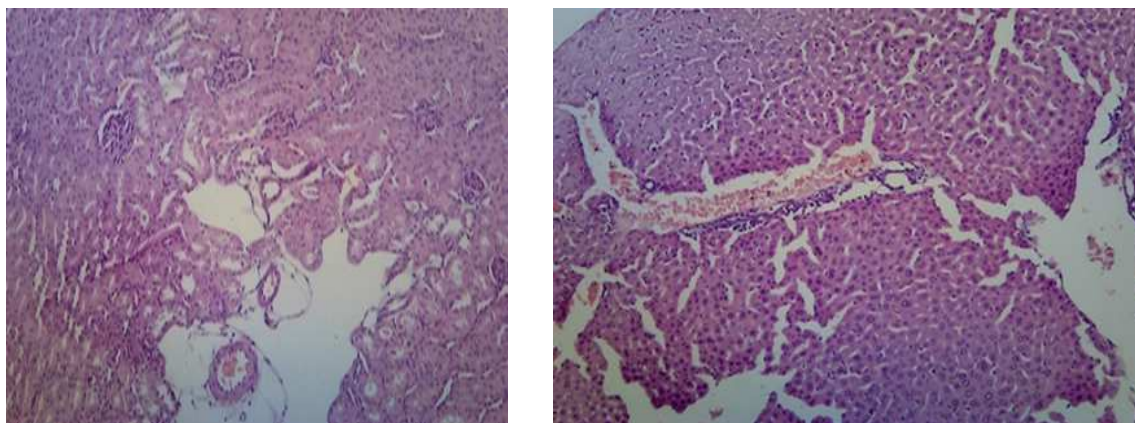
Cr-Vildagliptin treated liver, Moderate dysplasia



Dapagliflozin treated kidney, U/R



Dapagliflozin treated liver, U/R



Cr- dapagliflozin treated kidney, U/R

Cr-dapagliflozin treated liver, Moderate Dysplasia

Figure 3.49. Histopathological reports of metformin, Cr-metformin, glimepiride, Cr-glimepiride, vildagliptin, Cr-vildagliptin, dapagliflozin and Cr-dapagliflozin treated mice liver and kidney tissues. (U/R= Unremarkable).

3.4. COMPLEXATION OF HEAVY METAL LEAD WITH FOUR ANTIDIABETIC DRUGS: SYNTHESIS, CHARACTERIZATION AND ASSESSMENT OF BIOLOGICAL ACTIVITY AND TOXICITY

The complexes of lead with four antidiabetic drugs, metformin, glimepiride, vildagliptin and dapagliflozin was done by co-evaporation method and the synthesized complexes were named as Pb-metformin (Pb-met), Pb-glimepiride (Pb-glim), Pb-vildagliptin (Pb-vilda) and Pb-dapagliflozin (Pb-dapa). The synthesized complexes were characterized by different R_f values on TLC plate and new peak patterns in FT-IR spectral analysis. From TGA analysis the thermal stability and thermochemical characteristics of the complexes were evaluated. Furthermore, their antidiabetic property was evaluated on mice model and the toxicological studies were also performed by measuring serum creatinine level and uric acid level. Histopathological study of nephrotic and hepatic tissues of mice treated with drugs and lead drug complexes was also performed.

3.4.1. TLC characterization of drugs and lead drug complexes

TLC of the Pb-drug complexes was carried out using methanol-dichloromethane in different ratios as mobile phase. The spot of each of the new drug complex appeared at different places from their precursor drugs (Table 3.31). Each individual spot in the TLC plate represented the evolution of newer compound.

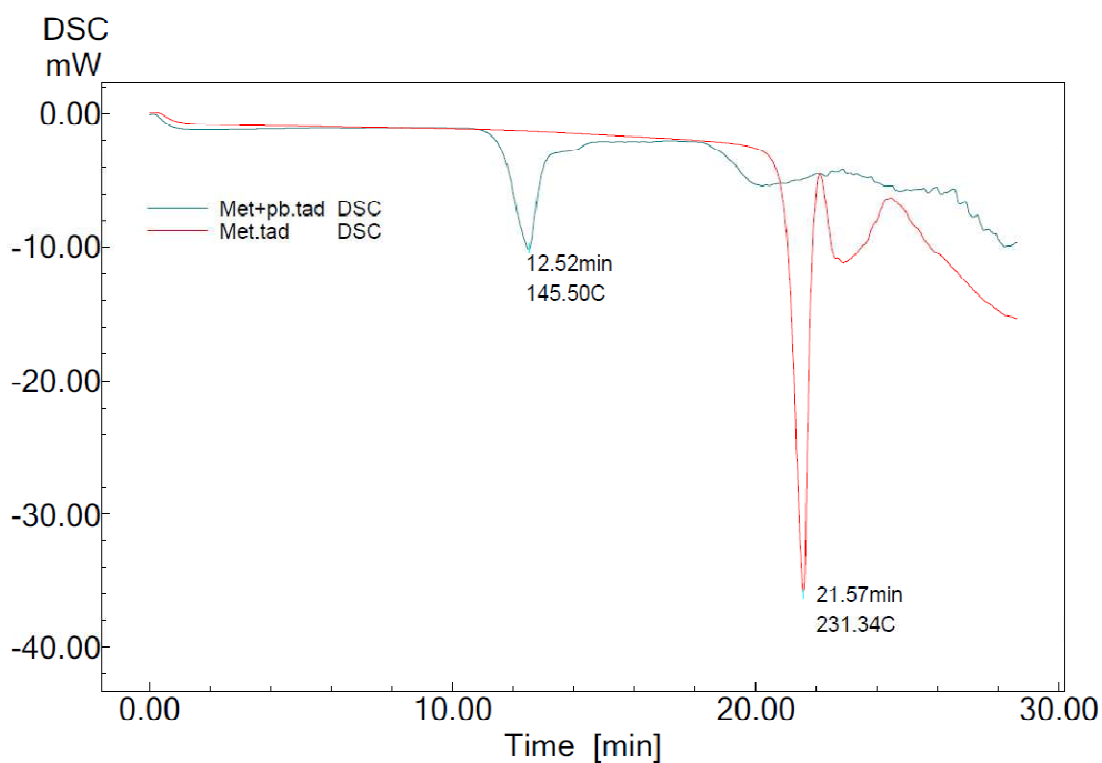
Table 3.31. R_f values of reference drugs and their respective lead complexes on silica gel H₂₅₄TLC plate.

Item	Mobile phase	R_f value
Metformin HCl	Methanol/dichloromethane (2:8)	0.5
Pb-met complex		0.45
Glimepiride	Methanol/dichloromethane (7:3)	0.6
Pb-glim complex		0.75
Vildagliptin	Methanol/dichloromethane (8:2)	0.7
Pb-vilda complex		0.55
Dapagliflozin	Methanol/dichloromethane (7:3)	0.5
Pb-dapa complex		0.3

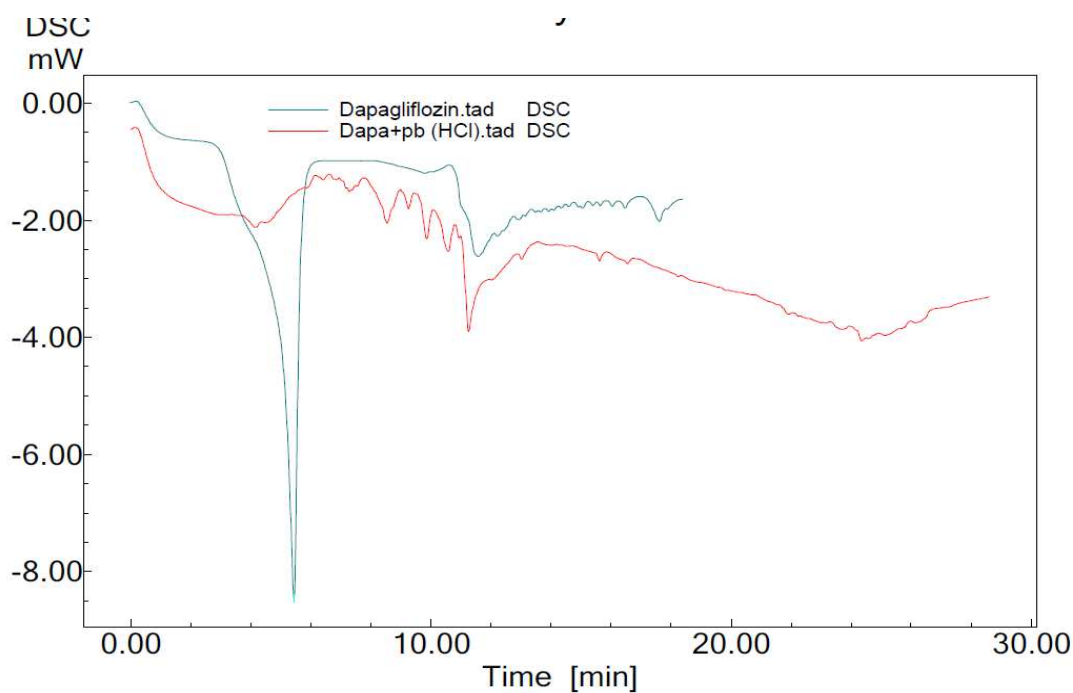
3.4.2. Analysis of drugs and lead drug complexes by DSC

The phase changes of the standard drugs and their Pb-complexes were studied by DSC and recorded as melting endotherm. Pure metformin showed melting endotherm at 231 °C and its Pb-complex (Pb-met) gave melting endotherm at 145 °C [Figure 3.50(1)].

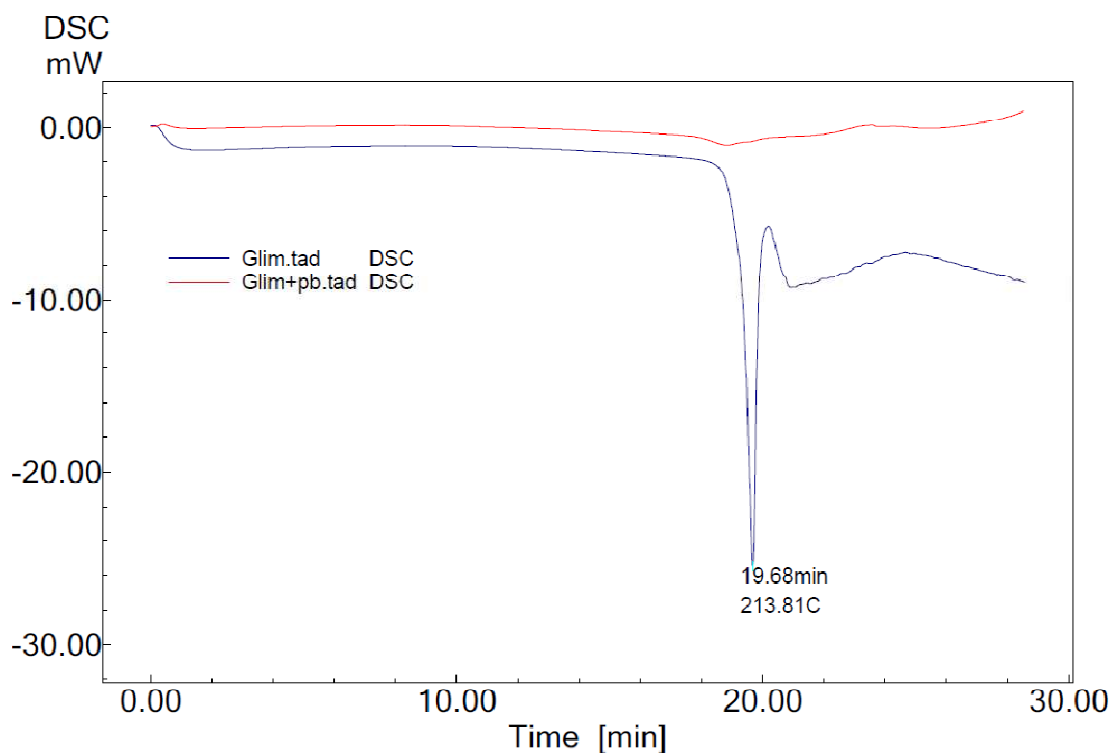
Dapagliflozin exhibited melting endotherm at the point of 77.98 °C but its Pb-complex revealed different fragmented peaks in the thermogram [Figure 3.50(2)]. Glimepiride and vildagliptin showed melting points at 213 °C and 152 °C, respectively whereas their Pb-complexes displayed different melting endotherms, which indicated the formation of new complexes [Figure 3.50(3) and 3.50(4)].



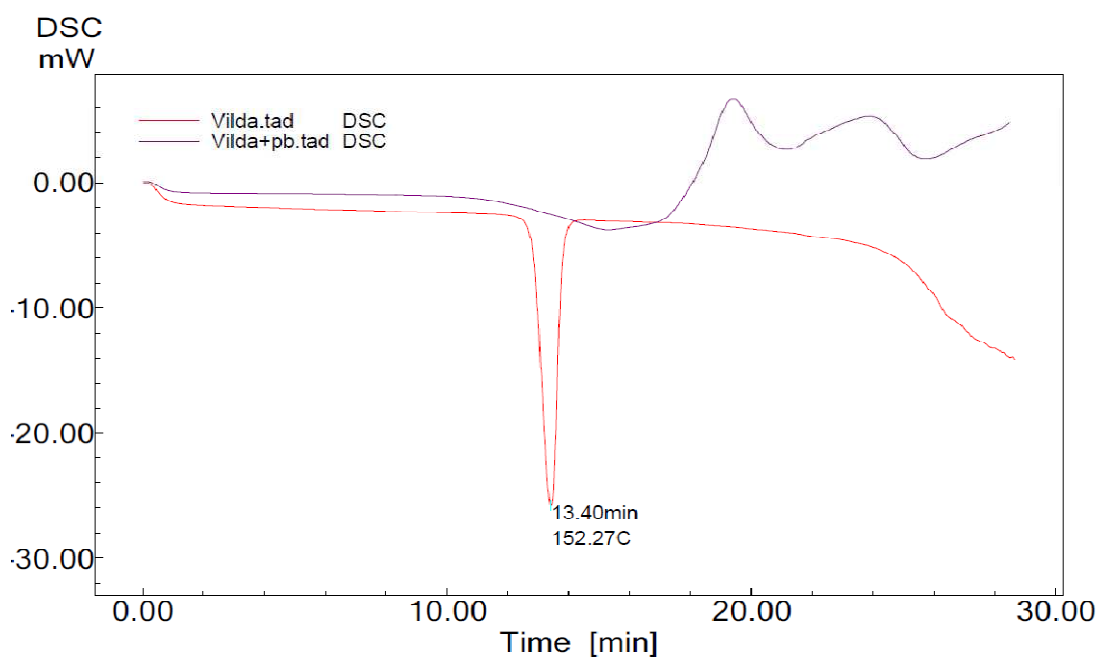
(1) DSC thermogram of metformin and Pb-metformin complex.



(2) DSC thermogram of dapagliflozin and Pb-dapagliflozin complex.



(3) DSC thermogram of glimepiride and Pb-glimepiride complex.

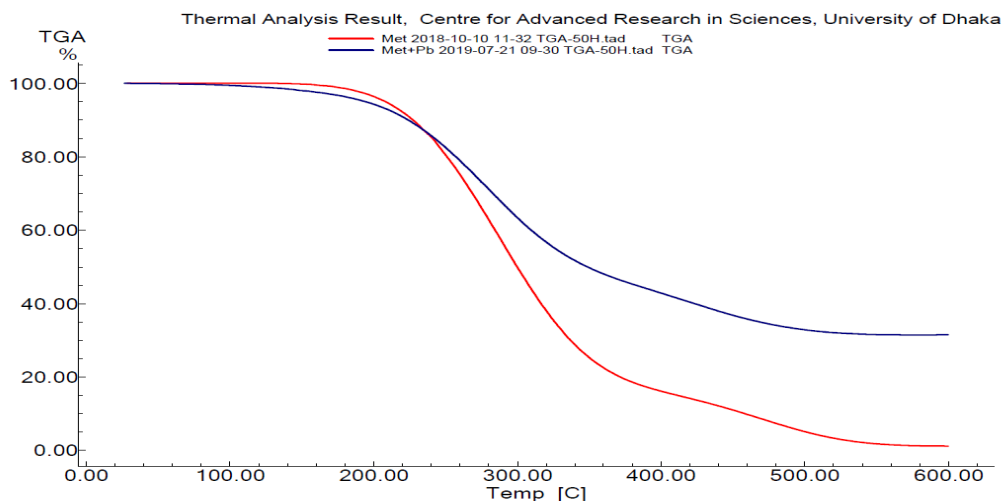


(4) DSC thermogram of vildagliptin and Pb-vildagliptin complex.

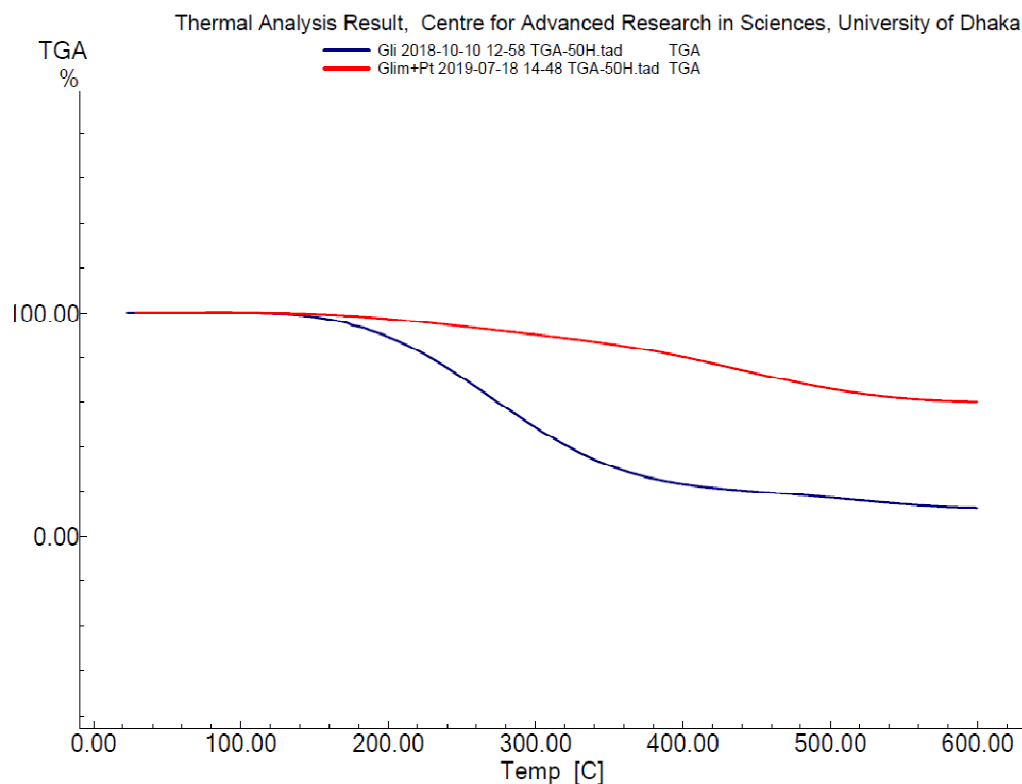
Figure 3.50. Overlaid DSC thermograms of: (1) metformin and Pb-metformin, (2) dapagliflozin and Pb-dapagliflozin, (3) glimepiride and Pb-glimepiride and (4) vildagliptin and Pb-vildagliptin complex.

3.4.3. Analysis of drugs and lead drug complexes by TGA

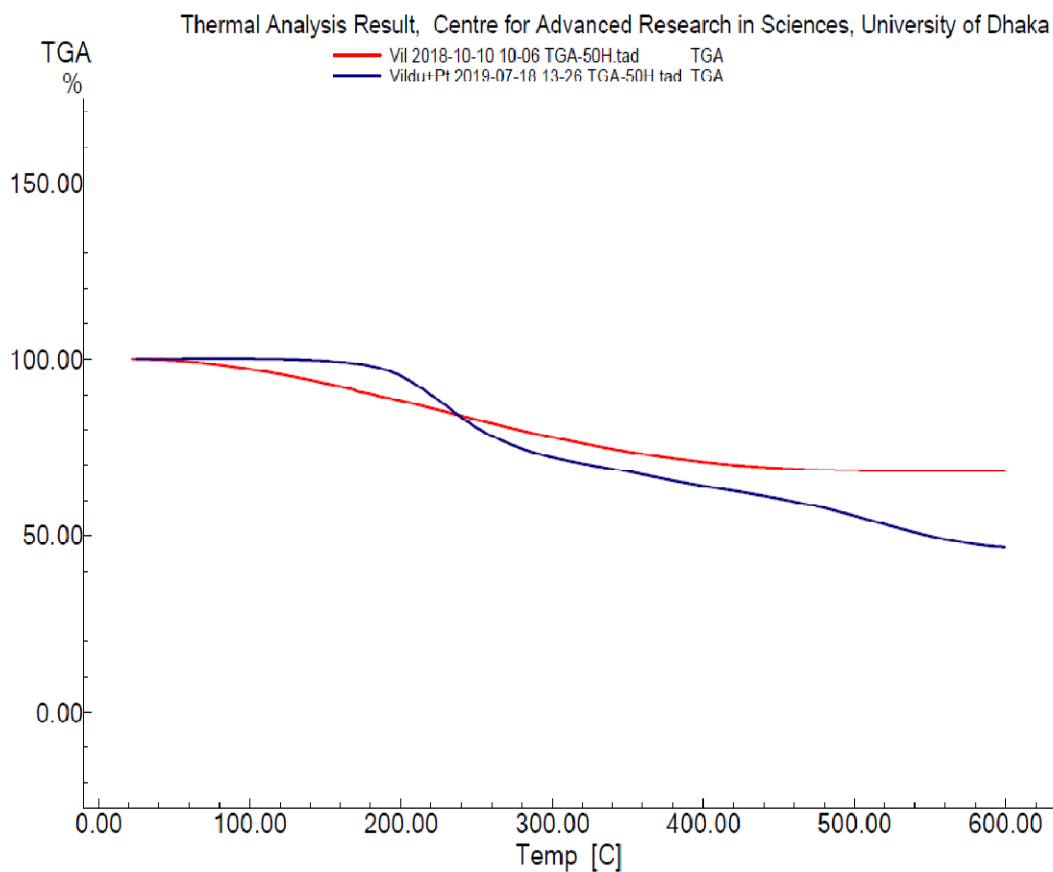
The percentages of weight loss for pure antidiabetic drugs and their lead(II) complexes were analyzed by thermogravimetric experiment at definite increase in temperature. Standard metformin was degraded 4.29% at 205 °C, whereas Pb-metformin complex showed different degradation pattern [Figure 3.51(1)].



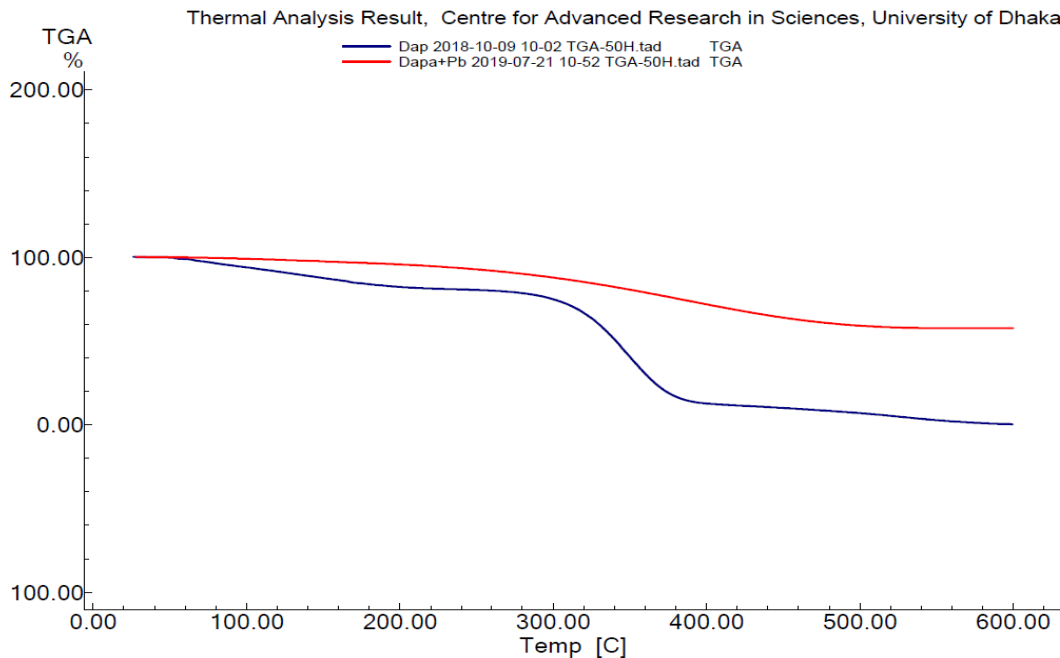
(1) TGA thermogram of metformin and Pb-metformin complex.



(2) TGA thermogram of glimepiride and Pb-glimepiride complex.



(3) TGA thermogram of vildagliptin and Pb-vildagliptin complex.



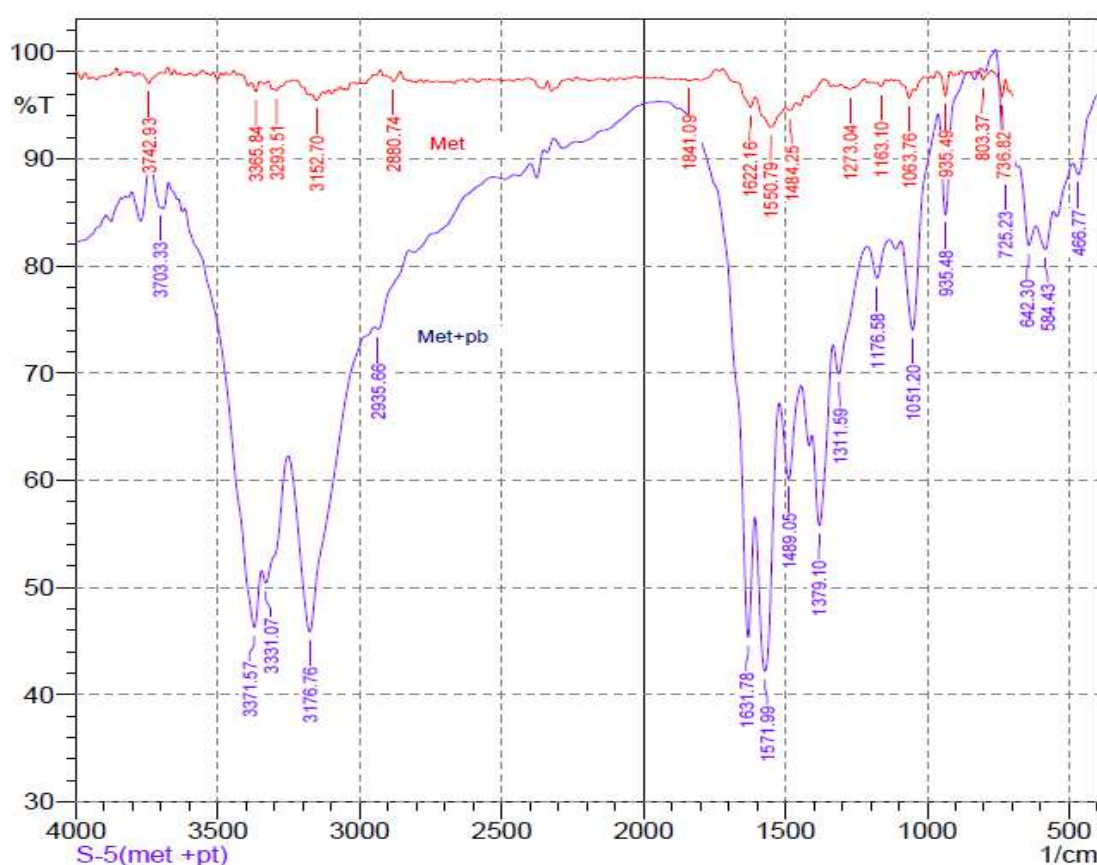
(4) TGA thermogram of dapagliflozin and Pb-dapagliflozin complex.

Figure 3.51. Overlaid TGA thermograms: (1) metformin and Pb-metformin complex, (2) glimepiride and Pb-glimepiride complex, (3) vildagliptin and Pb-vildagliptin complex and (4) dapagliflozin and Pb-dapagliflozin complex.

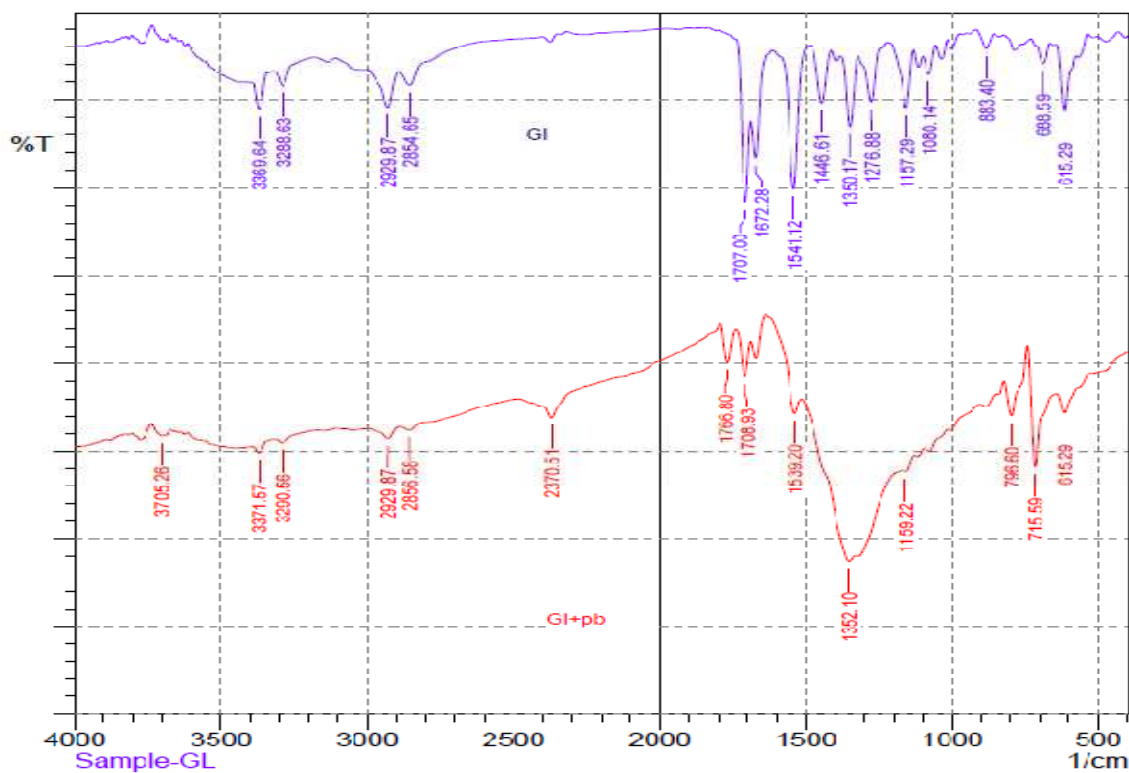
In glimepiride analysis 2.36% degradation was found at 160 °C and 87.70% degradation at 600 °C, whereas in case of Pb-glimepiride complex 1.45% degradation occurred at 175 °C and at 600 °C only 40% degradation was found [Figure 3.51(2)]. Vildagliptin showed 2.47% degradation at 92 °C and 31.89% degradation at 600 °C but the Pb-vildagliptin showed different degradation pattern. In Pb-vildagliptin thermogram 2.55% degradation was occurred at 185 °C and 45% degradation happened at 600 °C [Figure 3.51(3)]. In case of pure dapagliflozin, the breakdown pattern showed 17% degradation at 189 °C and 94% at 516 °C but for Pb-dapagliflozin complex degradation showed different pattern [Figure 3.51(4)].

3.4.4. Analysis of drugs and lead drug complexes by FT-IR

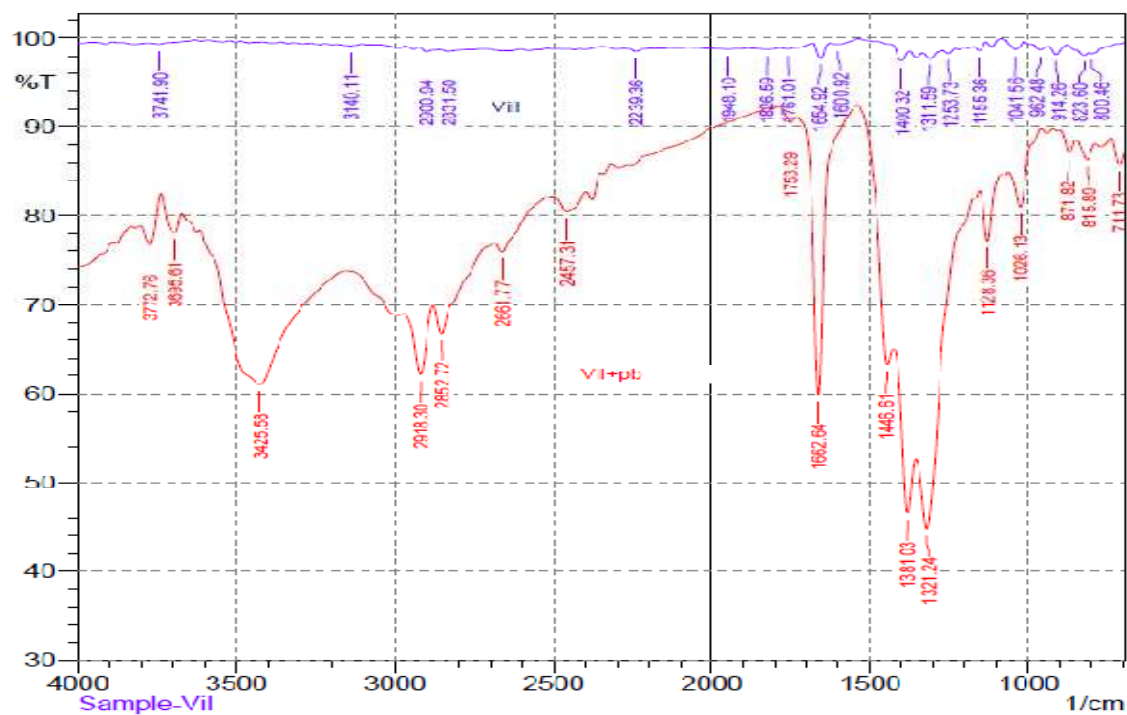
The FTIR spectra of pure drugs metformin, glimepiride, vildagliptin, dapagliflozin and their Pb-complexes are shown in Figure 3.52. The pure drugs and their lead complexes displayed different IR patterns which could be assigned as different compounds. The FTIR spectra of newly synthesized complexes exhibited characteristics specific types of molecular vibration.



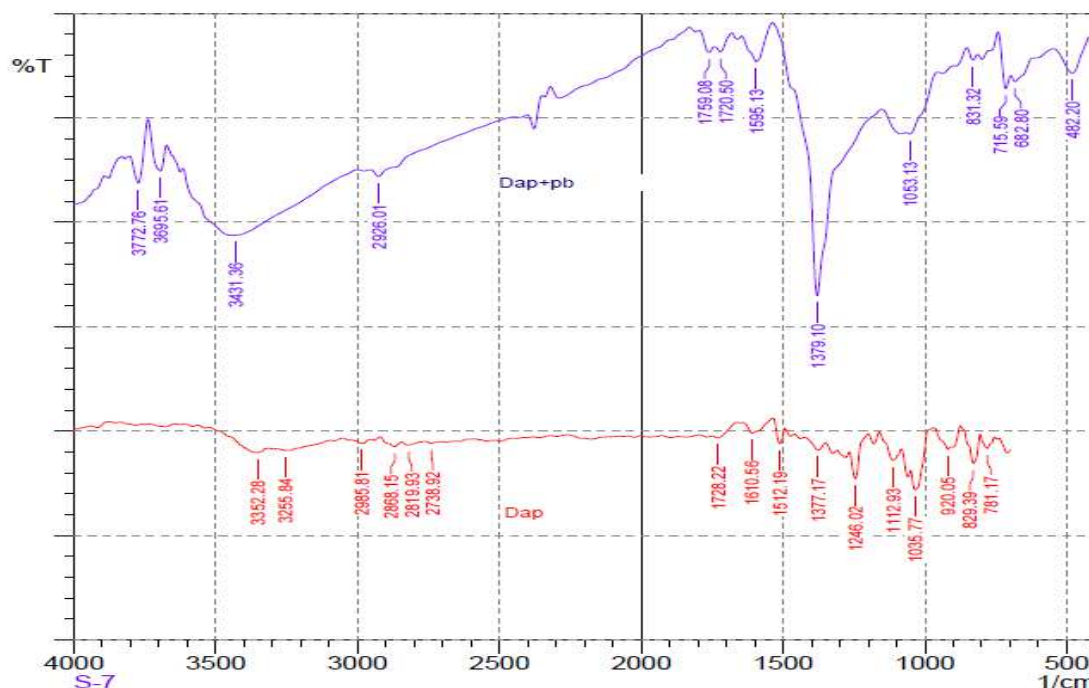
(1) FT-IR spectra of metformin and Pb-metformin.



(2) FT-IR spectra of gimepiride and Pb-gimepiride complex.



(3) FT-IR spectra of vildagliptin and Pb-vildagliptin complex.



(4) FT-IR spectra of dapagliflozin and Pb-dapagliflozin complex.

Figure 3.52. Overlaid IR spectra of: (1) metformin and Pb-met complex, (2) glimepiride and Pb-glime complex, (3) vildagliptin and Pb-vilda complex and (4) dapagliflozin and Pb-dapa complex.

The characteristic -NH stretching peak of metformin was yielded at 3742.93 cm^{-1} whereas the -NH peak of Pb-metformin complex was obtained in the downfield at 3703 cm^{-1} [Figure 3.52(1)]. Similarly, the -NH vibration stretching peak of glimepiride displayed at 3369.64 cm^{-1} was shifted to 3371.57 cm^{-1} in Pb-glimepiride complex [Figure 3.52(2)]. In vildagliptin the major vibration peak for -OH at 3140.11 cm^{-1} moved up field at 3425.58 cm^{-1} for Pb-vildagliptin [Figure 3.52 (3)]. The -OH vibration peak for dapagliflozin displayed at 3352.28 cm^{-1} shifted in the IR spectra of the corresponding Pb-drug complexes to 3431.36 cm^{-1} [Figure 3.52(4)]. These modifications in the IR spectra suggested that the lead complexes were synthesized newly and are different from the precursor drugs.

3.4.5. Evaluation of antidiabetic activity of drugs and lead drug complexes

The pure antidiabetic drugs and Pb-drug complexes were administered to alloxan induced diabetic mice to evaluate the antidiabetic activity of the new complexes. The pure drugs significantly reduced the blood glucose level as compared to control mice which received distilled water and normal food. But Pb-drug complexes did not show remarkable positive change after 14 days of treatment (Figure 3.53 and Table 3.32) to

reduce blood glucose level. After 14 days of treatment with metformin, glimepiride, vildagliptin, dapagliflozin, it was found that the average glucose levels of mice reduced from 31.54 to 19.02, 30.24 to 17.20, 31.50 to 19.70 and 30.37 to 17.60 mmol/L, respectively. Whereas the complexes Pb-met, Pb-glim, Pb-vilda and Pb-dapa did not reduce blood glucose levels considerably and blood sugar measured were found as 25.82, 29.23, 25.32 and 29.32 mmol/L, respectively.

Table 3.32. *In vivo* antidiabetic property of pure drugs (metformin, glimepiride, vildagliptin and dapagliflozin) and their Pb-complexes (Pb-met, Pb-glim, Pb-vilda and Pb-dapa) in mice model.

Sample	Fasting blood sugar (mmol/L)	SD	After alloxan blood sugar (mmol/L)	SD	After drug treatment blood sugar (mmol/L)	SD
Control	5.74	0.8562			5.76	0.9044
Metformin	5.24	0.6427	31.54	0.6768	19.02	0.6380
Pb-met	5.3	1.25	30.6	0.8889	25.82	2.9072
Glimepiride	5.4	0.7749	30.24	1.2896	17.2	1.1203
Pb-glim	5.35	1.25	30.23	0.8846	29.23	3.1565
Vildagliptin	5.2	0.7071	31.5	0.8477	19.7	0.9428
Pb-vilda	5.42	1.8759	31.93	1.9721	25.32	3.0037
Dapagliflozin	5.44	1.2702	30.37	0.8021	17.6	1.372
Pb-dapa	5.39	1.5342	32.25	0.9416	29.32	0.8656

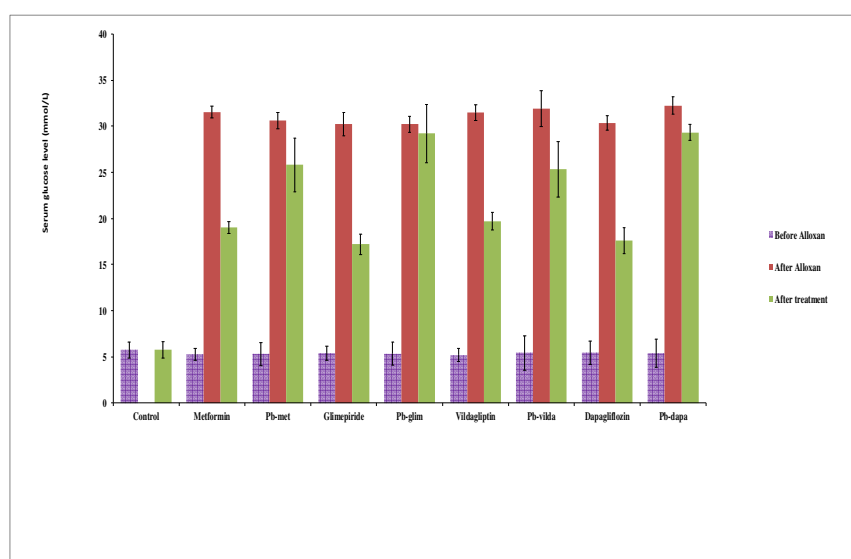


Figure 3.53. *In vivo* antidiabetic property of pure drugs (metformin, glimepiride, vildagliptin and dapagliflozin) and their Pb-complexes (Pb-met, Pb-glim, Pb-vilda and Pb-dapa) in mice model.

3.4.6. Evaluation of toxicity in terms of serum creatinine and uric acid level determinations in mice

Toxicity of antidiabetic drug-Pb⁺⁺ complexes were evaluated by studying the serum creatinine and uric acid level after 14 days of treatment. There was no toxicity observed in renal function of mice as measured by serum creatinine and serum uric acid levels when pure antidiabetic drugs viz. metformin, glimepiride, vildagliptin and dapagliflozin were used to reduce the blood sugar. But the complexes of Pb with those respective drugs elevated both serum creatinine and uric acid levels suggesting the renal impairment (Figures 3.54 and 3.55). After 14 days of treatment with metformin, glimepiride, vildagliptin, dapagliflozin, the serum creatinine levels of mice were found 3.38, 3.96, 3.60 and 3.42 mg/dL, respectively whereas for Pb-met, Pb-glim, Pb-vilda and Pb-dapa the creatinine level was increased and found 4.57, 5.36, 5.21 and 5.24 mg/dL, respectively (Table 3.33 and Figure 3.54)

Table 3.33. Serum creatinine levels after treatment with pure drugs (metformin, glimepiride, vildagliptin and dapagliflozin) and their Pb-complexes (Pb-met, Pb-glim, Pb-vilda and Pb-dapa) in mice model.

Sample	Serum creatinine level (mg/dL)	Serum creatinine level (mg/dL)	Serum creatinine level (mg/dL)	Average	SD
Control	3.41	3.57	3.13	3.37	0.223
Metformin	3.58	3	3.56	3.38	0.329
Pb-met	4.36	4.77		4.57	0.291
Glimepiride	3.46	4.46		3.96	0.707
Pb-glim	5.14	5.58		5.36	0.312
Vildagliptin	2.99	4.32	3.51	3.61	0.670
Pb-vilda		4.96	5.46	5.21	0.354
Dapagliflozin	3.43	3.14	3.7	3.42	0.280
Pb-dapa	4.90	5.58		5.24	0.478

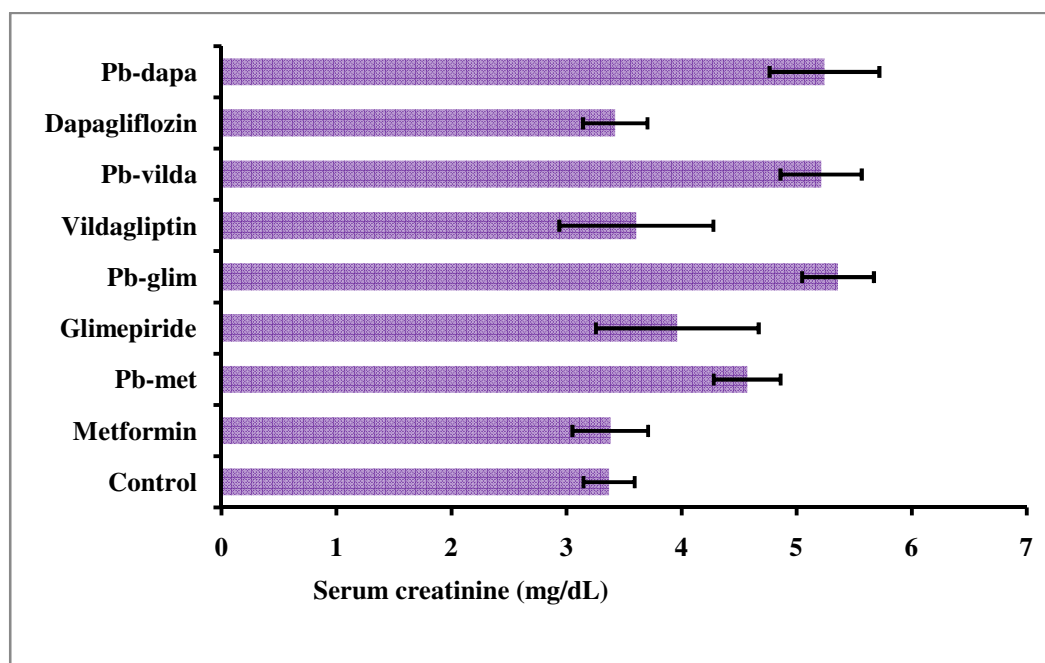


Figure 3.54. Serum creatinine levels after treatment with pure drugs (metformin, glimepiride, vildagliptin and dapagliflozin) and their Pb-complexes (Pb-met, Pb-glim, Pb-vilda and Pb-dapa) in mice model.

The serum uric acid level also increased after treatment with Pb-met, Pb-glim, Pb-vilda and Pb-dapa than that with metformin, glimepiride, vildagliptin, dapagliflozin treatment. The level of uric acid was elevated into 53.13 mg/dL from 42.91 mg/dL, 57.40 mg/dL from 44.83 mg/dL, 49.36 mg/dL from 40.21 mg/dL and 53.32mg/dL from 41.49 mg/dL, respectively for Pb-met, Pb-glim, Pb-vilda and Pb-dapa treated mice than that of metformin, glimepiride, vildagliptin, dapagliflozin treated mice. (Table 3.34 and Figure 3.55)

Table 3.34. Serum uric acid levels after treatment with pure drugs (metformin, glimepiride, vildagliptin and dapagliflozin) and their Pb-complexes (Pb-met, Pb-glim, Pb-vilda and Pb-dapa) in mice model.

Sample	Serum Uric (mg/dL)	SD (\pm)
Control	40.191067	1.904434
Metformin	42.90818859	3.637966
Pb-met	53.12903226	2.379655
Glimepiride	44.82878412	5.371964
Pb-glim	57.40198511	4.778807
Vildagliptin	40.2133995	3.881108
Pb-vilda	49.36228288	7.459893
Dapagliflozin	41.49379653	3.603282
Pb-dapa	53.31513648	5.122522

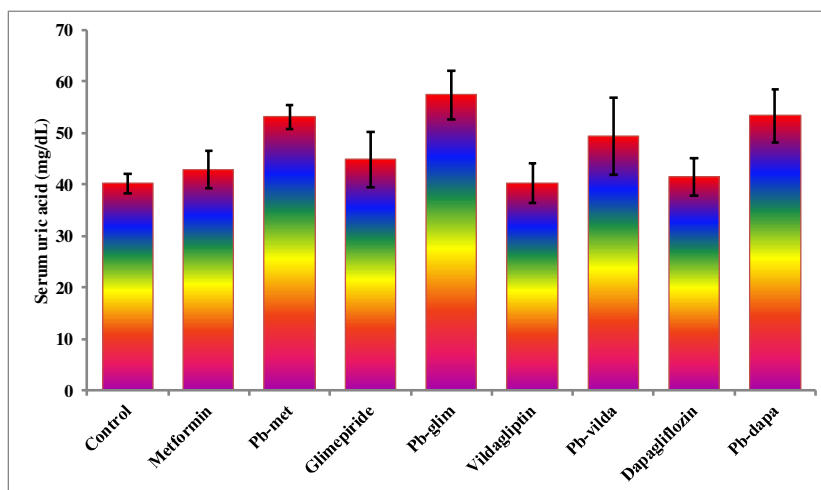
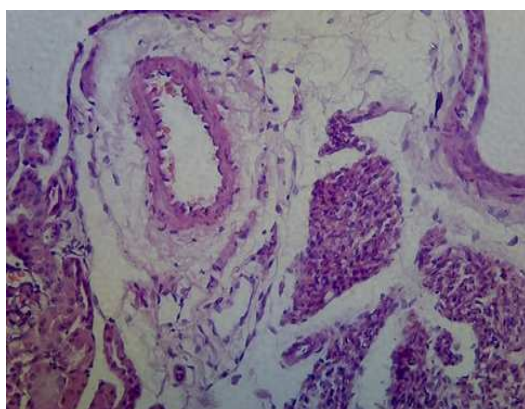


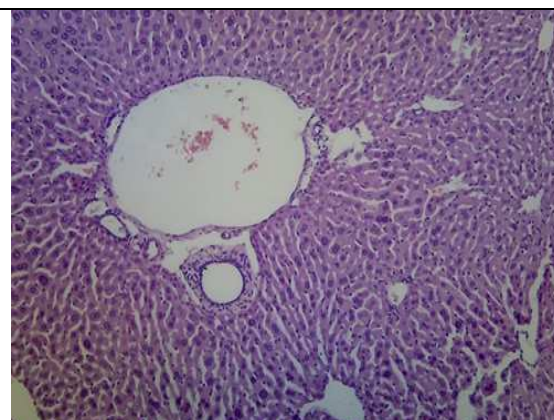
Figure 3.55. Serum uric acid levels after treatment with pure drugs (metformin, glimepiride, vildagliptin and dapagliflozin) and their Pb-complexes (Pb-met, Pb-glim, Pb-vilda and Pb-dapa) in mice model.

3.4.7. Histopathological studies of mice treated with drugs and lead drug complexes

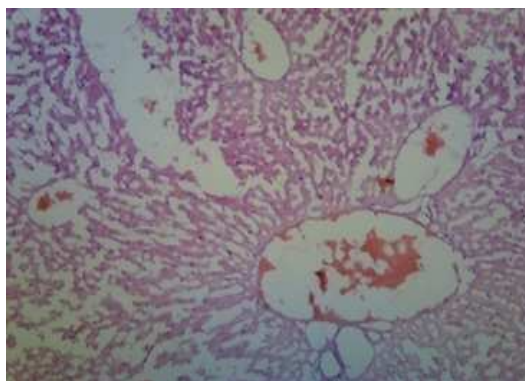
After the 14 days experimental period the mice were sacrificed, and the hepatic and nephrotic tissues were collected for histopathological studies. The experiment was conducted in pathological lab of BSMMU (Bangabandhu Sheikh Mujib Medical University), Dhaka. The results are shown in Figure 3.56. Metformin, Pb-metformin, dapagliflozin and Pb-dapagliflozin treated mice kidney and hepatic tissues exhibited no remarkable change. Same was found for glimepiride and vildagliptin treated kidney and hepatic tissues. But Pb-glimepiride and Pb-vildagliptin treated hepatic tissues revealed dysplasia.



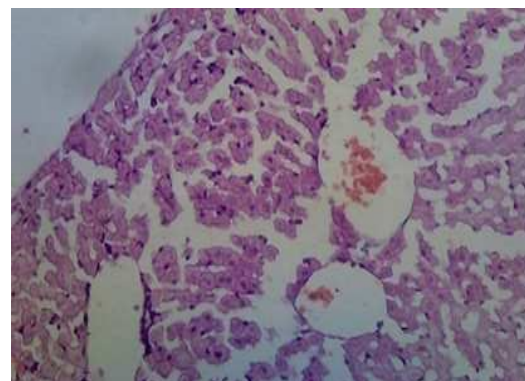
Metformin treated kidney, U/R



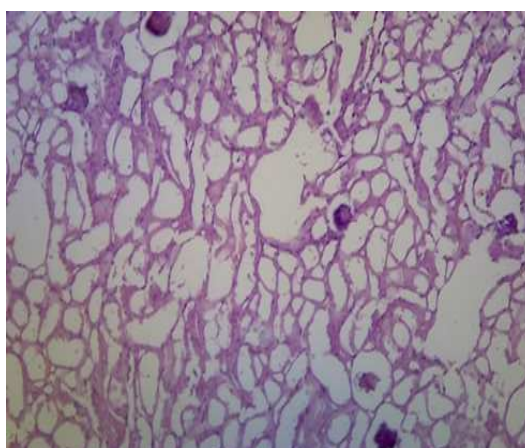
Metformin treated Liver, U/R



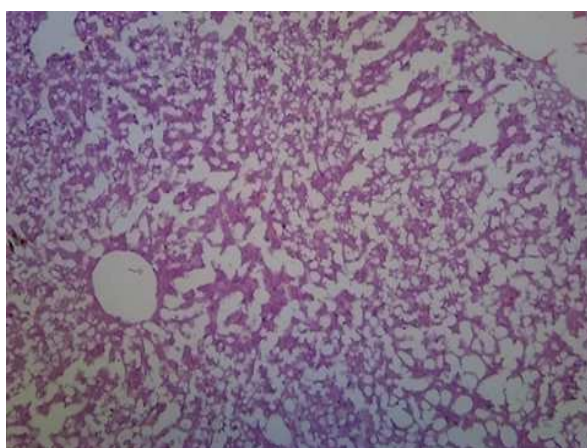
Pb-met complex treated Kidney, U/R



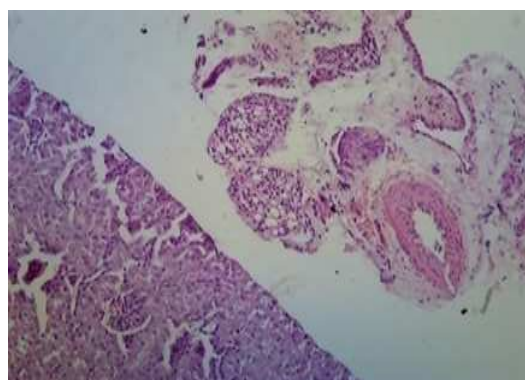
Pb-met complex treated Liver, U/R



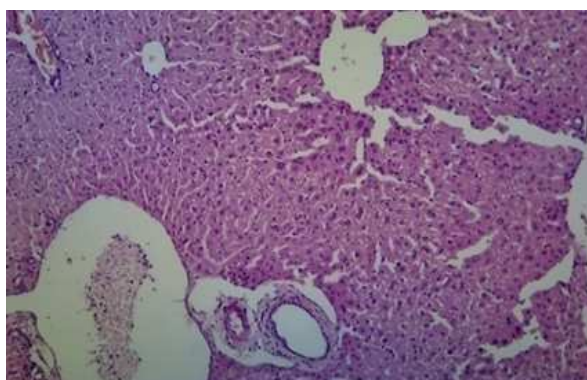
Glimepiride treated Kidney, U/R



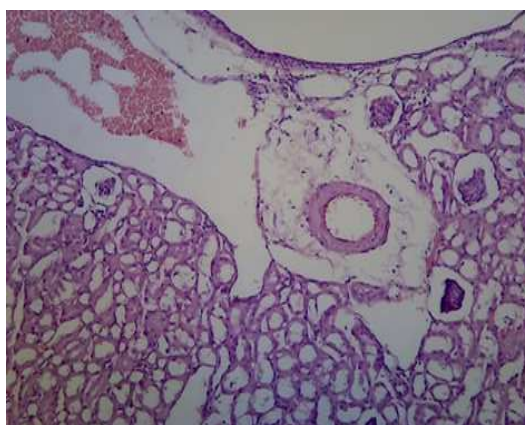
Glimepiride treated Liver, U/R



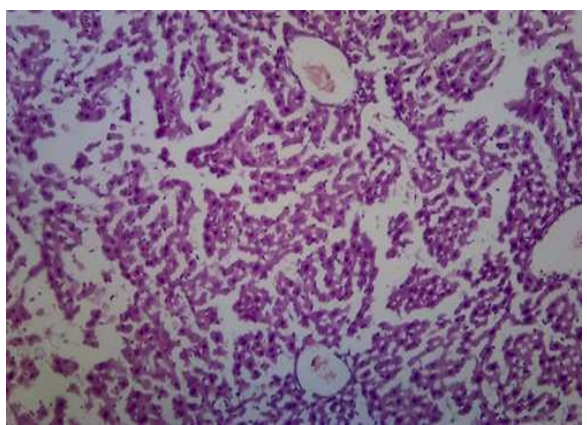
Cr-glim complex treated Kidney, U/R



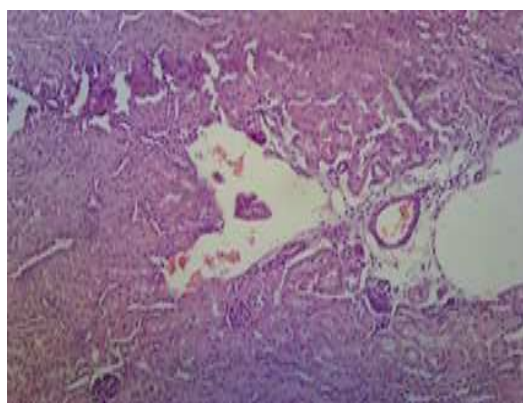
Pb-glim treated Liver, Severe dysplasia



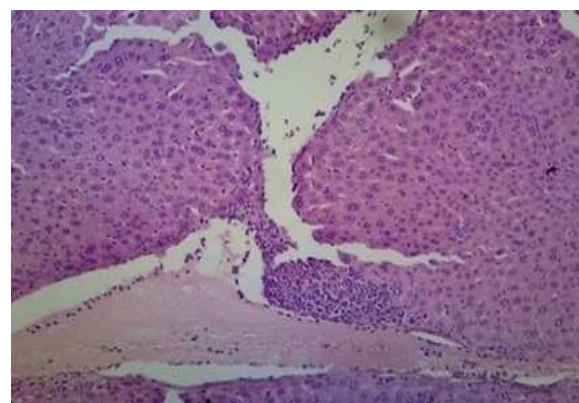
Vildagliptin treated Kidney, U/R



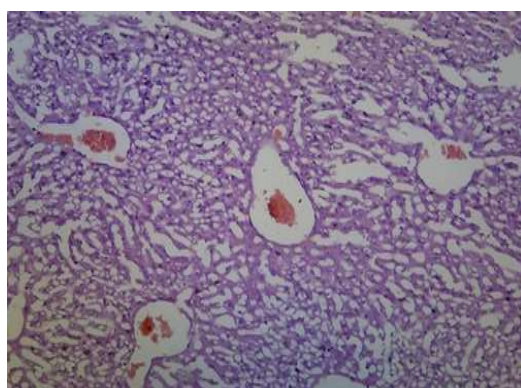
Vildagliptin treated Liver, U/R



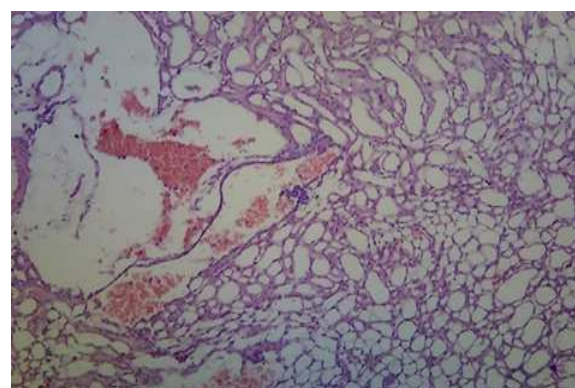
Pb-vilda complex treated Kidney, U/R



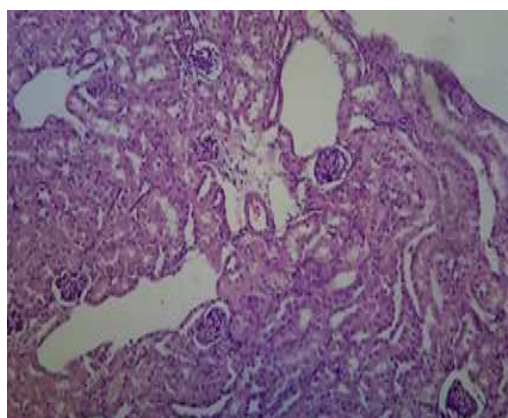
Pb-vilda treated Liver, dysplasia



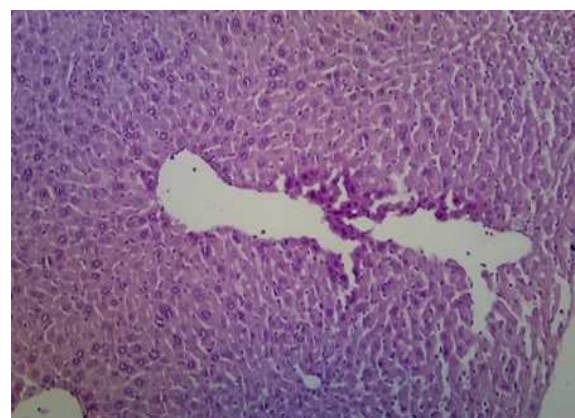
Dapagliflozin treated Kidney, U/R



Dapagliflozin treated Liver, U/R



Pb-dapa complex treated Kidney, U/R



Pb-dapa complex treated Liver, U/R

Figure 3.56. Histopathological reports of metformin, Pb-metformin, Glimpiride, Pb-glimpiride, Vildagliptin, Pb-vildagliptin, Dapagliflozin and Pb-dapagliflozin treated mice liver and kidney tissues. (U/R= Unremarkable).

3.5. LIPID LOWERING DRUG ATORVASTATIN CALCIUM TRIHYDRATE COMPLEXATION WITH COPPER(II), IRON(II) AND ZINC(II): SYNTHESIS AND CHARACTERIZATION

Three new complexes of lipid lowering drug atorvastatin with three divalent metals called iron-atorvastatin complex, Copper-atorvastatin and Zinc-atorvastatin complexes were synthesized by co-evaporation process. Then the complexes [Fe(II)-atorvastatin, Cu(II)-atorvastatin and Zn(II)-atorvastatin complexes] were investigated and characterized by different R_f values from TLC plate, melting point analyses, new peak patterns of FT-IR and ^1H NMR spectral analyses.

3.5.1. Physical, analytical and thermal characteristics of drug and metal drug complexes



Figure 3.57. Crystals of Fe-atorvastatin, Cu-atorvastatin and Zn-atorvastatin.

The colour of synthesized crystalline solid complexes was deep brown (Figure 3.57). The melting points of the newly formed complexes were less than the parent compound atorvastatin calcium. Using ethyl acetate: toluene: methanol at a ratio of 2:7:1 as mobile phase few unique spots were found in TLC plate with different R_f values. The results are shown in Table 3.35.

Table 3.35. Physical, analytical and thermal characteristics of atorvastatin and its three complexes.

Compound	color	R _f value	Melting point, T _m (°C)
Atorvastatin calcium	White	0.2	163 °C -167 °C
Fe-atorvastatin	Brown	0.6	105.6 °C- 110 °C
Cu-atorvastatin	Brown	0.65	106.5 °C-111 °C
Zn-atorvastatin	Brown	0.63	102 °C-107.6 °C

3.5.2. TLC characteristics of the drug and metal drug complexes

The analysis was carried out in ethyl acetate: toluene: methanol at a ratio of 2:7:1 as mobile phase to confirm complexation. The three clear spots of the formed complexes with different retardation factor (R_f) values from the parent drug were observed (Table 3.35). The characteristic R_f values are informative of different compounds.

3.5.3. Analysis of drug and metal drug complexes by UV Spectroscopy

The atorvastatin calcium showed peak around 250 nm, but its three new metal complexes Fe-atorvastatin, Cu-atorvastatin and Zn-atorvastatin showed peak around 240 nm. It was also observed that the newly formed complexes showed hypsochromic shift than that of atorvastatin calcium in Figure 3.58.

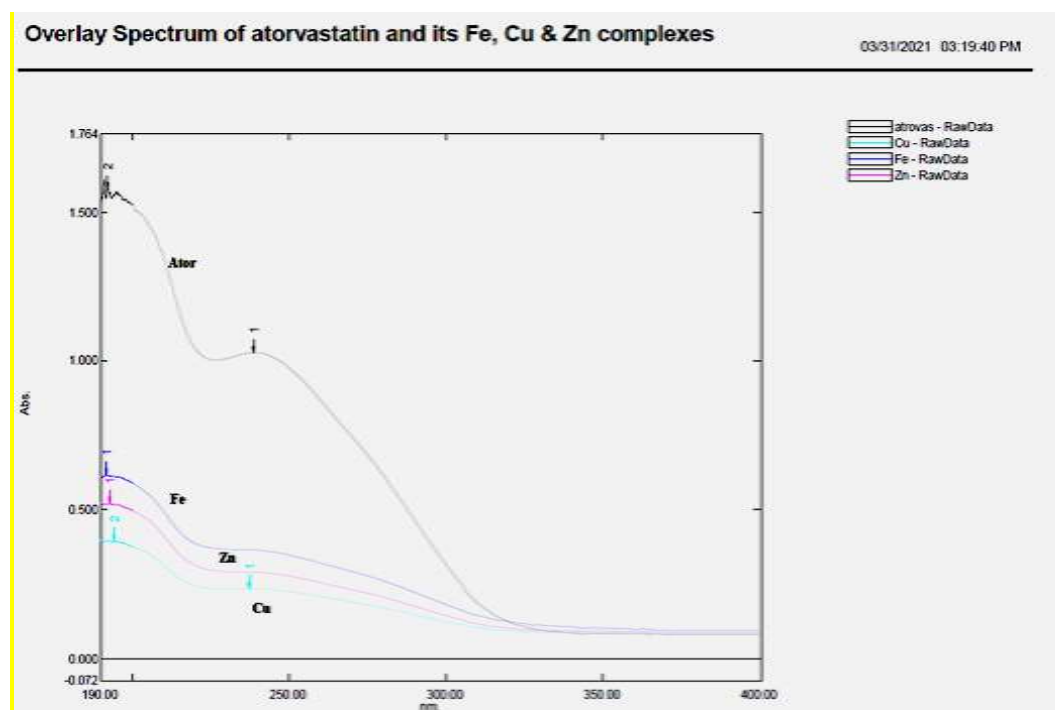
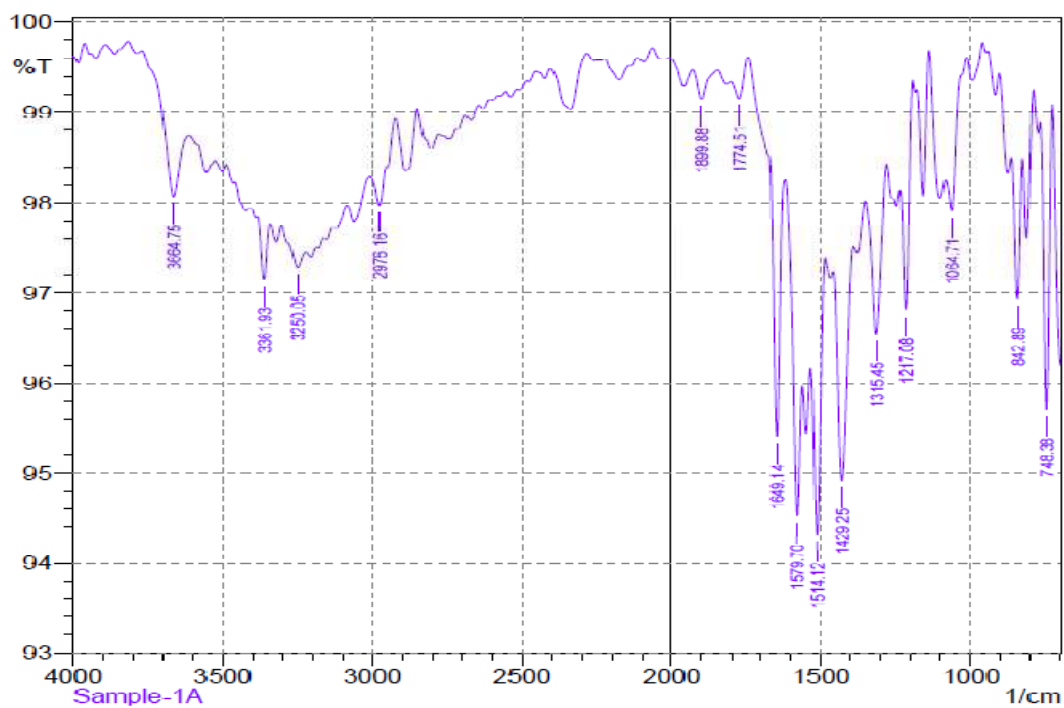


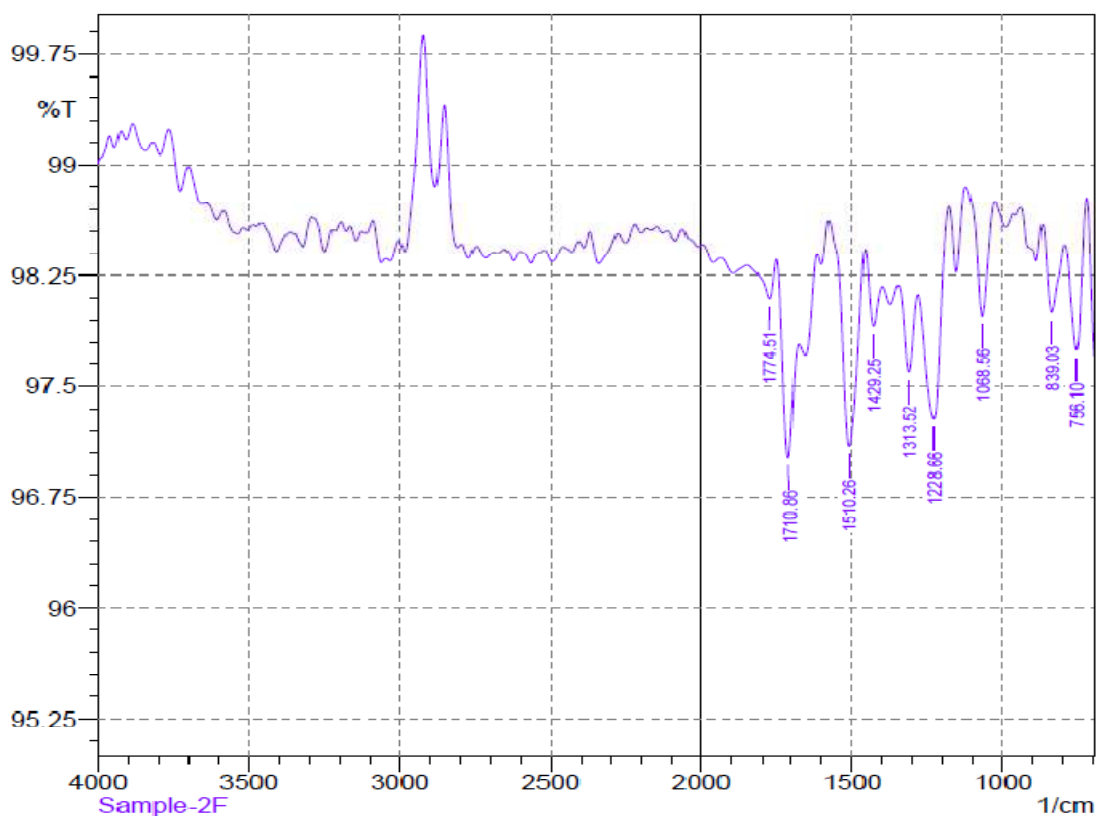
Figure 3.58. Overlaid UV spectra of atorvastatin calcium and three new complexes (Fe-atorvastatin, Cu-atorvastatin and Zn-atorvastatin).

3.5.4. Analysis of drug and metal drug complexes by FT-IR

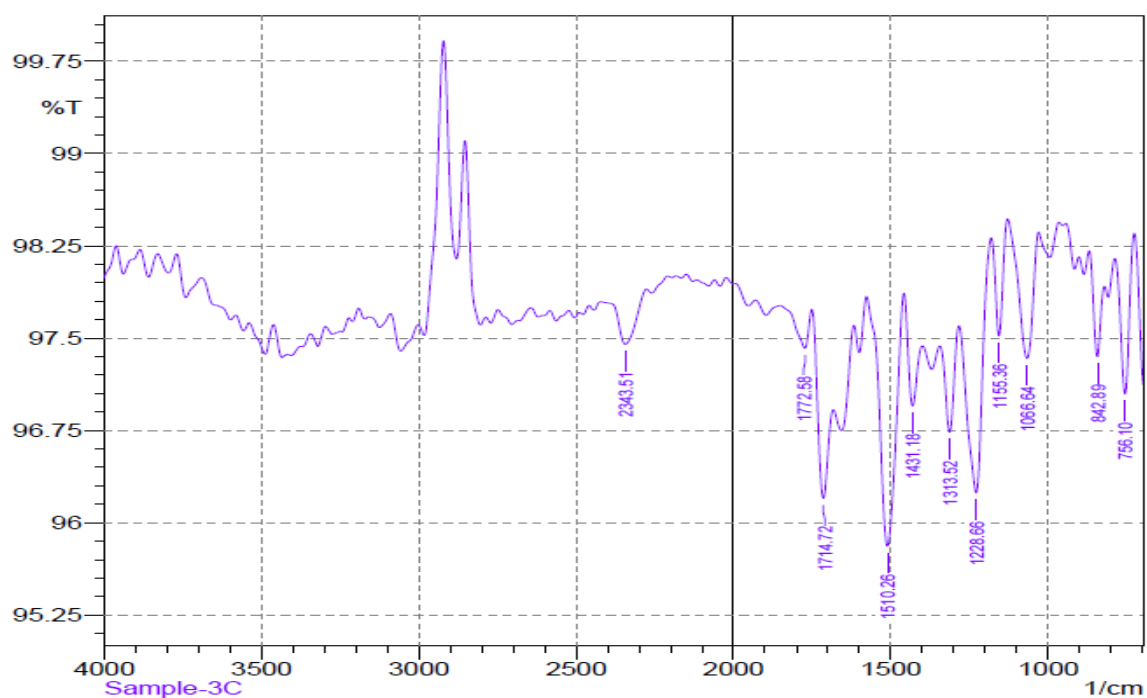
Characteristic peaks of atorvastatin calcium were found between 3700 and 3000 cm^{-1} , specifically at 3664 , 3361 , 3250 , 2976 , 1899 , 1774 , 1649 and 1579 cm^{-1} as shown in Figure 3.59 (1). The peak seen at 3664 cm^{-1} represented of free OH group. On the other hand, the peaks at 3361 cm^{-1} and from 1700 cm^{-1} to 1400 cm^{-1} were found to be characteristic for N-H and C-C bond stretching vibration of aromatic ring. Other peaks at 3250 cm^{-1} and 2976 cm^{-1} indicated asymmetrical as well as symmetrical stretching of OH bond, respectively.



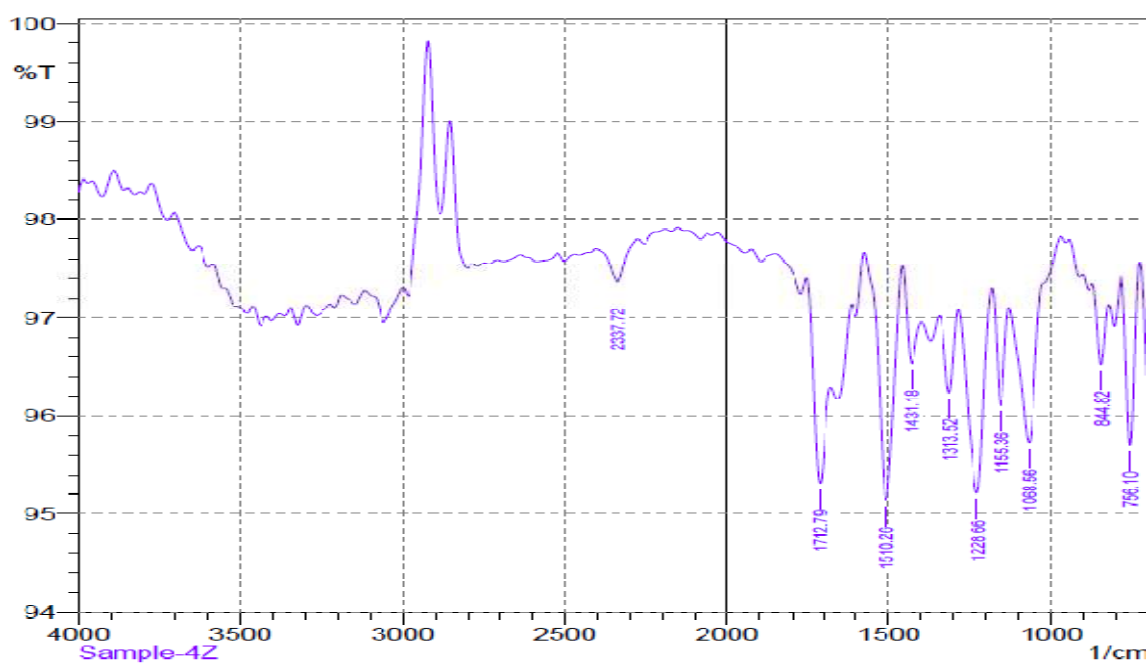
(1) FT-IR spectrum of atorvastatin calcium.



(2) FT-IR spectrum of the new complex Fe-atorvastatin.



(3) FT-IR spectrum of new complex Cu-atorvastatin.

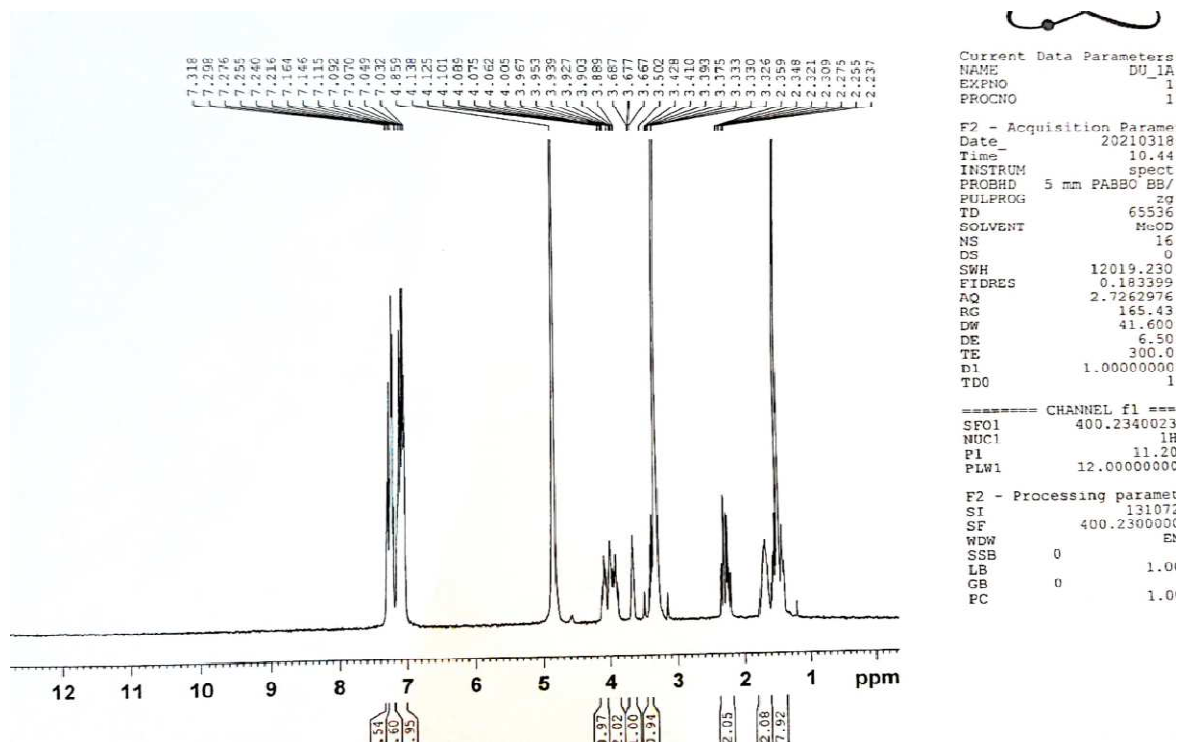


(4) FT-IR spectrum of new complex Zn-atorvastatin.

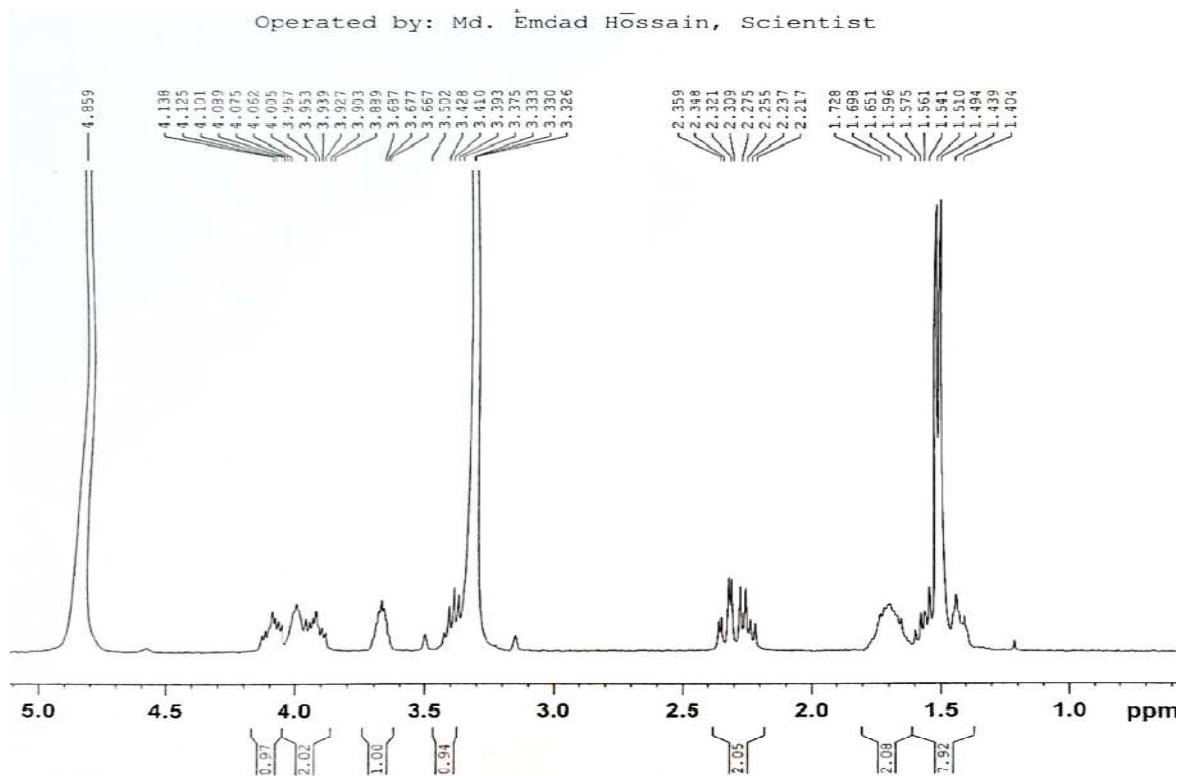
Figure 3.59. FT-IR spectra of: (1) atorvastatin calcium, (2) Fe-atorvastatin, (3) Cu-atorvastatin and (4) Zn-atorvastatin.

3.5.5. Analysis of atorvastatin and its metal complexes by ^1H NMR spectroscopy

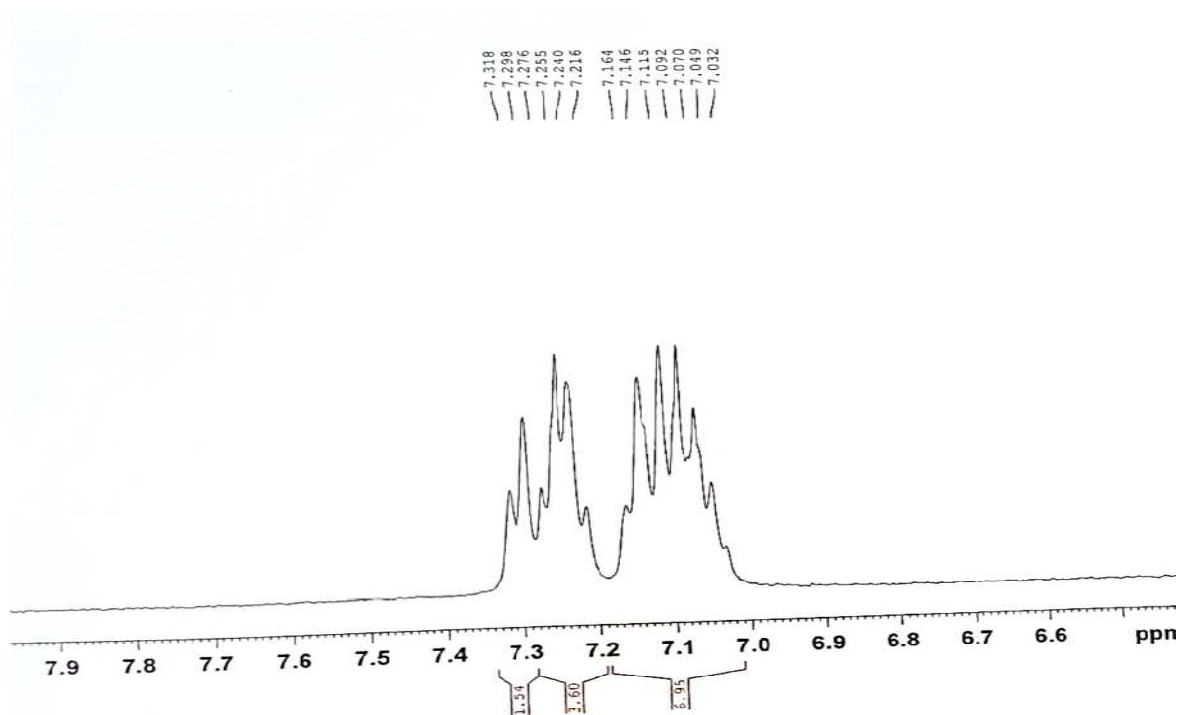
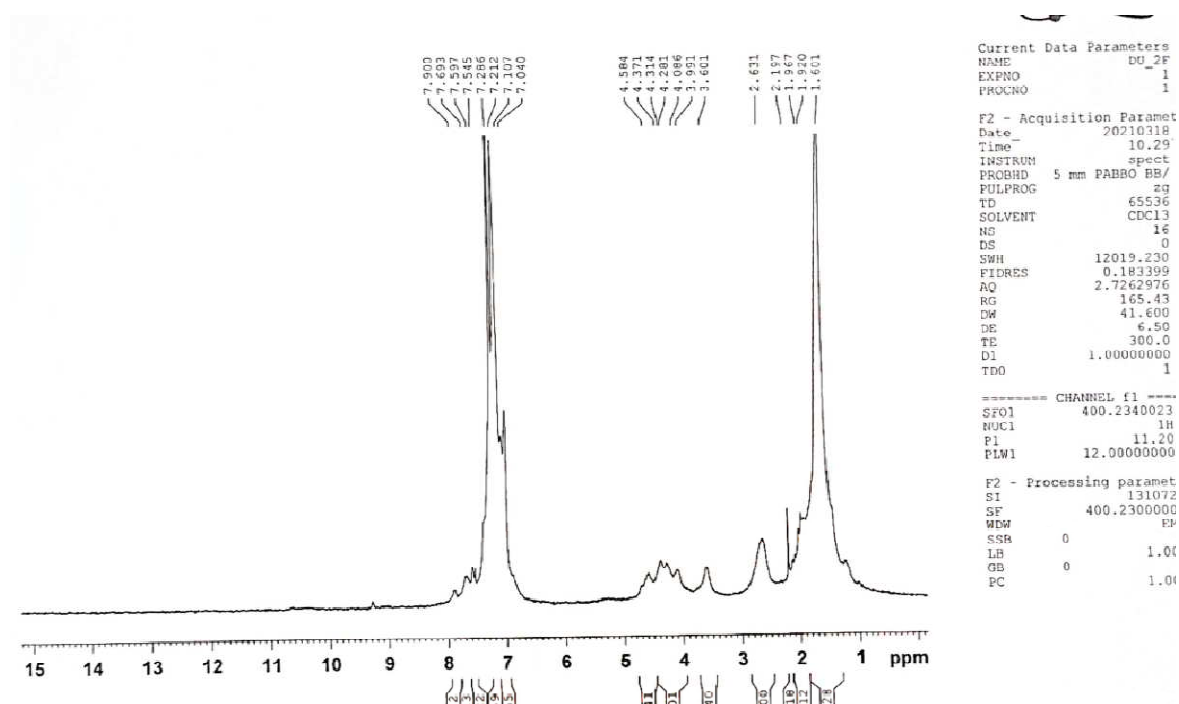
NMR data were analysed for the determination of the change in the spectra of the newly synthesized atorvastatin-metal complexes. The spectra are shown in Figure 3.60.

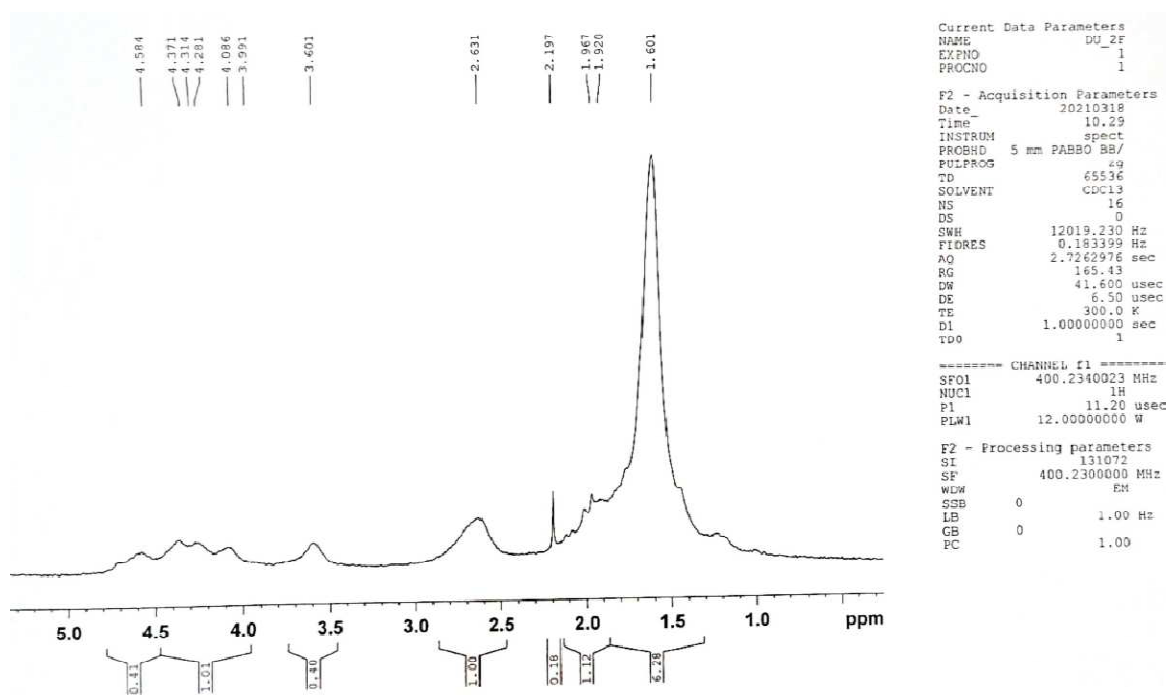
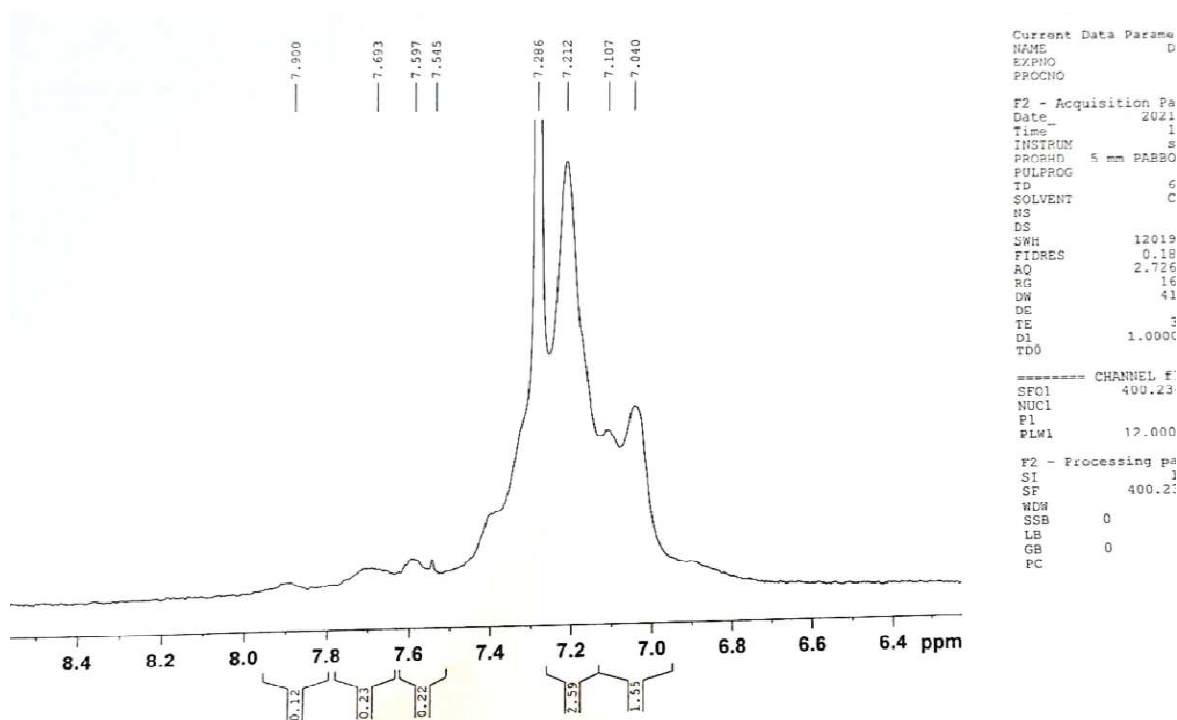


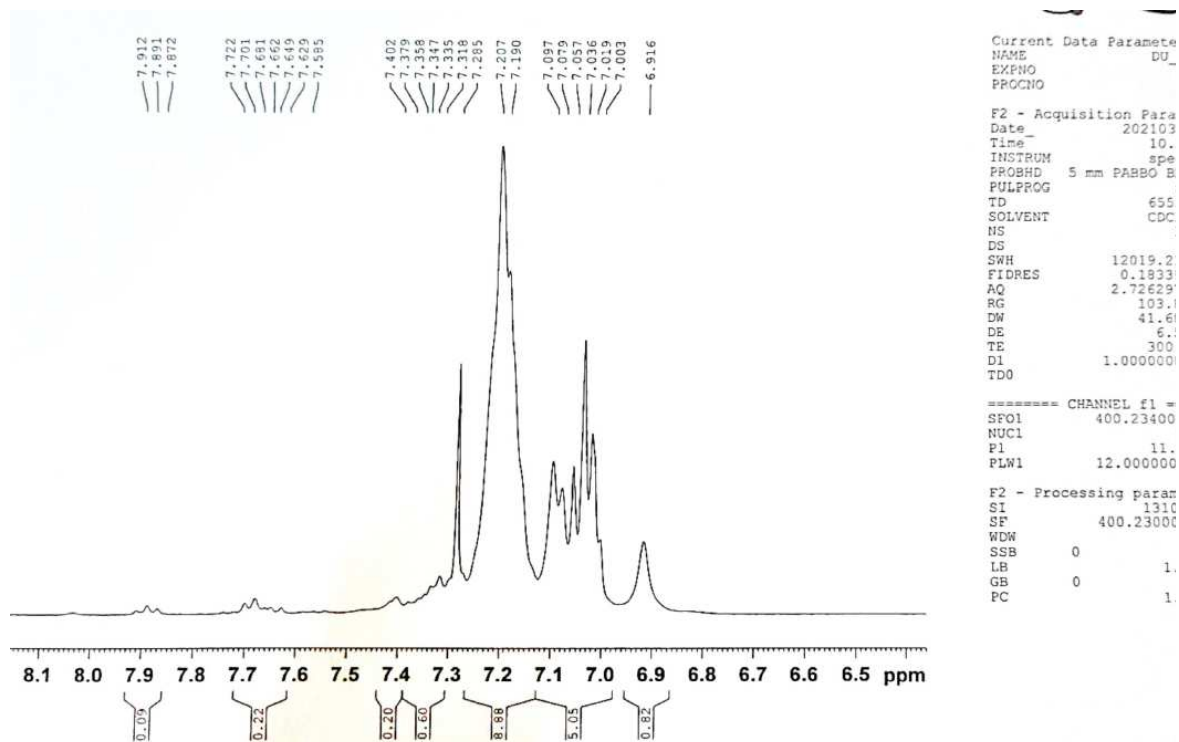
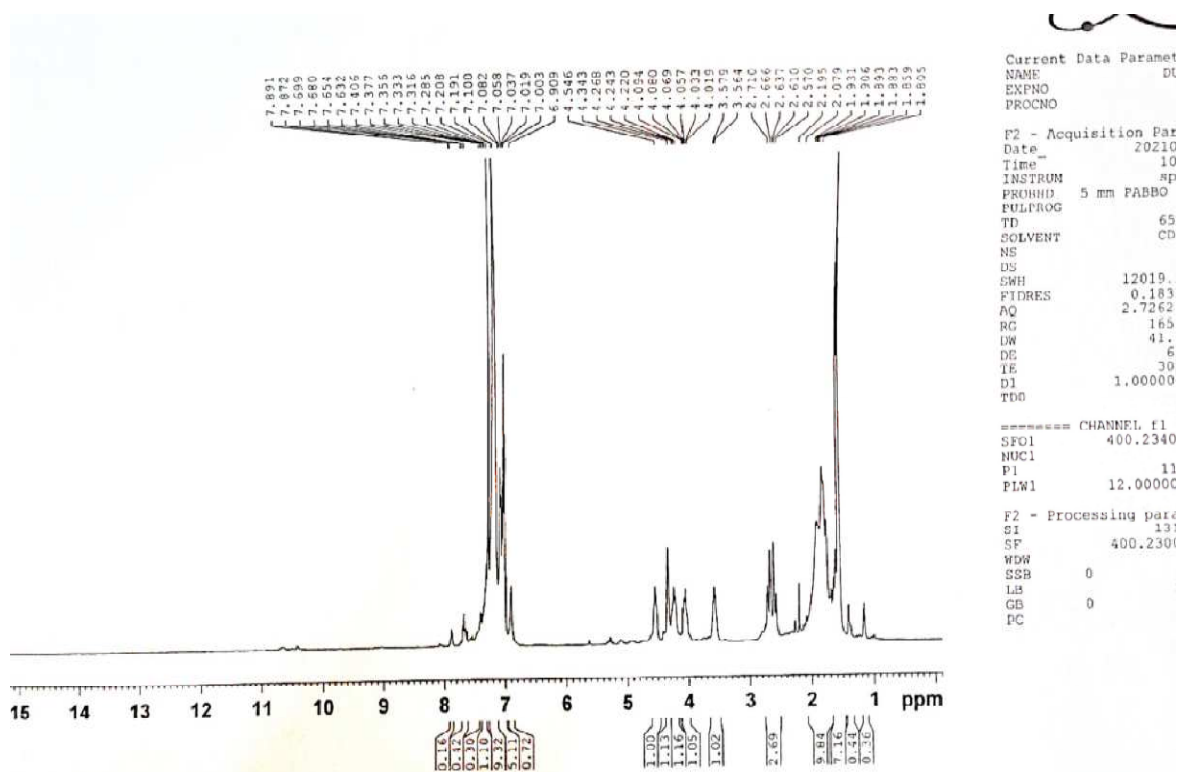
(1) ^1H NMR spectrum of atorvastatin calcium.



(2) ^1H NMR spectrum of atorvastatin calcium.

(3) ^1H NMR spectrum of atorvastatin calcium.(4) ^1H NMR spectrum of new metal complex Fe-atorvastatin.

(5) ^1H NMR spectrum of new metal complex Fe-atorvastatin.(6) ^1H NMR spectrum of new metal complex Fe-atorvastatin.

(9) ^1H NMR spectrum of new metal complex Cu-atorvastatin.(10) ^1H NMR spectrum of new metal complex Zn-atorvastatin.

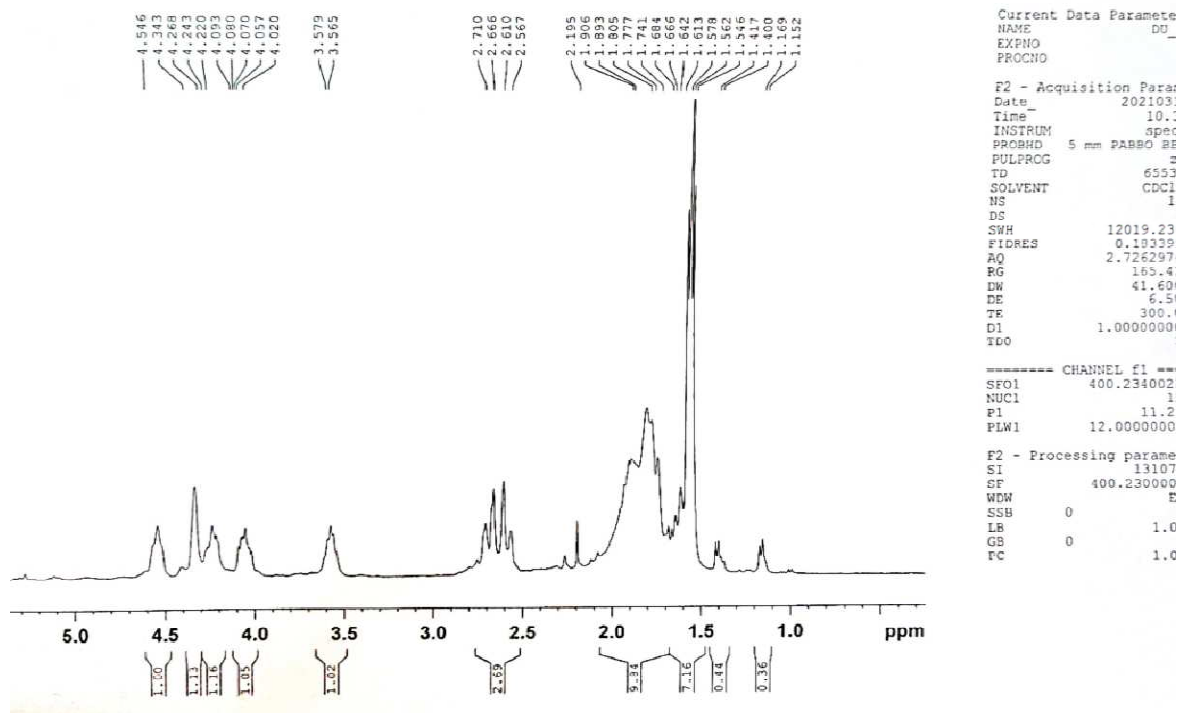
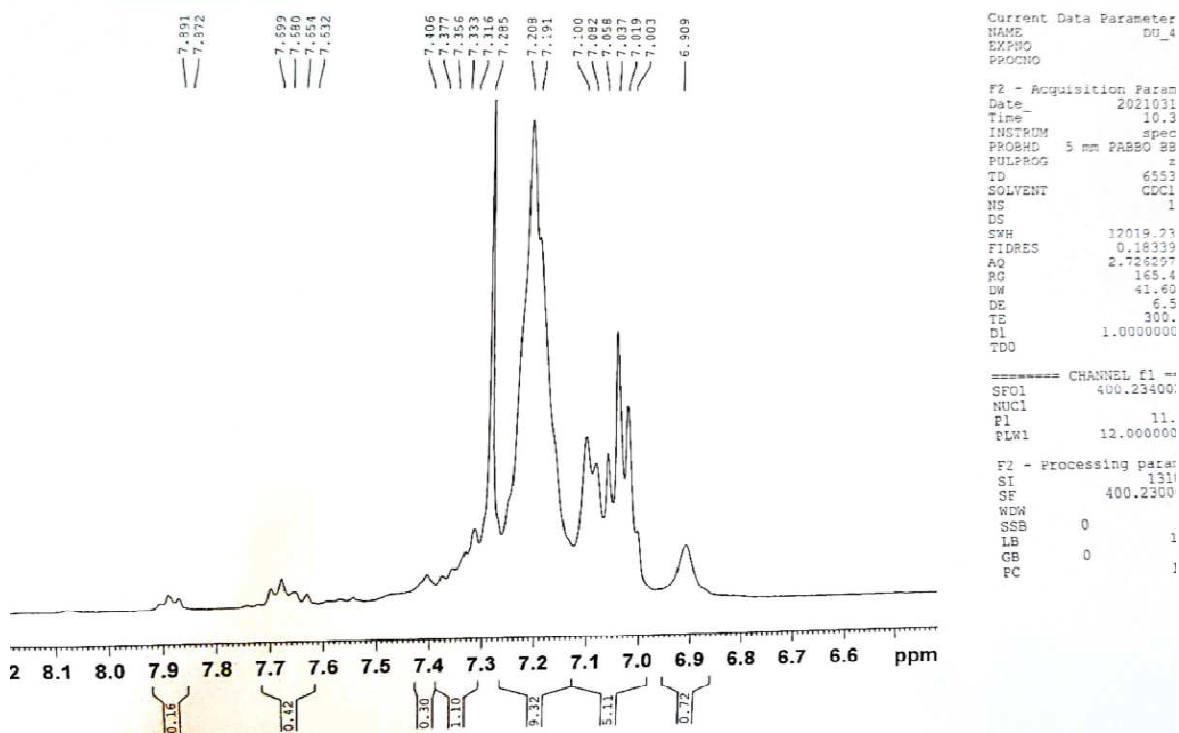
(11) ^1H NMR spectrum of new metal complex Zn-atorvastatin.(12) ^1H NMR spectrum of new metal complex Zn-atorvastatin.

Figure 3.60. ^1H NMR spectra: (1-3) atorvastatin calcium, (4-6) Fe-atorvastatin, (7-9) Cu-atorvastatin and (10-12) Zn-atorvastatin.

CHAPTER FOUR

CONCLUSION

CHAPTER FOUR

CONCLUSION

Drug-drug and drug-metal interactions of some selected antidiabetics, antihypertensives and lipid lowering drugs were carried out, and *in vivo* pharmacological effects of the formed complexes were studied. Diverse types of *in vitro* physicochemical properties were also investigated for the selected drugs while interacting with each other and with some metal ions like chromium(III), lead(II), zinc(II), iron(II) and copper(II).

The co-evaporated dispersion method was used for the synthesis of both drug-drug and drug-metal complexes. Three complexes by interacting between antidiabetic and antihypertensive drugs were formed as olmesartan-metformin (OM), olmesartan-dapagliflozin (OD) and olmesartan-vildagliptin (OV). Three complexes as perindopril-vildagliptin (PV), perindopril-rosuvastatin (PR) and rosuvastatin-vildagliptin (RV) were also formed as part of drug-drug interactions. In addition eleven drug-metal complexes were synthesized viz., Cr- metformin, Cr-glimepiride, Cr-vildagliptin, Cr-dapagliflozin, Pb-metformin, Pb-glimepiride, Pb-vildagliptin, Pb-dapagliflozin, Zn-atorvastatin, Cu-atorvastatin and Fe-atorvastatin.

To characterize the complexation different analytical techniques like melting point determination, TLC, HPLC, DSC, TGA, FT-IR and ^1H NMR were performed. The melting points, DSC and TGA analyses demonstrated the thermal stability as well as thermochemical properties of the synthesized complexes. For NMR spectra no attempt was taken for in-depth analysis of the spectral data. Careful analysis of the ^1H NMR spectra exhibited the differences between the spectra of the parent drugs and synthesized complexes. This was further supported by TLC, TGA, DSC and FT-IR analyses. Melting points were found to be 221-225 °C, 80-85 °C, 150-154 °C, 175-180 °C, 126-130 °C, 156-160 °C and 163-167 °C for metformin, dapagliflozin, vildagliptin, olmesartan medoxomil, perindopril, rosuvastatin and atorvastatin, respectively. The synthesized complexes exhibited melting points at 68-72 °C, 80-85 °C, 100-105 °C, 55-60 °C, 110-115 °C, 115-118 °C, 102-107.6 °C, 106.5-111 °C and 105.6-110 °C for OM, OD, OV, PR, RV, PV, Zn-atorvastatin, Cu-atorvastatin and Fe-atorvastatin, respectively which were also different from the precursor drugs and the complexes. The DSC thermograms of metformin, dapagliflozin, vildagliptin, olmesartan medoxomil, OD, OV, OM, Cr-metformin, Cr-glimepiride, Cr-vildagliptin, Cr-dapagliflozin, Pb-metformin, Pb-glimepiride, Pb-vildagliptin and Pb-dapagliflozin revealed the melting endotherms which were found to be different from each other. The R_t of HPLC

chromatograms were found to not be identical of some parent drugs and drug complexes in the same analytical conditions. The thermodynamic parameters of the interactions of BSA (bovine serum albumin) with these pure drugs and synthesized complexes were observed using fluorescence quenching method.

The drug protein interaction study was also performed using fluorescence spectrophotometry for dapagliflozin, vildagliptin and metformin, and their new complexes with olmesartan medoxomil. The interaction mechanism of these drugs and drug-complexes with BSA were possibly by dynamic quenches as the values of K_{sv} were increased by increasing temperature. The thermodynamic factors were determined from the linear plot of van't Hoff and the results indicated the spontaneous (negative value of ΔG) interaction where hydrophobic interaction was the major contributing force (positive values of ΔH and ΔS) except for olmesartan. It was found that $\Delta H < 0 < \Delta S$ for olmesartan which indicated that the interaction between the drug and BSA was electrostatic force driven. It was also analyzed the binding constants and number of binding sites and found that one mole of the reactant (drug) or complex interacted with one mole of BSA.

The *in vivo* assessment of antidiabetic activity suggested that among the three synthesized complexes namely OD, OV and OM, only OM demonstrated synergistic effect as the complex reduced the blood sugar level more than the metformin alone did. The complex OM, OD and OV reduced the blood sugar by 42.95%, 50.50% and 48.66%, respectively while metformin, dapagliflozin and vildagliptin reduced the blood sugar by 39.70%, 56.73% and 51.22%, respectively. Other complexes OD and OV did not produce better effects as they reduced the blood sugar not more than the parent drugs dapagliflozin and vildagliptin, respectively. From the histopathological studies it was revealed that OM did no damage to the hepatic and nephrotic tissues but OD and OV produced moderate to severe dysplasia in kidney and liver tissues after 14 days of treatment. After 14 days of drug treatment the mice blood was also investigated for determining the levels of serum creatinine and uric acid. OD, OV and OM all three complexes elevated the levels of serum creatinine and uric acid than that of metformin, dapagliflozin and vildagliptin alone. Serum SGPT and SGOT were also determined, which revealed that OV elevated the serum SGPT and SGOT levels but OM reduced the serum SGPT and SGOT levels than that produced by metformin treatment. After observing all the experimental data, the complex OM can be demonstrated as safe and promising and it is suggested for further extensive studies to determine its safety and efficacy as a therapeutic agent.

To demonstrate the complexation among antidiabetic drug vildagliptin, antihypertensive drug perindopril erbumine and lipid lowering drug rosuvastatin, diverse analytical techniques like melting point determination, TLC, TGA and FT-IR analyses were performed. TLC and FT-IR experiments suggested that rosuvastatin, perindopril and vildagliptin formed complexes with each other. The measured melting point and TGA analyses revealed the thermal stability of the synthesized complexes. The drug protein interaction was done with fluorescence spectrophotometry and found that the interactions were probably a dynamic quenching mechanism for the perindopril, vildagliptin, the complex PV and PR with BSA, but the rosuvastatin-BSA and RV-BSA system was developed by static quenching mechanism. Thermodynamic parameters were also measured to conclude that perindopril, vildagliptin, PR, PV interactions with BSA was mediated by enthalpy driven hydrophobic interaction (negative ΔG value). But for rosuvastatin-BSA and RV-BSA system interactions were driven by vander Waal's forces and H-bonds as ΔH value was found negative along with $\Delta S < 0$. It was also analyzed to determine the binding constants and number of binding sites and found that one mole of the reactant (drug) or complex interacted with one mole of BSA.

The *in vivo* analysis for lipid lowering activity of the synthesized complexes was performed in rabbits. The results revealed that all three synthesized complexes designated by complex PR, PV and RV reduced cholesterol, triglycerides, low density lipoprotein (LDL) cholesterol, very low-density lipoprotein (VLDL) cholesterol, non-high-density lipoprotein (HDL) cholesterol levels but enhanced the high-density lipoprotein (HDL) cholesterol level. In support of lipid lowering activity of the complexes PR, PV and RV, the antioxidant, thrombolytic and membrane stabilizing activities were also evaluated *in vitro*. These complexes showed better thrombolytic activity than the standard lipid lowering drug rosuvastatin. The synthesized complexes PR, PV and RV displayed better antioxidant activity than the active drug rosuvastatin. They also revealed significant membrane stabilizing activity. Therefore, three synthesized complexes PR, PV and RV are good candidate as lipid lowering drugs as they are better in reducing blood lipid level as well as they displayed good antioxidant than rosuvastatin.

Transition metal chromium(III) was reacted with four antidiabetic drugs viz. metformin, glimepiride, vildagliptin and dapagliflozin at high temperature. The synthesized complexes viz. Cr-metformin, Cr-glimepiride, Cr-vildagliptin and Cr-dapagliflozin were characterized by assessing the thermochemical behaviors like DSC, TGA and chromatographic properties like TLC, ^1H NMR and FT-IR spectroscopy. The *in vivo*

study was performed using mice model to evaluate the antidiabetic activity. Among the four Cr-drug complexes, Cr-dapagliflozin reduced blood glucose level significantly and it was found to be 64.20% more effective than standard dapagliflozin. The experimental result was followed by Cr-glimepiride (26.72% reduction), Cr-metformin (23.35% blood glucose reduction) and Cr-vildagliptin (7.61% blood glucose reduction) than standard glimepiride, metformin and vildagliptin, respectively. Histopathological studies revealed that Cr-vildagliptin and Cr-dapagliflozin showed moderate dysplasia in hepatic tissues after 14 days of treatment. Though the Cr-antidiabetic drugs complexes exhibited better hypoglycemic activity, whether Cr-complexes have long-term health benefits or not are still unknown as extensive toxicological data could not be established yet.

Heavy metal lead(II) was reacted with four anti-diabetic drugs viz. metformin, glimepiride, vildagliptin and dapagliflozin at 70-75 °C to produce four complexes. They were characterized by assessing their physicochemical behaviors using DSC, TGA, TLC and FT-IR spectrophotometry. To evaluate the antidiabetic activity *in vivo* mice model was used. The pure antidiabetic drugs and Pb-drug complexes called Pb-metformin, Pb-glimepiride, Pb-vildagliptin and Pb-dapagliflozin were administered to alloxan induced diabetic mice for 14 days. It was found that after the 14 days of experimental period the pure drugs significantly reduced the blood glucose level (average glucose levels of mice decreased from 31.54 to 19.02, 30.24 to 17.20, 31.50 to 19.70 and 30.37 to 17.60 mmol/L, respectively for metformin, glimepiride, vildagliptin and dapagliflozin) as compared to control mice which received only distilled water and normal food. But Pb-drug complexes did not show significant positive effect to reduce blood glucose level (blood sugar measured were found as 25.82, 29.23, 25.32 and 29.32 mmol/L, respectively for Pb-metformin, Pb-glimepiride, Pb-vildagliptin and Pb-dapagliflozin) after 14 days of treatment. Moreover, the Pb-complexes increased the levels of serum creatinine and serum uric acid of mice, and necrotized the hepatic and nephrotic tissues which suggested cellular damage in liver and kidneys of the experimental mice. Therefore, it can be concluded that lead is toxic as it produced oxidative stress and reduced insulin secretion.

Three new complexes of lipid lowering drug atorvastatin with three divalent metals e.g. Fe-atorvastatin, Cu-atorvastatin and Zn-atorvastatin complexes were synthesized by co-evaporation process. Then the complexes were investigated and characterized by different R_f values from TLC, melting point analyses, new peak patterns of FT-IR and ^1H NMR spectral analyses.

From the above scenario of the drug-drug and drug-metal interactions of some selected antidiabetics, antihypertensives and lipid lowering drugs it was explored that the drug-drug and drug-metal interactions are important topics of research in drug discovery and may introduce new molecules having new and/or more potent therapeutic properties.

CHAPTER FIVE

REFERENCES

REFERENCES

- Adekunle, F.A., Woods, J.A.O., Onawumi, O.O.E., Odunola, O.A. 2010. Synthesis and characterization of nickel(II) complexes of various substituted acid hydrazides. *Asian. J. Chem.* **22**, 5543–50.
- Afridi, H.I., Kazi, T.G., Kazi, N., Jamali, M.K., Arain, M.B., Jalbani, N., Baig, J.A. and Sarfraz, R.A. 2008. Evaluation of status of toxic metals in biological samples of diabetes mellitus patients. *Diabetes Res. Clin. Pract.* **80**, 280–288.
- Agrawal, Y.K., Gogoi, P.J., Manna, K., Bhatt, H.G. and Jain, V.K. 2010. A supercritical fluid chromatography/tandem mass spectrometry method for the simultaneous quantification of metformin and gliclazide in human plasma. *Indian J. Pharm. Sci.* **72**, 50-57.
- Ahren, B. 2008. Emerging dipeptidyl peptidase-4 inhibitors for the treatment of diabetes. *Expert. Opin. Emerg. Drugs* **13**, 593-607.
- Ahren, B. 2011. Are sulfonylureas less desirable than DPP-4 inhibitors as add-on to metformin in the treatment of type 2 diabetes? *Curr. Diab. Rep.* **11**, 83-90.
- Aktar, F., Sultan, Z. and Rashid, M. A. 2019. *In vitro* complexation of olmesartan medoxomil with dapagliflozin, vildagliptin and metformin. *Dhaka Univ. J. Pharm. Sci.* **18**, 271-180.
- Allain, C.C., Poon, L.S., Chan, C.S., Richmond, W. and Fu, P.C. 1974. Enzymatic determination of total serum cholesterol. *Clin. Chem.* **20**, 470-475.
- Al-Saleh, Y., Sabico, S., Al-Furqani, A., Jayyousi, A., Alromaihi, D., Ba-Essa, E., Alawadi, F., Alkaabi, J., Hassanein, M., Al-Sifri, S., Saleh, S., Alessa, T. and Al-
- Daghri, N.M. 2021. Sulfonylureas in the current practice of Type 2 diabetes management: Are they all the same? Consensus from the Gulf Cooperation Council (GCC) countries advisory board on sulfonylureas. *Diabetes Ther.* **12**, 2115-2132.
- Alves, M.G., Martins, A.D., Vaz, C.V., Correia, S., Moreira, P.I., Oliveira, P.F. and Socorro, S. 2014. Metformin and male reproduction: effects on Sertoli cell metabolism. *Br. J. Pharmacol.* **171**, 1033-1042.
- American Diabetes Association. 2008. Diagnosis and classification of diabetes mellitus. *Diabetes Care* **31** (Suppl 1), S55-60.

Amin, T. U., Islam, R., Sultan, Z., Sultana, S., Islam, S. and Hasnat, A. 2016. Study of interaction of dextromethorphan hydrobromide with deoxyribonucleic acid by fluorescence quenching. *Bangladesh Pharm. J.* **19**, 197-205.

Amit, S.K., Iain, G.R., Scott, O., Christopher, L.S., Ernesto, C., Kirk, R.H., Abdul, E.M., Deepak, K.D., Jae, S.L., Yasuhiro, N., John, P.O.D., Jason, B.7 and Shawn, P.H. 2005. A comprehensive listing of bioactivation pathways of organic functional groups. *Curr. Drug Metab.* **6**, 161-225.

Amundson, D.M. and Zhou, M. 1999. Fluorometric method for the enzymatic determination of cholesterol. *J. Biochem. Biophys. Meth.*, **38**, 43-52.

Anderson, R. 1981. Nutritional role of chromium. *Sci. Total Environ.* **17**, 13-29.

Anderson, R.A. 1993. Recent advances in the clinical and biochemical effects of chromium deficiency. WileyLiss, New York, pp. 221-234.

Anderson, R.A. 1995. Chromium and parenteral nutrition. *Nutr.* **11**, 83-86.

Anderson, R.A. 1995. Chromium, glucose tolerance, diabetes and lipid metabolism. *J. Adv. Med.* **8**, 37-49.

Anderson, R.A. 1998. Chromium, glucose intolerance and diabetes. *J. Am. Coll. Nutr.* **17**, 548-555.

Anderson, R.A. 2000. Chromium in the prevention and control of diabetes. *Diabetes Metab.* **26**, 22-27.

Anderson, R.A., Cheng, N., Bryden, N.A., Polansky, M.M., Chi, J. and Feng, J. 1997. Beneficial effects of chromium for people with diabetes. *Diabetes* **46**, 1786-1791.

Anderson, R.A., Polansky, M.M., Bryden, N.A. and Canary, J. 1991. Supplemental-chromium effects on glucose, insulin, glucagon, and urinary chromium losses in subjects consuming controlled low-chromium diets. *Am. J. Clin. Nutr.* **54**, 909-916.

Anderson, R.A., Polansky, M.M., Bryden, N.A., Bhathena, S.J. and Canary, J. 1987. Effects of supplemental chromium on patients with symptoms of reactive hypoglycemia. *Metab.* **36**, 351-355.

Arad, Y., Ramakrishnan, R. and Ginsberg, H.N. 1992. Effects of lovastatin therapy on very-low-density lipoprotein triglyceride metabolism in subjects with combined hyperlipidemia: evidence for reduced assembly and secretion of triglyceride-rich lipoproteins. *Metab.* **41**, 487-493.

- Arredondo, M. and Unez, M.T.N. 2005. Iron and copper metabolism. *Mol. Aspects Med.* **26**, 313-327.
- Arsman, G., Jabs, H.U., Kuhnert, U., Nolte, W. and Schriewer, H. 1984. LDL-cholesterol, polyvinyl sulphate method. *Clin. Chim. Acta.* **140**, 77.
- Asadullah, M.M., Ekwai, S.A., Imran, D.Z. Hussain, N.M., Ranjha, M.I., Khan, M.A., Muhammad, A.M. and Hassam, Z. 2014. FTIR drug-polymer interactions studies of perindopril erbumine. *J. Chem. Soc. Pak.* **36**, 1064-1070.
- AstraZeneca Pharmaceuticals LP. Crestor (rosuvastatin calcium) prescribing information. 2020. <https://www.astrazeneca.ca/content/dam/az-ca/downloads/productinformation/crestor-product-monograph-en.pdf> (Access on July, 2020).
- ATSDR (Agency for toxic substances and disease registry), Case Studies in Environmental Medicine (CSEM) chromium toxicity course: WB 1466 Original; 2011. <https://www.atsdr.cdc.gov/csem/chromium/docs/chromium.pdf> (Access on January, 2020).
- Bailey, C.J. 1992. Biguanides and NIDDM. *Diabetes Care* **15**, 755-772.
- Balamurugan, K. and Schaffner, W. 2006. Copper homeostasis in eukaryotes: teetering on a tightrope. *Biochim. Biophys. Acta* **1763**, 737-746.
- Barham, D. and Trinder, P. 1972. An improved colour reagent for the determination of blood glucose by the oxidase system. *Analyst.* **97**, 142-145.
- Barry, N. P. E. and Sadler, P. J. 2013. Exploration of the medical periodic table: towards new targets. *Chem. Commun.* **49**, 5106-5131.
- Bellary, S. 2011. For Type 2 diabetes poorly controlled by metformin monotherapy, the addition of any non-insulin antidiabetic drug reduces HbA1c to a similar extent, but with differing effects on weight and hypoglycaemic risk. *Evid. Based Med.* **16**, 39-40.
- Bener, A., Obineche, E., Gillett, M., Pasha, M.A. and Bishawi, B. 2001. Association between blood levels of lead, blood pressure and risk of diabetes and heart disease in workers. *Int. Arch. Occup. Environ. Health* **74**, 375-378.
- Berthon, G. 1995. Handbook of Metal-ligand Interactions in Biological Fluids; Marcel-Dekker Inc.: New York, Vol. 1 and 2.

- Bevilacqua, L., Lorenzon, M.G., Massari, G., Vasselli, M., Angerame, D., Maglione, M., Di Lenarda, R. and Di Lenarda, A. 2019. Gingival overgrowth caused by olmesartan medoxomil: Observational study. *J. Med. Res.* **5**, 180-184.
- Bielicka, A., Bojanowska, I. and Wiśniewski, A. 2005. Two faces of chromium - pollutant and bioelement. *Pol. J. Environ. Stud.* **14**, 5-10.
- Bokara, K.K., Blaylock, I., Denise, S.B., Bettaiya, R., Rajanna, S. and Yallapragada, P.R. 2009. Influence of lead acetate on glutathione and its related enzymes in different regions of rat brain. *J. Appl. Toxicol.* **29**, 452-458.
- Borhade, S. 2011. Synthesis, characterisation and spectrophotometric determination of Fe(II) complex of 2,4-dihydroxybenzaldehyde isonicotinoyl hydrazone {(E)-N0-(2,4-dihydroxybenzylidene) isonicotinohydrazide}, it's application & biological activity. *Der Chemica. Sinica* **2**, 64-71.
- Bousser, M.G. and Ferro, J.M. 2007. Cerebral venous thrombosis: An update. *Lancet Neurol.* **6**, 162-170.
- Braca, A., Tommasi, N.D., Bari, L.D., Pizza, C., Politi, M. and Morelli, I. 2001. Natural anti-oxidants from plant material in phenolic compounds in food and their effects on health. *J. Nat. Prod.* **64**, 892-895.
- Brewer, G.J. 2009. The risks of copper toxicity contributing to cognitive decline in the aging population and to Alzheimer's disease. *J. Am. Coll. Nutr.* **28**, 238-242.
- Brody, T. 2018. FDA's Drug review process and the package label strategies for writing successful FDA Submissions, Academic Press, pp. 255-335.
- Brouwers, M.C., VanGreevenbroek, M.M., Stehouwer, C.D., Graaf, J. and Stalenhoef, A.F. 2012. The genetics of familial combined hyperlipidaemia. *Nat. Rev. Endocrinol.* **8**, 352-362.
- Brown, R.O., Forloines, L.S., Cross, R.E. and Heizer, W.D. 1986. Chromium deficiency after long-term total parenteral nutrition. *Dig. Dis. Sci.* **31**, 661-664.
- Buckett, L.B.P., Davidson, R., Dunkley, C., Martin, L., Stafford, J. and McTaggart, F. 2000. Selectivity of ZD4522 for inhibition of cholesterol synthesis in hepatic versus non-hepatic cells. *Atherosclerosis* **151**, 41-41.
- Bucolo, G. and David, H. 1973. Quantitative determination of serum triglycerides by the use of enzymes. *Clin. Chem.* **19**, 476.

- Burstein, M., Scholnick, H.R. and Morfin, R. 1980. Severe combined hyperlipidemia. *Scand. J. Clin. Lab. Invest.* **40**, 560-572.
- Caterina, P., Antonello, D.P., Chiara, G., Chiara, C., Giacomo, L., Antonio, S., Giovambattista, D.S., and Luca, G. 2013. Drug target protein-protein interaction networks: A systematic perspective. *J. Res. Med. Sci.* **18**, 601-610.
- Cave, M., Appana, S., Patel, M., Falkner, K.C., McClain, C.J. and Brock, G. 2010. Polychlorinated biphenyls, lead, and mercury are associated with liver disease in American adults: NHANES 2003-2004. *Environ. Health Perspect.* **118**, 1735-1742.
- Chen, C.J., Wang, S.L., Chiou, J.M., Tseng, C.H., Chiou, H.Y., Hsueh, Y.M., Chen, S.Y., Wu, M.M. and Lai, M.S. 2007. Arsenic and diabetes and hypertension in human populations: A review. *Toxicol. Appl. Pharmacol.* **222**, 298-304.
- Chen, Y.W., Yang, C.Y., Huang, C.F., Hung, D.Z., Leung, Y.M. and Liu, S.H. 2009. Heavy metals, islet function and diabetes development. *Islets.* **1**, 169-176.
- Clarke, M. J. 1989. Progress in Clinical Biochemistry and Medicine, Berlin, Springer, Verlag, Vol. 10, pp. 25-39.
- Clarke, M. J. and Sadler, P. J. 1999. Metallopharmaceuticals I: DNA Interactions, Springer-Verlag: Berlin. Vol. 1, pp. 199-220.
- Coban, T.A., Senturk, M., Ciftci, M. and Kufrevioglu, O.I. 2007. Effects of some metal ions on human erythrocyte glutathione reductase: An *in vitro* study. *Protein Pept. Lett.* **14**, 1027-1030.
- Colberg, S.R., Sigal, R.J., Fernhall, B., Regensteiner, J.G., Blissmer, B.J., Rubin, R.R., Chasan, T.L., Albright, A. L. and Braun, B. 2010. Exercise and type 2 diabetes the American College of Sports Medicine and the American Diabetes Association: Joint position statement. *Diabetes Care* **33**, e147-e167.
- Crichton, R.R. 2019. Biological Inorganic Chemistry, 3rd ed., Academic Press, Cambridge, MA, USA, Chapter 12, pp. 339-362.
- Crichton, R.R. 2019. Biological Inorganic Chemistry, 3rd ed., Academic Press, Cambridge, MA, USA, Chapter 22, pp. 599-623.
- Crisponi, G., Nurchi, V.M., Fanni, D., Gerosa, C., Nemolato, S. and Faa, G. 2010. Copper-related diseases: From chemistry to molecular pathology. *Coord. Chem. Rev.* **254**, 876-889.

Dams, I., Ostaszewska, A., Puchalska, M., Chmiel, J., Cmoch, P., Bujak, I., Białońska, A. and Szczepek, J.W. 2015. Synthesis and physicochemical characterization of the process-related impurities of olmesartan medoxomil. Do 5(Biphenyl-2-yl)-1-triphenylmethyltetrazole intermediates in sartan syntheses exist? *Molecules* **20**, 21346-21363.

Daniel, K.G., Gupta, P., Harbach, R.H., Guida, W.C. and Dou, Q.P. 2004. Organic copper complexes as a new class of proteasome inhibitors and apoptosis inducers in human cancer cells. *Biochem. Pharmacol.* **67**, 1139-1151.

Davis, C.M. and Vincent, J.B. 1997. Chromium oligopeptide activates insulin receptor kinase activity. *Biochem.* **36**, 4382-4385.

DeFronzo, R.A. 1999. Pharmacologic therapy for Type 2 diabetes mellitus. *Ann. Intern. Med.* **131**, 281-303.

DePalma, R.G., Hayes, V.W., Cafferata, H.T., Hamid, A.M., Bruce, K.C., Leo, R.Z. and Mark, R.H. 2003. Cytokine signatures in atherosclerotic claudicants. *J. Surg. Res.* **111**, 215-221.

Depalma, R.G., Hayes, V.W., Chow, B.K., Shamayeva, G., May, P.E. and Zacharski, L.R. 2010. Ferritin levels, inflammatory biomarkers, and mortality in peripheral arterial disease: a substudy of the iron (Fe) and atherosclerosis study (FeAST) trial. *J. Vasc. Surg.* **51**, 1498-1503.

DePalma, R.G., Hayes, V.W., May, P.E., Cafferata, H.T., Mohammadpour, H.A., Brigg, L.A., Chow, B.K., Shamayeva, G. and Zacharski, L.R. 2006. Statins and biomarkers in claudicants with peripheral vascular disease. *Vascular* **14**, 193-200.

Domecq, J.P., Prutsky, G., Leppin, A., Sonbol, M.B., Altayar, O., Undavalli, C., Wang, Z., Elraiyah, T., Brito, J.P., Mauck, K.F., Lababidi, M.H., Prokop, L.J., Asi, N., Wei, J., Fidahusseini, S., Montori, V.M. and Murad, M.H. 2015. Drugs commonly associated with weight change: a systematic review and meta-analysis. *J. Clin. Endocrinol. Metab.* **100**, 363-370.

Dorr, M. and Meggers, E. 2014. Metal complexes as structural templates for targeting proteins. *Curr. Opin. Chem. Biol.* **19**, 76-81.

Drucker, D.J. 2007. Dipeptidyl peptidase-4 inhibition and the treatment of Type 2 diabetes: preclinical biology and mechanisms of action. *Diabetes Care* **30**, 1335-1343.

Dubois, F. and Belleville, F. 1991. Chromium: physiologic role and implications in human pathology. *Pathol. Biol.* **39**, 801-808.

Dunne, L.J. and Kirschmann J.D. 1990. Nutrition Almanac. 3rd Ed, Mc-Graw-Hill, New York, pp. 70-71.

Dyson, P.J. and Sava, G. 2006. Metal-based antitumour drugs in the post genomic era. *Dalton Trans.* **2006**, 1929-1933.

Dzau V.J., Antman, E.M., Black, H.R., Hayes, D.L., Manson, J.E., Plutzky, J., Jeffrey J., Popma, J.J. and Stevenson, W. 2006. The cardiovascular disease continuum validated: Clinical evidence of improved patient outcomes: Part I: Pathophysiology and clinical trial evidence (risk factors through stable coronary artery disease). *Circulation* **114**, 2850-2870.

Ercal, N., Gurer, O.H. and Aykin, B.N. 2001. Toxic metals and oxidative stress part I: Mechanisms involved in metal-induced oxidative damage. *Curr. Top. Med. Chem.* **1**, 529-539.

Evans, G.W. 1989. The effect of chromium picolinate on insulin controlled parameters in humans. *Int. J. Biosoc. Med. Res.* **11**, 163-180.

Fang, J. and Alderman, M.H. 2000. Serum uric acid and cardiovascular mortality the NHANES I epidemiologic follow-up study, 1971-1992. National Health and Nutrition Examination Survey. *JAMA* **283**, 2404-2410.

Farrell, N. 1989. Transition metal complexes as drugs and chemotherapeutic agents, Kluwer Academic Publishers, London, pp. 1-30.

Farrell, N. 1999. The uses of inorganic chemistry in medicine, the Royal Society of Chemistry: Cambridge, UK.

Ferrari, R., Pasanisi, G., Notarstefano, P., Campo, G., Gardini, E. and Ceconi, C. 2005. Specific properties and effect of perindopril in controlling the rennin-angiotensin system. *Am. J. Hypertens.* **18**, 142S-154S.

Ferro, A., Gilbert, R. and Krum, H. 2006. Importance of renin in blood pressure regulation and therapeutic potential of renin inhibition. *Intern. J. Clin. Prac.* **60**, 577-581.

Finney, L.A. and O'Halloran, T.V. 2003. Transition metal speciation in the cell: Insights from the chemistry of metal ion receptors. *Science* **300**, 931-936.

- Fossati, P., Prencipe, L. and Berti, G. 1980. Use of 3,5-dichloro-2-hydroxy benzene sulfonic acid/4-aminophenazone chromogenic system in direct enzymic assay of uric acid in serum and urine. *Clin. Chem.* **26**, 227-231.
- Fossati, R. and Prencipe, L. 1982. Serum triglycerides determined colorimetrically with an enzyme that produces hydrogen peroxide. *Clin. Chem.* **28**, 2077-2079.
- Fraiji, L.K., Hayes, D.M. and Werner, T.C. 1992. Static and dynamic fluorescence quenching experiments for the physical chemistry laboratory. *J. Chem. Edu.* **69**, 424-428.
- Franvis, C.W. 2005. Direct thrombin inhibitors for treatment of heparin induced thrombocytopenia, deep vein thrombosis and atrial fibrillation. *Curr. Pharm. Des.* **11**, 3931-3941.
- Freund, H., Atamian, S. and Fischer, J.E. 1979. Chromium deficiency during total parenteral nutrition. *JAMA* **241**, 496-498.
- Fricke, S.P. 1994. Metal Complexes in Cancer Therapy. Chapman and Hall: London, Vol. 1, pp. 215-217.
- Fridlyand, L. and Philipson, L. 2006. Reactive species and early manifestation of insulin resistance in type 2 diabetes. *Diabetes Obes. Metab.* **9**, 136-145.
- Ginghina, C., Bejan, I. and Ceck, C.D. 2011. Modern risk stratification in coronary heart disease. *J. Med. Life.* **4**, 377-386.
- Grossman, E., and Messerli, F.H. 2008. Hypertension and diabetes. *Adv. Cardiol.* **45**, 82-106.
- Grundy, S.M. 1984. Pathogenesis of hyperlipoproteinemia. *J. Lipid Res.* **25**, 1611-1618.
- Guariguata, L., Whiting, D.R, Hambleton, I., Beagley, J., Linnenkamp, U. and Shaw, J.E. 2014. Global estimates of diabetes prevalence for 2013 and projections for 2035. *Diabetes Res. Clin. Pract.* **103**, 137-149.
- Guo, Z. and Sadler, P. J. 1999. Metals in medicine. *Angew Chem. Int. Ed. Engl.* **38**, 1512-1531.
- Haas, K.L. and Franz, K.J. 2009. Application of metal coordination chemistry to explore and manipulate cell biology. *Chem. Rev.* **109**, 4921-4960.

- Habib, S.I., Baseer, M.A. and Kulkarni, P.A. 2011. Synthesis and antimicrobial activity of cobalt(II), nickel(II), and copper(II) complexes of some 20-hydroxychalcones. *Der Chemica. Sinica* **2**, 27-32.
- Hambley, T.W. 2007. Developing new metal-based therapeutics: Challenges and opportunities. *Dalton Trans.* **2007**, 4929-4937.
- Harrison, T.R., Petersdorf, R.G., Braunwald, E. and Martin, J.B. 1994. Harrison's Principles of Internal Medicine, 13th edition, McGraw-Hill, New York, pp. 444-445.
- Hayden, M.R. and Tyagi, S.C. 2004. Uric acid: A new look at an old risk marker for cardiovascular disease, metabolic syndrome, and Type 2 diabetes mellitus: The urate redox shuttle. *Nutr. Metab.* **1**, 10-10.
- Heinegaard, D. and Tindstrom, G. 1973. Determination of serum creatinine by a direct colorimetric method. *Clin. Chim. Acta* **43**, 305-310.
- Herrington, W., Lacey, B., Sherliker, P., Armitage, J. and Lewington, S. 2016. Epidemiology of atherosclerosis and the potential to reduce the global burden of atherothrombotic disease. *Circ. Res.* **118**, 535- 546.
- Hines, L.E. and Murphy, J.E. 2011. Potentially harmful drug-drug interactions in the elderly: A review. *Am. J. Geriatr. Pharmacother.* **9**, 364-377.
- Howard, J.K. 1974. Human erythrocyte glutathione reductase and glucose6-phosphatedehydrogenase activities in normal subjects and in persons exposed to lead. *Clin. Sci. Mol. Med.* **47**, 515-520.
- Hu, Y.J., Yang, Y.O., Dai, C.M., Xiao, Y.L. and Xiao, H. 2010. Binding of berberine to bovine serum albumin: Spectroscopic approach. *Mol. Biol. Rep.* **37**, 3827-3832.
- Hunaiti, A.A. and Soud, M. 2000. Effect of lead concentration on the level of glutathione, glutathione S-transferase, reductase and peroxidase in human blood. *Sci. Total Environ.* **248**, 45-50.
- Ikeda, T., Iwata, K. and Murakami, H. 2000. Inhibitory effect of metformin on intestinal glucose absorption in the perfused rat intestine. *Biochem. Pharmacol.* **59**, 887-890.
- Inzucchi, S.E., Bergenstal, R.M., Buse, J.B., Diamant, M., Ferrannini, E., Nauck, M., Peters, A.L., Tsapas, A., Wender, R. and Matthews, D.R. 2012. Management of hyperglycemia in type 2 diabetes: a patient-centered approach: position statement of the

American Diabetes Association (ADA) and the European Association for the Study of Diabetes (EASD). *Diabetes Care* **35**, 1364-1379.

Istvan, E.S. and Deisenhofer, J. 2001. Structural mechanism for statin inhibition of HMG-CoA reductase. *Science* **11**, 1160-1164.

Jeejeebhoy, K.N., Chu, R.C., Marliss, E.B., Greenberg, G.R. and Bruce, R.A. 1977. Chromium deficiency, glucose intolerance, and neuropathy reversed by chromium supplementation in a patient receiving long-term total parenteral nutrition. *Am. J. Clin. Nutr.* **30**, 531-538.

Jeyabalan, S. and Palayan, M. 2009. Antihyperlipidemic activity of *Sapindus emarginatus* in Triton WR-1339 induced albino rats. *Res. J. Pharm. Tech.* **2**, 319-323.

Johnstone, T.C., Suntharalingam, K. and Lippard, S.J. 2016. The next generation of platinum drugs: Targeted Pt(II) agents, nanoparticle delivery, and Pt(IV) prodrugs. *Chem. Rev.* **116**, 3436-3486.

Jones, O.A., Maguire, M.L. and Griffin, J.L. 2008. Environmental pollution and diabetes: A neglected association. *Lancet* **371**, 287-288.

Jorgensen, T., Capewell, S., Prescott, E., Allender, S., Sans, S. and Zdrojewski, T. 2013. Population-level changes to promote cardiovascular health. *Eur. J. Prev. Cardiol.* **20**, 409-421.

Joshu, C.E., Boehmer, T.K., Brownson, R.C. and Ewing, R. 2008. Personal, neighbourhood and urban factors associated with obesity in the United States. *J. Epidemiol. Commun. Health.* **62**, 202-208.

Jovanovic, P.L., Gutierrez, M. and Peterson, C.M. 1995. Chromium supplementation for gestational diabetic women (GDM) improves glucose tolerance and decreases hyperinsulinemia. *J. Am. Coll. Nutr.* **14**, 530-530.

Kahn, C.R. 1985. Current concepts of the molecular mechanism of insulin action. *Ann. Rev. Med.* **36**, 429-451.

Kahn, C.R. 1985. Current concepts of the molecular mechanism of insulin action. *Ann. Rev. Med.* **36**, 429-451.

Kanai, F., Ito, K., Todaka, M., Hayashi, O., Kamohara, S., Ishii, K., Okada, T., Kakakie, O., Ui, M. and Ebina, Y. 1993. Insulin-stimulated GLUT 4 translocation is relevant to the

phosphorylation of IRS 1 and the activity of PI3-kinase. *Biochem. Biophys. Res. Comm.* **195**, 762-768.

Kawsar, M.H., Sikder, M.A.A., Rana, M.S., Nimmi, I. and Rashid, M.A. 2011. Studies of thrombolytic, antioxidant and cytotoxic properties of two asteraceous plants of Bangladesh. *Bangladesh Phar. J.* **14**, 103-106.

Kelland, L. 2007. The resurgence of platinum-based cancer chemotherapy. *Nat. Rev. Cancer* **7**, 573-584.

Keppler, B. 1993. Metal complexes in cancer chemotherapy; VCH: Basel, pp. DM 196.

Knowles, S.O. and Donaldson, W.E. 1990. Dietary modification of lead toxicity: Effects on fatty acid and eicosanoid metabolism in chicks. *Comp. Biochem. Physiol. C Comp. Pharmacol. Toxicol.* **95**, 99-104.

Kolachi, N.F., Kazi, T.G., Afridi, H.I., Kazi, N., Khan, S., Kandhro, G.A., Shah, A.Q., Baig, J.A., Wadhwa, S.K., Shah, F., Jamali, M.K. and Arain, M.B. 2011. Status of toxic metals in biological samples of diabetic mothers and their neonates. *Biol. Trace Elem. Res.* **143**, 196-212.

Kostova, I. and Momekov, G. 2006. New zirconium (IV) complexes of coumarins with cytotoxic activity. *Eur. J. Med. Chem.* **41**, 717-726.

Krum, H. and Gilbert, R. 2007. Novel therapies blocking the renin-angiotensin aldosterone system in the management of hypertension and related disorders. *J. Hypertens.* **25**, 25-35.

Kumar, D., Parcha, V., Maithani, A. and Dhulia, I. 2012. Effect and evaluation of antihyperlipidemic activity guided isolated fraction from total methanol extract of *Bauhinia variegata* (Linn.) in Triton WR-1339 induced hyperlipidemic rats. *Asian Pac. J. Trop. Dis.* **2**, 909-913.

Kundu, S.P., Amjad, F.M., Sultana, S. and Sultan, M.Z. 2012. Study of differential scanning calorimetry of complex of magnesium sulfate with aspirin, paracetamol and naproxen. *Bangladesh Phar. J.* **15**, 7-12.

Lakowicz, J.R. 1999. Principles of fluorescence spectroscopy, 2nd ed. Springer, Kluwer Academic, New York.

Lakowicz, J.R. 2006. Principles of fluorescence spectroscopy, 3rd ed., Springer, New York.

- Lang, J. 1999. Molecular mechanisms and regulation of insulin exocytosis as a paradigm of endocrine secretion. *Eur. J. Biochem.* **259**, 3-17.
- Larsen, K. 1972. Creatinine assay by a reaction-kinetic principle. *Clin. Chim. Acta* **41**, 209-217.
- Lawton, L.J. and Donaldson, W.E. 1991. Lead-induced tissue fatty acid alterations and lipid peroxidation. *Biol. Trace Elem. Res.* **28**, 83-97.
- Linder, M.C. 1991. Nutritional biochemistry and metabolism with clinical application, 2nd Ed., Prentice-Hall Int., pp. 215-276.
- Lucas, C., Byles, J. and Martin, J.H. 2016. Medicines optimisation in older people: Taking age and sex into account. *Maturitas* **93**, 114-120.
- MacDonald, P.E., Joseph, J.W. and Rorsman, P. 2005. Glucose-sensing mechanisms in pancreatic beta-cells. *Philos. Trans. R. Soc. Lond. B. Biol. Sci.* **360**, 2211-2225.
- Makrilakis, K. 2019. The role of DPP-4 inhibitors in the treatment algorithm of Type 2 diabetes mellitus: When to select, what to expect. *Int. J. Environ. Res. Public Health* **16**, 2720.
- Mandrup, P.T., Pickersgill, L. and Donath, M.Y. 2010. Blockade of interleukin 1 in Type 1 diabetes mellitus. *Nat. Rev. Endocrinol.* **6**, 158-166.
- Mather, A. and Pollock, C. 2011. Glucose handling by the kidney. *Kidney Int.* **79**, S1-S6.
- Mathieu, C. 2009. The scientific evidence: Vildagliptin and the benefits of islet enhancement. *Diabet. Obes. Metab.* **11**(Suppl. 2), 9-17.
- Matovic, V., Buha, A., Dukic, C.D. and Bulat, Z. 2015. Insight into the oxidative stress induced by lead and/or cadmium in blood, liver and kidneys. *Food Chem. Toxicol.* **78**, 130-140.
- McCarthy, M.I. 2010. Genomics, Type 2 diabetes, and obesity. *New Eng. J. Med.* **363**, 2339-2350.
- McTaggart, F. 2003. Comparative pharmacology of rosuvastatin. *Atherosclerosis* **4**, 9-14.
- Meggers, E. 2007. Exploring biologically relevant chemical space with metal complexes. *Curr. Opin. Chem. Biol.* **11**, 287-292.

- Mertz, W. 1993. Chromium in human nutrition: A review. *J. Nutr.* **123**, 626-633.
- Mertz, W., Abernathy, C.O. and Olin, S.S. 1994. Risk assessment of essential elements, ILSI Press, Washington DC, pp. 19-38.
- Mire, D.E., Silfani, T.N. and Pugsley, M.K. 2005. A Review of the structure and functional features of olmesartan medoxomil, an angiotensin receptor blocker. *J. Cardiovasc.Pharmacol.* **46**, 585-593.
- Mishra, P.R., Panda, P.K., Apanna, K.C. and Panigrahi, S. 2011. Evaluation of acute hypolipidemic activity of different plant extracts in Triton WR-1339 induced hyperlipidemia in albino rats. *Pharmacologyonline* **3**, 925-934.
- Mitra, S.K., Sundaram, R., Venkataranganna, M.V. and Gopumadhavan, S. 1999. Pharmacokinetic interaction of diabecon (D-400) with rifampicin and nifedipine. *Eur. J. Drug Metab. Pharmacokinet.* **24**, 79-82.
- Mjos, K.D. and Orvig, C. 2014. Metallo drugs in medicinal inorganic chemistry. *Chem. Rev.* **114**, 4540-4563.
- Moon, S.S. 2013. Association of lead, mercury and cadmium with diabetes in the Korean population: The Korea National Health and Nutrition Examination Survey (KNHANES) 2009-2010. *Diabet. Med.* **30**, e143–e148.
- Mostafalou, S., Baeri, M., Bahadar, H., Soltany, R.R.M., Gholami, M. and Abdollahi, M. 2015. Molecular mechanisms involved in lead induced disruption of hepatic and pancreatic glucose metabolism. *Environ. Toxicol. Pharmacol.* **39**, 16-26.
- Movahedian, A., Sadeghi, H., Ghannadi, A., Gharavi, M. and Azarpajoo, S. 2006. Hypolipidemic activity of *Allium porrum* L. in cholesterol fed rabbits. *J. Med. Food* **9**, 98-101.
- Munde, A.S., Shelke, V.A., Jadhav, S.M., Kirdant, A.S., Vaidya, S.R. and Shankarwar, S.G. 2012. Synthesis, characterization and antimicrobial activities of some transition metal complexes of biologically active asymmetrical tetradentate ligands. *Adv. Appl. Sci. Res.* **3**, 175-182.
- Musi, N., Hirshman, M.F., Nygren, J., Svanfeldt, M., Bavenholm, P., Rooyackers, O., Zhou, G., Williamson, J.M., Ljunqvist, O., Efendic, S., Moller, D.E., Thorell, A. and Goodyear, L.J. 2002. Metformin increases AMP-activated protein kinase activity in skeletal muscle of subjects with Type 2 diabetes. *Diabetes* **51**, 2074-2081.

- Naik, J.B. and Waghulde, M.R. 2018. Development of vildagliptin loaded Eudragit® microspheres by screening design: in vitro evaluation. *J. Pharmaceutic. Invest.* **48**, 627-637.
- Nakagawa, T., Hu, H., Zharikov, S., Tuttle, K.R., Short, R.A., Glushakova, O., Ouyang, X., Feig, D.I., Block, E.R., Herrera, A.J., Patel, J.M. and Johnson, R.J. 2006. A causal role for uric acid in fructose-induced metabolic syndrome. *Am. J. Physiol. Renal Physiol.* **290**, F625-F631.
- National Institutes of Health. Zinc-Fact Sheet for Health Professionals. Available online: <https://ods.od.nih.gov/factsheets/Zinc-HealthProfessional/> (accessed on 8 December 2020).
- National Research Council. 1989. Recommended Dietary Allowance, 10th ed. National Academy Press, Washington, DC.
- Neeraj, K., Subba, R.D., Gurmeet, S., Kadirappaa, A., Shailendra, K.D. and Pramod, K. 2016. Identification, isolation and characterization of potential process-related impurity and its degradation product in vildagliptin. *J. Pharm. Biomed. Anal.* **119**, 114-121.
- Okaka T., Sakuma L., Fukui Y., Hageki, O. and Ui, M. 1994. Blockage of chemotactic peptide-induced stimulation of neutrophils by wortmannin as a result of selective inhibition of phosphatidylinositol kinase. *J. Biol. Chem.* **269**, 3563-3567.
- Orvig, C. and Abrams, M.J. 1999. Medicinal Inorganic Chemistry: Introduction. *Chem. Rev.* **99**, 2201-2204.
- Othman, A.I. and ElMissiry, M.A. 1998. Role of selenium against lead toxicity in male rats. *J. Biochem. Mol. Toxicol.* **12**, 345-349.
- Padilla, M.A., Elobeid, M., Ruden, D.M. and Allison, D.B. 2010. An examination of the association of selected toxic metals with total and central obesity indices: NHANES 99–02. *Int. J. Environ. Res. Public Health* **7**, 3332–3347.
- Pechova, A. and Pavlata, L. 2007. Chromium as an essential nutrient: A review. *Vet. Med.* **52**, 1-18.
- Pernicova, I. and Korbonits, M. 2014. Metformin- mode of action and clinical implications for diabetes and cancer. *Nat. Rev. Endocrinol.* **10**, 143-156.
- Plosker, G.L. 2012. Dapagliflozin: a review of its use in type 2 diabetes mellitus. *Drugs.* **72**, 2289-2312.

- Prasad, S., Kashyap, R.S., Deopujari, J.Y., Purohit, H.J., Taori, G.M. and Daginawala, H.F. 2007. Effect of *Fagonia arabica* (Dhamasa) on *in vitro* thrombolysis. *BMC Complement Alternat. Med.* **7**, 36.
- Puig, S. and Thiele, D.J. 2002. Molecular mechanisms of copper uptake and distribution. *Curr. Opin. Chem. Biol.* **6**, 171-180.
- Ratnaparkhi, M.P. 2012. Formulation and development of taste masked orally disintegrating tablets of perindopril erbumine by direct compression method. *Pharmaceutic. Anal. Acta* **3**, DOI: 10.4172/2153-2435.1000162.
- Ravina, A., Slezak, L., Rubal, A. and Mirsky, N. 1995. Clinical use of the trace element chromium(III) in the treatment of diabetes mellitus. *J. Trace Elem. Exper. Med.* **8**, 183-190.
- Reitman, S. and Frankel, S.A. 1957. Colorimetric method for the determination of serum glutamic oxalacetic and glutamic pyruvic transaminases. *J. Clin. Pathol.* **28**, 56-63.
- Rendell, M. 2004. The role of sulphonylureas in the management of Type 2 diabetes mellitus. *Drugs* **64**, 1339-1358.
- Ribarov, S.R. and Benov, L.C. 1981. Relationship between the hemolytic action of heavy metals and lipid peroxidation. *Biochim. Biophys. Acta* **640**, 721-726.
- Ribarov, S.R. and Bochev, P.G. 1982. Lead-hemoglobin interaction as a possible source of reactive oxygen species- A chemiluminescent study. *Arch. Biochem. Biophys.* **213**, 288-292.
- Ribarov, S.R., Benov, L.C. and Benchev, I.C. 1981. The effect of lead on hemoglobin-catalyzed lipid peroxidation. *Biochim. Biophys. Acta* **664**, 453-459.
- Rikitake, Y. and Liao, J.K. 2005. Rho GTPases, statins and nitric oxide. *Circ. Res.* **97**, 1232-1235.
- Ris, M.D., Dietrich, K.N., Succop, P.A., Berger, O.G. and Bornschein, R.L. 2004. Early exposure to lead and neuropsychological outcome in adolescence. *J. Int. Neuropsychol. Soc.* **10**, 261-270.
- Roat, R. M. 2002. Bioinorganic Chemistry: A Short Course, Wiley Interscience, Hoboken, New Jersey.

- Robert, L.L., Katelijne, E.M., Gert, A.V., Patrick, C.P., Max, D., Jean, C.S. and Norbert, H. L. 2003. Pharmacokinetics of atorvastatin and its metabolites after single and multiple dosing in hypercholesterolaemic haemodialysis patients. *Nephrol. Dial. Transplant.* **18**, 967-976.
- Roblek, T., Deticek, A., Leskovar, B., Suskovic, S., Horvat, M., Belic, A., Mrhar, A. and Lainscak, M. 2016. Clinical-pharmacist intervention reduces clinically relevant drug-drug interactions in patients with heart failure: a randomized, double-blind, controlled trial. *Int. J. Cardiol.* **203**, 647-652.
- Rodrigues, M.C.S. and Oliveira, C. 2016. Drug-drug interactions and adverse drug reactions in polypharmacy among older adults: an integrative review. *Rev. Latino-Am. Enfermagem.* **24**, e2800.
- Rorsman, P. 1997. The pancreatic beta-cell as a fuel sensor: An electrophysiologist's view point. *Diabetologia* **40**, 487-495.
- Rosenberg, B., Van, C.L. and Krigas, T. 1965. Inhibition of cell division in *Escherichia coli* by electrolysis products from a platinum electrode. *Nature* **205**, 698-699.
- Ross, P.D. and Subramanian, S. 1981. Thermodynamics of protein association reactions: Forces contributing stability. *Biochem.* **20**, 3096-3102.
- Roth, R.A., Lui, F. and Chin, J.E. 1994. Biochemical mechanisms of insulin resistance. *Hormone Res.* **41**(suppl2), 51-55.
- Saad, M.J. 1994. Molecular mechanisms of insulin resistance. *Braz. J. Med. Biol. Res.* **27**, 941-957.
- Sabastiyan, A., Suvaikin, M.Y. 2012. Synthesis, characterization and antimicrobial activity of 2-(dimethylaminomethyl)isoindoline-1,3- dione and its cobalt(II) and nickel(II) complexes. *Adv. Appl. Sci. Res.* **3**, 45-50.
- Sadler, P. J. 1999. Metals in medicine. *Adv. Inorg. Chem.* **49**, 183-306.
- Saha, S., Begum, R., Sultan, Z., and Amjad, F. 2012. *In vitro* interaction of metformin with diclofenac in aqueous medium. *Dhaka Univ. J. Pharma. Sci.* **11**, 2-7.
- Sarkar, B. 1999. Treatment of Wilson and Menkes Diseases. *Chem. Rev.* **99**, 2535-2544.
- Sasmal, P.K., Streu, C.N. and Meggers, E. 2013. Metal complex catalysis in living biological systems. *Chem. Commun.* **49**, 1581-1587.

- Schanne, F.A., Dowd, T.L., Gupta, R.K. and Rosen, J.F. 1989. Lead increases free Ca^{2+} concentration in cultured osteoblastic bone cells: Simultaneous detection of intracellular free Pb^{2+} by ^{19}F NMR. *Proc. Natl. Acad. Sci. U.S.A.* **86**, 5133-5135.
- Schermaier, A.J., O'Connor, L.H. and Pearson, K.H. 1985. Semi-automated determination of chromium in whole blood and serum by Zeeman electrothermal atomic absorption spectrophotometry. *Clin. Chim. Acta* **152**, 123-134.
- Schumm, D.P.M., Burgess, L., Koranyi, L., Hrubá, V., Hamer, M.J.E. and de Bruin, T.W.A. 2015. Twice-daily dapagliflozin co-administered with metformin in Type 2 diabetes: A 16-week randomized, placebo-controlled clinical trial. *Diabetes Obes. Metab.* **17**, 42-51.
- Searle, A.K., Baghurst, P.A., Hooff, M., Sawyer, M.G., Sim, M.R., Galletly, C., Clark, L.S. and McFarlane, A.C. 2014. Tracing the long-term legacy of childhood lead exposure: A review of three decades of the port Pirie cohort study. *Neurotoxicol.* **43**, 46-56.
- Shankar, G., Pragney, D. and Ramakrishna, S. 2014. Simultaneous determination of atorvastatin calcium and olmesartan medoxomil in rat plasma by liquid chromatography electrospray ionization tandem mass spectrometry and its application to pharmacokinetics in rats. *Int. J. Pharm. Pharm. Sci.* **6**, 464-468.
- Sheikhshoai, I., Badii, A. and Ghazizadeh, M. 2012. Synthesis and spectroscopic studies of two new complexes containing Fe(III) and Mo(VI) of two tridentate ONO donor sets ligands. *Der. Chemica. Sinica* **3**, 24-28.
- Shoji, A., Yamanaka, H. and Kamatani, N. 2004. A retrospective study of the relationship between serum urate level and recurrent attacks of gouty arthritis: Evidence for reduction of recurrent gouty arthritis with antihyperuricemic therapy. *Arthritis Rheum.* **51**, 321-325.
- Shrestha, P. and Ghimire, L. 2012. A review about the effect of life style modification on diabetes and quality of life. *Glob. J. Health Sci.* **4**, 185-190.
- Sirken, G., Kung, S.C. and Raja, R. 2003. Decreased erythropoietin requirements in maintenance hemodialysis patients with statin therapy. *ASAIO J.* **49**, 422-425.
- Soldevila, B.J.J. and Sadler, P.J. 2015. Approaches to the design of catalytic metallodrugs. *Curr. Opin. Chem. Biol.* **25**, 172-183.

- Song, Y., Chou, E.L., Baecker, A., You, N.C.Y., Song, Y., Sun, Q. and Liu, S. 2016. Endocrine-disrupting chemicals, risk of Type 2 diabetes, and diabetes-related metabolic traits: A systematic review and meta-analysis. *J. Diabetes* **8**, 516-532.
- Stancu, C. and Sima, A. 2001. Statins: mechanism of action and effects. *J. Cell. Mol.* **5**, 378-387.
- Star, M. and Flaster, M. 2013. Advances and controversies in the management of cerebral venous thrombosis. *Neurol. Clin.* **31**, 765-783.
- Steinhardt J., Krijn, J. and Leidy, J.G. 1971. Differences between bovine and human serum albumins: Binding isotherms, optical rotatory dispersion, viscosity, hydrogen ion titration, and fluorescence effects. *Biochem.* **10**, 4005-4015.
- Stoecker, B.J. 1996. Present Knowledge in Nutrition. 7th Ed., ILSI Press, Washington DC, pp. 344-352.
- Stumvoll, M. Goldstein, B.J. and Haeften, T.W. 2005. Type 2 diabetes: Principles of pathogenesis and therapy. *Lancet* **365**, 1333-46.
- Stumvoll, M., Nurjhan, N., Perriello, G., Dailey, G. and Gerich, J.E. 1995. Metabolic effects of metformin in non-insulin-dependent diabetes mellitus. *New Eng. J. Med.* **333**, 550-554.
- Sturgess, N., Cook, D., Ashford, M.J. and Hales, C.N. 1985. The sulphonylurea receptor may be an ATP-sensitive potassium channel. *Lancet* **326**, 474-475.
- Sugiyama, M., Ohashi, M., Takase, H., Sato, K., Ueda, R. and Dohi, Y. 2005. Effects of atorvastatin on inflammation and oxidative stress. *Heart Vessels.* **20**, 133- 136.
- Surkan, P.J., Zhang, A., Trachtenberg, F., Daniel, D.B., McKinlay, S. and Bellinger, D.C. 2007. Neuropsychological function in children with blood lead levels <10 micro gm/dL. *Neurotoxic.* **28**, 1170-1177.
- Suryawanshi, V.D., Walekar, L.S., Gore, A.H., Anbhule, P.V. and Kolekar, G.B. 2016. Spectroscopic analysis on the binding interaction of biologically active pyrimidine derivative with bovine serum albumin. *J. Pharm. Anal.* **6**, 56-63.
- Suryawanshi, V.D., Walekar, L.S., Gore, A.H., Anbhule, P.V. and Kolekar, G.B. 2016. Spectroscopic analysis on the binding interaction of biologically active pyrimidine derivative with bovine serum albumin. *J. Pharm. Anal.* **6**, 56-63.

- Tabassum, A., Arayne, M.S., Sultana, N. and Mehjabeen. 2016. Synthetic characterization of complexes of rosuvastatin and some ACE inhibitors: Pharmacological evaluation. *Pharm. Anal. Acta* **7**, 6.
- Tanwir, A., Jahan, R., Quadir, M.A., Kaiser, M.A. and Hossain, K. 2012. Spectroscopic studies of the interaction between metformin hydrochloride and bovine serum albumin. *Dhaka Univ. J. Pharm. Sci.* **11**, 45-49.
- Targher, G., Bertolini, L., Padovani, R., Rodella, S., Tessari, R., Zenari, L., Day, C. and Arcaro, G. 2007. Prevalence of nonalcoholic fatty liver disease and its association with cardiovascular disease among Type 2 diabetic patients. *Diabetes Care* **30**, 1212-1218.
- Tatineni, V., An, J.Y. Leffew, M.R. and Mahesh, S.A. 2020. Anemia from A to zinc: Hypocupremia in the setting of gastric bypass and zinc excess. *Clin. Case Rep.* **8**, 745-750.
- Tsaih, S.W., Korrick, S. and Schwartzetal, J. 2004. Lead, diabetes, hypertension, and renal function: The normative aging study. *Environ. Health Perspect.* **112**, 1178-1182.
- Tsunekawa, T., Hayashi, T., Suzuki, Y., Matsui, H.H., Kano, H., Fukatsu, A., Nomura, N., Miyazaki, A. and Iguchi, A. 2003. Plasma adiponectin plays an important role in improving insulin resistance with glimepiride in elderly Type 2 diabetic subjects. *Diabetes Care* **26**, 285-289.
- Turel, I. and Kljun, J. 2011. Interactions of metal ions with DNA, its constituents and derivatives, which may be relevant for anticancer research. *Curr. Top. Med. Chem.* **11**, 2661-2687.
- Ukinc, K., Ersoz, H.O., Erem, C., Hacıhasanoglu, A.B. and Karti, S.S. 2009. Effects of one year simvastatin and atorvastatin treatments on acute phase reactants in uncontrolled type 2 diabetic patients. *Endocrine* **35**, 380-388.
- Uriu-Adams, J.Y. and Keen, C.L. 2005. Copper, oxidative stress, and human health. *Mol. Aspec. Med.* **26**, 268-298.
- vanBommel, E.J.M., Muskiet, M. H.A., Tonneijck, L., Kramer, M.H.H., Nieuwdorp, M. and vanRaalte, D.H. 2017. SGLT2 Inhibition in the diabetic kidney-From mechanisms to clinical outcome. *CJASN* **12**, 700-710.
- Viollet, B. and Foretz, M. 2013. Revisiting the mechanisms of metformin action in the liver. *Ann. Endocrinol.* **74**, 123-129.

Weaver, V.M., Ellis, L.R., Lee, B.K. Todd, A.C., Shi, W., Ahn, K.D. and Schwartz, B.S. 2008. Associations between patella lead and blood pressure in lead workers. *Am. J. Ind. Med.* **51**, 336-343.

Weaver, V.M., Griswold, M., Todd, A.C., Jaar, B.G., Ahn, K.D., Thompson, C.B. and Lee, B.K. 2009. Longitudinal associations between lead dose and renal function in lead workers. *Environ. Res.* **109**, 101-107.

Weaver, V.M., Lee, B.K., Ahn, K.D., Lee, G.S., Todd, A.C., Stewart, W.F., Wen, J., Simon, D.J., Parsons, P.J. and Schwartz, B.S. 2003. Associations of lead biomarkers with renal function in Korean lead workers. *Occup. Environ. Med.* **60**, 551-562.

Weaver, V.M., Lee, B.K., Todd, A.C., Jaar, B.G., Ahn, K.D., Wen, J., Shi, W., Parsons, P.J. and Schwartz, B.S. 2005. Associations of patella lead and other lead biomarkers with renal function in lead workers. *J. Occup. Environ. Med.* **47**, 235-243.

Wells, G. B., Dipiro, J., Schwinghammer, T. and Hamilton, C. 2007. *Pharmacotherapy Handbook*, 7th ed, The McGraw Hill Companies, USA, pp. 98-108.

White, C.M. 2002. A review of the pharmacologic and pharmacokinetic aspects of rosuvastatin. *J. Clin. Pharmacol.* **42**, 963-970.

Whittle, E., Singhal, R., Collins, M. and Hrdina, P. 1983. Effects of subacute low level lead exposure on glucose homeostasis. *Res. Commun. Chem. Pathol. Pharmacol.* **40**, 141-154.

Williams, R.H. and Palmer, J.P. 1975. Farewell to phenformin for treating diabetes mellitus. *Ann. Int. Med.* **83**, 567-568.

Williamson, R.M., Price, J.F., Glancy, S., Perry, E., Nee, L.D., Hayes, P.C., Frier, B.M., Van Look, L.A.F., Johnston, G.I., Reynolds, R.M. and Strachan, M.W.J. 2011. Edinburgh Type 2 Diabetes study investigators prevalence of and risk factors for hepatic steatosis and nonalcoholic fatty liver disease in people with Type 2 diabetes: The Edinburgh Type 2 Diabetes Study. *Diabetes Care* **34**, 1139-1144.

World Health Organization (WHO), 2017, Global Health Observatory (GHO) data. World Health Organization (WHO), Geneva, Switzerland. Available at: http://www.who.int/gho/ncd/risk_factors/cholesterol_text/en/ [Accessed on 17th July 2017].

Zacharski, L.R., Shamayeva, G. and Chow, B.K. 2011. Effect of controlled reduction of body iron stores on clinical outcomes in peripheral arterial disease. *Am. Heart J.* **162**, 949-957.

Zhai, H., Chen, C., Wang, N., Chen, Y., Nie, X., Han, B., Li, Q., Xia, F. and Lu, Y. 2017. Blood lead level is associated with non-alcoholic fatty liver disease in the Yangtze River Delta region of China in the context of rapid urbanization. *Environ. Health* **16**, 93. DOI: 10.1186/s12940-017-0304-7

Zhao, L., Liu, R., Zhao, X., Yang, B., Gao, C., Hao, X. and Wu, Y. 2009. New strategy for the evaluation of CdTe quantum dot toxicity targeted to bovine serum albumin. *Sci. Total Environ.* **407**, 5019-5023.

Zhao, X., Liu, R., Chi, Z., Teng, Y. and Qin, P. 2010. New insights into the behavior of bovine serum albumin adsorbed on to carbon nano tubes: Comprehensive spectroscopic studies. *J. Phys. Chem. B* **114**, 5625-5631.

Zohdi, H., Emami, M. and Reza, H. 2012. Galvanic corrosion behavior of dental alloys. *Environmental and Industrial Corrosion -Practical and Theoretical Aspects*; pp. 157-168. DOI: 10.5772/52319.

List of Papers Published from the Thesis

1. **Aktar, F.**, Sultan, M.Z. and Rashid, M.A. 2021. Chromium (III) complexes of metformin, dapagliflozin, vildagliptin and glimepiride potentiate antidiabetic activity in animal model. *Int. J. Curr. Res. Rev.* **13**, 64-69.
2. **Aktar, F.**, Sultan, M.Z. and Rashid, M.A. 2020. Study of the effects of complexation of lead with metformin, glimepiride, vildagliptin and dapagliflozin in mice model, *Microb. Bioact.* **3**, 125-133.
3. **Aktar, F.**, Sultan, M.Z. and Rashid, M.A. 2019. *In vitro* complexation of olmesartan medoxomil with dapagliflozin, vildagliptin and metformin. *Dhaka Univ. J. Pharm. Sci.* **18**, 271-280.